Synthesis of aminoacyl-tRNA analogues for the study and inhibition of Fem-transferases, new targets for the development of antimicrobials

Nicolas Sakkas

Université Paris Descartes

Ecole doctorale Médicament, Toxicologie, Chimie, Imageries

Thèse

Présentée pour obtenir le grade de Docteur de l'Université Paris Descartes

Discipline : **Chimie** – Spécialité : **Interface Chimie-Biologie**

Par

Nicolas SAKKAS

Synthèse d'analogues d'aminoacyl-ARNt pour l'étude et l'inhibition de Fem-transférases, nouvelles cibles pour le développement d'antibactériens.

Préparée au Laboratoire de Chimie et Biochimie Pharmacologiques et Toxicologiques
CNRS UMR8601 – Université Paris Descartes

Sous la direction du Professeur Mélanie ETHÈVE-QUELQUEJEU

Soutenue le Lundi 7 novembre 2016 devant un jury composé de :

Pr Thomas CARELL	Université Louis-et-Maximilien de Munich	Rapporteur
Pr Michael SMIETANA	Université de Montpellier	Rapporteur
Pr Olivia REINAUD	Université Paris Descartes	Examinatrice
Pr Tom BROWN	Université d'Oxford	Examinateur
Pr Mélanie ETHÈVE-QUELQUEJEU	Université Paris Descartes	Examinatrice
Dr Emmanuelle GUILLOT-COMBE	Direction Générale de l'Armement	Membre invitée
Dr Sarah HARDING	Defence Science and Technology Laboratory	Membre invitée

Université Paris Descartes

Ecole doctorale Médicament, Toxicologie, Chimie, Imageries

Thèse

Présentée pour obtenir le grade de Docteur de l'Université Paris Descartes

Discipline : **Chimie** – Spécialité : **Interface Chimie-Biologie**

Par

Nicolas SAKKAS

Synthèse d'analogues d'aminoacyl-ARNt pour l'étude et l'inhibition de Fem-transférases, nouvelles cibles pour le développement d'antibactériens.

Préparée au Laboratoire de Chimie et Biochimie Pharmacologiques et Toxicologiques
CNRS UMR8601 – Université Paris Descartes

Sous la direction du Professeur Mélanie ETHÈVE-QUELQUEJEU

Soutenue le Lundi 7 novembre 2016 devant un jury composé de :

Pr Thomas CARELL	Université Louis-et-Maximilien de Munich	Rapporteur
Pr Michael SMIETANA	Université de Montpellier	Rapporteur
Pr Olivia REINAUD	Université Paris Descartes	Examinatrice
Pr Tom BROWN	Université d'Oxford	Examinateur
Pr Mélanie ETHÈVE-QUELQUEJEU	Université Paris Descartes	Examinatrice
Dr Emmanuelle GUILLOT-COMBE	Direction Générale de l'Armement	Membre invitée
Dr Sarah HARDING	Defence Science and Technology Laboratory	Membre invitée

Acknowledgments

Acknowledgments

First of all, I would like to thank the members of the panel who have agreed to evaluate this work. I am particularly honored that Prof. Thomas Carell and Prof. Michael Smietana accepted to be the *rapporteurs* of this doctoral thesis. I am very happy that Prof. Olivia Reinaud accepted to be part of this panel, as I would probably not be here today without her inspiring lectures and helpful advice. I am very grateful to Prof. Tom Brown for giving me the opportunity to come and work in his group in Oxford for several months during this PhD. I would also like to warmly thank Prof. Mélanie Ethève-Quelquejeu for welcoming me into her lab during my Master's and my PhD. Her optimistic, energetic and motivational supervision is gratefully acknowledged.

This PhD was funded by a scholarship from the Direction Générale de l'Armement (DGA) through the Fr/UK PhD scheme of the DGA and the British Defence Science and Technology Laboratory (DSTL). The collaborative work between the groups of Prof. Ethève-Quelquejeu and Prof. Brown would not have been possible without this funding, which is gratefully acknowledged. On a more personal note, this scheme also was an amazing opportunity to travel between two groups, work in two languages, and learn so much.

I would like to deeply thank our collaborators Dr Michel Arthur and Dr Matthieu Fonvielle, from the Centre de Recherche des Cordeliers (Paris, France). Their precious knowledge and explanations regarding Fem-transferases, biochemistry, and biomolecule chemistry were of a great help for me. This project would not be possible without such a stimulating collaboration. Our other collaborators are gratefully acknowledged: the group of Dr Dominique Mengin-Lecreulx for the enzymatic synthesis of peptidoglycan precursors analogs; the group of Prof. Herman Van Tilbeurgh for the crystallography studies; the group of Prof. Alain Burger for the fluorescent nucleosides.

I spent more than three years in the *Laboratoire de Chimie et Biochimie Pharmacologiques et Toxicologiques*. I would like to warmly thank all the members from the group of Prof. Etheve-Quelquejeu in particular: Laura Iannazzo who taught me all there is to know about chemistry (and some invaluable life lessons as well), Emmanuelle Braud, Expédite Yen-Pon, Colette Atdjian, and from the lab in general.

Over my two stays in Oxford, I had the chance to meet great people in the group of Prof. Brown, and of course I would like to thank Afaf El-Sagheer for her patience and kindness during her teaching of solid-phase synthesis.

Finally, I would like to thank all of my friends who supported me during this PhD, in good times and in bad. I feel blessed to have such amazing people in my life. Expédite, Anne-Doriane : on y est ! Armelle,

Camille, Candie, Chloé et Patrick, Chloé, Clotilde, Mathilde, Maud, Sarah, Sophie, et bien d'autres que je ne peux malheureusement pas tous citer ! And to finish, I thank my parents and my family for their inconditional support in all my endeavors.

Table of contents

PART 2: GOALS, RESULTS AND DISCUSSION

CHAPTER 1: SYNTHESIS OF ELECTROPHILIC AMINOACYL-TRNA ANALOGS FOR SITE-SPECIFIC CROSS-LINKING WITH FEMX$_{WV}$ AND PEPTIDE-RNA CONJUGATION

EXPERIMENTAL PART

List of abreviations

A	Adenine
aaRS	Aminoacyl-tRNA-synthetase
aa-tRNA	Aminoacyl-tRNA
Ac	Acetyl
ACE	2'-bis(2-Acetoxyethoxy)methyl
Ala	Alanine
Arg	Arginine
Asn	Asparagine
ASp	Aspartate
ATP	Adenosine triphosphate
BET	Ethidium bromide
Bn	Benzyl
BNA	Bridged Nucleic Acids
Boc	*tert*-butoxycarbonyl
BSA	Bovine Serum Albumine
Bu	Butyl
Bz	Benzoyl
C	Cytidine
cDNA	Complementary DNA
CDP	Cyclodipeptide
CDPS	Cyclodipeptide-synthase
CEO	2-Cyanoethoxy
CPG	Controlled-pore glass
CuAAC	Copper(I)-catalyzed Azide Alkyne Cycloaddition
DAST	Diethylaminosulfur trifluoride
DCC	Dicyclocarbodiimide
DCM	Dichloromethane
DIPEA	Di-*iso*-propylethylamine
DKP	Diketopiperazine
DMAP	*N,N*-dimethylaminopyridine
DMF	*N,N-dimethylformamide*
DMP	Dess-Martin Periodinane

DMSO	Dimethylsulfoxide
DMTr	Dimethoxytrityl
DNA	Deoxyribonucleic acid
E coli	*Escherichia coli*
EDC	1-Ethyl-3-(3-dimethylaminopropyl)carbodiimide
EF-Tu	Elongation Factor Thermo unstable
Et	Ethyl
Fem	factors essentials for methicillin resistance
FITC	Fluorescein Isothiocyanate
Fmoc	Fluorenylmethyloxycarbonyl
G	Guanine
GlcNAc	*N*-acetylglucosamine
Gln	Glutamine
Glu	Glutamate
Gly	Glycine
GTP	Guanosine triphosphate
HEPES	(4-(2-hydroxyethyl)-1-piperazineethanesulfonic acid
His	Histidine
HPLC	High Performance Liquid Chromatography
IC50	Half maximal inhibitory concentration
Ig	Immunoglobulin
Ile	Isoleucine
iPr	*iso*-propyl
IRES	Internal Ribosome Entry Site
Lac	Lactoyl
Leu	Leucine
LNA	Locked Nucleic Acids
Lys	Lysine
m-DAP	*meso*-diaminopimelic acid
Me	Methyl
Met	Methionine
mh	microhelix
mRNA	messenger RNA
MSH	O-(2,4,6-Trimethylbenzenesulfonyl)hydroxylamine

MurNAc	*N*-acetylmuramic acid
NHS	*N*-hydroxysuccinimide
NMR	Nuclear Magnetic Resonance
NRPS	Non-Ribosomal Peptide Synthetase
Orn	Ornithine
PG	Protecting Group
Ph	Phenyl
Phe	Phenylalanine
Pyr.	Pyridine
RNA	Ribonucleic Acid
rRNA	Ribosomal RNA
rt	room temperature
S aureus	*Staphylococcus aureus*
S noursei	*Streptomyces noursei*
SAR	Structure-Acivity Relationship
Sec	Selenocysteine
Ser	Serine
SM	Starting Material
SPS	Solid-Phase Synthesis
T	Thymidine
TBA	Tetrabutylammonium
TBAF	Tetrabutylammonium fluoride
TBDMS	*Tert*-butyldimethylsilyl
TBS	*Tert*-butyldimethylsilyl
tBu	*Tert-butyldimethylsilyl*
TC	2'-Thiomorpholine-4-carbothioate
TCA	Trichloroacetic Acid
TCEP	Tris-carboxyethyl phosphine
Tf	Triflyl
TFA	Trifluoroacetic Acid
THF	Tetrahydrofurane
THPTA	Tris(3-hydroxypropyltriazolylmethyl)amine
TMS	Trimethylsilyl
TOM	2-O-Triisopropylsilyloxymethyl

Tris	Tris(hydroxymethyl)aminomethane
tRNA	Transfer RNA
Trt	Trityl
U	Uridine
UDP	Uridine diphosphate
UM5K	UDP-MurNAc-pentapeptide
Val	Valine
Wv	*Weissella viridescens*

Part 1

Introduction, context and state of the art

1. Introduction: From antibiotic discovery to resistance emergence

Antibiotics are compounds able to either kill bacteria or inhibit their growth. The story of antibiotics is considered to start with the serendipitous discovery of penicillin from the fungus *Penicillium* by Sir A. Fleming in 1929.[1] Then followed what is considered to be a golden age of antibiotics, with the discovery of many new chemical classes of antibiotics, most of them deriving from natural compounds isolated from living organisms.

In a second phase, medicinal chemistry techniques allowed to obtain optimized antibiotics deriving from natural product-based scaffolds, giving birth to powerful drugs with excellent pharmacological profiles. This resulted in very efficient control and treatment of bacterial infections, drastic increase in the quality of life and life expectancy, and allowed the development of modern medicine as we know it.[2]

These first stages were however quickly followed by the "resistance era". Bacteria always had the ability to fight and resist naturally occurring antimicrobials, and it has been shown that the bacterial "resistome" precedes the age of antibiotic use by millennia.[3] Still, the modern use, overuse, and misuse of antibiotics have laid out an ideal set of conditions to mobilize and spread the bacterial resources for resistance.

Along with this resistance era came a decrease of successful drug discoveries. In the mid-1960s, new natural metabolites-based antibiotic scaffolds got harder to identify, and during this period innovation mainly happened through the optimization of pre-existing scaffolds. The emergence of new drug-discovery methods in the 1990s, with a "genes-to-drug" model, gave great results in biomedical research[4] and was applied to research for new antimicrobials. However, those systematic genetic studies and high-throughput biochemical and pharmacological screenings did not allow the discovery of compounds that are effective, that display acceptable physical and chemical properties, and that possess a broad spectrum of pathogenic bacteria. Moreover, poor understanding of drug penetration and efflux systems, and rapid emergence of resistance in single-target approaches are additional reasons explaining that no new suitable antibiotic could be obtained through these methods.

The conjunction of the emergence, spreading, and persistence of resistant bacterial strains on the one hand, and of the failure to deliver new antibiotics on the other hand, results in a major threat for public health. The appearance of multidrug resistance, in both healthcare and community settings, is damaging our ability to fight bacterial infections with efficacy and lead to cases with no more available

therapeutic options. In the European Union, it is estimated that drug-resistant bacteria are responsible for 25.000 deaths every year, and for a 1.5 billion USD cost.[5] This context dramatically justifies the need for new antibiotics. Keeping in mind the previous drawbacks and failures of classical drug discovery methods, efforts should be made for the research for unconventional targets, for the understanding of the complex mechanism of action of the pre-existing and effective antibiotics, and for the tackling of the problem of drug-vectorization, membrane permeability and target accessibility.[2]

Among the various bacterial processes that are targetable is the biosynthesis of the bacterial cell wall peptidoglycan, a process that is reviewed in Part 2. In this doctoral thesis, inhibitors and molecular tools have been synthesized in order to study targets for the development of antimicrobials: the transferases from the FemABX family, which are reviewed in Part 3. These enzymes use, as a substrate, an aminoacyl-tRNA (aa-tRNA), whose characteristics are reviewed in part 4, as aa-tRNA will be the scaffold used for the synthesis of the described compounds.

2. The bacterial peptidoglycan

2.1. Nature and role of the bacterial peptidoglycan

The peptidoglycan, also called murein, is the main component of the bacterial cell-wall. It is a biopolymer consisting of polyosidic and peptide parts (**Figure 1**). It is present in almost all the bacterial reign, although it is much thicker in Gram-positive bacteria than in Gram-negative bacteria.

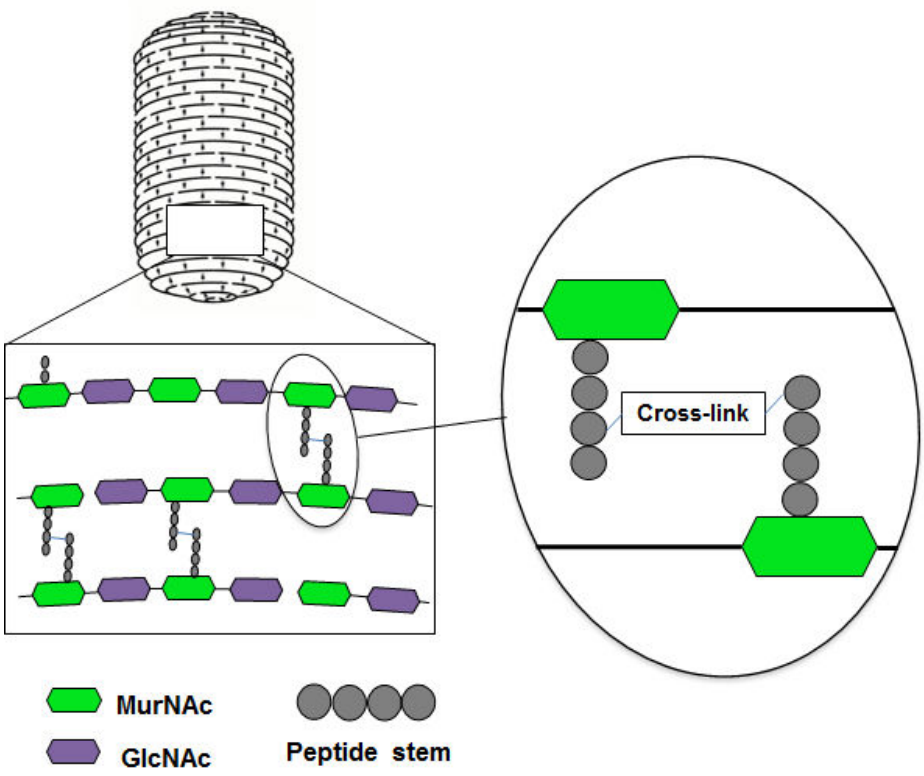

Figure 1: General structure of the peptidoglycan. In this example, the cross-linking between peptide stem is 3-4. Other linkages exist and are later mentioned.

Its main role is structural, maintaining the bacterial cell against mechanical constraints and osmotic pressure from the cytoplasm. Other known and notable roles are its use as an anchoring point for other envelope protein components, teichoic acids, or signaling osidic motifs.[6]

Because of these essential roles, inhibition or deregulation of the peptidoglycan biosynthesis lead to cell lysis, which is why this process has been one of the most investigated for antibiotic discovery.

2.2. Molecular structure of the peptidoglycan

2.2.1. Glycan strands

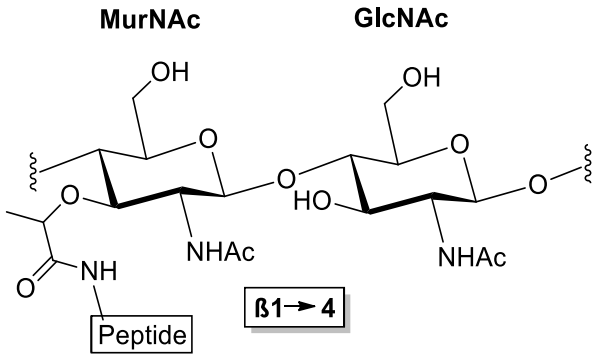

Figure 2: Structure of the MurNAc-GlcNAc disaccharide motif.

The glycan strands consist of alternating N-acetylglucosamine (GlcNAc) and N-acetylmuramic acid (MurNAc) residues with beta-1→4 linkages (**Figure 2**). These osidic linkages are biosynthesized at the very last step between peptidoglycan precursors. The carboxylic acid group of the MurNAc is substituted by a peptide stem (c*f* part 2.2.2.). This general structure is found in all bacterial species possessing murein, however secondary modifications or structural variations are frequent, notably at the reducing end between species. For example, *S. aureus* can possess either a MurNAc or GlcNAc residue at the reducing end depending whether N-acetylglucosaminidase-mediated cleavage has occurred, while Gram-negative bacteria and some Gram-positive bacteria (e.g. *Bacillus* spp.) terminate not with a reducing end but with a bridged 1,6-anhydroMurNAc residue.

Regarding the length of the glycan strands, important variability is observed between species and also within a species, with no obvious correlation with the cell-wall thickness: for example, while *S. aureus* and *B. subtilis* both possess a thick peptidoglycan layer, the former species shows short glycan strands (about 18 disaccharide units in average) while the latter shows long ones (between 50 and 250 disaccharide units).

Secondary modifications also exist on the glycan strands, such as *O*-acetylation, *N*-deacetylation, *N*-glycosylation, and affect hydrolysis and enlargement of peptidoglycan.[6] Such modifications can cause resistance by preventing the recognition of bacteria by immunity systems.

2.2.2. Peptide stem

The peptide stems most generally consist of five amino acid residues and are biosynthesized by Mur enzymes. They are connected to the glycan strands *via* the MurNAc lactoyl group and are linked between each other, depending on the nature of the residues, either directly or through an

interpeptide bridge (*cf* Part 2.2.3.). Some residues are widely found in the bacterial reign while other are the source of much variability (**Table 1**):

1. The first residue is often L-Ala. Some other residues can be present instead of L-Ala in rare cases.
2. The second residue added is always D-Glu, but latter modifications, posterior to the action of Mur enzymes, lead to a variability in this position.
3. The third residue is the source of much more variations compared to the other ones. It can be either a diamino acid (*meso*-diaminopimelic acid in most cases) or a monoamino acid (L-Lys in most cases). In a similar way as for the second position, post-synthetic modifications can be observed at this position.
4. The fourth and fifth position generally consist of a D-Ala-D-Ala dipeptide, synthesized before the action of Mur enzymes by the Ddl enzyme, and incorporated into the peptide stem by MurF. Little variability is observed at this position. The fifth residue is often lost in the mature biomolecule upon transpeptidation reactions.

Position	Mur-enzyme	Observed residue	Occurrence
1st	MurC	L-Ala	Most bacteria
2nd	MurD	D-iGlu D-iGln	Most Gram-negative bacteria Most Gram-positive bacteria
3rd	MurE	*m*-DAP L-Lys L-Orn	Most Gram-negative bacteria Most Gram-positive bacteria Spirochetes
4th, 5th	MurF	D-Ala-D-Ala D-Ala-D-Lac	Most bacteria Vancomycin-resistant *Enterococci*

Table 1: Main examples of amino acid variations in the peptide stem

2.2.3. Cross-linkages and peptide interbridges

Cross-linking is the most important source of inter-species variability for the peptidic part of the peptidoglycan. Cross-linking happens in two fashions:

1. 3-4 cross-linkage: the amino group of the 3rd amino acid residue of the peptide acyl-acceptor stem is linked to the carboxyl group of the 4th amino acid residue, a D-Ala, of the peptide acyl-donor stem. This linkage can either be direct (for most Gram-negative bacteria), or through a peptide interbridge (most Gram-positive bacteria).
2. 2-4 cross-linkage: the carboxyl group of the D-Glu in the 2nd position of the peptide acyl-acceptor stem is linked to the carboxyl group of the 4th amino acid residue, a D-Ala, of the peptide acyl-donor stem. This linkage can only happen through an interpeptide bridge containing a diamino acid.

Cross-linking, or transpeptidation, happens in the last phases of the peptidoglycan biosynthesis.

The biosynthesis of the interbridge, when it exists, is performed in the early phases of the biosynthesis, by enzymes from the FemABX family, or Fem-enzymes (*cf* Part 3), in the case of 3-4 cross-linkage, or *via* acyl-phosphate-activated amino acids for the 2-4 cross-linkage. The interbridge is the source for numerous differences between bacterial species, regarding either its amino acid sequence or the step of the peptidoglycan biosynthesis at which incorporation of the peptide interbridge happens. As a result, enzymes involved in the synthesis of the interbridge can be considered as promising targets for the development of selective antimicrobials.

2.3. Biosynthesis and potential targets for drug discovery.

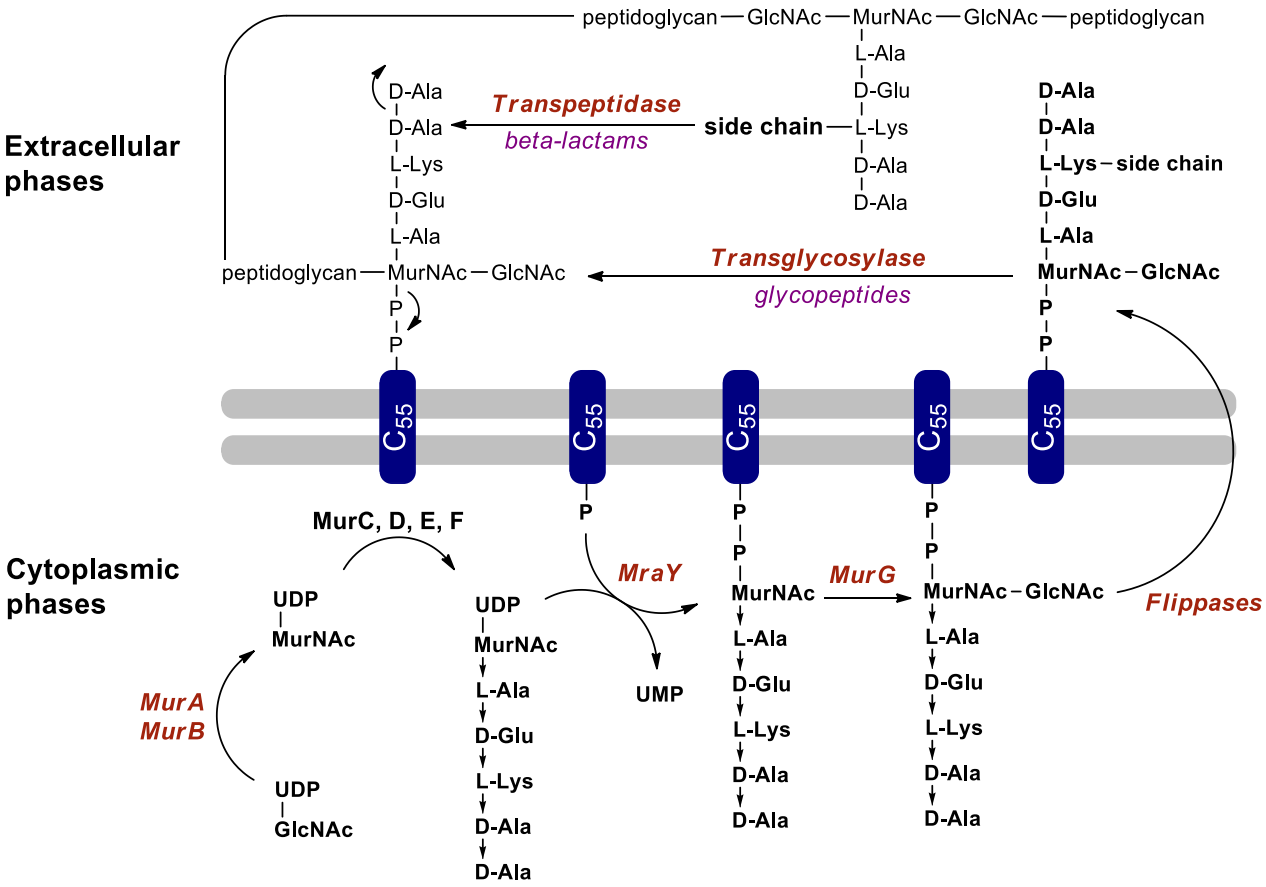

Scheme 1: Biosynthesis of the peptidoglycan for most Gram-positive bacteria

The biosynthesis of the peptidoglycan starts inside of the bacterial cell, where peptidoglycan precursors are biosynthesized during the cytoplasmic phase of the biosynthesis. The precursors are then translocated outside the cell, where the peptidoglycan can be formally assembled in the cytoplasmic phase. In this step, the macromolecule can grow and take on its various roles (**Scheme 1**). Historically, the enzymes involved in the extracellular phases have been studied and targeted before the ones involved in the intracellular phases.

2.3.1. Extracellular phases

Two types of reactions are involved in the tridimensional assembling of the peptidoglycan precursors outside the bacterial cell: transpeptidation and transglycosylation.

Transpeptidation is the cross-linking between the peptide stems in various fashions (*cf* part 2.2.3.). This reaction is performed by transpeptidases. These enzymes have been heavily targeted in the past by antibiotics belonging to the beta-lactams group, and bacterial resistance to such compounds is already well-established (**Scheme 2A**).

Transglycosylation is the assembling of the polyosidic motif. They have also been heavily targeted in the past by glycopeptide (**Scheme 2B**).

The enzymes involved in the extracellular phases are still under close investigation, but the identification of new targets in the extracellular phases is not probable.

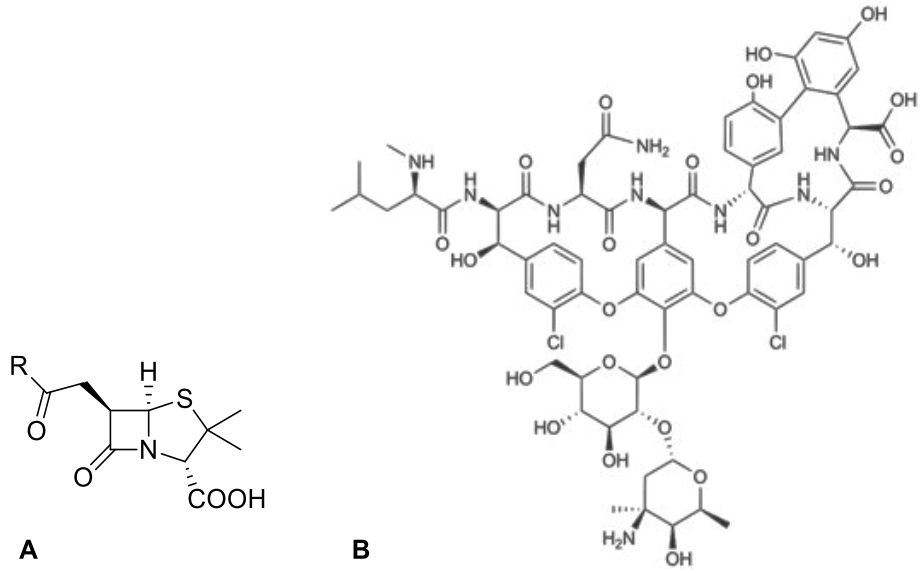

Scheme 2: Structure of compounds targeting extracellular biosynthetic enzymes. **A:** Structure of the transpeptidase-targeting penicillin. **B:** Structure of a glycopeptide, vancomycin, inhibiting the transglycosylation reaction.

2.3.2. Cytoplasmic phase

2.3.2.1. MurA-F enzymes

In the cytoplasm, UDP-GlcNAc is converted into UDP-MurNAc through the sequential actions of MurA and MurB. Then, MurC, MurD and MurE each catalyze the transfer of an amino acid onto the lactoyl group of the UDP-MurNAc. MurF catalyzes the transfer of the terminal dipeptide, previously synthesized by the Ddl enzyme from D-Ala generated by Alanine-racemase Alr.

MurA is targeted by fosfomycin, a clinically used antibiotic working through covalent inhibition of MurA. Other compounds have been identified through high-throughput screenings and SAR experimentation as efficient *in vitro* inhibitors, but to date, none of them has led to a selective inhibitor or to a potent antimicrobial.

MurB inhibitors have also been identified, and the peptidoglycan biosynthesis inhibiting properties of pyrazolidine are suspected to be caused by MurB inhibition. However, due to MurA feedback regulation by MurNAc, dual MurA/B inhibitors are considered to be more promising: thiazolyl ureas

and pyrazolidinediones antimicrobial properties are suspected to be linked to the fact that they are MurA/B inhibitors. [7]

MurC, D, E, F are ligases transferring amino acids. Because of abundant structural data which show similarities between these ligases, much effort has been made to obtain inhibitors that are active on more than one Mur ligase, with significant results in hit-identification. However, again, to date, none of these allowed to obtain suitable drug candidates.[8]

MurF substrate D-Ala-D-Ala dipeptide is synthetized through racemization of L-Ala by Alanine racemase Alr and condensation by Ddl.[8] Both of them are targets of D-cycloserine, a clinically used antibiotic for treatment of tuberculosis.[9]

2.3.2.2. MraY

MraY, or phospho-MurNAc-pentapeptide translocase, attach the MurNAc-pentapeptide onto the lipid carrier undecaprenyl-phosphate, thus yielding lipid I. This essential enzyme is heavily investigated for antimicrobial discovery, and the crystallographic structure of the apoenzyme has been resolved in 2013.[10] Natural scaffolds such as liposidomycins are known to inhibit MraY,[11] but to date, no clinical candidate has been identified.

2.3.2.3. MurG

MurG is responsible for the biosynthesis of lipid II from lipid I through the addition of a GlcNAc moiety. Among all the studies related to MurG, notable work is the one of Walker *et al.*: they reported the structure of both MurG alone[12] and the MurG:UDP-GlcNAc complex.[13] High-throughput screenings allowed them to identify several scaffolds showing good activity on this transferase, mostly five or six-membered heteroaromatic rings.[14,15]

2.3.2.4. Flippases

Translocation of the lipid II towards the periplasm is mediated by an ensemble of proteins of the SEDS family (shape, elongation, division, sporulation).[16] Some of them have been identified as essential for bacterial survival and as such, they are investigated as potential targets.

2.3.2.5. Fem-transferases

The enzymes belonging to the FemABX family are considered as attractive new targets. They are responsible for the biosynthesis of the peptide interbridge in the bacteria for which such a structure exists. These enzymes are more precisely detailed in the following part 3.

3. The FemABX family

3.1. General characteristics of the FemABX family members.

During studies of methicillin resistance in staphylococci, transposon-mediated mutagenesis[17] led to the identification of loci whose inactivation deleted methicillin resistance, for which the term “fem” for “factors essential for methicillin resistance” was coined.[18,19] Mutants for these factors showed loss of methicillin resistance and hypersusceptibility even to unrelated antibiotics.[20] Identification of the proteins coded by these genes led to the discovery of the FemABX family, or Fem-transferases.

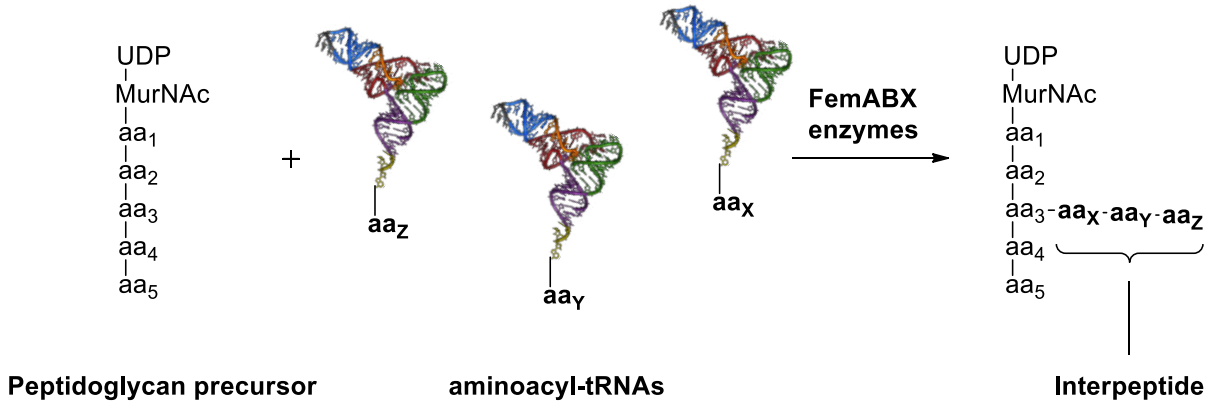

Scheme 3: General reaction catalyzed by enzymes from the FemABX family.

Fem-transferases are non-ribosomal aminoacyl-transferases that are responsible for the biosynthesis of the peptide interbridge of the peptidoglycan (**Scheme 3**),[21,22] as all bacteria possessing a FemABX analog in their genome bear such an interbridge in their peptidoglycan (**Table 2**).

Bacterial species	Interpeptide	FemABX homolog
Weissella viridescens	L-Ala-L-Ser	FemX
Staphylococcus aureus	Gly_5	FmhB, FemA, FemB
Staphylococcus epidermidis	Gly_{4-5}-L-Ala	FemA, FemB
Streptococcus pneumoniae	L-Ala-L-Ala	FibA, FibB, MurMN
Streptococcus pyogenes	L-Ala_{2-3}	
Enterococcus faecalis	L-Ala_{2-3}	
Clostridium perfringens	Gly	BAB87796
Treponema pallidum	Gly	AAC65773
Borrelia sp.	Gly	AAB91521

Table 2: Examples of peptide interbridges synthesized by Fem-transferases.

They are present in many Gram-positive bacteria, among them *Staphylococcus* spp., *Streptococcus* spp., *Enterococcus faecalis, Clostridium perfringens, Streptomyces coelicolor*, etc. and also in some Gram-negative bacteria, for example the pathogenic spirochetes *Treponema pallidum* and *Borrellia* spp.

Little structural data is known to date, but relative similarity can be expected between most of the members of the FemABX family members, with more or less phylogenetic distance (**Figure 3**).

Figure 3: Dendrogram of the FemABX family, reproduced from Rohrer, S.; Berger-Bachi, Antimicrob. Ag. Chemother. 2003, 47 (3), 837–846.

A source of variability between Fem-transferases is the nature of the peptidoglycan precursor onto which they attach the interpeptide: it can be soluble early precursors such as UDP-MurNAc-pentapeptide (UM5K) (e.g. FemX for *Weissella viridescens*) or later membrane-bound precursors such as lipid II (e.g. FmhB for *Staphylococcus aureus*).

The other substrates of Fem-transferases are aminoacyl-tRNA that act as amino acid donors. Aa-tRNA are also involved in the translation process. As a result, FemABX enzymes have to compete with the translation process and to divert aa-tRNA from the translation process. For some amino acids, there are more than one tRNA isoacceptors per amino acid: in that case, it has been hypothesized that one isoacceptor can be more prone to interact with Fem-enzymes than with translation factors.[23]

The work presented here mostly deals with two members of the FemABX family: FemX of *Weissella viridescens* and FmhB of *Staphylococcus aureus*.

3.2. Weissella viridescens FemX

3.2.1. A good model

Weissella viridescens is a non-pathogenic Gram-positive bacterium. It possesses a member of the FemABX family, FemX, which catalyzes the transfer of L-Ala onto the L-Lys of the UDP-MurNAc-pentapeptide (UM5K) (**Scheme 4**).

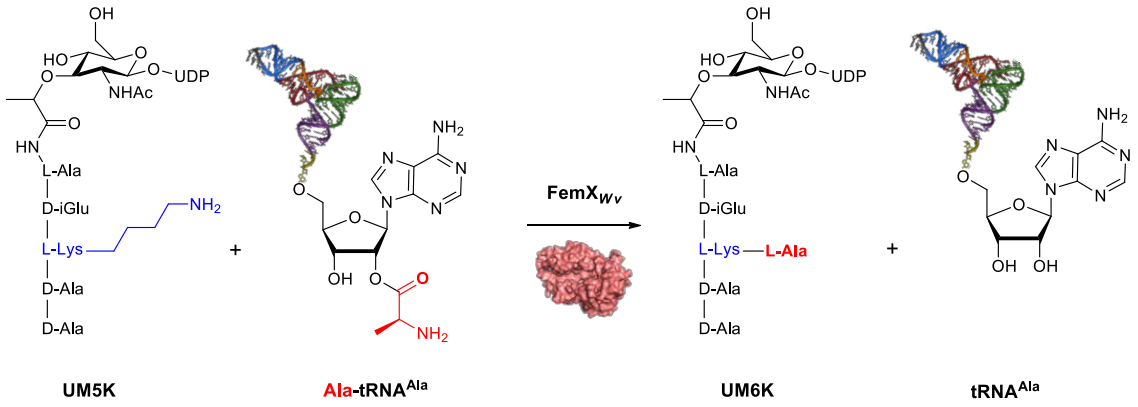

Scheme 4: Reaction catalyzed by $FemX_{Wv}$

As $FemX_{Wv}$ can be easily purified and used, and because the UM5K substrate is conveniently hydrosoluble, it is a practical model for the study of Fem-transferases.

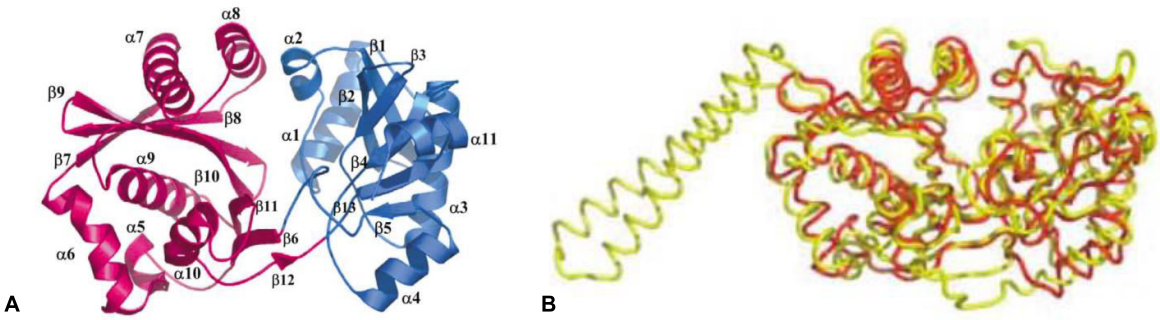

Figure 4: **A:** Structure of $FemX_{Wv}$; **B:** Superimposition of the structures of $FemX_{Wv}$ (red) and FemA (yellow). Reproduced from Biarrote-Sorin *et al.*, Structure, **2004**, 12.

Its crystal structure has been resolved in 2004,[24] both alone and in complex with the UM5K substrate (**Figure 4A**). The structure of the apoenzyme shows similarity to *Staphyloccocus aureus* FemA (**Figure 4B**).[25] the two major differences are the presence of a coiled-coil domain in FemA, and a different environment for the pocket welcoming the peptidoglycan precursor. This makes sense as for $FemX_{Wv}$,

the UM5K substrate is hydrosoluble in contrast to the lipid II for $FemA_{Sa}$. The channel recognizing the aa-tRNA substrate is very similar for both of them, thus confirming that $FemX_{Wv}$ is a valid model for the study of Fem-transferases in general, and their interactions with aa-tRNA in particular. For this reason, the group of Prof. Mélanie Ethève-Quelquejeu, in collaboration with the group of Dr Michel Arthur, developed the syntheses of several substrates analogues and inhibitors to study this interesting enzyme.

3.2.2. Previous studies on FemX

The work to study and understand the FemX enzyme consisted in synthesizing first analogs for the Ala-$tRNA^{Ala}$ substrate by modifying parts of the substrate and then monitoring its ability to transfer the alanyl group. Insight could be gained into the key parameters for substrate recognition.

3.2.2.1. Recognition mode of the aa-tRNA substrate

A model was developed for the hemisynthesis of Ala-$tRNA^{Ala}$ analogs.[26] After establishing that all key determinants for a substrate analog to be used by FemX are located in the acceptor stem of the $tRNA^{Ala}$, a coupled assay FemX/AlaRS allowed to study the recognition parameters for the Ala-$tRNA^{Ala}$ substrate.

The synthesis of compounds associating various tRNA moieties ($tRNA^{Gly}$, $tRNA^{Ala}$, $tRNA^{Ser}$) with amino acids (Gly, Ala, Ser) allowed to show that FemX:[27]

- Discriminates the amino acid carried by the tRNA on the basis of bulkiness, thus excluding any residue larger than Ala.
- Discriminates the RNA sequence of the aa-tRNA on the basis of the nucleotide sequence of the acceptor arm, more specifically the C^{2}-G^{71} bases-pair. It is interesting to note that this discrimination is different than the one operated by Ala-$tRNA^{Ala}$-synthetase, thus suggesting that this process evolved by deriving aminoacyl-tRNA from translation for the purpose of cell-wall synthesis.

3.2.2.2. 2'-position specificity and logic of the enzyme

The synthesis of 2' or 3' deoxy analogs of Ala-$tRNA^{Ala}$ (**Figure 5**) allowed to obtain non-isomerizable analogs. Biological assays with both of them led to the conclusion that:

- FemX can only transfer the amino acid from the 2' position of the aa-tRNA onto the peptidoglycan precursor.
- FemX recognizes both the 2' and the 3'-loaded aa-tRNA and is able to catalyze the 3'-2'-transacylation of the aa-tRNA to generate a suitable substrate.

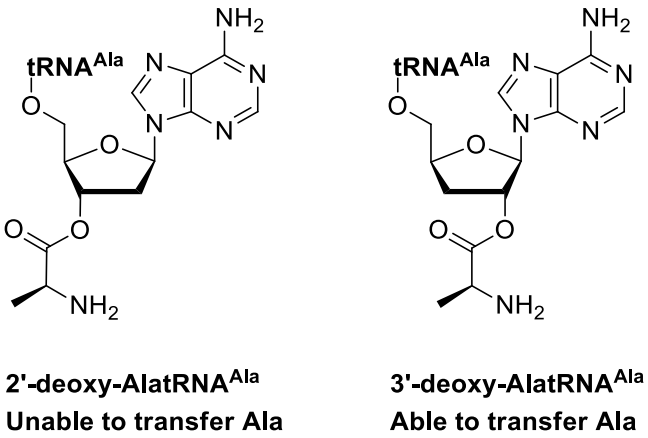

Figure 5: Chemical structure of the deoxy-Ala-tRNA^{Ala} analogues used to study FemX regioselectivity

As a result, FemX and the ribosome, which is thought to catalyze the transfer of amino acids from the 3'-loaded aa-tRNA[28] onto the peptidyl-tRNA, compete for the same pool of aa-tRNA, and FemX seems to have developed the ability to efficiently derives aa-tRNA from the translation process towards peptidoglycan biosynthesis.[29]

3.2.2.3. Structural data

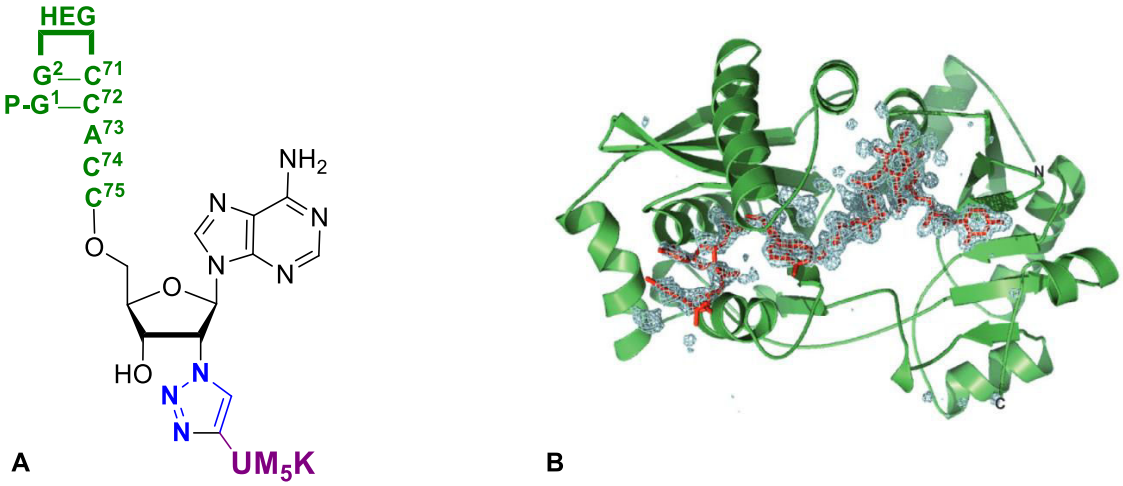

Figure 6: A: Structure of the peptidyl-RNA conjugate used for co-crystallization. HEG = Hexaethyleneglycol linker. **B:** Structure of FemX$_{Wv}$ in complex with the peptidyl-RNA conjugate

Even though the structures of both the apoenzyme and the UM5K/FemX complex were resolved in 2004, crystallization of Fem-enzymes in complex with tRNA substrates is a challenge because of the high flexibility of nucleic acids. As a result, a precise knowledge of the interactions between FemX and its Ala-tRNA^{Ala} substrate remained unavailable at that time.

Recently, the synthesis of a peptidyl-oligoribonucleotide conjugate that can be called a “bi-substrate” inhibitor allowed co-crystallization with FemX. This compound containing a RNA moiety mimicking $tRNA^{Ala}$ and a peptide moiety mimicking the UM5K substrate (**Figure 6A**), presented a high affinity with FemX and low flexibility for the RNA moiety. Those two parts are linked by a triazole ring. The crystallographic structure was resolved with a 1.6 angström resolution (**Figure 6B**). The structure shows all FemX residues, the UM5K part of the inhibitor and the three first nucleotides of the RNA part of the inhibitor, thus all data concerning the catalytic pocket of FemX were accessible.[30]

Associated with directed mutagenesis, key amino acid could be identified and an interaction map at the catalytic site could be drawn (**Figure 7**).

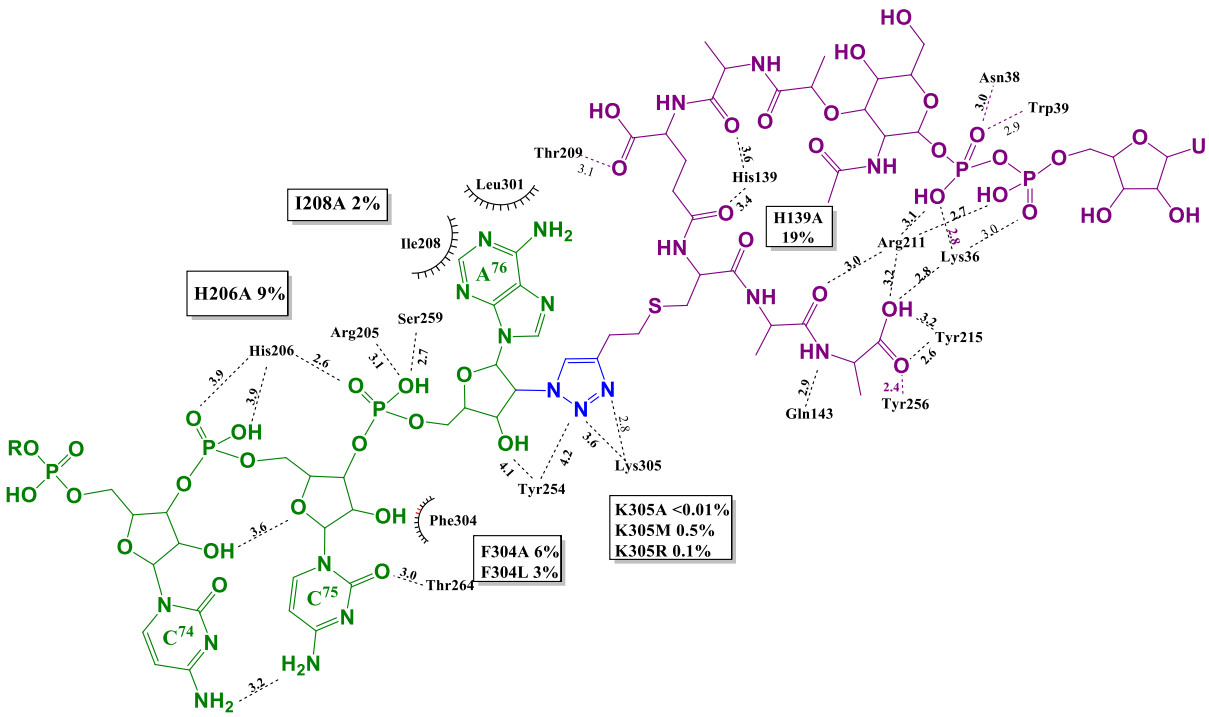

Figure 7: Interaction map of the catalytic site of $FemX_{Wv}$ in presence of the peptidyl-RNA conjugate. Frames indicate results of directed mutagenesis. Values on dashed bonds indicate inter-atomic distance in angströms.

Among all the amino acids that seem to be important for interaction with the aa-tRNA substrate we can cite:

- His206, Arg205 and Ser259 that are well-positioned to anchor the phosphodiester backbone of the 3’-end of the aa-tRNA through a hydrogen bond network.
- Ile208 and Leu301 that, when the enzyme is active, form a “sandwich” anchoring the terminal adenine nucleobase through hydrophobic interactions.

- Lys305 that is absolutely critical for enzymatic activity and that is well-positioned to interact with the 2'-born amino acid during transfer. Prof. Etheve-Quelquejeu *et al*. postulated that this Lysine residue stabilizes the oxyanion intermediate formed during aminoacyl transfer through electrostatic interaction.

3.3. *Staphylococcus aureus* FmhB, FemA and FemB.

The peptidoglycan in *S. aureus* bacterial strains naturally possesses a pentaglycine peptide interbridge cross-linking the peptidoglycan strands. Three enzymes participate in its biosynthesis (**Scheme 5**): FmhB, responsible for the ligation of the first Gly residue; FemA, responsible for the sequential addition of 2 Gly residues; and FemB, responsible for the addition of the fourth and final fifth Gly residues. FmhB (previously referred to as *Staphylococcus aureus* FemX) is coded separately from FemA and FemB, which come from the *femAB* operon, and all of them utilize Gly-tRNA^{Gly} as a glycyl donor substrate. To this day, only the crystallographic structure of the apoenzyme FemA has been resolved.[25]

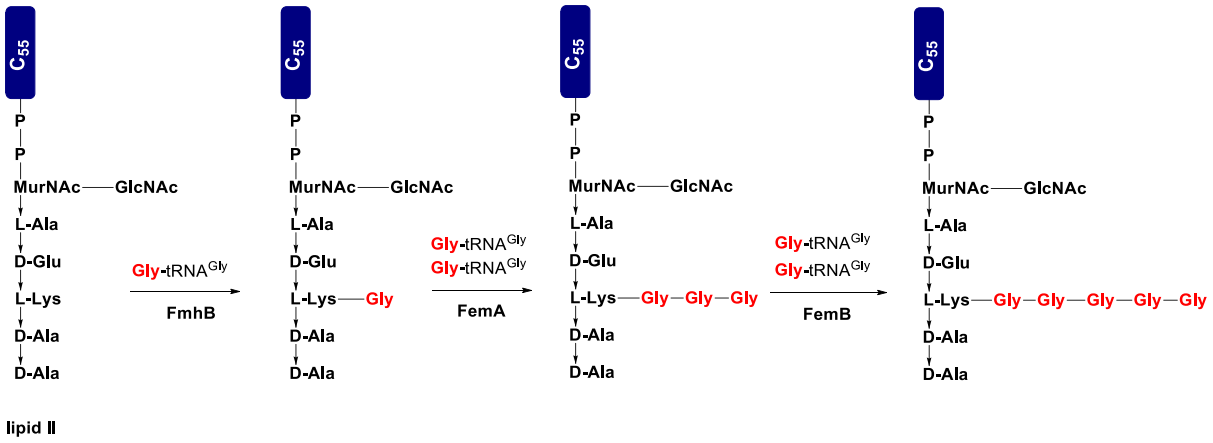

Scheme 5: Biosynthesis of the pentaglycine interbridge for *S. aureus*

Inhibition of the *femAB* operon leads to high disruption of cell viability despite some resiliency mechanisms, suggesting that no bridge is lethal, and a shortened bridge is very damageable for bacterial survival.[31]

One of the main mechanisms for methicillin resistance is the role of PBP2a, a transpeptidase that remains active in the presence of methicillin. PBP2a, however, can only function with a complete pentaglycine bridge. As a result, inhibition of the biosynthesis of the bridge is thought to be a way to restore methicillin-susceptibility to resistant strains.[32,33]

The fifth and final glycyl residue can be the point of anchoring for virulence factors.[34]

For these reasons, FmhB, FemA and FemB are considered as promising targets for inhibiting bacterial survival, restore susceptibility to known antibiotics, and decrease infection virulence. The

development of antimicrobials able to target them requires detailed structural data and better knowledge of their key interactions.

3.4. Conclusion

An overview of the FemABX family and a focus on some of its members has been presented: FemX of Weissella viridescens, used as a model for all Fem-transferases, has already been studied in the group; FmhB, FemA, and FemB, the Fem-transferases present in *S. aureus*, are therapeutically relevant targets that require investigation. The objective of the work presented herein is to synthesize compounds as tools for the study of these enzymes or as inhibitors. Because these enzymes use aa-tRNA as an amino acid donor substrate, aa-tRNA, tRNA and RNA-conjugates were used as scaffolds for the design and the synthesis of our compounds. The features of tRNAs and aa-tRNAs are presented in the following part, as well as the strategies to obtain modified RNA and aa-tRNA analogs reported in the literature.

4. tRNAs, aminoacyl-tRNAs and analogs.

4.1. Introduction

Because of their involvement in the synthesis of the bacterial cell-wall through the action of FemABX enzymes, tRNAs and aa-tRNAs are the main scaffolds used in this work, to synthesize compounds able to interact with FemABX enzymes in order to develop new antimicrobials. For this reason, this part first presents the key structural and functional features of tRNAs and aa-tRNAs. Secondly, the main methods used to artificially obtain these biomolecules will be overviewed. Finally, the different strategies aiming at the synthesis of tRNA and aa-tRNA analogs will be reviewed, as well as the aa-tRNA analogs reported in the literature.

4.2. General features of tRNA and aa-tRNA

4.2.1. Structure

Transfer RNAs (tRNAs) are small, ubiquitous, non-coding RNAs defined by their main function as interpret during translation. Structurally, they are characterized by their typical highly-organized secondary and tertiary structures and their high content in modified nucleobases in the nucleotide sequence and post-transcriptional modifications (*cf* Part 4.1.3.). Base-pairings are responsible for the "clover-leaf" secondary structure (**Figure 8A**) that allows to clearly distinguish:[35]

- The acceptor arm, with the 3-terminal CCA sequence onto which is attached the appropriate aminoacid to form aa-tRNA.
- The T-loop, also named the TψC arm as it contains an unusual Thymine (T) followed by a characteristic pseudouridine (ψ).
- The D-arm.
- The anticodon arm, bearing the trinucleotide sequence corresponding to the appropriate mRNA codon.
- The variable arm, which, as its name indicates, is a source of variability in shape and size.

X-ray crystallography indicates that bacterial tRNA can also adopt an L-shaped tridimensional tertiary structure (**Figure 8B**), as a result of interaction between modified nucleobases on the different arms.

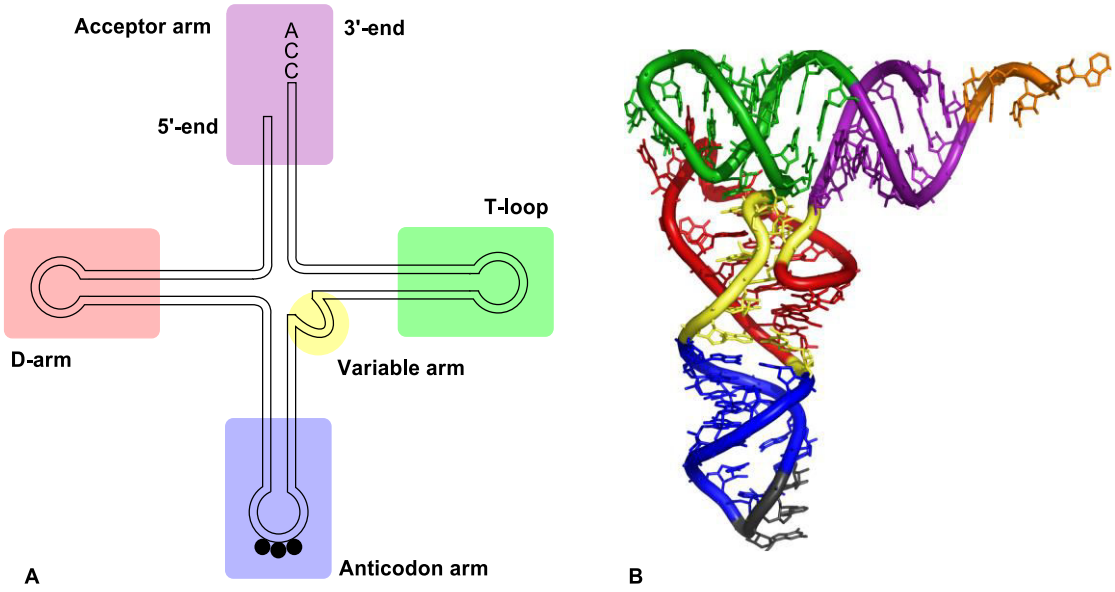

Figure 8: **A:** Secondary "clover-leaf" structure of tRNA. **B:** Tertiary structure of tRNA. D-Arm is represented in red, anticodon arm in blue, acceptor arm in purple, variable arm in yellow and T-loop in green.

4.2.2. tRNA modifications

tRNA modifications are primordial steps of tRNA maturation, roles, and degradation, and they are responsible for the high molecular diversity of tRNAs. Over a 100 modifications are reported in the literature,[36] a majority of which are located in the anticodon loop. It is estimated that 1 to 10 percent of a given genome encode for enzymes involved in the tRNA-modification processes, greatly outnumbering the number of genes encoding for tRNA themselves[37]. Hence, the tRNA modifications are the subject of great investigation for their implication in gene expression,[38] response to cellular stress,[39] or disease.[40]

Modifications in the anticodon loop, especially at position 34 (anticodon) and 37 (anticodon-adjacent) are of the highest importance for proper mRNA decoding and adequate aminoacylation by aa-tRNA-synthetases. Modifications in the other stems are most capital for the structure and stability of the tRNA.

The modifications of tRNA are too numerous to be exhaustingly reviewed here, but the most frequent ones are:[35]

- Pseudouridine (ψ): pseudouridylation of the tRNA is performed by pseudouridine-synthases, a group of 4 families: TruA, TruB, TruD and RluA. The extra-hydrogen bond at position 5 of the nucleobase is key for interaction with the ribosome. This modification is present, of course, in the TψC arm (or T-loop) but can also be found in the other stems.

- Methylation (m): methylation of the nucleobases, by steric hindrance or charge-introduction can induce significant structural changes. Methylation can also occur at the 2'-position of the ribose, thus protecting the tRNA against degradation and increasing its stability.
- Dihydrouridine (D): this reduced form of U, yielded by the action of dihydrouridine synthases, is notably present in the D-arm, to which it gave its name. It is responsible for an increase in stability as well as it affects the flexibility and conformation of the tRNA molecule. It is interesting to note that D levels are increased in cancerous tissues.

4.2.3. The life of a tRNA

4.2.3.1. tRNA biogenesis

The first step of tRNA biogenesis is the transcription of the tRNA genes by RNA Polymerase III[41]. In bacteria, these genes are found in cistrons, associated together and/or with protein-coding regions. In eukarya, they appear as dispersed units across the linear genome, but they are often physically clustered in a close localization to the nucleolus,[42] along with ribosomal RNA, thus forming a functionally consistent unit that can be mobilized for translation.[41]

4.2.3.2. tRNA maturation

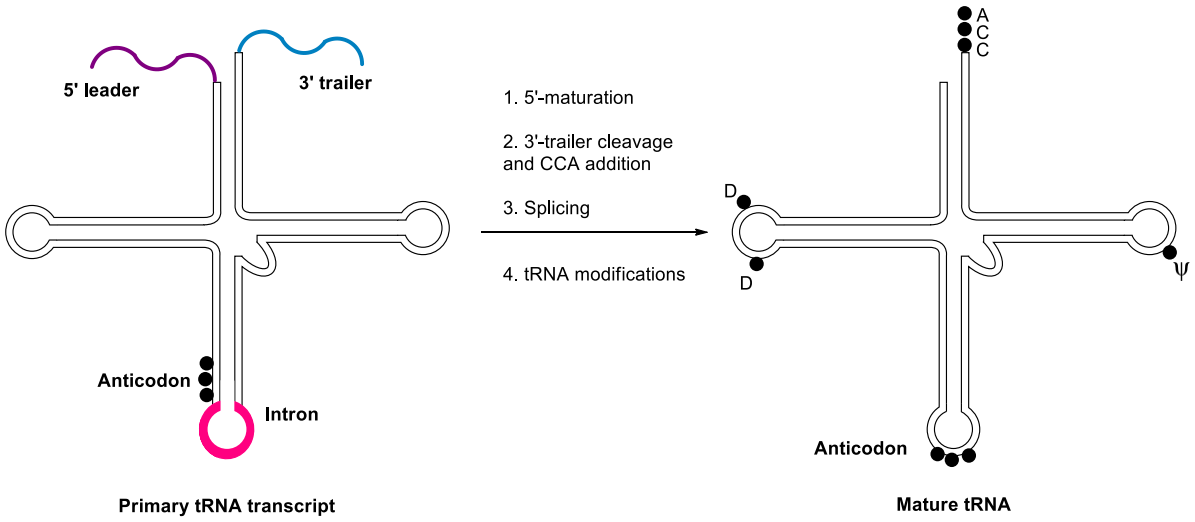

Scheme 6: Representation of the tRNA maturation process

The tRNA transcript is still immature as it contains fragments that are not found in functional tRNA (**Scheme 6**): a 5'-fragment referred to as the 5' leader sequence, a 3'-fragment referred to as the 3' trailer and, in some cases, introns, *ie* non-coding sequence, that have to be removed.

The 5' maturation involves cleavage of the 5' leader sequence by the RNase P complex.[43] In bacteria, RNase P is a ribonucleic particle consisting of protein RnpA and RNA RnpB,[44] which solely manages the

catalytic activity, making it a true ribozyme that cleaves RNA through Mg^{2+}-dependent phosphodiester bond-breaking.

The 3' maturation can happen through two mechanisms depending on the presence of the 3'-terminal CCA sequence. If it does, the 3' trailer is cleaved either by the sequential action of endonuclease (RNase E) then exonucleases (RNase T, RNase PH), or directly by the endonuclease tRNase Z. If the tRNA does not possess the CCA sequence, the 3' trailer is completely removed by tRNAse Z, and the CCA trinucleotide is then added by nucleotidyltransferases referred to as "CCA-adding enzymes" using CTP and ATP as substrates.[45] It is interesting to note that tRNase Z enzymes are metallo-endonucleases that structurally belong to the family of metal-containing beta-lactamases.[46]

The splicing process, *ie* the removal of introns, of tRNA is enzymatically distinct from mRNA splicing. Introns are generally short (14 to 60 nucleotides) and located in the anticodon loop. In Eukarya and Archaea, they are removed by endonucleases. TRNA ligase and 2'-phosphotransferase finish the process. In Bacteria, introns are self-splicing with no enzymatic involvement whatsoever. Modifications are crucial for maturation of tRNAs. They can appear either inside or outside the nucleus.

4.2.3.3. Nuclear export

The properly maturated tRNAs can travel toward the cytoplasm where they can take on their roles. Nuclear export is a selective process in which only mature tRNAs are allowed to leave the nucleus. The export is mediated by the exportin-t receptor, which interacts with secondary structures within the tRNA.[47] Adequate tRNAs form exportin-t/tRNA/Ran-GTP complexes that travel through nuclear pores into the cytoplasm, where hydrolysis of GTP causes the complex to dissociate into Ran-GDP, free exportin-t and exported tRNA. The exported tRNAs can then be aminoacylated by aa-tRNA-synthetases (*cf* Part 4.1.4.) and take on their roles (*cf* Part 4.1.5.).

4.2.3.4. tRNA cleavage

Mature tRNA are extremely stable, with half-lives from hours to days. Misprocessed or hypomodified tRNAs are degraded by exonucleases.[48] Cleavage of tRNAs is a drastically different process: under stress conditions, endoribonuclease-mediated cleavage of mature and functional tRNAs appear to have signaling functions. The fragments generated by these cleavages, generally in the anticodon loop, are now known to be responsible for reducing translation or activating genes for stress-response.[49,40] These processes add themselves to the previously known role of tRNA as sensors of amino acids depravation and translation modulators.[50,51,52]

For most of their biological duties, tRNAs act as amino acids donors in the form of aa-tRNAs. The biogenesis and the roles of aa-tRNAs will now be presented.

4.2.4. Aminoacyl-tRNA

4.2.4.1. Aminoacyl-tRNA biosynthesis

The aminoacylation of tRNAs is performed by highly specialized enzymes referred to as aminoacyl-tRNA-synthetases, or aaRS. Canonically, one aaRS exists for each amino acid. This aaRS is able to recognize and aminoacylate only the tRNAs bearing the cognates anticodons for this one amino acid, which are plural due to the genetic code degeneracy.

Mechanistically, this process takes place in two steps: first, the amino acid and ATP are bound to the aaRS which catalyzes the phosphorylation of the amino acid. The subsequent phosphorylated amino acid remains bound to the aa-RS for the second step in which the tRNA is recruited by the enzyme to see its 3'-terminal position aminoacylated.

Some organisms do not encode an aa-RS for every amino acid; in those cases, access to the corresponding aa-tRNA is achieved by enzymatic modification of other aa-tRNA. For example, many Archeae lack Gln-RS and Gln-tRNA^{Gln} is obtained from Glu-tRNA^{Gln}, which is itself synthesized by a non-discriminating Glu-RS. A similar process allows the formation of Asn-tRNA^{Asn} from Asp-tRNA^{Asn} in the Gln-RS-lacking prokaryotes.[53] Another example of indirect aa-tRNA formation is the case of the rare seleno-cystein tRNA Sec-tRNA formed upon modification of the Cys-tRNA.[54]

4.2.4.2. The tRNA identity problem

For their purposes in translation, tRNAs must all be able to interact similarly with the A- and P-site in the ribosome, thus they must possess close structural features. However, every group of tRNA decoding for one given amino acid must be selectively aminoacylated by the correspond aa-RS, meaning that every one of the 20 groups of tRNAs must be able to be adequately identified by the one among 20 corresponding aa-RS, thus suggesting necessary structural differences. This paradox is known as the tRNA identity problem.

Both *in vitro* and *in vivo* assays lead to the understanding that aa-RS rely on positive and negative recognition signals to selectively aminoacylate the cognate tRNAs.[55] These recognition elements are mainly but not only situated in the amino acid acceptor region and the anticodon loop and are now heavily documented.[56,57,58]

Among the positive identity elements, many are situated in the amino acid acceptor region, which is coherent with this region being at the active site of the aa-RS. The most convincing argument is the possibility to replace a whole tRNA by a mini or microhelix mimicking the acceptor arm of the tRNA, and still have them correctly aminoacylated by aa-RS. This possibility was reported for both class I – Ala,[59] His,[60] Gly,[61] Ser,[62] Asp[63] – and class II – Met,[64] Ile,[65] Gln,[66] Val[67] – aa-RS. Such scaffolds thus are

useful tRNA mimics for studies of tRNA-related processes.[58] The most notable identity features are the nature of the base 73 and the 3-70 base pair.

Some positive recognition elements are situated in the anticodon region, which, although it is situated 75 angströms away from the active site of aa-RS, still holds many identity elements for almost all tRNA families. Notable exceptions are the tRNA families for Ser, Leu, and Ala as, due to the genetic code degeneracy, they respectively recognize six, six and four anticodons and thus already bear diversity at this region. Instead, the long variable arms of $tRNA^{Ser}$ and $tRNA^{Leu}$ bear recognition elements.

Global 3D arrangement and folding can be an identity element, ruled by critical base pair such as the 15-48 interaction – eg $tRNA^{Cys}$ in *E. coli*,[68] and the folding between the D and T loops can create a tridimensional variable pocket important for recognition – eg $tRNA^{Arg}$ and $tRNA^{Phe}$ in *E. coli*.[69]

Base modifications play a relatively unimportant role in the tRNA identity. When they do, they are situated in the anticodon loop and are also crucial to anticodon recognition. In addition, they can be discriminating elements.[70]

4.2.5. Involvement of tRNAs and aa-tRNAs in biological processes

4.2.5.1. In the ribosome: the translation process

Translation is the process during which the messenger RNA (mRNA) is translated into a polypeptide chain. Aa-tRNAs function as translators as their nucleotide sequence bear an anticodon sequence, specifically complementary to the codon to translate, and they also bear the cognate amino acid.

The translation process is carried out in the ribosome, and can be divided into three major steps: initiation, elongation, and termination. The ribosome is a ribonucleoprotein particle composed of ribosomal RNAs (rRNA) and protein assembled in the nucleolus. Though similar in structure in prokaryotes and eukaryotes, eukaryotes possess larger and more complex ribosomes. In Bacteria, for example in *E. coli*, it is a spheroid particle of 250 A in size and 25 kDa in molecular weight, and consists of one third protein and two thirds rRNA. It can be separated into two subunits, the small one that sediments 30S (thus called the 30S subunit) and the large one, referred to as the 50S subunit. The two subunits assemble around the mRNA for translation, forming a 70S ribosomal complex. The ribosome possesses three tRNA-biding sites: The A-site (for interaction with the aminoacylated tRNA), the P-site (for interaction with the peptidyl-tRNA) and the E site (for the deacylated tRNA before it departs from the ribosome).

The translation initiation requires numerous factors, which differ between prokaryotes and eukaryotes. In eukaryotes, the initiator Met-tRNA, the ribosome and no less than 12 multisubunit complexes are associated to the 5'-cap of mRNA to initiate the translation process. In bacteria, the

three initiation factors IF1, IF2 and IF3 allow binding of the initiator formyl-Met-tRNA^{i} with the ribosome and the mRNA. In some cases, mostly for viruses, the translation can be initiated in a 5'-cap-independent fashion through the presence of IRES (Internal Ribosome Entry Sites), which are highly structured internal mRNA sequences able to recruit the ribosomal machinery.

The elongation step is quite similar between the three reigns. The process begins with the initiator Met-tRNA in the P site, with a vacant A site. The aa-tRNA corresponding to the following amino acid then forms a complex with GTP and the elongation factor – eEF1A in Eukarya and EF-Tu in Bacteria – and enters the A site, where complementarity between the codon and anticodon can occur. This interaction causes GTP to be hydrolyzed by the elongation factor and dissociation of the complex, leaving the free aa-tRNA in the A site. Peptide bond formation can occur between the amino group of the aa in the A site towards the ester-activated carboxyl group of the Met in the P site, thus forming a Met-aa-tRNA in the A site and a deacylated initiator tRNA in the P site. The peptidyl-transferase activity is carried out by coordinated action of ribosomal proteins and rRNA in the ribosome center. The deacylated initiator tRNA moves to the E site. Another elongation factor – eEF2-GTP in Eukarya, EF-G in Bacteria – assists the departure of the initiator tRNA from the E-site and the transfer of the dipeptide-tRNA toward the P-site, leaving the A-site vacant. The following aa-tRNA can enter the A-site as described above, and the cycle of polypeptide chain elongation can go on.

When there is a stop-codon in the A site, it is recognized by release factors – that, again, differ significantly between the three reigns – and promote the release of the polypeptide chain from the tRNA in the P site.

The ribosome with a deacylated tRNA in the A or E site and still associated with mRNA is then recycled by dissociation of the complex by a variety of ribosome release factors (RRF).

4.2.5.2. Outside the ribosome

Aa-tRNAs are also involved as amino acid donors in many non-ribosomal biological processes:[71]

- Glu-tRNA^{Glu} is part of the biosynthesis of porphyrins.[72]
- Aminoacylation of the bacterial cell wall phosphatidyl glycerol requires aa-tRNA.[73]
- Cyclodipeptide synthases (CDPS) are aminoacyl-tRNA-dependent enzymes for the biosynthesis of cyclodipeptides in many organisms.[74,75,76]
- Some natural nucleosidic antibiotics are biosynthesized using aa-tRNA.[77]
- N-end tagging of protein by amino acids and subsequent degradation is an important process mediated by transferases using aa-tRNA as substrates, e.g. the L/F transferase.[78,79,80]
- The cross-linking of peptidoglycan in many Gram-positive bacteria and some Gram-negative bacteria is ruled by the FemABX family, or Fem-transferases (*cf* Part 3).

Because of their numerous roles in vivo, researchers have developed methods to artificially obtain nucleic acids in general and tRNA in particular. The two main approaches, enzymatic and chemical synthesis, will now be presented.

4.3. Synthetic methods to obtain tRNAs

4.3.1. Enzymatic methods

Like other RNAs, tRNAs can be obtained through *in vitro* transcription of the complementary DNA (cDNA) by a RNA polymerase. A suitable cDNA template must be preceded by a promoter recognized by the chosen RNA polymerase, and be properly framed by ATG and stop codons.

The use of RNA ligases allows ligation of previously synthesized RNA sequences. These are particularly suitable for hemisynthetic strategies in which chemically synthesized oligoribonucleotides, modified or not, can be ligated into large RNA sequences.

4.3.2. Chemical methods

4.3.2.1. Principle for solid-phase synthesis of nucleic acids

Chemical synthesis of nucleic acids, as other biopolymers, is based on the use of modified monomers bearing a reactive function in either the 3' or the 5' position and a protected function in the 5' or 3' position. Coupling and deprotection steps allow elongation of the polymer, and final orthogonal deprotection of the other functional groups – phosphates and nucleobases – yield the final synthetic nucleic acid.

Attachment of the first monomer onto a solid support and elongation of the chain on this support allowed more convenient synthesis techniques, better yields and automation of the process for maximal efficiency.

4.3.2.2. Towards solid-phase phosphoramidite chemistry

Ever since the discovery of the structure of nucleic acid, nucleic acid chemists have developed methods to obtain quickly and efficiently the natural 3'-5' phosphodiester linkage between nucleotides.[81,82] The first reported method in 1955 was from Michelson and Todd,[83] with a phosphate diester approach. Exploration of phosphate diester,[84] then phosphate triester[85,86,87,88] and phosphite triester[89,90] approaches allowed to obtain oligonucleotides with better yields,[91] more convenient reaction conditions and suitable nucleosidic buildings blocks. Progress in automation and the use of solid-support such a silica[92] or controlled-pore glass (CPG)[93] allowed to initiate solid-supported automated oligonucleotide synthesis.

The development of phosphoramidite nucleosides[94] allowed to improve the overall stability of the building blocks. Improvement of the chemical features[95,93] of the method and automation made

phosphoramidite chemistry the method of choice for the synthesis of oligonucleotides and oligoribonucleotides.[96,97]

4.3.2.3. The solid-phase synthetic process for RNA

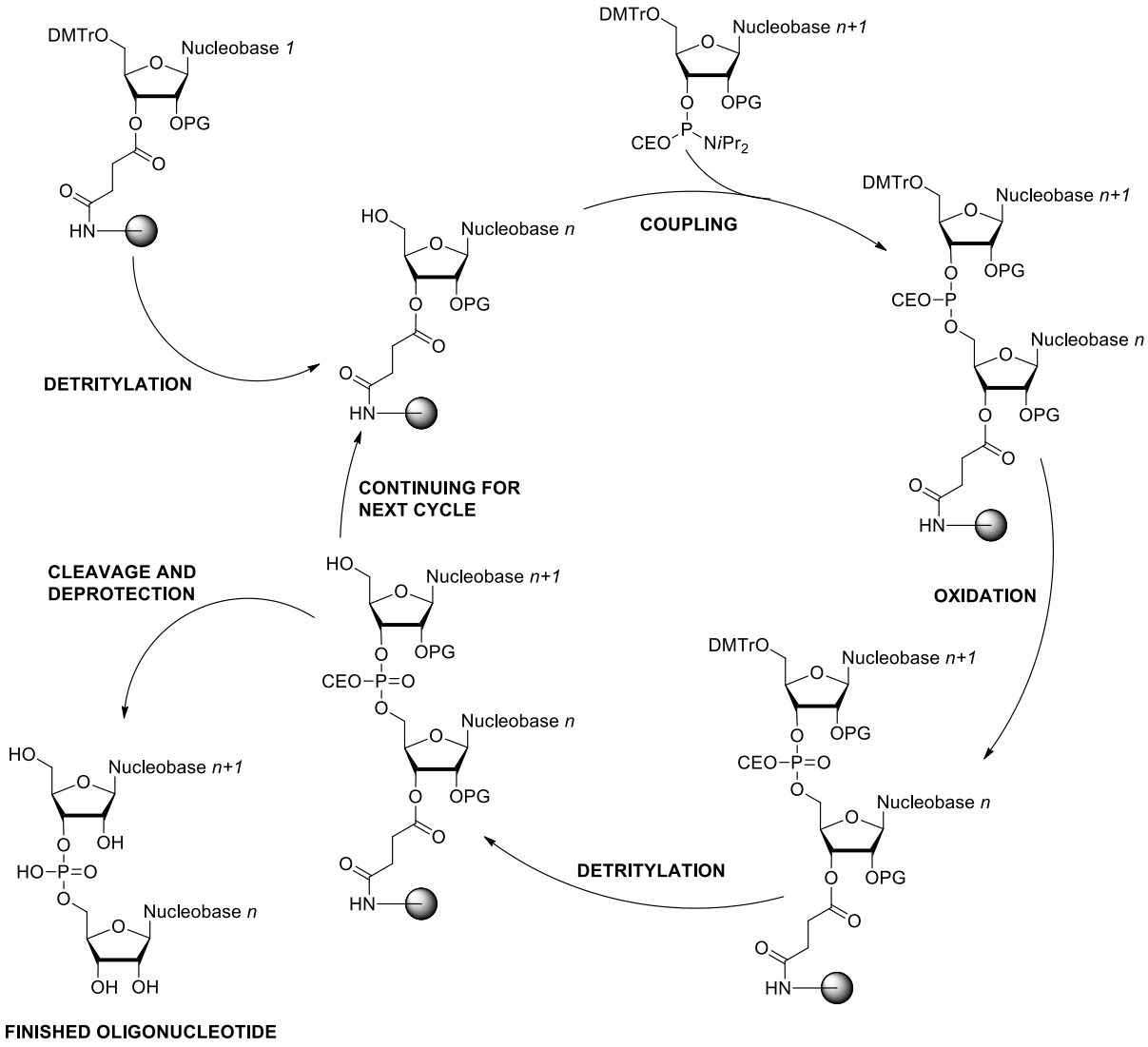

Scheme 7: Typical phosphoramidite-mediated solid-phase oligoribonucleotide synthesis cycle

A classical phosphoramidite synthetic cycle usually takes place as follows (**Scheme 7**):

1. A solid-support functionalized with 5'-DMTr protecting group is deprotected by trichloroactic acid.
2. Addition of the following nucleotide phosphoramidite, which, when activated by a weak acid such as tetrazole, is attacked by the 5'-deprotected nucleotide to form the linkage.
3. Oxidation of the phosphorus (III) into phosphorus (V) leads to a proper phosphodiester linkage. A typical oxidant is aqueous iodine.

4. Detritylation of the 5'-terminal nucleotide leads back to the first step and allows to continue elongating the sequence.

When the sequence has been correctly synthesized, deprotection, solid-support cleavage, and purification yield the desired oligonucleotide.

This process is identical for DNA synthesis, without, of course, protecting groups for the 2'-position.

The classically used protecting groups are:

- The dimethoxytrityl group for the 5'-OH: rapidly deprotected in the presence of TCA, its cleavage leads to the dimethoxytrityl cation which is orange and is used for evaluating couplings yields.
- The cyanoethoxy group (CEO) for the phosphate: deprotected in basic conditions to generate the appropriate final phosphate.
- The nucleobases that require protection (G, A, C) are generally protected with basic-labile groups to limit the number of deprotection steps.

Compared to DNA synthesis, the main challenge of RNA solid-phase synthesis is the handling of the 2'-OH that is absent in DNA. Thus RNA chemistry has been developed and evolved in parallel with DNA chemistry[98] with some adjustments. It requires a protecting group that does not prevent efficient coupling of the vicinal 3'-phosphoramidite, does not migrate, and can be deprotected in conditions compatible with the process. Overall instability of RNAs can also make the deprotection and purification steps more challenging than for DNA. The most commonly used protecting groups for the 2'-OH are (**Figure 9**):

- Silylated groups such as *tert*-butyldimethylsilyl (TBS) or tri-*iso*-propylsilyloxymethyl (TOM). TOM can be preferred to TBS due to less steric hindrance thanks to the linker. Deprotection steps proceed with sources of fluoride such as tetrabutylammonium fluoride (TBAF) or fluorhydric acid – trimethylamine (NEt_3.3HF).
- The thiomorpholine-4-carbothioate (TC) group. It has the advantage to be deprotected in basic conditions as well as the nucleobases, thus providing a deprotection step-economy. Typical deprotection proceeds with anhydrous ethylenediamine (EDA) solution.
- The bis(2-acetoxyethoxy)methyl (ACE) group, which is acid-labile. In that case, the 5'-DMTr group must be replaced by silylated group so that the 2' and the 5' remain orthogonally protected. Deprotection can also proceed first by deacylation in basic conditions, usually during nucleobase deprotection, and subsequent acidic treatment. In addition to excellent coupling yields, the advantage of ACE is the possibility to purify the oligo with the ACE and to

store it protected, and thus resistant to RNAses, with very quick and clean deprotection steps immediately prior to use.

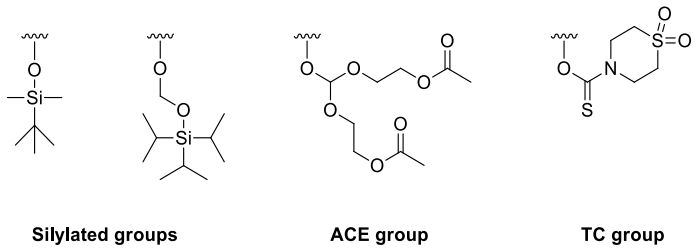

Figure 9: Chemical structure of the groups used for 2'-OH protection during RNA synthesis

Leaning on those efficient methods to obtain tRNAs, researchers have developed the synthesis of tRNA and aa-tRNA analogs in order to study the biological processes involving tRNAs and aa-tRNAs. The different approaches and the pros and cons of the different oligomerization methods will now be presented.

4.4. tRNA and aa-tRNA analogs

4.4.1. Pre- or post-synthetic approach

The study of biological processes involving tRNAs and aa-tRNAs has required the synthesis of analogs possessing useful analytical tags, enhanced stability, and unusual reactivity. These features generally related to a chemical modification incorporated in a nucleoside. The synthesis of such modified tRNAs and aa-tRNAs can proceed according two main approaches: the pre- and post-synthetic approaches.

In the pre-synthetic approach, access to the modified analogs is carried out by, first, the synthesis of a modified nucleoside, and then its incorporation into an RNA sequence through various oligomerization methods yielding the final tRNA analog. In the post-synthetic approach, the modification born by the nucleoside is light but has the ability to react selectivity in later steps.

After oligomerization, chemoselective modification on the full tRNA analog allow the functionalization of the RNA with the desired motif of interest. (**Scheme 8**).[99,100]

The pre-synthetic methods, though more straightforward, have the following drawbacks:

- Large amounts of modified nucleoside are often needed.
- The modification can be either not orthogonal to the oligomerization methods or too bulky, preventing efficiency.
- Access to unstable motifs or molecular diversity is difficult.

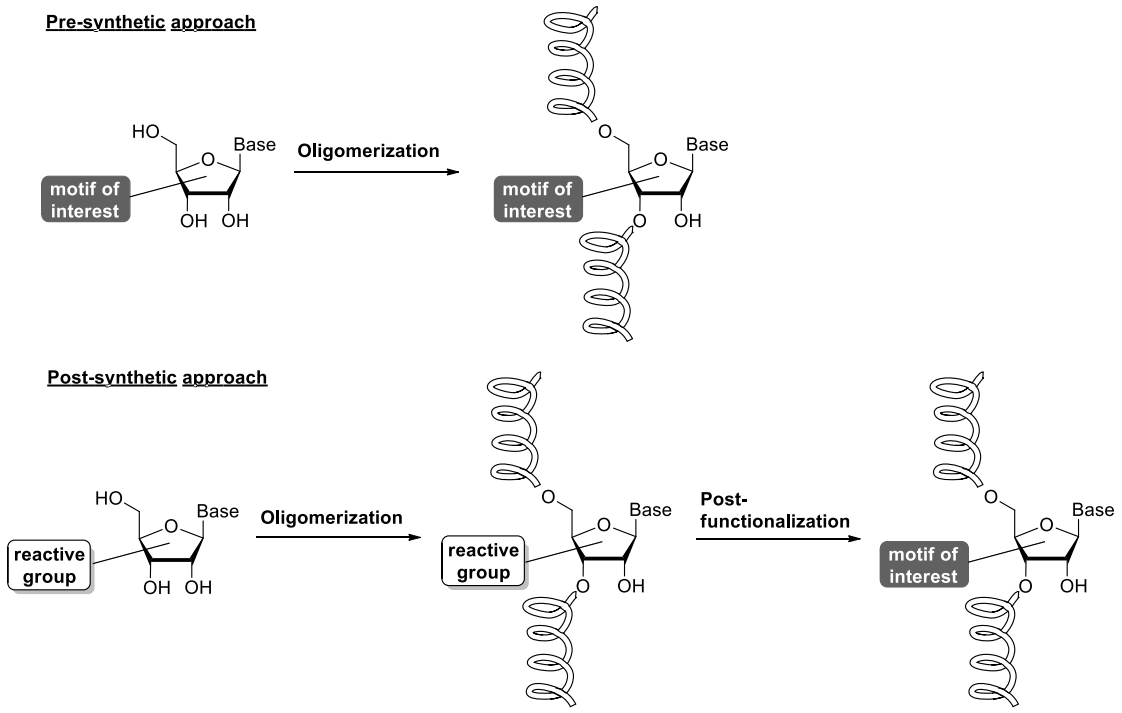

Scheme 8: Differences between the pre- and post-synthetic approaches for the synthesis of modified analogs

The post-synthetic methods allow chemoselective and site-specific modification and incorporation of a wide variety of motifs. However, chemistry on tRNA-like biomolecules can be challenging and remains little studied in comparison, for example, to peptide chemistry.

4.4.2. Choice of oligomerization methods

The incorporation of a modified nucleoside or nucleoside analog requires that the modification is well-tolerated by the chosen oligomerization method. The oligomerization method will also be different whether the modification is intended to be internal or terminal (**Scheme 9**).

Enzymatic synthesis through the use of RNA polymerases requires, first of all, the use of nucleotide triphosphates, the synthesis of which can be very challenging and not always compatible with the desired modification. The nucleotide analog must remain similar enough to the natural nucleotides

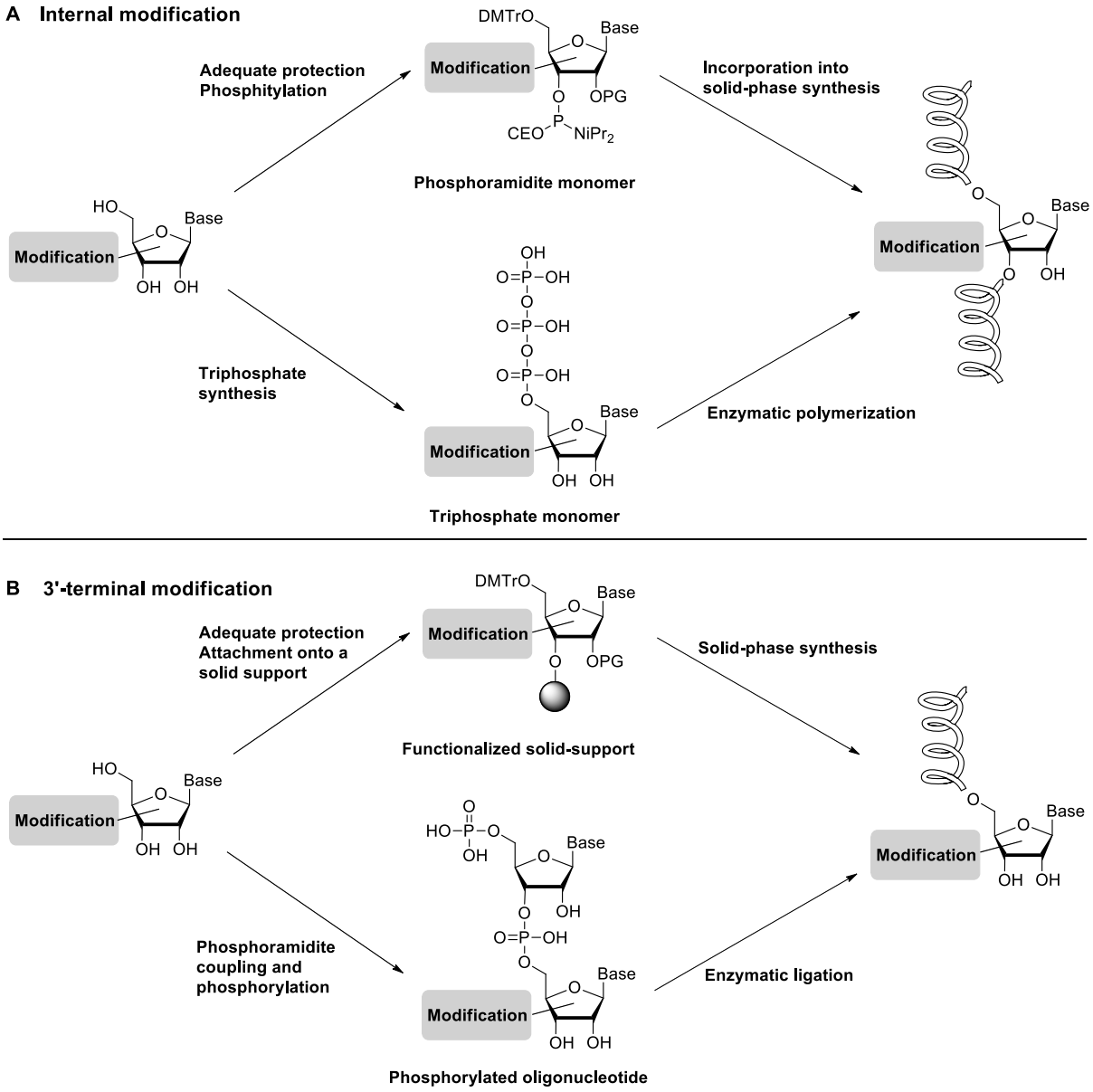

Scheme 9: Oligomerization methods and their requirements to yield modified RNA. **A:** Internally modified RNA. **B:** 3'-terminally modified RNA

in order to be correctly and efficiently incorporated into the polymerization process, thus interacting correctly with the complementary template and being well-recognized by the polymerase. Enzymatic incorporation can be interesting, for example, for the complete replacement of a natural nucleobase. It is however not ideal to incorporate one unique modification at a specific position.

Chemically-synthesized nucleic acids are generally obtained through solid-phase synthesis (SPS) using phosphoramidite chemistry. The modification must not interfere with the SPS reagents and conditions. The nucleoside analog is thus required to be either inert or orthogonally protected towards the SPS reagents and conditions. They must bear the correct functional groups, meaning a dimethoxytrityl

protecting group in the 5'-position and the phosphoramidite functional group in the 3'-position, the introduction of which can be, again, challenging. In the case of analogs for the 3'-terminal nucleoside for tRNA analog, the nucleoside must bear the DMTr group in the 5' and be grafted onto the solid support previous to the automated synthesis.

Mixed syntheses can also be carried out, in which short sequences bearing modifications are synthesized through chemical ways, and then ligated *via* RNA ligases resulting in longer sequences obtained by enzymatic polymerization.

These general approaches have been used by researchers to obtain analogs for tRNA and aa-tRNA. Because aa-tRNAs are substrates of Fem-transferases and the main scaffold used for the design of our compounds, we will now review the examples of aa-tRNA analogs reported in the literature and their syntheses.

4.5. Known aa-tRNA analogs

Most of the aminoacyl-tRNA analogs reported in the literature share some common features: they all possess an unmodified adenosine core mimicking the 3'-terminal adenosine of the tRNA. Most of them also comprise an oligoribonucleotides mimicking either the acceptor arm of the tRNA or the full tRNA. A general natural scaffold is the one of puromycin, a natural aminonucleoside antibiotic isolated in from *Saccharomyces alboniger* (**Figure 10**). Most groups took part in the synthesis of both substrate analogs able to transfer amino acids as natural tRNA, and stable non-transferring or non-hydrolysable analogs that can act as inhibitors of the studied enzyme. Finally, a major part of the effort was invested for the study of the ribosomal peptidyl-transferase and the translation pathway in general. Here is presented an overview of the reported analogs, their chemical features and their syntheses.

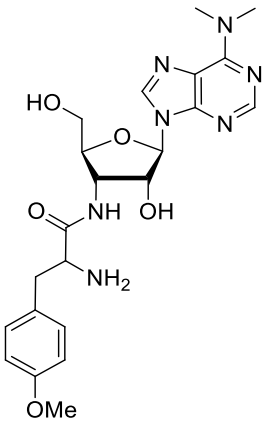

Figure 10: Chemical structure of puromycin

4.5.1. First analogs for the substrate of the ribosomal peptidyl-transferase.

The ribosomal peptidyl-transferase is a ribonucleoprotein catalyzing the transfer of the growing peptide born by the tRNA in the P-site onto the amino acid loaded on the aminoacyl-tRNA in the A-site. In 2000, Nissen *et al.* reported the use, for structural studying purposes, of two analogues for the aminoacyl-tRNA and for the reactional intermediate. The first one is a tRNA-like minihelix aminoacylated similarly to the puromycin in the 3'-position. The second one is a phosphoramidate conjugate between puromycin and a CCA trinucleotide (**Figure 11**).[101]

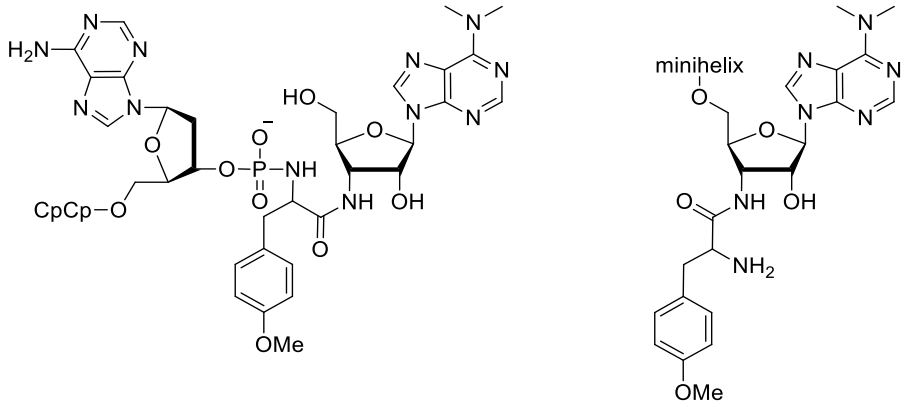

Figure 11: Chemical structures of two puromycine-derived peptidyl transferase substrate analogs

The synthesis of a similar aminoacylated CCA trinucleotide was reported in 2002 by Zhang *et al.* Chemical synthesis of a 3'-phenylalanyladenosine monomer preceded solution-phase phosphoramidite coupling to yield the functionalized trinucleotide (**Scheme 10**).[102]

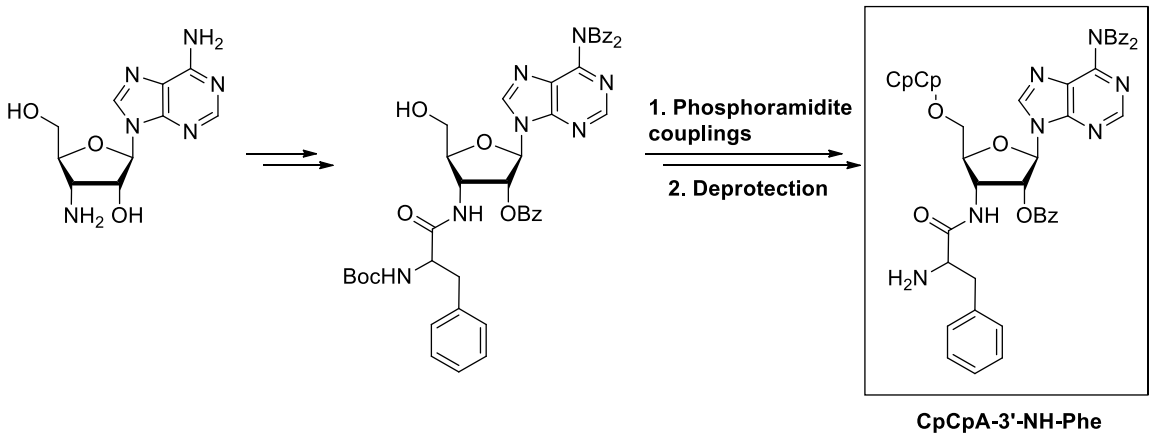

Scheme 10: Synthesis of 3'-phenylanalyl-trinucleotide

The group of Strobel described the syntheses of several analogues. In a similar strategy, a 3'-biotinylated CCA trinucleotide was synthesized (**Scheme 11**).[103]

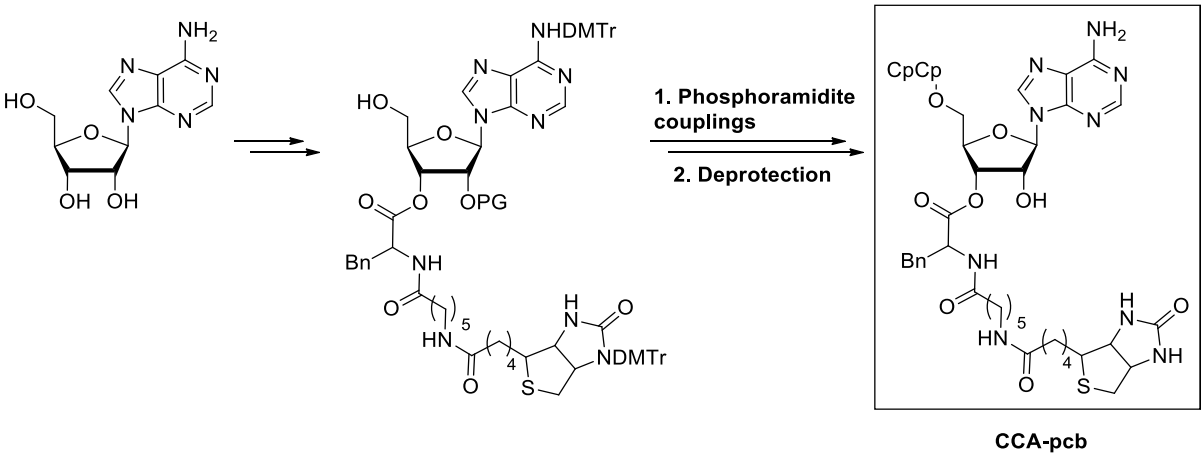

Scheme 11: Synthesis of 3'-biotinylated-trinucleotide

Transition state analogues were also synthesized, using phosphate or phosphoramidate oligo-oligo conjugates (**Figure 12**). These compounds allowed to study the stereochemistry of the peptidyl transferring in the ribosome.[103,104,105,106]

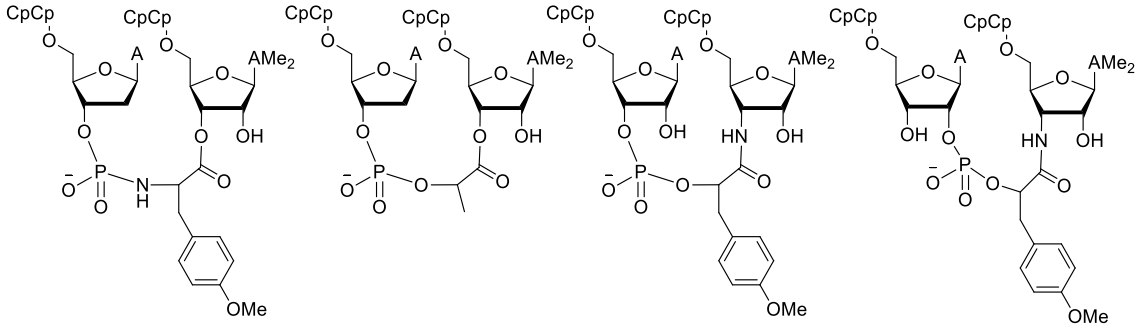

Figure 12: Chemical structures of phosphoramidate and phosphate oligonucleotides conjugates

4.5.2. Puromycine analogs

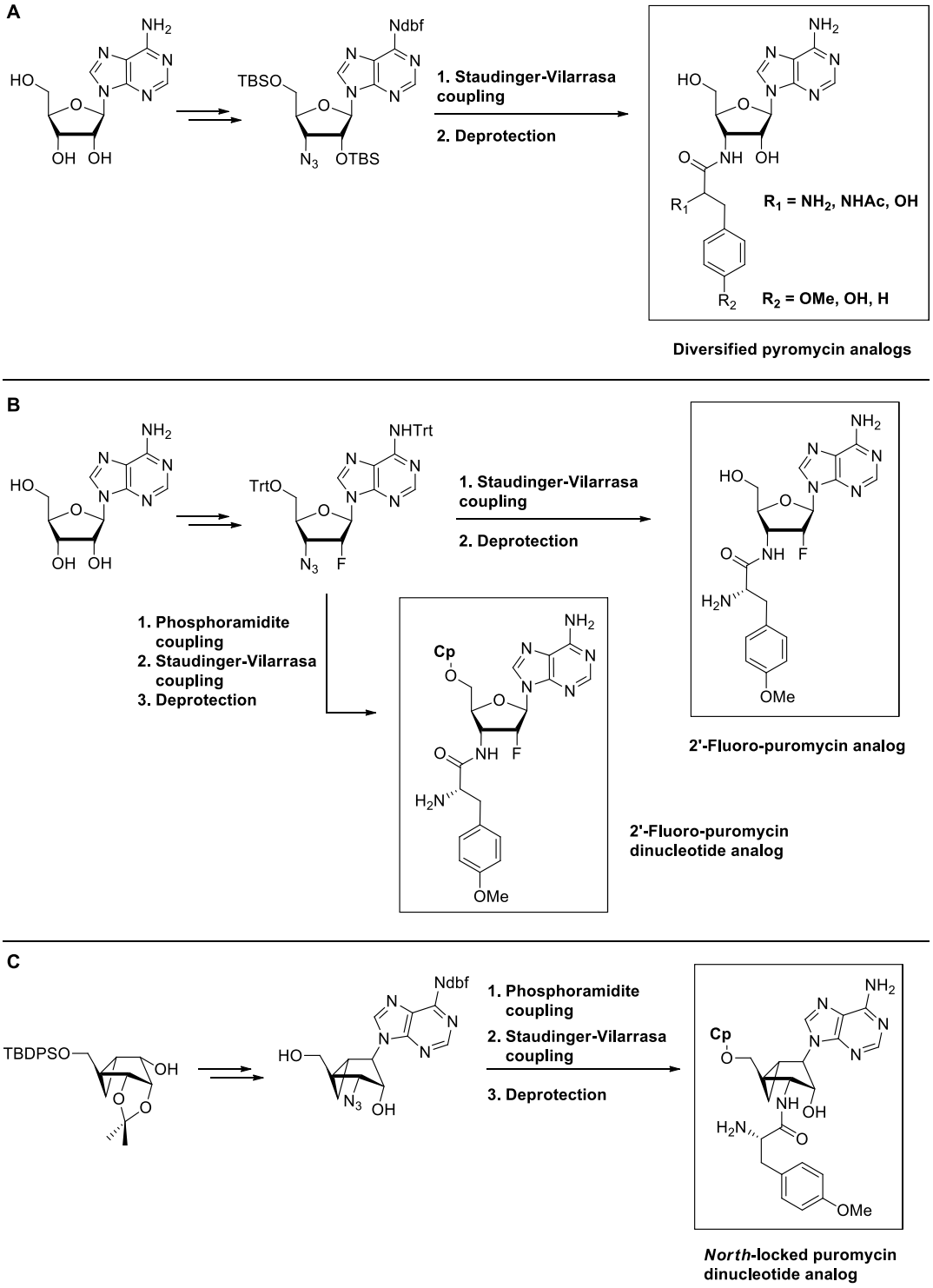

Scheme 12: Synthetic routes to puromycin analogs developed by Strazewski *et al.* **A:** Puromycin analogs with molecular diversity. **B:** 2'-fluorinated puromycin analog (di)nucleotide. **C:** *North*-locked puromycin dinucleotide analog.

The group of Strazewski reported the syntheses of several analogs of the puromycin as tools for the study of translation-related processes (**Scheme 12**). Analogs with molecular diversity in the 3'-position

were synthesized,[107] and methodological and mechanistic studies were carried out in the process of obtaining these analogs *via* Staudinger reactions; for these purposes, fluorinated analogs were synthesized.[108] Eventually, the investigation of the role of the terminal adenosine sugar ring conformation became possible through the synthesis of a *North*-locked analogues of puromycin.[109]

4.5.3. Hemisynthetic (mis)acylated tRNAs

The group of Hecht reported the hemisynthesis of aa-tRNA and misacylated aa-tRNAs[110,111,112] relying on the following strategy (**Scheme 13**): first, the chemical synthesis of a phosphorylated dinucleotide. The dinucleotide can then by acylated. This acylated dinucleotide can be recognized by an RNA ligase to introduce the desired RNA sequence.

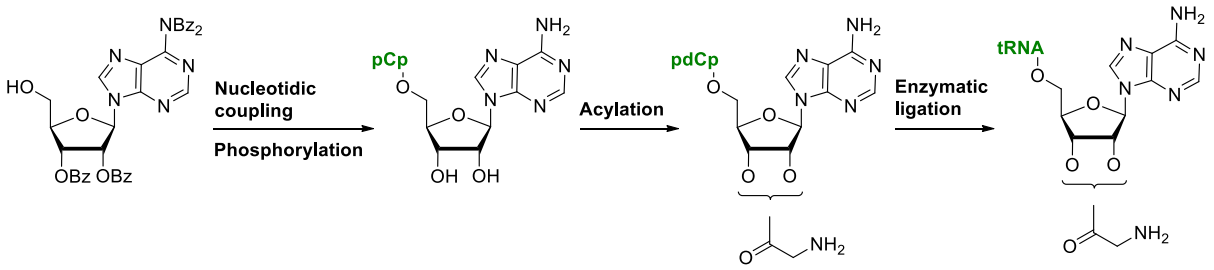

Scheme 13: Synthetic strategy of Hecht *et al.* for artificial aa-tRNAs

This method allows the synthesis of a wide variety of aa-tRNA analogs bearing modifications on the terminal A76.

4.5.4. 3'-peptidyl-RNA conjugates to study the translation process.

The group of Micura reported the synthesis of numerous analogs for aminoacyl-tRNA in the form of peptidyl-RNA conjugates relying on both solid-phase nucleic acid and peptide syntheses, and applying peptide chemistry techniques to RNA-peptides conjugates.[113-115]

Starting from functionalized 3'-azido-3'-deoxyadenosine, solid-phase synthesis, post-functionalization and enzymatic ligation led to non-hydrolysable aminoacyl-tRNA, for example fMet-tRNA^{fMet} with an amide bond instead of the natural ester bond (**Scheme 14A**).[113] Glycyl-, alanyl- and isoleucyl-RNA were also reported,[114] as well as N^6,N^6-dimethylated analogues resembling puromycin.[115]

Several methods were developed to obtain 3'-*NH*-peptidyl-RNA conjugates (**Scheme 14B**). They were first synthesized combining peptide solid-phase synthesis and oligoribonucleotides solid-phase synthesis. This requires first the synthesis of a versatile 3'-aminoacyl-adenosine monomer bearing protecting groups compatible with both SPS processes. Peptide synthesis first yields a 3'-peptidyl-adenosine monomer, and subsequent oligoribonucleotide synthesis leads to 3'-peptidyl-RNA conjugates.

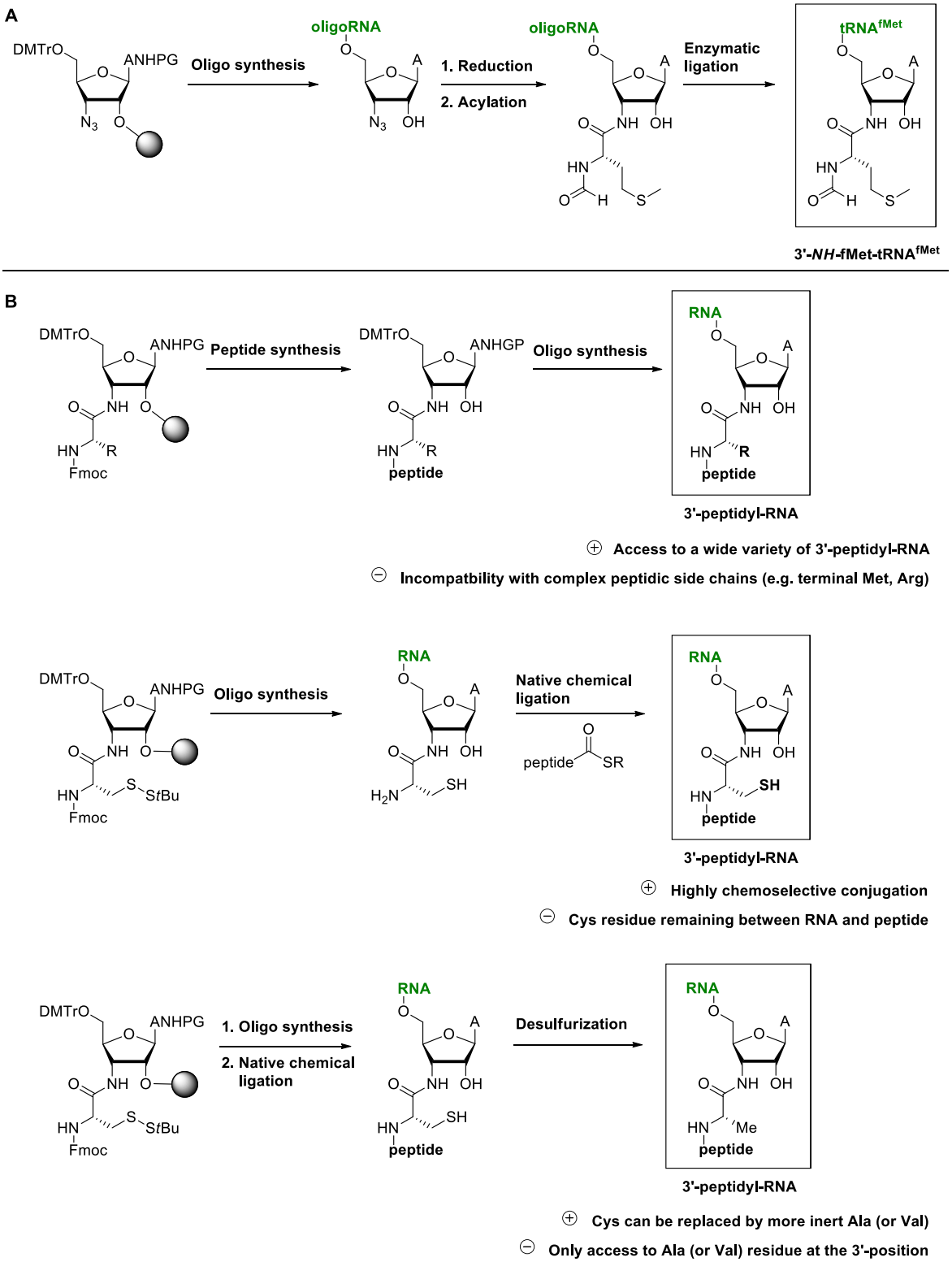

Scheme 14: Synthetic pathways leading to aminoacyl-tRNA analogues. **A:** Synthesis of a stable 3'-*NH*-aminoacyl-tRNA. **B:** Synthetic methods for peptidyl-RNA conjugates developed by Micura *et al.*

In a later strategy, starting from a 3'-cysteinyl-adenosine monomer as a precursor to 3'-cysteinyl-RNA, the use of native chemical ligation (NCL) allowed to conjugate, on the 3'-cysteine, virtually any

thioester-activated peptide [116] – the only drawback of this method is the remaining of a Cys residue between the peptide and the RNA. This problem could later be overcome by the use of desulfurization methods post-NCL allowing to convert the Cys residue into an Ala or a Val residue.[117]

These methods were also applied to obtain conjugates with hydrolysis-resistant RNA bearing nucleotide modifications[118] or with amino acid *N*-methylation, *O*-phosphonation or *O*-phosphorylation.[119]

4.5.5. Phosphonate transition state analogs for study of FemABX family members

Cressina *et al.* reported in 2007 the synthesis of a phosphonate Ala-deoxyadenosine and described it as a first inhibitor of MurM, a member of the FemABX family of bacterial transferases (**Figure 13**).[120] Although the best inhibiting potency of such compound remained modest (IC_{50} = 100 µM), it showed that the aminoacyl-tRNA analog for inhibition of Fem-transferases was promising.

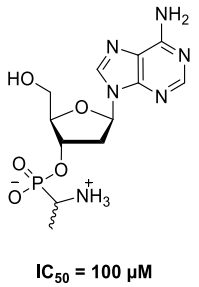

IC_{50} = 100 µM

Figure 13: Structure of the 2'-deoxyadenosine phosphonate MurM inhibitor

4.5.6. Previous work concerning the synthesis of Ala-tRNA^{Ala} analogs for the study and inhibition of FemX$_{Wv}$

The group of Prof. M. Ethève-Quelquejeu, in collaboration with the group of Dr M. Arthur, designed substrates analogues and inhibitors for the FemX transferase of Weissella viridescens, a model enzyme for the FemABX family. The general strategy was a hemisynthesis: a modified nucleoside in the 2' or 3' position was synthesized, then coupled *via* phosphoramidite chemistry to a deoxycytidine. The corresponding dinucleotide was then phosphorylated and enzymatically ligated to either the full tRNA^{Ala} or a microhelix mimicking the acceptor arm of the tRNA^{Ala}. Two classes of analogs were obtained: substrates analogs, able to transfer an amino acid, and stable analogs, non-transferring compounds. For this purpose, the general strategy of Hecht was adapted and combined with complex modifications on the terminal A76.

Concerning the substrate analogs: In order to look at their ability to transfer the amino acid and thus identify the recognition elements (amino acid, nucleotide sequence, etc.) for the enzyme, mimics of the natural substrate still possessing an amino acid with an ester bond were targeted (**Scheme 15**).

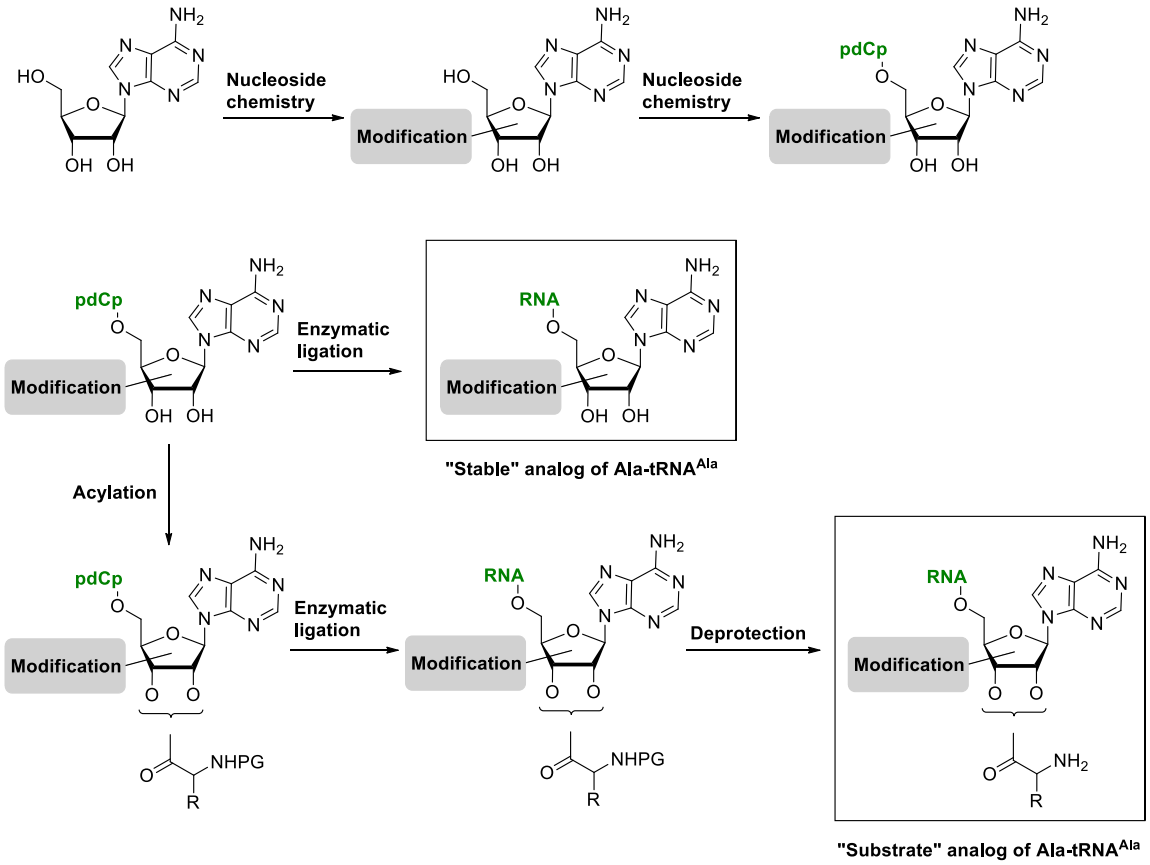

Scheme 15: General synthetic routes leading to either "stable" or "substrates" analogs of Ala-tRNA^{Ala} developed by Ethève-Quelquejeu *et al.*

Concerning the stable analogs: the same synthetic strategy was used to obtain compounds mimicking the substrates both not able to transfer an amino acid, thus acting as a competitive inhibitor. In those compounds, the ester bond is either absent or replaced by more stable linkages. First, analogs of Ala-tRNA^{Ala}, Ser-tRNA^{Ala} and Gly-tRNA^{Ala} (**Figure 14A**) and of Ala-tRNA^{Gly} and Ala-tRNA^{Ser} (**Figure 14B**) were synthesized.[27]

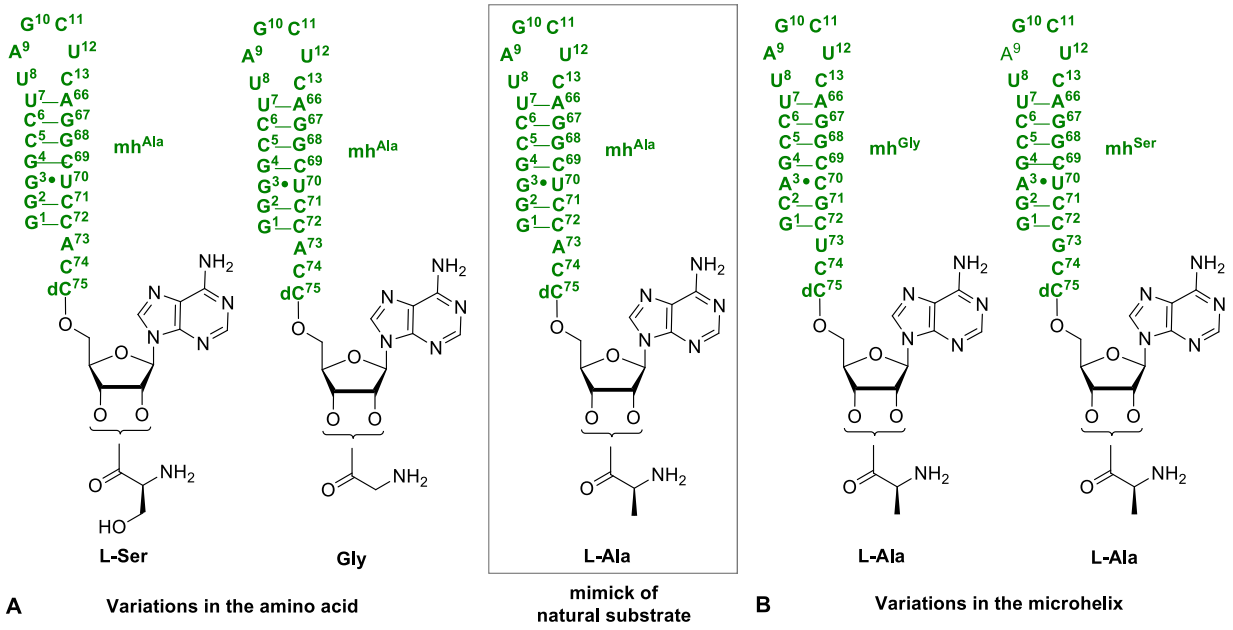

Figure 14: Structure of the substrates analogues evaluated for amino acid transfering. A: "Mis-acylated" $tRNA^{Ala}$ microhelix (mh^{Ala}). B: Alanyl-microhelixes for Gly and Ser

Deoxy substrates analogs, lacking one of the two alcohol groups, either in the 2' or the 3' position, allowed to understand the logic and regioselectivity of FemX (**Scheme 16**).[29]

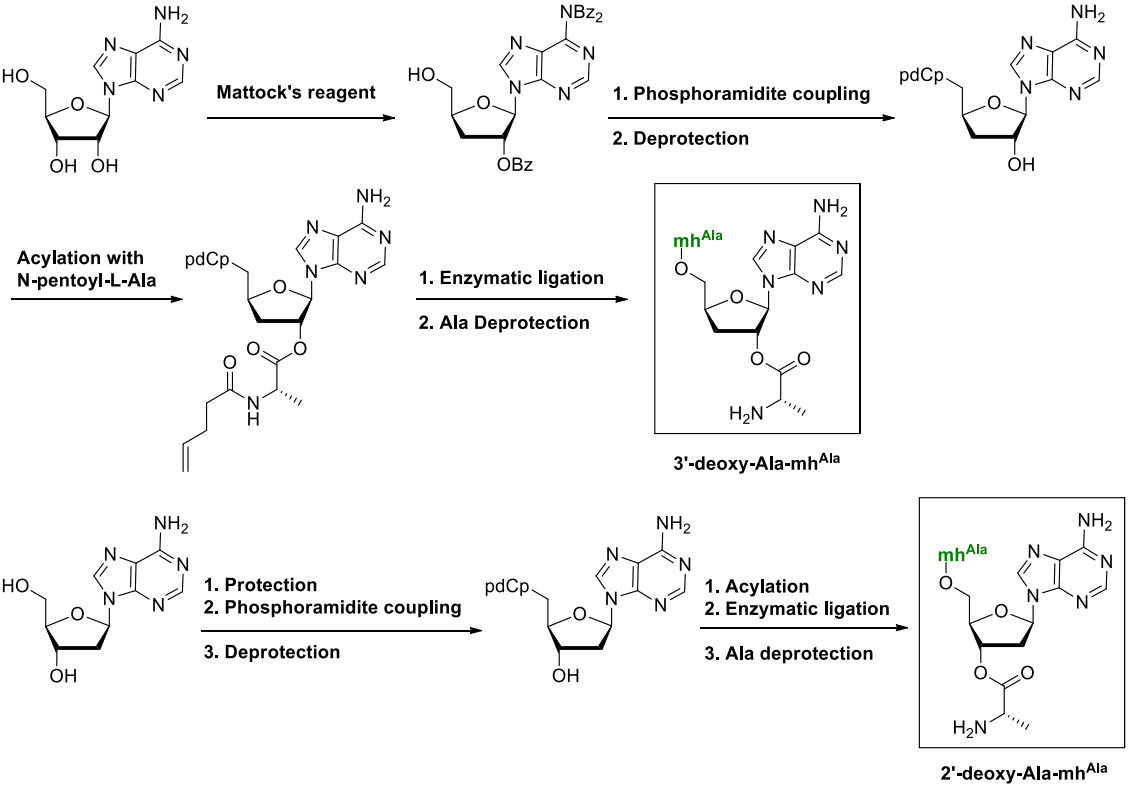

Scheme 16: Synthetic pathways leading to the 2' and 3' deoxy-Ala-$tRNA^{Ala}$ analogs

Another class of synthesized compounds is the one of inhibitors, in which the natural labile ester bond between the Ala and the $tRNA^{Ala}$ is replaced by a more stable amide bond, or by heteroaromatic rings such as triazole[121] or oxadiazole[122] (**Scheme 17**). Those compounds are unable to transfer their amino acid but are still recognized by FemX. They are inhibitors in the micromolar range when the tRNA moiety is a microhelix for $tRNA^{Ala}$.

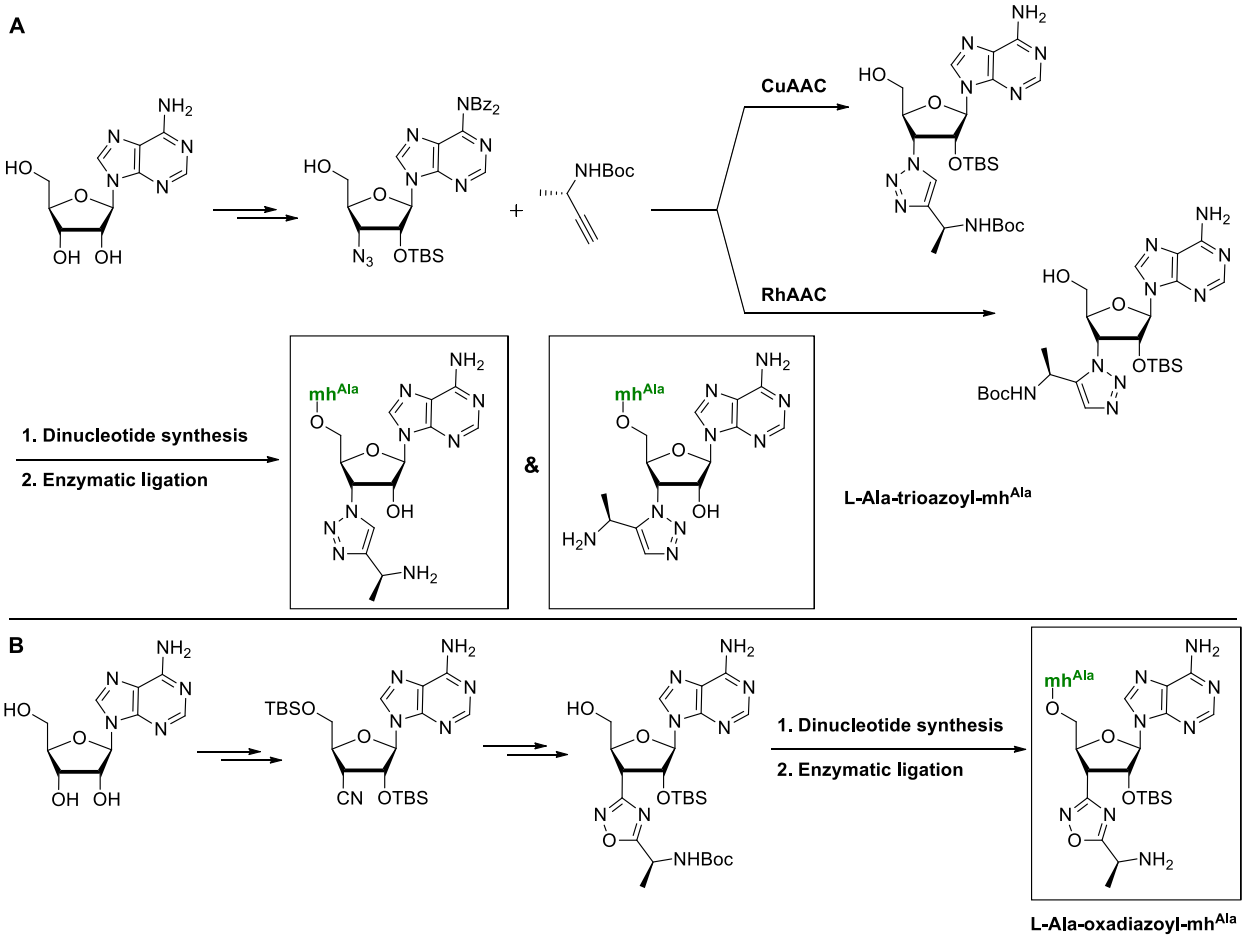

Scheme 17: Synthetic pathways leading to the stable Ala-tRNAAla analogues with A: triazole linkage and B: oxadiazole linkage

More recently, in order to increase the affinity, inhibitors referred to as "bi-substrate inhibitors" were obtained. These compounds contain a UDP-MurNAc-pentapeptide (UM5K) unit and a RNA part (**Scheme 18A**). Those peptidyl-RNA conjugates can be termed "bi-substrates" inhibitors as they interact with both substrate-pockets of the enzyme, and they are good candidates for high-affinity inhibition. For this purpose, since the triazole ring had previously shown good results at the 2'-position, the "Click-chemistry" copper(I)-catalyzed azide-alkyne cycloaddition (CuAAC) reaction appeared to be the method of choice for the synthesis of such compounds.

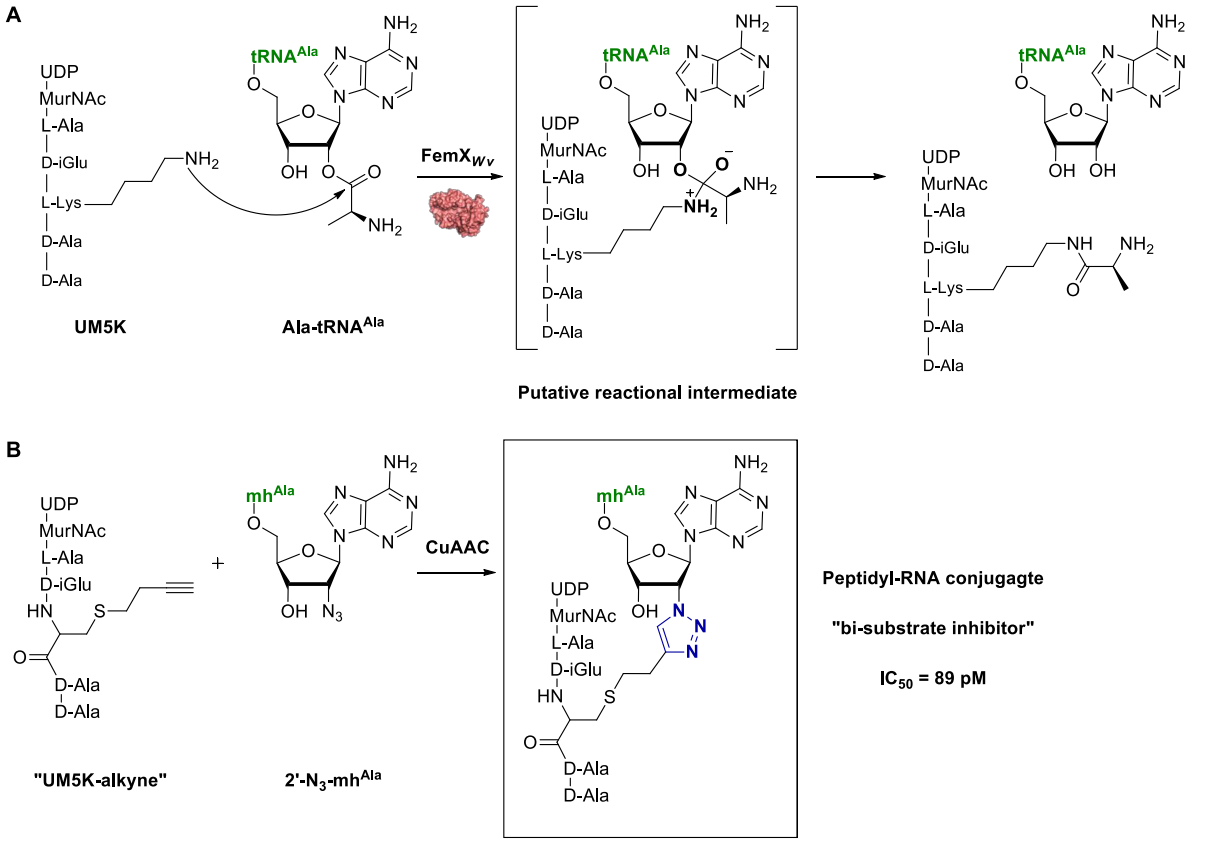

Scheme 18: A: Putative mechanism for amino acid transfer catalyzed by FemX**. B:** Synthesis of a peptidyl-RNA conjugate resembling the reactional intermediate.

A microhelix for $tRNA^{Ala}$ modified in the terminal 2'-position with an azide group could react with a modified alkyne-bearing UM5K to yield peptidyl-RNA conjugates with inhibition constants down to 89 pM (**Scheme 18B**).[123] UM5K-alkyne was obtained through a chemo-enzymatic synthesis thanks to collaboration with the group of Dr. Dominique Mengin-Lecreulx (Paris Sud University).

Structural studies of FemX and particularly the identification of the structures and amino acids residues interacting with the tRNA substrate are challenging because of the high flexibility of the tRNA in the enzyme, which prevents co-crystallization of tRNA-mimics with FemX. In order to decrease that flexibility, the $tRNA^{Ala}$ microhelix was replaced by a series of short oligonucleotide duplexes still bearing the azide group in the 2' terminal position. These duplexes were obtained through solid-phase oligoribonucleotide synthesis in collaboration with the group of Prof. Tom Brown (University of Oxford) (**Scheme 19A**). "Clicked" compounds with the UM5K-alkyne yielded a series of "bi-substrates" inhibitors, with, because of the loss of the major part of the RNA moiety, showed less affinity than previously synthesized compounds. However, despite the loss of affinity, these compounds show better ability to co-crystallize with the enzyme, and allowed to obtain the first structure of a FemABX

enzyme in complex with an analog for the tRNA substrate (**Scheme 19B**).[30] This 1.6 Å resolved structure includes all FemX residues, all the UM5K analogue atoms, and the terminal CCA nucleotides.

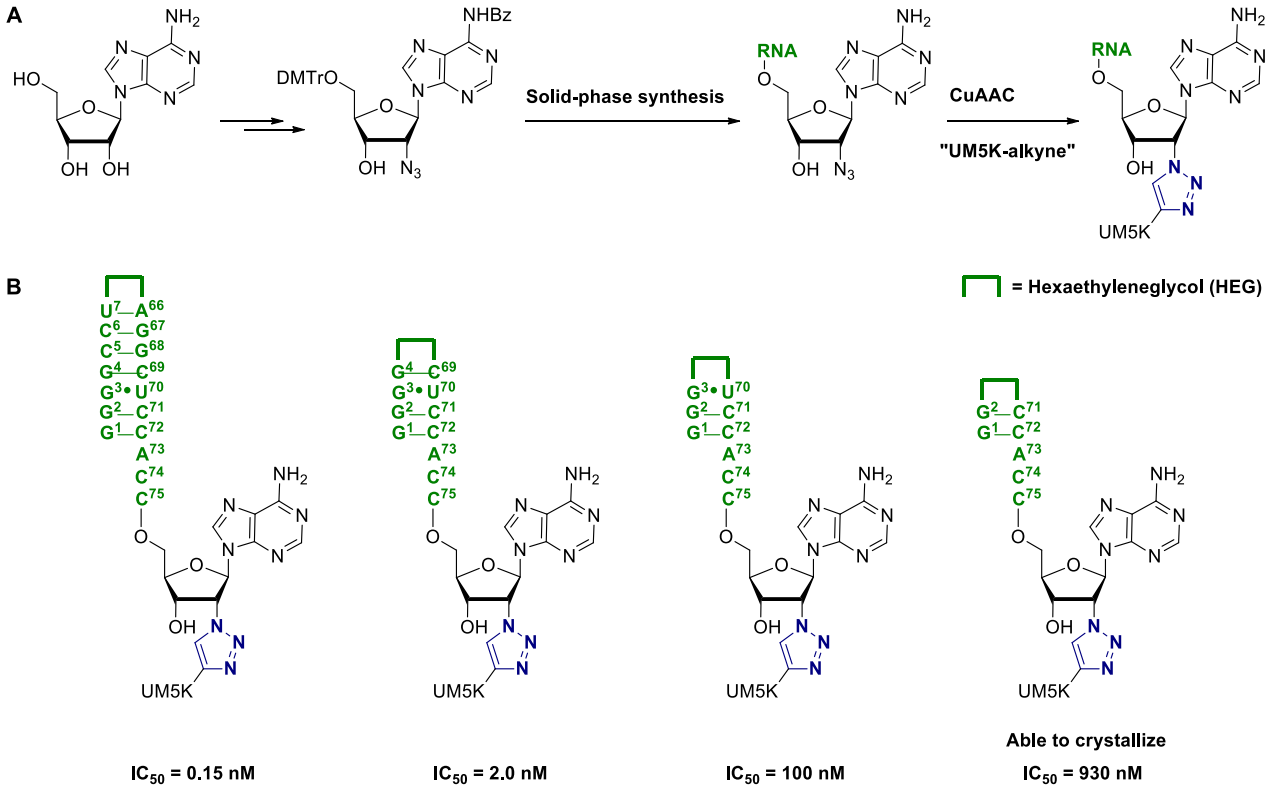

Scheme 19: A: Synthetic pathway leading to RNA-peptidyl conjugates with short RNA duplexes. **B:** Structure and biological evaluation of the obtained compounds.

The work presented in this doctoral thesis is in the continuity of these results. The first chapter presents the synthesis of "electrophilic" tRNA analogs able to label an aminoacyl-tRNA dependent enzyme, e.g. FemX, in a site-specific fashion. The second chapter deals with the synthesis of fluorinated nucleosides as precursors of tRNA analogs that will be used as tools to study the role of the 3'-hydroxyl group of aa-tRNAs as well as the conformational preference of FemX. In the third chapter, the knowledge and know-how developed on FemX is applied to *Staphylococcus aureus* FmhB to develop first inhibitors of FmhB and for structural studies of this crucial enzyme. Eventually, the fourth chapter presents the synthesis of analogs for the study of cyclodipeptide synthases, another class of aminoacyl-tRNA-dependent enzyme.

Part 2

Goals, results, and discussion

Chapter 1

Synthesis of electrophilic aminoacyl-tRNA analogs for site-specific cross-linking with FemX$_{Wv}$ and peptide-RNA conjugation.

1. Design of electrophilic aa-tRNA analogs

1.1. Goals

As previously described (*cf* Part 1; 4.1.5), aa-tRNA are involved in a wide variety of biological processes and, despite a growing interest in the field of tRNA biology, many enzymes interacting with aa-tRNA remain unidentified. The use of molecular tools able to selectively interact and bind – covalently or not – with such enzymes could lead to their identification.

In the case of Fem-transferases, identification of yet unknown Fem-enzymes is an interesting strategy for target discovery for antimicrobials research. Moreover, synthesis of compounds able to covalently bind Fem-transferases could be a first step toward the synthesis of suicide-inhibitors that could act as antibiotics. For these reasons, the work presented here deals with the synthesis of aa-tRNA analogs bearing ean electrophilic motif able to covalently bind the model FemX and to do so in a residue- and site-specific fashion. The design of such "electrophilic" RNA relies on previously acquired structural and mechanistic data (*cf* Part 1; 3.2.).

1.2. The 2'-terminal position of aa-tRNA and FemX K305

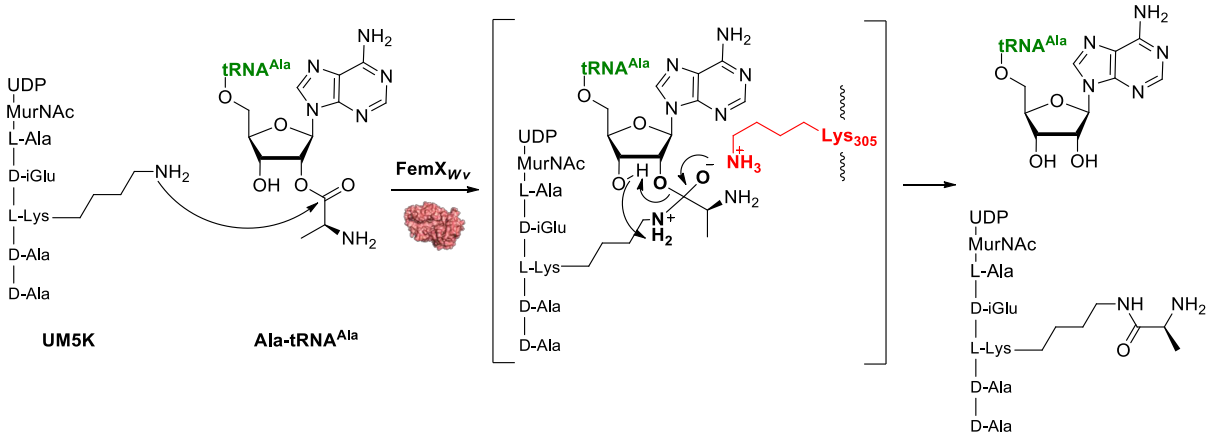

Scheme 20: Role of Lys305 during the FemX-catalyzed amino acid transfer

Among all the important amino acid residues in the active site of FemX, Lys305 is particularly interesting. It is perfectly positioned to play a key role in catalysis, and when mutated, the activity of the enzyme drops dramatically. The postulated mechanism for amino acid transfer catalyzed by FemX reported in the group of Prof. Mélanie Ethève-Quelquejeu in 2013[30] suggests that K305 can stabilize the oxyanion intermediate during the reaction (**Scheme 20**). Its close proximity with the 2'-position makes it a good candidate for covalent labeling by an electrophilic motif placed at the 2'-position of the terminal adenosine of a tRNA analog. Thus, the desired compound would need to be not only

selective toward Lys among all amino acids, but also to the Lys305 among all 19 Lys residues present on FemX by placing the electrophilic motif on a recognized RNA-sequence with an affinity that is important enough to position the motif in proximity of Lys305. As a result, Lys-selective motifs were searched with the requirement of moderate reactivity to insure site-specificity.

Another interesting lysine involved in the Fem-catalyzed reaction is the one on the UM5K that naturally attacks the Ala-tRNA^{Ala}. An electrophilic motif at the 2'-position could also be able to trap the UM5K, either *in vitro* for synthesis of peptidyl-RNA conjugates acting as bi-substrates inhibitors and *in situ* with FemX assistance, which could lead to enzyme-assisted synthesis of inhibitors.

UM5K and UM5K analogs can be obtained through enzymatic synthesis. During these processes, the natural lysine can be replaced by other nucleophilic residues such as Cys. FemX possesses no Cys in its sequence, and one Cys residue can be incorporated through site-directed mutagenesis at many positions. For these reasons, even though electrophilic motifs reacting with Lys were more thoroughly studied, motifs reacting with Cys residues were also investigated.

1.3. Electrophilic motifs

1.3.1. A first general approach: the maleimide motif

The first envisioned motif was the maleimide group. In the beginning of this study, the role of Lys305 was still being uncovered, and maleimide was a good first example to optimize the introduction of the electrophilic motif, the peptidyl-RNA synthesis, and the enzymatic cross-linking experiments. The maleimide group is considered to be a major Cys-selective reactive group.[124,125] Though FemX does not comprise a Cys residue in its sequence, site-directed mutagenesis allows the introduction of Cys residues. Also, the UM5K substrate can be replaced by a Cys-containing analog. For these reasons, development of Cys-trapping compounds remains interesting.

Maleimide reactivity relies on the 1,4-addition of nucleophiles onto its double bond. Two reasons exist for its enhanced reactivity:[126,127] In the reaction with a nucleophile, the nucleophilic species attacks in the lowest unoccupied molecular orbital (LUMO), here the π*. The keto groups act as electron-withdrawing groups, decreasing the energy of both π and π* molecular orbitals. The cyclic constraint generates an angle smaller than 120° which decreases the gap between the π and π* molecular orbitals. As a result, the lower-in-energy π* molecular orbital is more prone to react with nucleophiles.

Considered very selective for Cys residues, maleimide can also react with amines in the case of high pH conditions, and the thiol-maleimide adduct hydrolyzes quickly in alkaline conditions. Amines can lead to ring-opening of the maleimide adduct, leading to cross-linking.[128,129] Maleimide is described as unreactive toward Tyr, Met and His residues.[130,131]

In order to obtain a first general electrophilic RNA, the synthesis of RNA-maleimide in the 2'-position was investigated, as well as its ability to cross-link with aa-tRNA-dependent enzymes such as FemX, aa-tRNA synthetases and non-tRNA-dependent enzymes (*cf* 1.4.).

1.3.2. A selective approach: lysine-reactive motifs

The Lys residues can react through their lateral amino group, or, when terminal, their alpha-amino group. They are normally protonated at physiological pH; however, the pKa of lysine can vary greatly depending on the enzymatic microenvironment.[132] Many motifs have been reported in the literature for lysine labeling, the most frequently used being NHS-activated[133] ester and iso(thio)cyanates.[134,135] These motifs differ in reactivity, selectivity and stability. We focused on the motifs for which site-specific Lys labeling was achieved. Examples of such specific Lys labeling are now reviewed.

Selective labeling of Lys338 of a Cytochrome p450 enzyme with fluorescein-isothiocyanate (FITC) was reported in 1974.[136] In that study, treatment with one equivalent of FITC yielded quantitative adduct formation, 75 % of which was proved to be on Lys338, and 25 % on other Lys residues. The cause of this site-specificity remains unclear but is believed to be linked to the high affinity of the FITC for the pocket in which lies Lys338. The high hydrophobicity of the pocket could also be suspected for decreasing the pKa of this specific Lys residue. The same FITC reagent was also reported to be able to label specifically Lys61 of actin,[137] again without rationalizing this specificity other than the suspicion of a lower pKa value of this Lys residue as opposed to the other 33 other Lys residues of actin.[138,139]

Activated esters and notably NHS-activated esters, though selective toward Lys residues, have not been described for site-specific Lys labeling. Their high reactivity, which is the reason for their quicker hydrolysis,[140] can also be thought to be the reason of their inability to select one Lys from another. Reaction with other amino acids residues such as Tyr, His, Ser, Thr has been reported.[141,142,143] Reaction with thiols does not lead to stable adducts but promotes degradation of the reagent and can affect the yield of the labeling reaction.

Aldehydes can be used as electrophilic motifs for reaction with Lys residues through sodium borohydride-mediated reductive amination. Though this method has mostly been used for conjugation of proteins with carbohydrates (which possess aldehyde groups),[144,145] it was also reported for tagging of four out of fifty-nine Lys residues of BSA.[146] Again, only unusually low pKa values can be suspected to explain this selectivity among Lys residues.

The use of fluorescent imidoesters for fluorescent tagging of horse liver alcohol dehydrogenase led to specific tagging of Lys228.[147] The authors took advantage of the proximity of this Lys residue with an excess of substrate of the enzyme to protect all Lys residues but Lys228, and then they were able to

tag it as the only free Lys residue remaining. This method was first used for mechanistic studies and enzymatic activity enhancement for this same enzyme.[148]

Azetidinone-bearing bifunctional linkers were also used to specifically target the Lys93 of the heavy chain of immunoglobulin G (IgG),[149,150] again taking advantage of the unusually low pKa value – around 6.0 – of this particular Lys residue.

In all those examples, no common strategies can be identified for site-specific Lys labeling. In every case, the authors took advantage of one peculiarity of the studied system such as low pKa values, probe affinity, or used derivatization strategies. With those elements in mind, we then wanted to design compounds for site-specific lysine-labeling of FemX.

In the case of Lys305 of $FemX_{Wv}$, we have no knowledge of an unusual pKa value; given its suspected role in catalysis as a cation, it is most probably completely protonated. A way to target specifically this Lys residue would be to attach the electrophilic motif to a compound with an affinity for the catalytic site of FemX that is high enough to place the motif in close proximity to Lys305. This brings three requirements for the desired compounds: first of all, they must possess an aa-tRNA mimicking sequence that is long enough to be efficiently recognized by the enzyme. Second, the motif must be structurally compatible – meaning, not too big – with the previous FemX structural data to be appropriately positioned in close proximity to Lys305. Finally, the motif must not be as reactive as those previously described: designed for labeling and tagging purposes, they were optimized for enhanced reactivity. In our case, excessive reactivity could lead to unspecific Lys labeling.

Few examples of electrophilic nucleic acids are reported in the literature. In 2013, the group of Hocek did report vinylsulfonamide- and acrylamide-functionalized DNA to study DNA/proteins interactions.[151] Even though the vinylsulfone motif could, in some conditions, react with Lys residues,[152,153,154] those motifs react strongly with Cys and other amino acid residues,[135] thus they do not meet the aforementioned requirements. Even though these examples are interesting in that they prove that it is possible to introduce electrophilic motifs on nucleic acids, we cannot use them in our case and we looked into other lysine-reactive motifs meeting our criteria.

Among all the bioconjugation strategies, the use of squaric acid esters show interesting properties in view of our goals.[155,156] They are derivatives of squaric acid, a four-membered aromatic ring. Their most promising properties in their ability to react with only one first equivalent of amine, leading to a squaramate, and in harsher conditions, to react with a second equivalent of amine, leading to a squaramide (**Scheme 21**). The use of different amines leads to asymmetric squaramides, and is a convenient and convergent synthetic pathway for the coupling of amines. Their use as amine-amine coupling agents has recently increased first in the field of bioconjugation as a linker between

biomolecules, and later in the field of medicinal chemistry as a linker between amine-bearing scaffolds.[157] They are attractive candidates for our application for the following reasons.

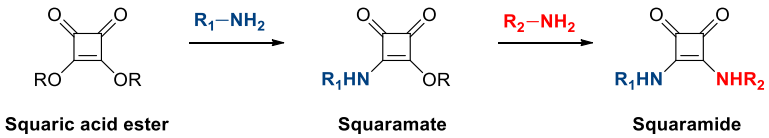

Scheme 21: Squaryl-mediated amine-amine coupling

Squaramates are able to discriminate the lysine residues over other nucleophilic amino acid residues such His, Arg or Ser.[158,159,160] Reaction with other nucleophiles can proceed but the instability of the formed adducts with thiolate or alcohol groups prevents undesired labeling. Very early description of their ability to react with the Lys residues of wool-based textiles.[161] They can trap the lysine residues of BSA, as repeatedly reported,[156,157] though in a non-site-specific fashion. Squaramates were also reported to be able to label the tetanus toxoid[162] and lysozyme.[159] More recently, over the course of our study, the group of Ito *et al.* reported the use of a squaramate attached to a compound binding to the UDP-glucose:glycoprotein glucosyl-transferase (UGGT) to site-specifically label a lysine residue in close proximity of the binding site.[163]

Its reactivity seems compatible with our purposes: unspecific tagging of BSA lysine residues requires high pH, generally above 9, and long reaction time, generally more than one day.[157]

The synthesis of RNA-squaramates has not been reported. However, squaramides were synthesized from oligo(ribo)nucleotides with carbohydrate-squaramates.[164,165] In all of those examples, the amino group was introduced in the 5'-position (**Scheme 22**) of the attached nucleotide. In our case, the introduction of a 2'-amino group is possible either from 2'-NH-protected group or from 2'-azido group, and has been previously obtained in our group.[166]

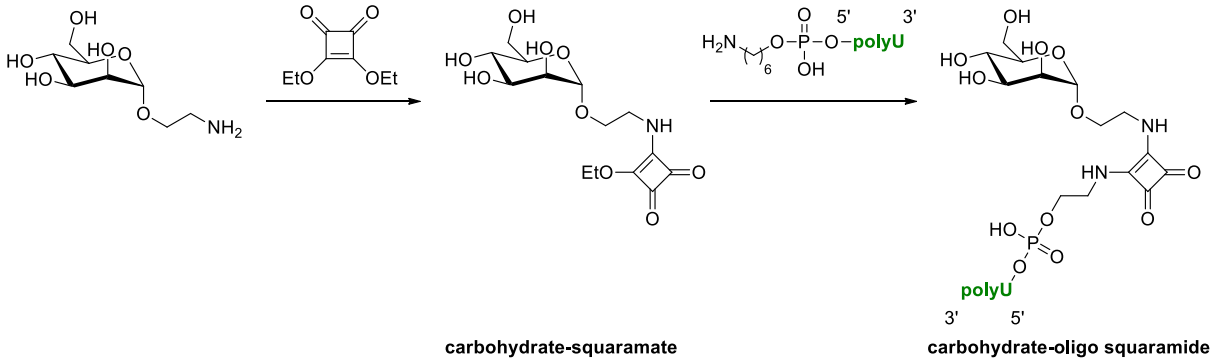

Scheme 22: Example of synthesis of carbohydrate-RNA squaramide conjugates by Yan *et al.*[164,165]

Structurally, squaryl, as well as triazole, is a small aromatic unit. Both of them have been described as possible analogs for the phosphodiester bond between nucleotides.[167,168,169] Thus, despite their structural differences, the squaryl moiety might then be an isostere of the previously used triazole[121] or an isostere of the natural ester bond.

Aside from their ability to cross-link with specific enzymatic Lys residues, squaramates can be thought of as precursors for peptide-RNA conjugates. In the case of FemX, the peptidic substrate UM5K possesses a lysine that would be able to react with a RNA-squaramate to form a peptide-RNA squaramide conjugate that could be a bi-substrate inhibitor of FemX.

To summarize, the squaramate functional group meets the following requirements: it is structurally compatible with our biological target; it might be possible to graft it on nucleic acids; its reactivity, moderate and exclusive towards lysine residues, might be able to achieve site-specific cross-linking; it also is a precursor to peptide-RNA conjugates.

For all these reasons, the synthesis of RNA-squaramate in the 2'-position and their applications for FemX cross-linking and peptidyl-RNA synthesis were investigated and are presented here.

1.4. Structure of the desired compounds

The targeted compounds must comprise (**Figure 15**):

- A RNA sequence mimicking the acceptor arm of $tRNA^{Ala}$ that is long enough to be well recognized by FemX. A good recognition by the enzyme is necessary to be assured that the electrophilic motif will be adequately positioned.
- An electrophilic motif, maleimidyl or squaryl, for cross-linking or conjugation, depending on the target.
- A linker between the RNA and the electrophilic motif. The number of methods compatible with the attachment of an electrophilic motif is not large. The linker is directly dependent on the chosen method: it can be a triazole obtained through CuAAC-mediated attachment of the electrophile, an amide bond through peptidic coupling or Staudinger ligation, or, in the case of the squaryl, a direct NH-squaramate linkage.

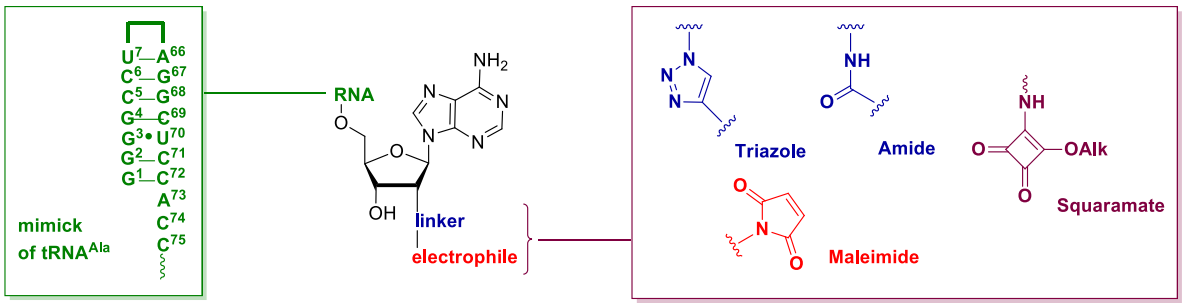

Figure 15: Structure of the targeted electrophilic tRNA analogs

2. Retrosynthetic analyses

The retrosynthetic scheme planed here is described in **Scheme 23A**.

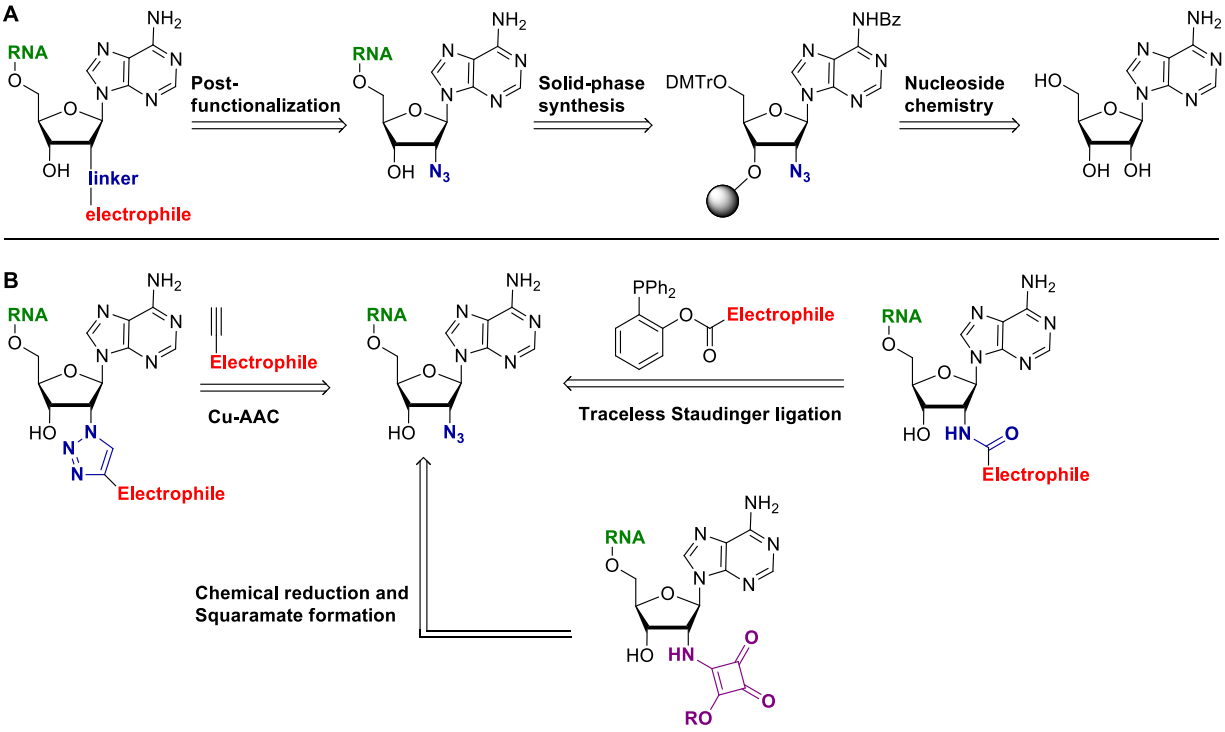

Scheme 23: A: Overall retrosynthetic scheme from the electrophilic RNA scaffold to adenosine. **B:** Retrosynthetic strategies for final post-functionalization.

The introduction of the electrophilic motif is intended to be the last step of the synthesis, as a post-functionalization on 2'-azido-RNA. This 2'-azido-RNA can be obtained by solid-phase synthesis from a 2'-azido-2'-deoxyadenosine monomer, that itself can be synthesized from commercially available adenosine.

The post-functionalization step depends on the desired linkage or the desired motif (**Scheme 23B**). A triazole linkage can be obtained directly from the 2'-azido-RNA through Cu-AAC with an alkyne-bearing electrophile partner: this method was used to obtain the maleimide-bearing RNA. To obtain the amide

linkage, we propose the use of the chemoselective traceless Staudinger ligation: a methodological study is herein presented for the application of this method on an oligoribonucleotide. Direct linkage of the squaramate requires the reduction of the azido group into an amino group and then squaramate formation, both of which are described here.

3. Synthesis

3.1. Monomer synthesis

To achieve the synthesis of the targeted compound, 2'-azido-2'-deoxyadenosine **8** was synthesized (**Scheme 24**).

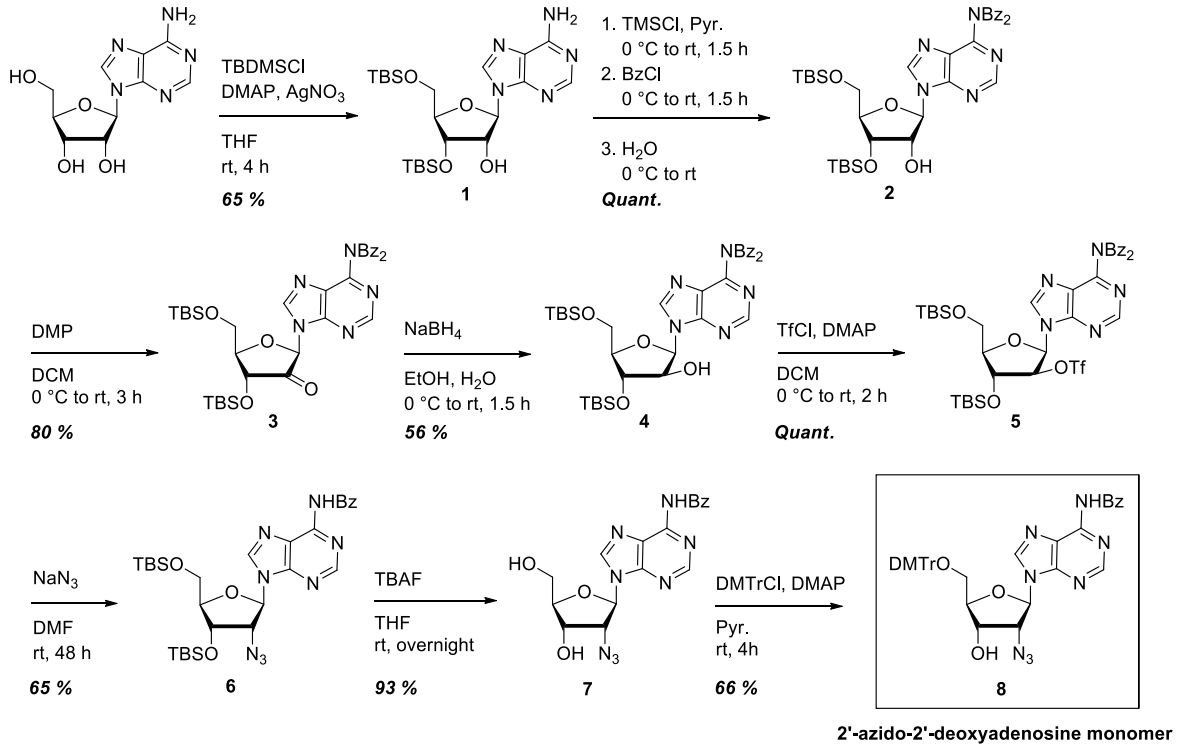

Scheme 24: Synthesis of the 2'-azido-2'-deoxyadenosine monomer.

The goal is the introduction of an azido group at the 2'-position *in lieu* of the natural -OH. Starting from the commercially available adenosine, an eight-step synthesis yields the appropriate 2'-azido-2'-deoxyadenosine monomer **8** that is compatible with the solid-phase synthesis process. The first two steps consist in protection steps: first the selective silylation of the 3' and 5' alcohols, then the benzoylation of the nucleobase exocyclic amine to give the adequately protected compound **2**. The following steps consist in the inversion of configuration of the 2'-OH in order to obtain a final 2'-azido compound in the same *ribo* configuration as the natural 2'-OH. This is achieved by an oxidation/reduction sequence. The oxidation was carried out smoothly with Dess-Martin periodinane. The sodium borohydride-mediated reduction yields the *arabino* diastereoisomer **4** thanks to the

hindrance of the nucleobase that favors hydride attack from the inferior side of the sugar-ring with an acceptable selectivity. Eventually, the *arabino* 2'-OH is transformed into a good leaving group in the form of the triflate **5**, which is then substituted by an azide group. One benzoyl group is lost upon azide substitution. The last steps consist in the introduction of the appropriate protecting groups for solid-phase synthesis: first, both silyl groups are removed through the use of tetrabutylammonium fluoride (TBAF), and then the 5'-OH is protected with a dimethoxytrityl group. The 3'-OH of compound **8** is left unprotected as it is intended to be the attachment point for the solid support.

3.2. Oligo synthesis

3.2.1. Attachment to the solid support

The chosen solid support for RNA synthesis is a Controlled-Pore Glass (CPG) support grafted with an amino group, with a porosity of 1000 Å, compatible with the synthesis of the desired 8 to 18-mer oligos.

The coupling between the amino group of the resin and the 3'-OH group of the nucleoside is mediated by a succinic linker (**Scheme 25**). The resin first reacts with succinic anhydride. The subsequent carboxylic acid functional group is activated by EDC and then substituted by the 3'-OH group of the nucleoside, forming an ester bond. This ester bond is stable throughout the solid-phase synthesis process and is cleavable in basic conditions as well as most protecting groups used for the solid-phase synthesis monomers.

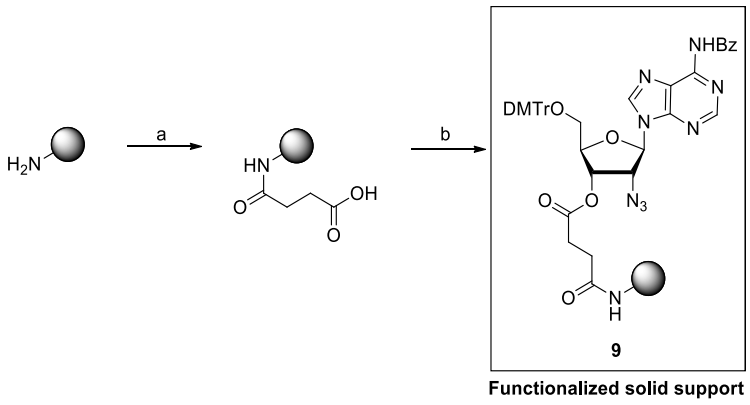

Scheme 25: Grafting of the modified adenosine monomer onto the solid support. a) succinic anhydride, DIPEA, Pyr., rt, 20 h. b) **8**, EDCI, DMAP, Pyr., rt, 20 h.

The loading of the resin is evaluated by taking a weighed sample of functionalized resin and treating it with trichloroacetic acid (TCA) to induce DMTr cleavage. Filtration and measurement of the optical density of the cleaved DMTr group allows to calculate a loading of 29 µmol/g. This modified A-solid support **9** is then introduced into SPS.

3.2.2. Oligomerization

The functionalized resin is introduced into the oligo synthesizer. The RNA monomers used were 2'-TBS protected and the nucleobases for A, G, and C were protected by 4-*tert*butylphenoxyacetyl (tBpa) (**Scheme 26**). The hexaethyleneglycol (HEG) linker, introduced to favor base-pairings, was introduced in the form of a phosphoramidite monomer, as well as the phosphorylation reagent.

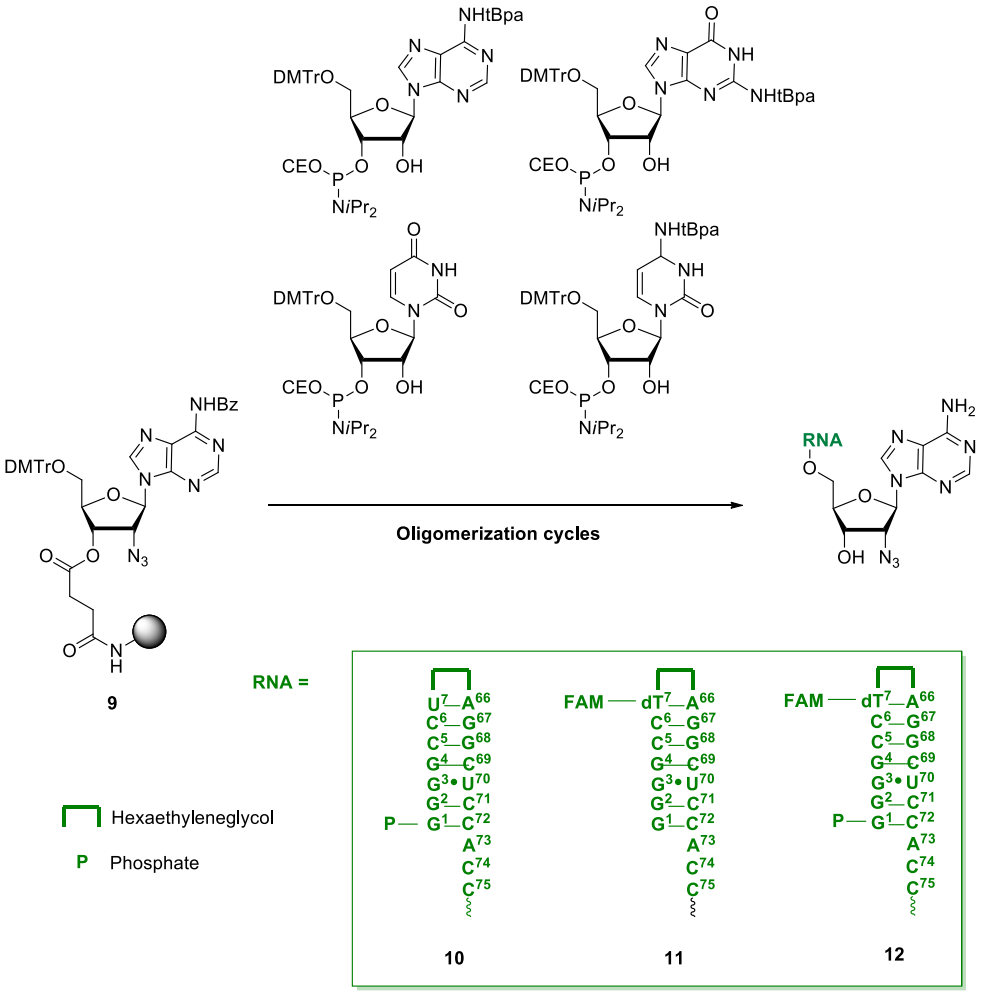

Scheme 26: Solid-phase synthesis of 2'-azido-RNAs mimicking $tRNA^{Ala}$. FAM: 6-CarboxyFluorescein-Aminohexyl Amidite.

The chosen sequence was the one previously used mimicking the acceptor arm of $tRNA^{Ala}$ consisting of the first four unpaired bases, and a duplex formed by seven base pairs linked by a hexaethyleneglycol hydrophilic linker for appropriate folding. To confirm previous results indicating that a phosphate in the 5' end was responsible for a 4-fold affinity increase, sequences ending with a 5'-OH and a 5'-phosphate were synthesized. For co-localization of the desired covalent adducts, sequences with either a fluorescent dT-FAM or a U at position 7 were synthesized.

3.2.3. Cleavage and deprotection

The cleavage and deprotection stages proceeds in two sequential steps. First, the finished oligo still attached to the solid support is treated with 3:1 NH_4OH:EtOH in the synthesizer. The ester bond linking the oligo to the solid support is quickly cleaved, and the free oligo is recovered. Basic deprotection of the nucleobases and of the phosphates requires a longer time at higher temperature, so the oligo is kept in the NH_4OH:EtOH solution and heated up to 55 °C during 2 hours to yield the partially deprotected oligo. Treatment with $HF.3Et_3N$ allowed deprotection of the 2'-silylated groups.

After HPLC purification, the obtained oligos can then undergo post-synthetic functionalization.

3.3. Post-synthetic functionalization

3.3.1. Maleimide motif with triazole linkage

3.3.1.1. The Cu-catalyzed azide/alkyne cycloaddition method

"Click"-chemistry is a relatively recent term coined to cover all reactions consisting in the heteroaromatic-forming association of small reactive groups that meet a number of requirements.[170,171] "Click"-chemistry reactions need to be carried out smoothly with high yields, a wide scope of application, easy purification, tolerance towards water, oxygen, or physiological conditions, and high regio- and chemoselectivity.

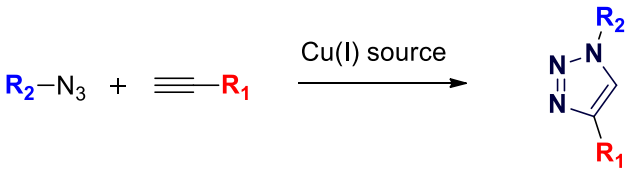

Scheme 27: Copper(I)-catalyzed azide/alkyne cycloaddition

"Click"-chemistry is often used to name the most emblematic and widely used Copper(I)-catalyzed azide/alkyne cycloaddition (CuAAC).[171,172] It consists in the reaction of a functionalized azide with a functionalized alkyne to form a 1,4-disubstituted 1,2,3-triazole through a copper(I)-mediated cycloaddition (**Scheme 27**). This reaction perfectly meets all the aforementioned requirements. Most importantly, both the precursor functions are stable, simple and compatible with water, oxygen, and most biomolecules.[173,174] As a result, it has been used extensively on all kind of compounds, from small molecules in medicinal chemistry to complex supramolecular constructs or large biomolecules.

The mechanism for this reaction is still under investigation. The latest reports suggest a binuclear mechanism involving two Cu atoms (**Scheme 28**).[175,176]

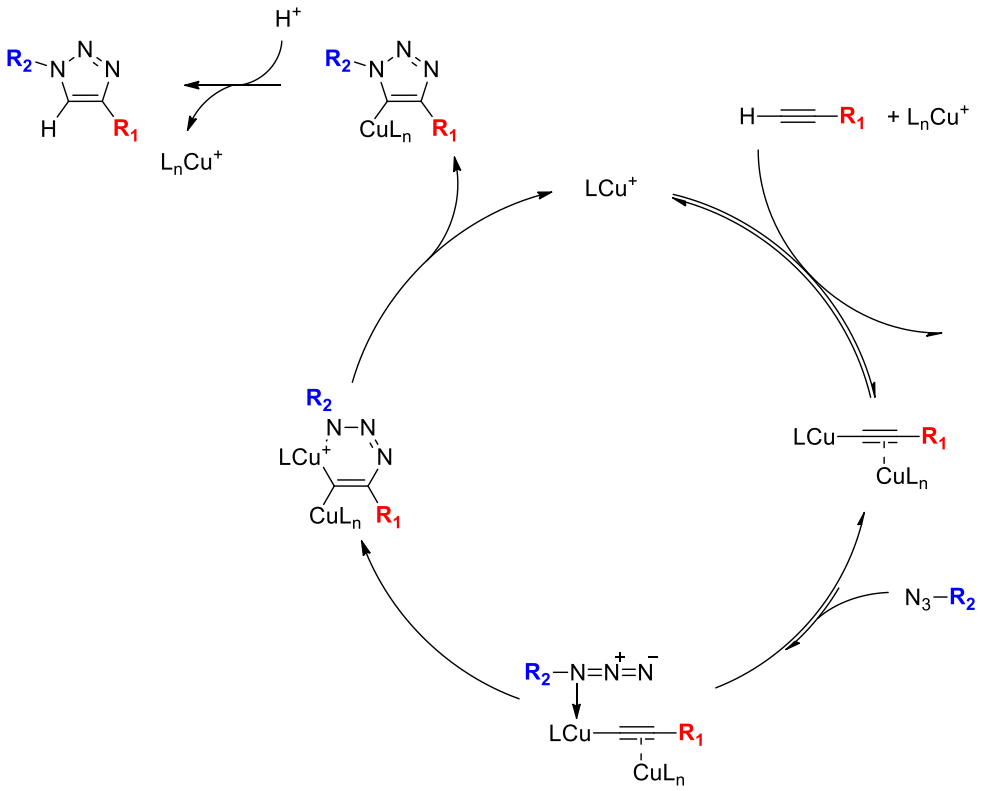

Scheme 28: Example of recently reported catalytic mechanism of the CuAAC reaction

Nucleic acid chemistry has made notable use of this method for multiple goals: labeling with dyes or other interesting tags, strand cross-linking, surface immobilization, metallization, oligo-oligo ligation or conjugation with peptides.[169] The alkyne group can be introduced into nucleic acids at the monomer level and is compatible with both enzymatic polymerization[177,178] and chemical solid-phase synthesis.[179] The azide function is trickier because of its ability to react with the Phosphorus (III) of the phosphoramidite monomer. The introduction of these small reactive groups allows post-synthetic approaches for labeling and thus access to tags that would be unfit for solid-phase synthesis conditions (unstable during deprotection, too bulky, etc.). Other than the special attention needed for the azide/phosphorus(III) reaction, another drawback of this method for nucleic acids is the sensitivity of nucleic acids toward Copper(I), resulting in its degradation within minutes.[180] However, this can be overcome by the use of Copper-free Click-chemistry methods, using strained activated alkynes that do not require copper for the reaction to proceed, or the use of Copper(I) ligands that stabilize the metal as well as they increase the rate of the reaction.[181]

In our post-synthetic approach for the synthesis of electrophilic RNA, this chemoselective method was the method of choice for our first attempts with the maleimide motif. For this purpose, the synthesis of an alkyne-bearing maleimide was necessary.

3.3.1.2. Synthesis of the alkyne-maleimide partner

The alkyne-bearing maleimide partner was synthesized with a procedure reported in the literature (**Scheme 29**). Maleic anhydride was reacted with propargylamine in 48 % yield, then the subsequent acid was cyclized in acetic anhydride. The product was isolated by distillation with a low yield. The obtained alkyne **13** was then used for ligation to the azido-RNA.

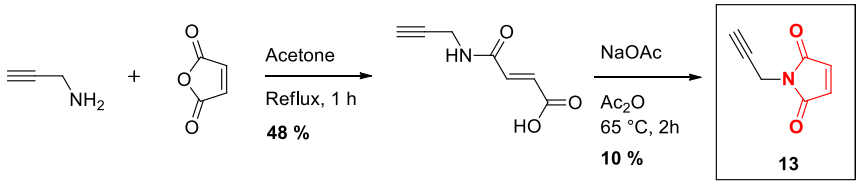

Scheme 29: Synthesis of alkyne-maleimide

3.3.1.3. Synthesis of maleimidyl-RNA

The chosen azido partner was the fluorescent sequence mimicking $tRNA^{Ala}$ **11**, for easier purification and identification of the subsequent products. The CuAAC was carried out in water with 10 % DMF as co-solvent for solubilization of the alkyne partner **13**. The copper(I) complex was generated by *in situ* reduction of copper(II) sulfate by sodium ascorbate, in the presence of THPTA as a copper(I) ligand (**Scheme 30**).

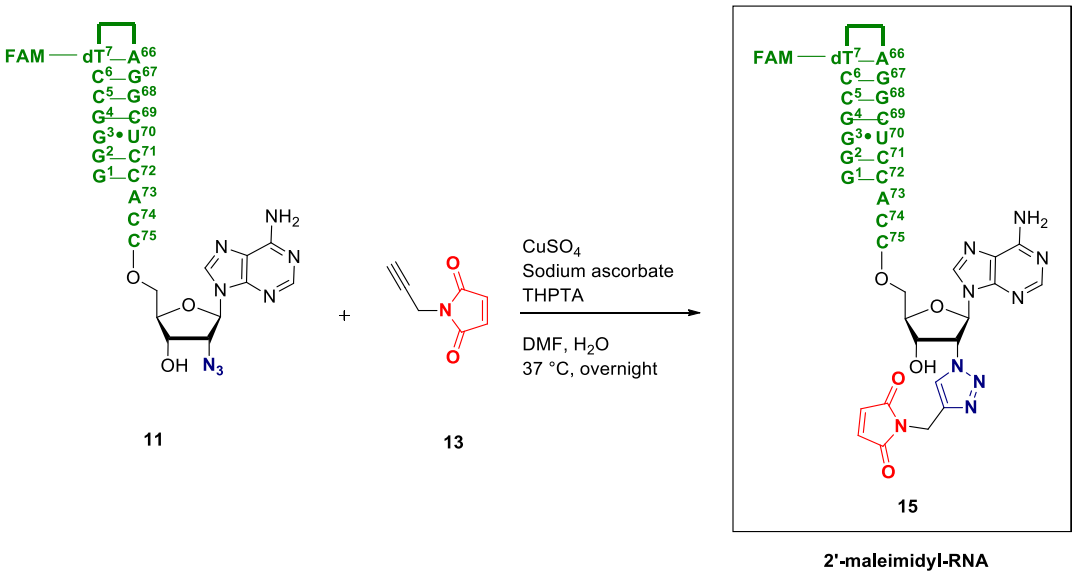

Scheme 30: CuAAC-mediated synthesis of maleimidyl-RNA

Reaction monitoring and purification were done with reversed-phase HPLC. Testing of compound **15** through the usual assay indicated a micromolar inhibiting constant. However, because the assay is designed to evaluate competitive inhibition, it was only an indication that the compound was

recognized by FemX. Further evaluation of the potential of the compound was done by looking at its ability to covalently bind to the enzyme.

3.3.1.4. Adduct formation and selectivity analysis

The results presented here have been obtained through collaboration with Dr Matthieu Fonvielle in the group of Dr Michel Arthur (Centre de Recherche des Cordeliers, Paris).

The electrophilic compound **15** was incubated with FemX for increasing times. Migration on gel and revelation of the gel with both coomassie blue and BET allowed the detection of both proteins and nucleic acids. Hence, co-revealed bands are most probably covalent nucleoproteic complexes (**Figure 16**).

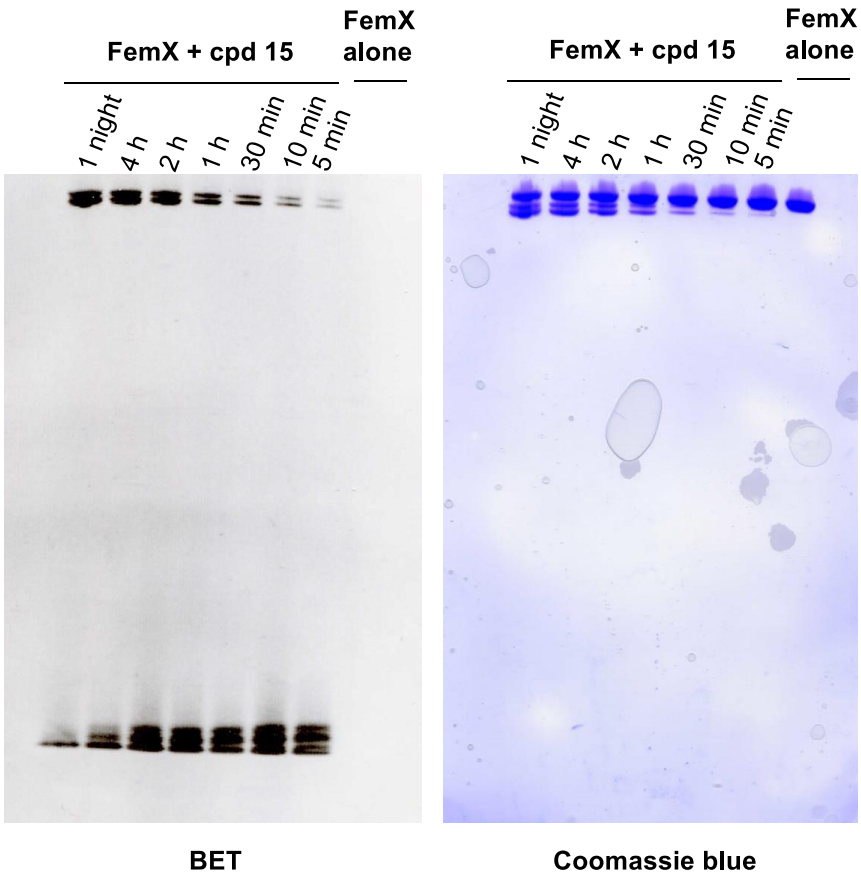

Figure 16: Gel showing the products of incubation of FemX with **15** at various times. Conditions: 30 µM $FemX_{Wv}$ (300 pmol), 20 µM cpd **15**, 30 mM Mes pH6 buffer, 10 µL volume. 37 °C under agitation at various times. Gel: 20 cm, 4 %, 12 % acryl/8M urea. Migration: 2 h, 600 V.

The maleimidyl-RNA **15** migrates much more than FemX, that stays on the top of the gel. After only 5 minutes of incubation with the electrophilic RNA, nucleoproteic complexes appear with similar migration as FemX, suggesting quick adduct formation. Very quickly, the electrophilic RNA shows degradation. Both these results indicate high reactivity and high instability of the motif. No Cys

residues being naturally present in FemX, the maleimide motif seems to be extremely reactive towards many amino acid residues.

To confirm this conclusion, the RNA-maleimide **15** was similarly incubated with various enzymes (**Figure 17**). FmhB, as well as FemX, is an aminoacyl-tRNA-dependent Fem-transferase. It possesses one Cys residue located in a beta foil, far from the RNA interaction site. AlaRS, GlyRS and SerRS are tRNA-dependent aminoacyl-tRNA synthetases. They respectively comprise 6, 8 and 5 Cys residues in their sequences. L,D-transpeptidase of *Enterococcus faecium* (Ldtfm) is a transpeptidase involved in the last steps of peptidoglycan synthesis. It is not a tRNA-dependent enzyme. The WT of LDtfm possesses one catalytic Cys residue, and the mutant has seen its Cys residue replaced by an Ala residue. The gel shows formation of covalent adducts with all of these enzymes, with no obvious correlation with the number of Cys residues or the recognition of a tRNA motif.

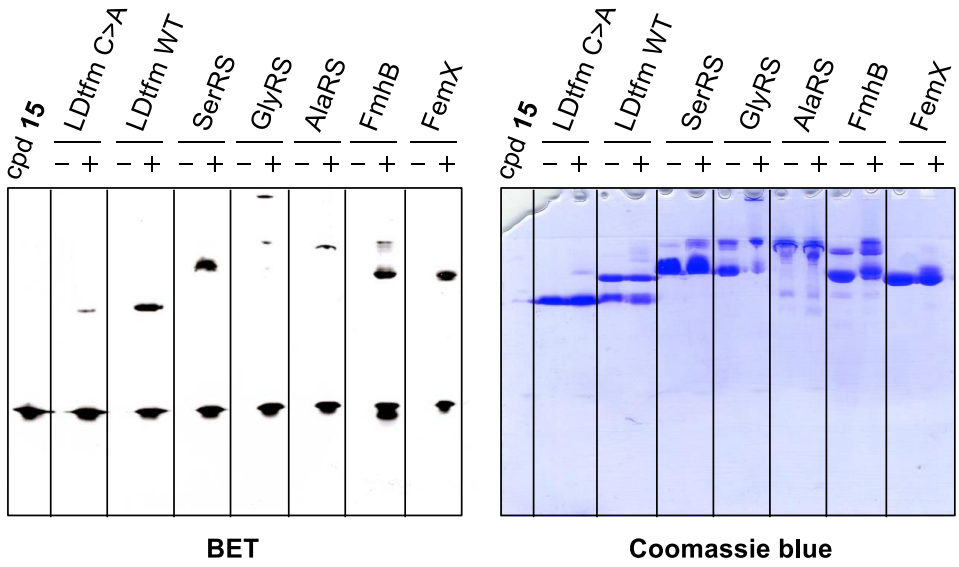

Figure 17: Gel showing the result of incubation of the electrophilic RNA **15** with various enzymes.

Those first results lead to the conclusion that the maleimide, despite supposed Cys specificity, reacts with many nucleophilic amino acid residues over all three types of tested enzymes. Site-specific introduction of a Cys residue into FemX sequence could therefore not lead to site-specific cross-linking. For this purpose, we moved on to the RNA-squaramates.

3.3.2. Synthesis of RNA-squaramates and RNA-squaramides

3.3.2.1. Chemical reduction

Starting from the intermediate 2'-azido-RNA, a prior reduction step yielding 2'-amino-RNA was necessary to graft the squaryl moiety. This synthesis was done on the azido-RNAs **10** and **12**, as well as

on a tetranucleotide ACCA **14** with the same 2'-azido modification. This last compound was used for optimization.

Such reductions, on 3'-azido-RNA, were reported by the group of Micura.[113] The use of the water-soluble triscarboxyethylphosphine (TCEP) in a Tris pH 8 buffer at -20 °C overnight yields the amino group with a 44 to 51 % yield after HPLC purification (**Scheme 31**). HPLC-monitoring shows complete conversion of the starting material after one night. Compounds **10**, **12** and **14** respectively lead to amino-RNAs **16**, **17** and **18**.

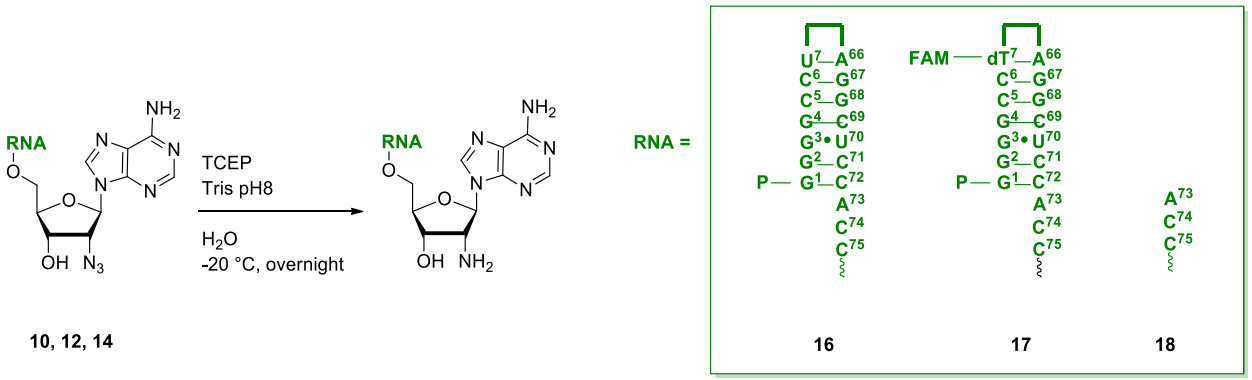

Scheme 31: Chemical reduction of the azido-RNA into amino-RNA

The amino-RNA can then be reacted with a squaric acid diester.

3.3.2.2. Squaramate synthesis

Despite the abundant literature concerning bioconjugation using squaric acid diester, in most examples, the squaramate is synthesized from a small molecule. Some optimization was thus necessary to synthesize RNA-squaramates.

First of all, to insure the viability of a squaryl linkage at the 2'-position, attempts were made at the nucleoside level. 2'-amino-2'-deoxyadenosine monomer **19** was reacted with diethylsquarate (**Scheme 32**). Subsequent squaramate **20** could be isolated in a good 80 % yield. Coupling of a lysine was then attempted with harsher and more basic conditions, which led to the corresponding nucleoside-lysine squaramide **21**. The loss of the benzoyl group due to basic conditions did not prevent the reaction from proceeding.

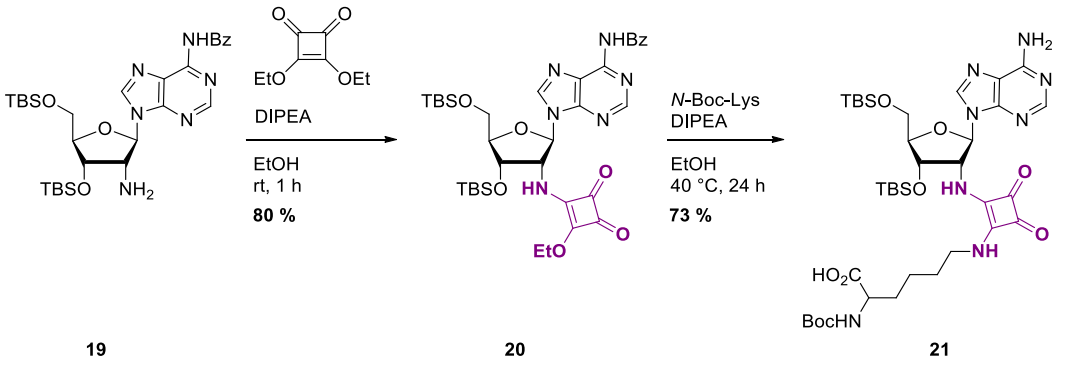

Scheme 32: Synthesis of adenosine-2'-squaramate and of adenosine-lysine squaramide.

Being now assured that the squaryl linkage was stable and able to react with a Lys residue at the 2'-position of a nucleoside, we moved on the oligoribonucleotide level. The ACCA-NH_2 **18** was used as a model. The diethylsquarate was dissolved in DMF and added to a solution of ACCA in an aqueous buffer. Tris pH8 buffer resulted in an unclean result, most probably because of reaction of Tris with the diethylsquarate. HEPES pH7.5 buffer gave cleaner results. 10 or 100 equivalents of diethylsquarate were tested and showed that conversion into the oligo-squaramate could be obtained in 3 h with 100 equivalents (**Scheme 33**).

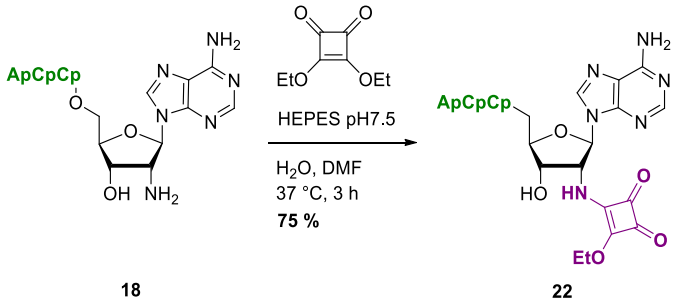

Scheme 33: Synthesis of a tetranucleotide-squaramate

The goal is to obtain oligonucleotides squaramates mimicking the acceptor arm of $tRNA^{Ala}$. Thus, those conditions were then applied to the oligos of interest, yielding the two RNA-squaramates **23** and **24** in 75 to 80 % yields, only differing by the presence or not of a fluorescent tag in position 7 (**Figure 18**). **24** was synthesized with dimethylsquarate to study the influence of the alkyl moiety on the squaramate.

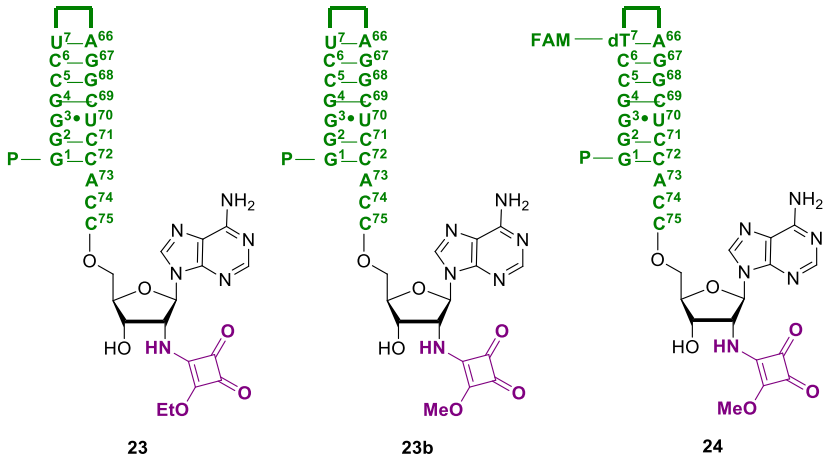

Figure 18: Structure of the $tRNA^{Ala}$ mimicking oligonucleotides-squaramates

These key intermediates were then investigated for enzymatic cross-linking and peptide conjugation.

3.3.2.3. Synthesis of a squaramide peptide-RNA conjugate

Squaramide peptide-RNA conjugates synthesis was realized in collaboration with Dr Matthieu Fonvielle in the group of Dr Michel Arthur (Centre de Recherche des Cordeliers, Paris).

The oligonucleotides-squaramates **22** and **23** were reacted with UDP-MurNAc-pentapeptide (UM5K). This peptide comprises an internal Lys residue that is aminoacylated during FemX-catalyzed reaction with Ala-$tRNA^{Ala}$. This second amine substitution, as described in the literature, requires more basic conditions and longer reaction times. In our case, successful couplings were observed in a borate pH9.2 buffer, at 37 °C over three days (**Scheme 34**).

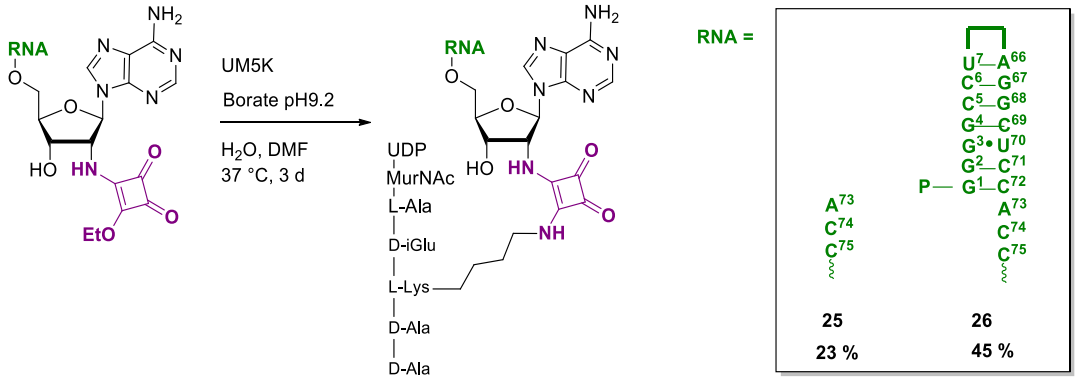

Scheme 34: Synthesis of peptidyl-RNA squaramide conjugates with UM5K

These peptidyl-RNA squaramide conjugates **25** and **26** are similar to bi-substrates inhibitors previously synthesized in the group through CuAAC, with the squaryl moiety replacing the triazole. Peptidyl-RNA conjugate **26** was evaluated as a competitive inhibitor of FemX and resulted in an IC_{50} value of 123 ± 6 nM. Although this submicromolar value is encouraging, it is a 1000-fold higher than the triazole linkage

analog. However, its synthesis is much more straightforward as it does not require a modified alkyne-bearing UM5K analog but the natural UM5K itself. Thus, the squaryl linkage, though less recognized by FemX than the triazole linkage, is still interesting for our studies.

These examples illustrate that deprotected peptides can be conjugated to RNA-squaramates through their lysine residues. The use of squaramide amine-amine coupling can be considered as a method of access to RNA-peptide conjugates.

On a larger scale, the interesting reactivity of squaramates towards terminal Cys residues could also be taken advantage of. Through initial attack by the thiol group and subsequent S to N acyl-transfer, terminal Cys can react with squaramates with enhanced kinetics.[182] RNA-squaramates could then be precursors to RNA-peptide conjugates with larger and more complex peptides with a Cys residue at their N-terminus. Combined with the work of Micura *et al.* regarding native chemical ligation and desulfurization methods,[116,117] the RNA-squaramates obtained simply from azido-RNA could be precursors to a wide variety of RNA-peptide conjugates.

3.3.2.4. Cross-linking between FemX and RNA-squaramates

Cross-linking experiments and characterization of these adducts have been done in collaborators with Dr Matthieu Fonvielle.

With the objective of cross-linking K305 among all 19 Lys residues of FemX, our RNA-squaramate **23** was incubated with FemX. Similar conditions as for the peptide-RNA conjugates synthesis were used, notably the borate pH9.2 buffer. Only marginal cross-linking could be observed in those conditions, suggesting very slow kinetics. In light of the relatively low affinity of the squaryl moiety for the enzymatic pocket, we hypothesized that the ethoxy group of the squaramate was a supplementary obstacle to the proper positioning of the squaramate in the catalytic pocket of FemX. Synthesis of a similar squaramate presenting a methoxy group instead of the ethoxy group was carried out. The subsequent **methyl-RNA-squaramate 23b** was incubated with FemX, and gave significant cross-linking (**Scheme 35**).

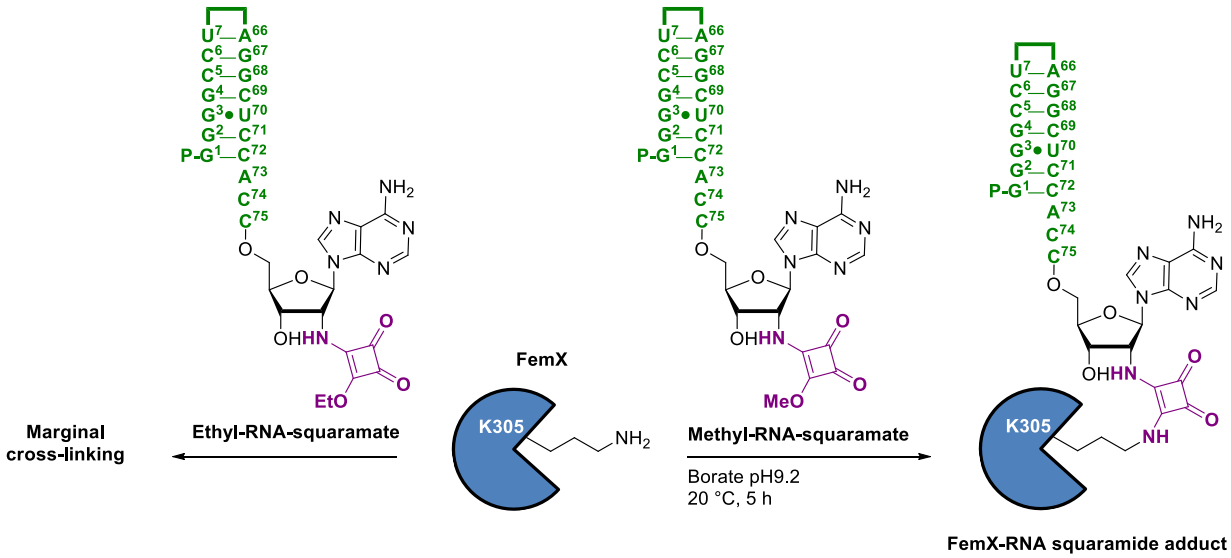

Scheme 35: Formation of covalent adduct between FemX and RNA-squaramates **23a** (ethyl-squaramate) and **23b** (methyl-squaramate).

Gel analyses of the cross-linking experiments show that RNA-squaramate **23b** site-specifically covalently labels K305 (**Figure 19A**). The gel was revealed with coomassie blue and anti-Fem antibodies. This adducts is not formed when FemX WT is replaced by a mutant FemX in which K305 has been replaced by an alanine residue.

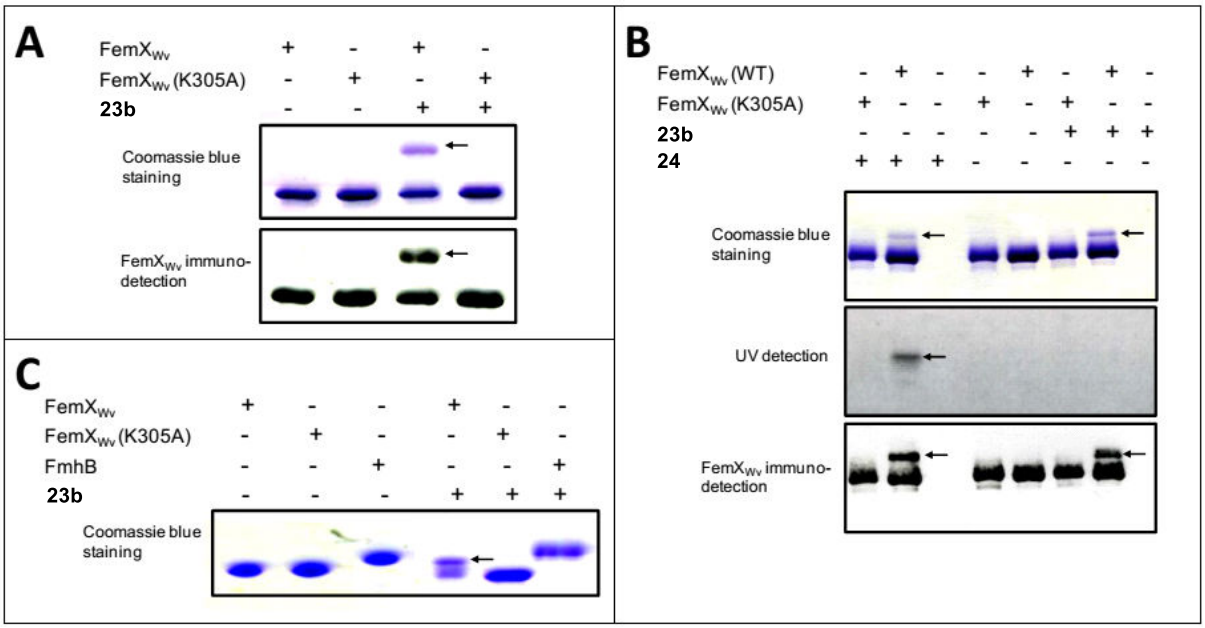

Figure 19: Gel analyses of cross-linking experiments. A: Cross-linking of **23b** with FemX WT and FemX K305A mutant. **B.** Cross-linking experiments with squaramates **23b** and fluorescent **24b**. **C:** Cross-linking experiments of **23b** with FemX WT and mutant and FmhB.

BET revelation did not allow the nucleoproteic nature of this adduct to be established. We hypothesize that the oligonucleotide is "hidden" in the catalytic pocket of FemX and therefore protected from BET intercalations. To fully identify the nucleoproteic complex, the RNA-methyl-squaramate **24** with the fluorescent tag on dT7 was cross-linked with FemX. The subsequent adduct was revealed with Fem antibodies, coomassie blue, and fluorescein detection, thus establishing the presence of our oligo-squaramate **24** in the observed adducts (**Figure 19B**).

Eventually, to validate our approach, attempts were made to cross-link squaramate **23b** with FmhB, an essential Fem-transferase of *Staphylococcus aureus*. This Fem-transferase does possess a K305-homolog Lys residue, conserved among all FemABX family members, in addition to 49 additional Lys residues. FmhB, however, catalyze the transfer of a Gly residue from a Gly-tRNA^{Gly}, unlike FemX that recognizes only Ala-tRNA^{Ala}. No cross-linking could be observed, confirming that our RNA-squaramate system requires the enzymatic recognition of the RNA moiety, and supports our strategy that only recognition and appropriate positioning of the squaramate allow squaramide formation and cross-linking with the enzyme.

To conclude, thanks to the moderate reactivity of squaramate, in addition to appropriate RNA recognition and positioning, we were able to site-specifically label the K305 residue, without side-reactivity with any other amino acid or any other Lys residue.

In the future, this RNA-squaramate platform can be adapted for other members of the FemABX family. Variations in the sequences will mimic different tRNAs and will allow recognition by various Fem-transferases. Cross-linking with their conserved Lys residue can then lead to adduct formation, which could help to get structural data. Another application would be the identification of new unknown members of the enzymatic family, making these RNA-squaramates suitable identification probes.

3.3.3. Optimization of traceless Staudinger ligation for aa-tRNA analogs

3.3.3.1. The traceless Staudinger ligation method and its applications for biomolecules

The traceless Staudinger ligation is a method first described by the groups of Bertozzi[183] and Raines[184] consisting in the transfer of the chemical group of interest from a functionalized phosphine toward an azido group, resulting in an amide bond (**Scheme 36**).

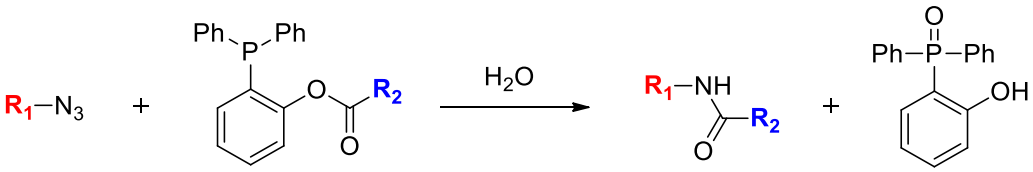

Scheme 36: Example of traceless Staudinger ligation

Mechanistically, the reaction starts as a Staudinger reaction with interaction between the phosphorus(III) and the azido group leading to nitrogen release (**Scheme 37**).[185] The nucleophilic nitrogen atom of the resulting iminophosphorane then attacks a (thio)ester positioned on the phosphine to form an amide bond. A final hydrolysis steps leads to the release of the amide ligated product and the oxidized phosphine.

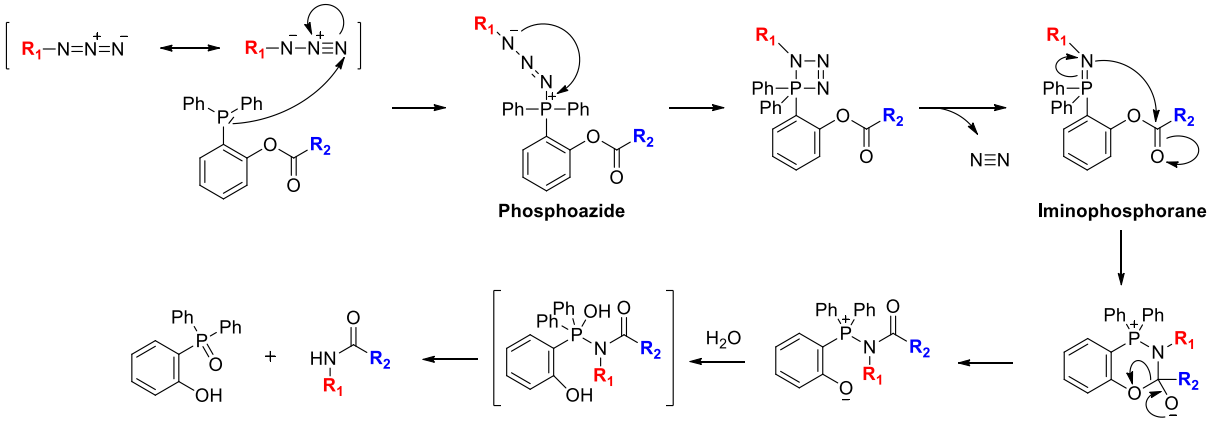

Scheme 37: Mechanism for the traceless Staudinger ligation

This ligation is interesting for bioconjugation as the azido group can be introduced in most biomolecules. Unlike CuAAC, it does not require a metal catalyst and leads to the formation of naturally occurring amide bonds. However, the nature of the functionalized phosphine with an activated ester is thought to be incompatible with a reductive milieu, and generally overly reactive with nucleophiles. For this reason, examples of the traceless ligation are less numerous than examples of the non-traceless Staudinger ligation.[186,187]

The traceless Staudinger ligation was reported for functionalization of proteins and polysaccharides.[188] Its use in the group of Bernardi with unprotected carbohydrates tends to show that the phosphine reagent can tolerate unprotected biomolecules and confirms the reaction's chemoselectivity.[189,190] For this reason, we decided to investigate the use of this method for functionalization of our 2'-azido-RNA.

The reaction conditions were first investigated at the 2'-position of a nucleoside, before being optimized on an oligo. To avoid side-reactions, optimization was carried out not with an electrophile but with a model acetyl group.

3.3.3.2. Optimization on a nucleoside

First, the required phosphine reagent needed to be synthesized. The corresponding acetyl-bearing phosphine reagent **27** was synthesized according to Bernardi *et al.* from (2-hydroxyphenyl)diphenylphosphine (**Scheme 38**).[189,191]

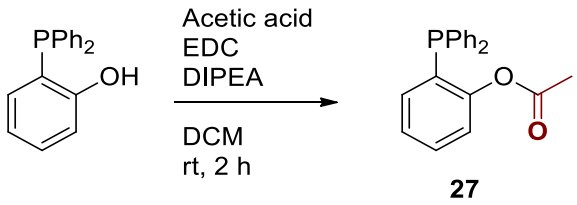

Scheme 38: Synthesis of the functionalized phosphine reagent

Attempts to perform traceless Staudinger ligation on a model 2'-azido-nucleoside with the conditions used by Bernardi *et al.* or by the original Bertozzi method were unsuccessful. Among examples in the literature of traceless Staudinger ligation conditions, we were interested in the one from Mamat *et al.* because of the nature of the solvent: a DMF/Water mixture that could be compatible with nucleic acid chemistry.[192] Attempts were performed with these conditions at various concentrations (**Scheme 39**).

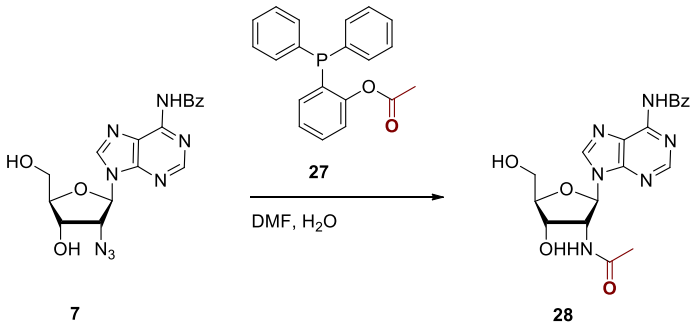

Scheme 39: Traceless Staudinger ligation attempts on a nucleoside using Mamat's conditions

At 0.3 M of both reagents, conversion was rapidly observed. After one night at room temperature, **28** could be isolated in 31 % yield.

At 0.03 M, no conversion was observed at room temperature during 1 day. Heating of the reaction mixture at 70 °C for four hours led to isolation of **28** in 71 % yield.

At 0.003 M, only traces of **28** could be observed, even after one day of heating.

This overview allowed these conditions to be adapted for an oligo.

3.3.3.3. Optimization on an oligoribonucleotide

Optimization was, again, done on the azido-tetranucleotide **16**. Because of the different concentrations in biomolecule chemistry, adaptations had to be made to Mamat's conditions. With a 100 µM concentration of oligo, we first tried the reaction using 300 equivalents of functionalized phosphine **27** to compensate the dilution. The mixture was heated at 37 °C overnight. Complete conversion of the starting material was observed on HPLC, but the new peak showed a retention time much higher than expected on RP-HPLC. MS analysis revealed that the transfer of acetyl was

successful, but the phosphine, instead of being oxidized with water, formed an adduct on a nucleobase and led to compound **29** (**Scheme 40**).

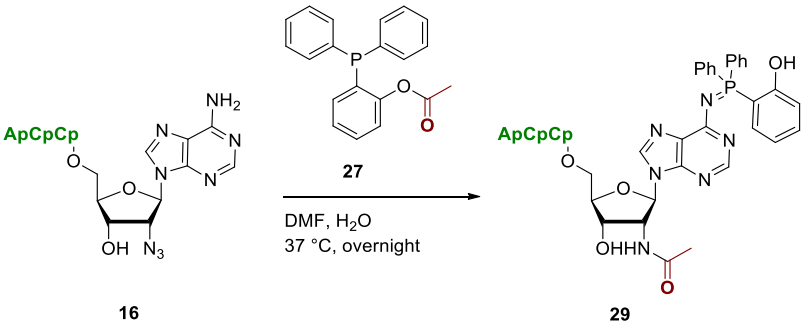

Scheme 40: Traceless Staudinger ligation on an azido-tetranucleotide

Similar adducts are common on nucleobases in reactions involving triphenylphosphine, for example halogenation reactions.[193] On nucleosides, acidic treatment is sufficient to remove this adduct. Treatment of **29** in an acidic buffer should then be able to remove the adduct. In the case of high stability of the adduct, this could be taken advantage of by labelling the triphenylphosphine reagent with another tag. That way, our method would allow bi-functionalization in one step. Many methods are reported for synthesis of further functionalized phosphine reagents.

3.3.3.4. Outlooks

This method provides access to amide bonds directly from azido groups at the 2' position in one step and with no catalyst. In the future, application of this method to electrophilic motifs will be carried out. In the case of reaction between the nucleophilic phosphorus(III) atom and the electrophilic motif, we could still introduce a "hidden" electrophile in the form of Cys that would be later converted into dehydroalanine.[194]

Other than electrophiles, this method can be an efficient way to label RNA with tags of interest in order to synthesize of RNA conjugates with many other biomolecules. Virtually any molecule bearing a carboxylic acid group can be coupled with the phosphine precursor, thus providing access to molecular diversity.

4. Conclusion

In this chapter we have developed:

- The synthesis of maleimidyl-RNA by CuAAC which is able to react with various proteins. The lack of selectivity, however, led us to develop more residue-selective and site-specific electrophilic RNA.
- The synthesis of RNA-squaramates, that were used first as precursors for RNA-peptide squaramide conjugates, and then for site-specific cross-linking with FemX on the crucial Lys 305 residue. These squaramates could, in the future, be used as probes for enzyme identification in RNA biology and as tools for the study of therapeutically relevant FemABX family members. The report of this study has been accepted for publication in Angewandte Chemie, International Edition (DOI: 10.1002/anie.201606843R1).
- Optimized conditions for application of the traceless Staudinger ligation method for the one-step chemoselective introduction of a motif of interest with a naturally-occurring amide bond. This method could be applied to electrophilic motifs, or any other useful tag for labeling. Bioconjugation of large biomolecules with RNA using this method can also be envisioned.

Part 2

Goals, results, and discussion

Chapter 2

Synthesis of fluorinated nucleosides for conformational studies

1. Introduction

1.1. The conformation of the ribose, a key parameter in nucleic acid chemistry

The sugar-ring of nucleosides exists in two major conformations in rapid equilibirum, generally referred to as the *North* and *South* types[195] (**Scheme 41**).

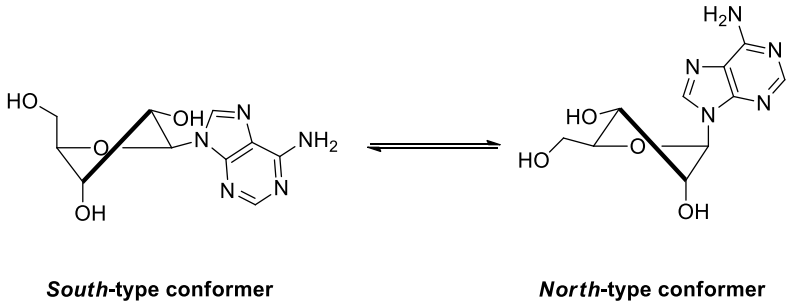

Scheme 41: Equilibrium between *North*- and *South*-types conformers for adenosine

The most favored conformation adopted by a nucleoside is the result of contributions of various factors, the most important of them being the electronic gauche and anomeric effects as well as steric hindrance from the nucleobase. This conformation can be classed within the pseudorotational cycle between the perfect *North*- and *South*-types which is a function of all conformational parameters such as torsional and rotational angles (**Figure 20**).[196] In the case of nucleosides and nucleotides, the conformation adopted by the sugar ring directly influences the positioning of the nucleobase and the hydroxyl groups. DNA and RNA differ in that regard, DNA mostly exhibiting *South*-conformation and RNA *North*-conformation. The backbone conformation is responsible for the stacking of the nucleobases. As a result, only one conformer of a given nucleos(t)ide can be expected to be recognized by a specific enzyme. Thus, it is not surprising that the conformation of nucleosides, nucleotides and nucleic acids is a key parameter for their *in vivo* destiny,[197] from metabolism to interaction with their targets. This feature has been notably important for nucleos(t)ide antiviral compounds: their efficiency relies in their ability to be first transformed into active triphosphate compounds, and then to be incorporated into nucleic acids by polymerases. It has been shown that the reverse transcriptase of HIV can discriminate nucleotides on the basis of conformation.[198,199] It has also been shown that a HSV kinase preferentially phosphorylate *South*-types nucleosides and its DNA polymerase rather incorporate *North*-types nucleosides.[200]

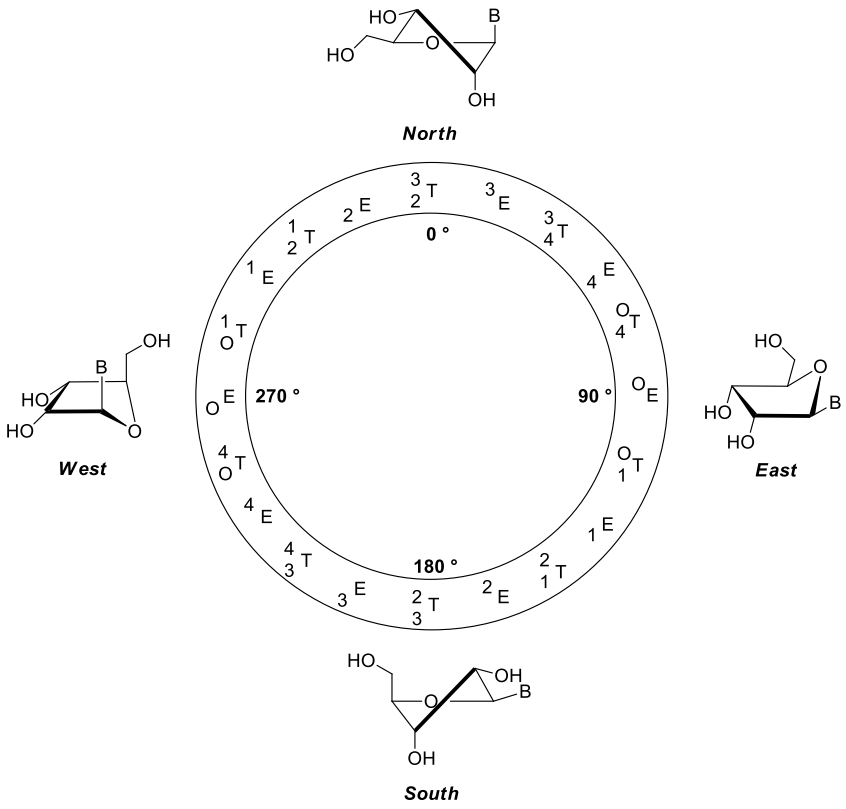

Figure 20: Pseudorotational cycle and major conformations. E: Envelope conformations. T: Twist conformations. Superscript numbers and subscripts numbers indicate the atoms away from the plane formed by the other atoms.

The acknowledgment of the pivotal role of sugar puckering has led to the need to control and modulate the conformation of the sugar ring of nucleosides. The principle approach to achieve control of conformation is the synthesis of modified pentafuranose rings in which bridges or cycles render one conformation impossible. These compounds and their derivatives are known as “locked” nucleic acids or “bridged” nucleic acids (LNA, BNA).[201,202] Their ability to exist in only one conformation makes them useful tools to evaluate one enzyme’s conformational preference or for structural studies of nucleic acids. Some of them, due to different binding properties or their resistance to nucleases, can also be considered for drug discovery. Numerous examples of such compounds have been reported in the literature (**Figure 21**).[203] The main drawback of this approach is the bulkiness of the bicyclic motifs that could prevent enzymatic recognition in the cases where the sugar-ring itself is a recognition element.

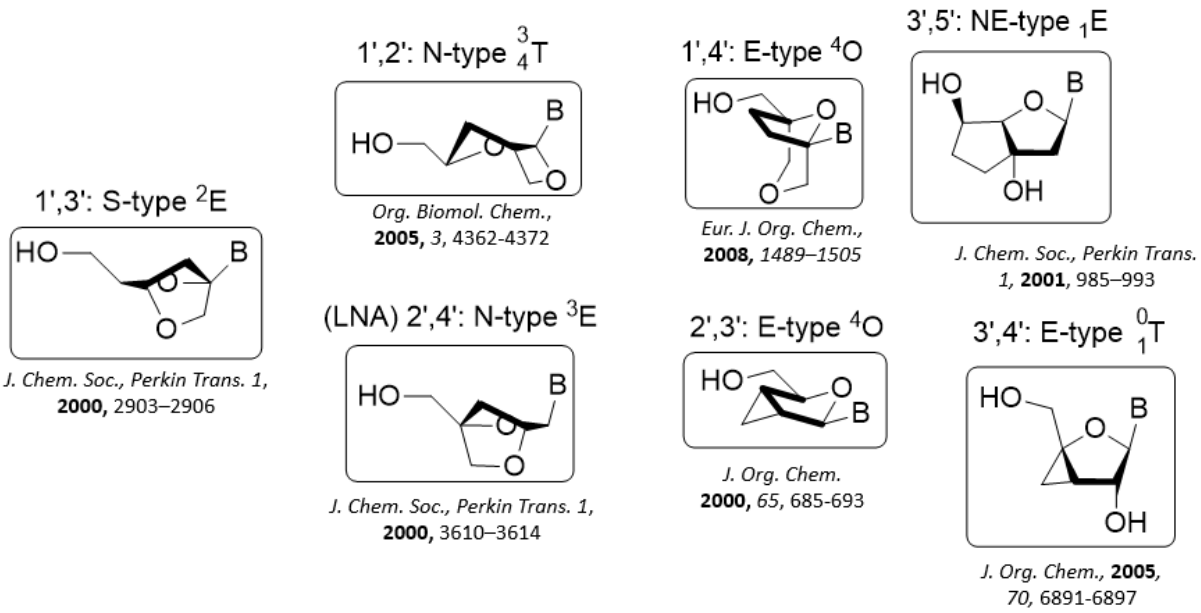

Figure 21: Examples of locked or bridged nucleosides and their adopted conformations

Another approach is the synthesis of "frozen" nucleoside: by introducing highly electronegative functional groups such as a fluorine atom, the contribution of the gauche effect increases and leads to a displacement of the equilibrium between *North* and *South*. Examples of such fluorinated "frozen" nucleosides have been reported in 2'-position,[108,204] in the 3'-position[205,206] or, more recently, in both the 2' and 3' positions[207] or both the 2' and 4'-positions.[208,209,210] Unlike BNA and LNA, such analogs still exhibit sugar rings similar to the natural ribose.

In the case of Fem-transferases, the amino acid transfer occurs at the 2'-position. Thus, we focused on the examples in which the fluorine atom is introduced at the 3'-position. At the 3'-position, a fluorine atom in the *ribo* configuration favors a *South*-type conformation, whereas a fluorine atom in the *xylo* configuration favors a *North*-type conformation (**Scheme 42**).[206]

For both of them, the favored conformation is the one in which the C-F bond is positioned in the same plane as a weakly-polarized C-C or C-H bond instead of a polarized C-O bond, as shown in the Newman projections.

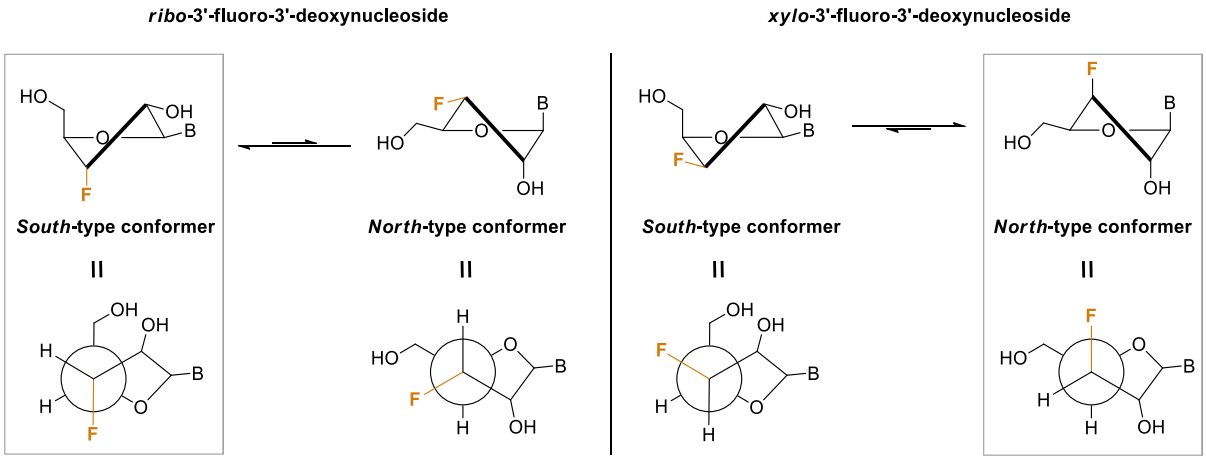

Scheme 42: Equilibrium between *North*- and *South*-types for 3'-fluoro-3'-deoxynucleosides, in Cram and C3'-C4'-Newman representations. The most stable conformations are shown framed.

1.2. The conformation of A76 in tRNAs and aa-tRNAs

The conformation of the 3'-terminal adenosine of tRNA and aa-tRNA is a key element for their roles in translation.

In the non-acylated tRNA in solution, the adenosine 76 sugar ring adopts a *North*-type conformation which allows stacking of the nucleobases of the terminal CCA sequence. This stacking is lost upon aminoacylation by aaRS that causes a shift in the conformational equilibrium, favoring *South*-type conformation in the A76 of aa-tRNA. This conformational shift is thought to be key for recognition of the aa-tRNA by the elongation factor EF-Tu. In crystallized complexes of EF-Tu with aa-tRNA, the conformation of A76 is definitely *South*-type.[211,212]

As previously mentioned, puromycin is an antibiotic resembling the 3'-end of aa-tRNA that acts as a chain terminator in translation. Puromycin comprises an adenosine moiety that mostly adopts *North*-type conformation in solution,[213] as well as in solid-phase as shown in the crystallographic structure of puromycin in the A-site of the ribosome.[214] This conformation appears to be necessary for the adequate position of the amino function attacking the peptidyl-tRNA in the P-site.

If puromycin is considered as a good model to study the conformation of aa-tRNA in the A-site of the ribosome, it would be logical that the A76 of aa-tRNA also adopts a *North*-type conformation to allow peptidyl-transfer. In that case, it follows that once freed from the elongation factor EF-Tu in the A-site, the A76 of aa-tRNA would again shift its conformation from *South*-type to *North*-type.

The exact variations of the A76 sugar-ring conformation remain unclear, but it is undeniable that its role is pivotal in the different stages of translation. This led us to wonder about its role in its recognition by the FemX transferase and in the mechanisms that allow Fem-transferases to recognize aa-tRNA and

divert them from the translation process. Given the apparent key role of conformation in recognition with elongation factor, it seems interesting to investigate the conformation of A76 in Fem-recognition.

Another reason to investigate the conformational preference of Fem-transferases is that, as previously shown with antiviral nucleosides, the development of drugs based on modified nucleosides and nucleotides can be greatly impacted by conformational preferences of the target.

1.3. Conformationally-restricted nucleic acids for FemX

In our group, the synthesis of 3'-fluorinated Ala-tRNA^{Ala} and tRNA^{Ala} analogs has been undertaken[215] for several reasons:

- The role of the vicinal 2' and 3' hydroxyl groups is extremely important in tRNAs. Aminoacylation of the 2' or the 3'-position and isomerization of these positions rule their interaction with enzymes and determine their fate, *ie* enter the translation process or move on to their other roles. In peptidoglycan synthesis, FemX catalyzes amino acid transfer from the 2'-position, and it has been shown that the free 3'-hydroxy group, though not essential for catalysis, remains important for catalytic efficiency. It has been hypothesized that this is due to its participation in the proton shuttling during the catalytic mechanism.[30] Replacing the 3'-hydroxy group by a fluorine atom that mimics its polarity and is a weak hydrogen bond acceptor, was interesting in order to gain access to non-isomerizable analogs in order to further explore the role of the 3'-hydroxy group.
- The implementation of a fluorine atom in the 3'-position also tends to "freeze" the conformation of the nucleoside, in the sense that its electronic properties tend to displace the *North-South* equilibrium and favor one conformation over the other.

Locked and bridged nucleic acids, despite their greater control on the sugar-ring conformation, generally present bulky bicyclic motifs that could be incompatible with FemX recognition.

For these reasons, "frozen" *xylo* and *ribo* 3'-fluoro analogs of tRNA^{Ala} and a *xylo* 3'-fluoro analog of Ala-tRNA^{Ala} were synthesized (**Figure 22**).[215] Though no conclusion has been yet drawn from biological evaluation concerning the role of the 3'-hydroxy, the percentages of *North* and *South* conformers populations were measured for the fluorinated compounds by ^{1}H NMR. An empirical method has indeed been reported allowing to deduce the relative percentage of *North* and *South* conformers from the scalar coupling constant between the protons H1' and H2' through the following formula: % *S*-type = 10 $J_{1'-2'}$.[216] In this work, this measurement on deprotected dinucleotide allowed to verify the influence of the 3'-fluorine atom: in the *xylo* configuration, *North* conformers are favored, and in the *ribo* configuration, *South* conformers are favored.

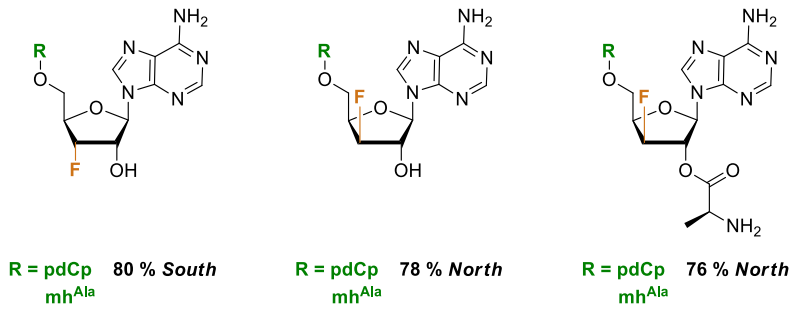

Figure 22: 3'-fluorinated compounds previously synthesized. The percentage of *North* and *South* conformers is indicated for dinucleotides according to ^{1}H NMR measurements. mh^{Ala} stands for microhelix mimicking the acceptor arm of tRNA^{Ala}.

Because there is a rapid and dynamic equilibrium between *North* and *South* conformers, it is difficult to monitor an enzyme conformational preference. Measurement of the affinity of both compounds through evaluation of their inhibition potencies, for example, would not allow us to deduce without doubt if FemX recognizes one conformer better than the other. Besides, the *xylo* and *ribo* compounds are diastereoisomers and any difference in affinity might also be caused by this configuration difference rather that by the conformational contribution. Overall, evaluation of the recognition by measuring the inhibition constant would not allow conclusions to be made regarding conformational preference.

In order to really monitor the conformation of the nucleoside preferred by FemX, the method of choice would be a crystallography study. The co-crystallization of fluorinated compounds in both *xylo* and *ribo* configurations would allow to see if they co-crystallize with FemX in their expected favored conformation or not. If both structures show the same conformation, that would be an argument for conformational preference.

Comparison to previously obtained crystallographic structures could also give information about the conformational preference of the enzyme. In previous work, the co-crystallization of FemX with a peptidyl-RNA conjugate with a triazole at the 2'-position and a OH at the 3'-position of the terminal adenosine exhibited a *South*-type conformation of the sugar ring (**Figure 23**).[30]

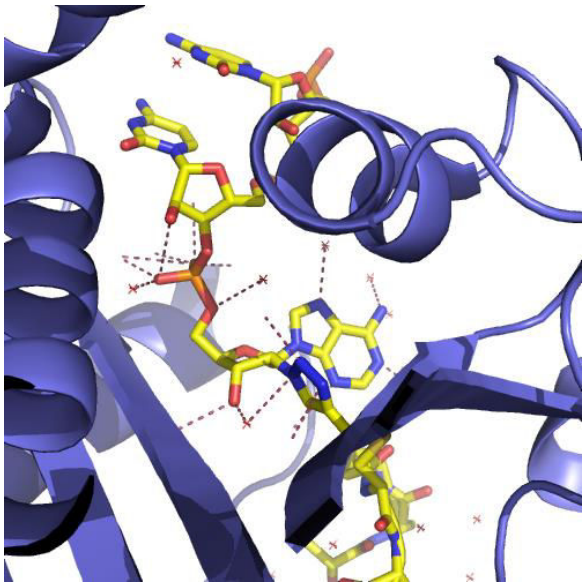

Figure 23: Crystallographic structure of the CCA terminal motif of the peptidyl-RNA conjugate in the catalytic site of FemX. The sugar-ring of A76 shows a *South* conformation.

In order to obtain such structures with fluorinated analogs, the synthesis of fluorinated compounds able to crystallize with FemX is required. Previous work in our group shows that a bi-substrate inhibitor comprising a minimal RNA moiety recognized by FemX is needed to achieve co-crystallization.[30] The targeted compounds are bases on this scaffold (**Figure 24**).

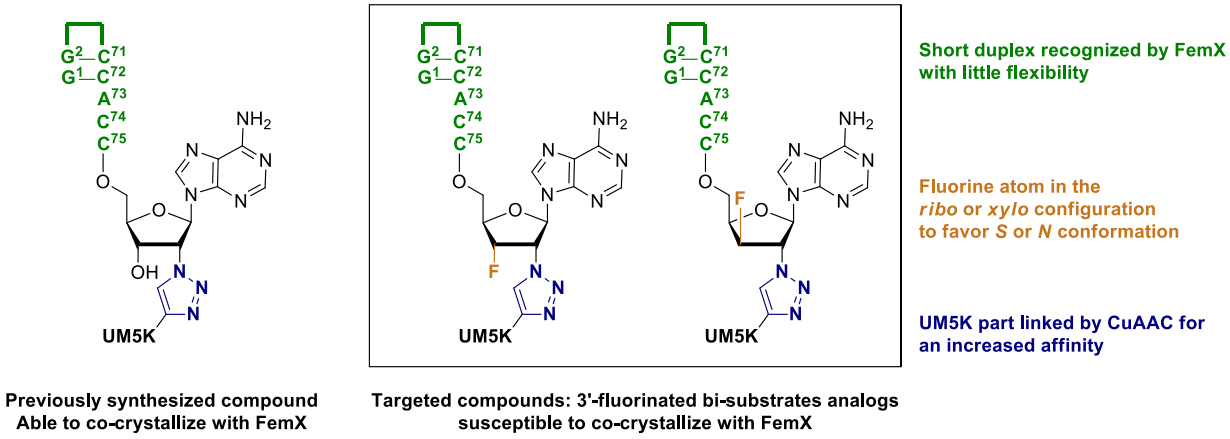

Figure 24: Previously synthesized and crystallized compound as a scaffold for the targeted fluorinated compounds

To access such compounds, a retrosynthetic scheme can be drawn, relying on the previous synthesis of bi-substrates compounds (**Scheme 43**). The CuAAC-mediated ligation of the alkyne-bearing UM5K analog is intended to be the last step as a chemoselective post-functionalization reaction. The 2'-azido-2',3'-dideoxy-3'-fluoro RNA can be obtained by solid-phase synthesis from the corresponding solid-support. This functionalized solid-support can itself be obtained through multi-step synthesis *via*

nucleoside chemistry from commercially available adenosine. CuAAC and SPS have been optimized for similar compounds, but the multi-step syntheses allowing functionalization of both the 2’ and 3’ positions with two different functional groups – the azido group and the fluoro group – and controlled stereochemistry were not optimized.

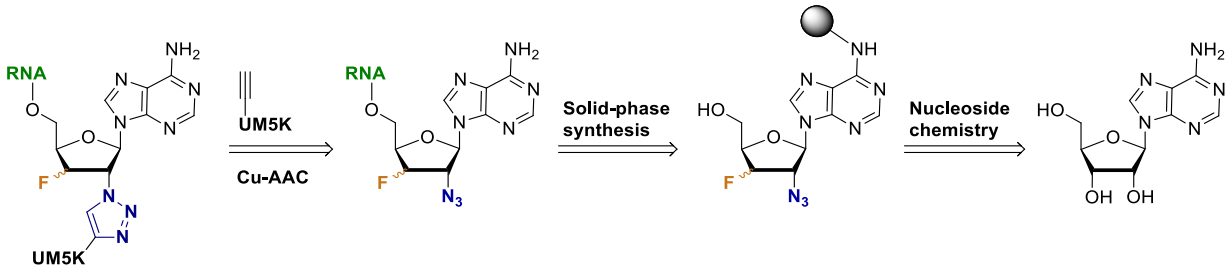

Scheme 43: Retrosynthetic scheme from 3'-fluorinated bi-substrate compound to commercially available adenosine.

In order to obtain separately the *ribo*- and *xylo*-configured fluoro-azido nucleosides, two synthetic routes must be developed from adenosine.

2. Synthesis of the *ribo* monomer

2.1. Retrosynthetic strategy

The functionalization of the 2’ and 3’ positions by azido and fluoro groups in *ribo* configuration was reported in the group of Strazewski.[108] In their study, the 3’-fluoro-2’-azido compound was a minor product, as they were looking to synthesize 2’-fluoro-3’-azido adenosine monomers (**Scheme 44**).

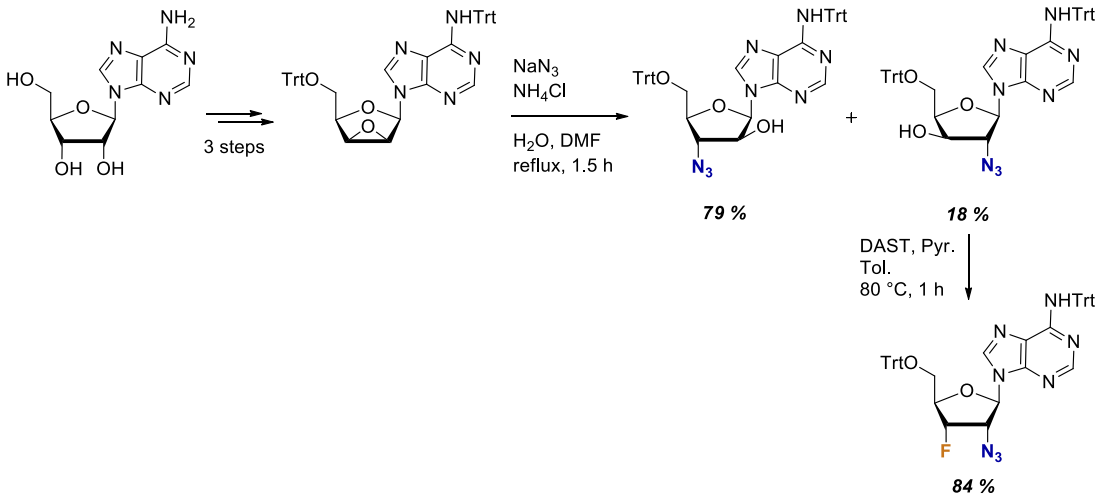

Scheme 44: Synthesis of a 2'-azido-2',3'-dideoxy-3'-fluoroadenosine monomer reported by Strazewski *et al.*[108]

Nevertheless, their strategy could still be modified to lead to our desired compound. The key intermediate in their synthetic route is the *lyxo*-epoxide **A**: nucleophilic opening of this epoxide allows to obtain *anti*-2',3'-difunctionalized adenosine **B** and **C** (**Scheme 45**). Both fluorination and azidation methods rely on SN2 mechanisms, thus, functionalization of this *anti* hydroxyl group leads to the desired *syn* 2',3'-bisfunctionalized compound.

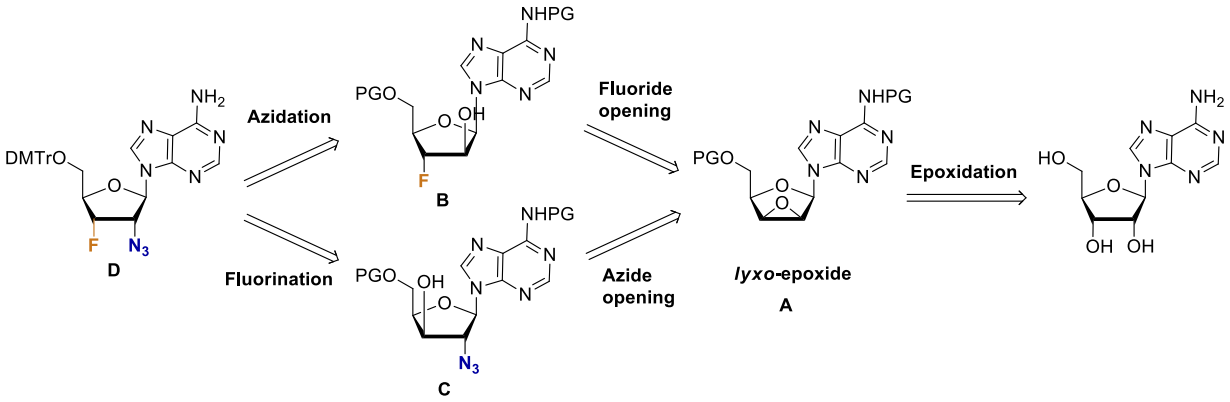

Scheme 45: Retrosynthetic scheme for the *ribo*-configured monomer

In the literature, such *lyxo*-epoxides are described as prone to regioselective 3'-nucleophilic opening,[108] presumably caused by electronic effects from the anomeric center[217] or sugar-ring conformation.[218] For this reason, we proposed that the targeted compound **D** could be obtained through fluoride opening of the *lyxo*-epoxide **A** and subsequent azidation of **B**.

An alternative strategy would be the azide-opening of the *lyxo*-epoxide **A** and subsequent fluorination **C**, but the expected 3'-regioselectivity would have to be addressed and modified by the reaction conditions to obtain acceptable yields.

2.2. Synthetic results

2.2.1. Synthesis of the *lyxo*-epoxide

The synthesis of the *lyxo*-epoxide is in accordance with the literature.[108] Commercially available adenosine is first tritylated in the 5'-position and on the nucleobase to give compound **30** (**Scheme 46**). The 2'- and 3'-hydroxyl groups are activated in the form of triflates to lead to the bis-triflate **31**. Epoxidation then proceeds in presence of water and TBA-NO_2 (tetrabutylammonium nitrite). In order to prevent the attack of two water molecules, the reaction is performed in a biphasic mixture of water and toluene, with TBA-NO_2 acting as a phase-transfer reagent. This method allowed us to obtain the epoxide **32** with an excellent 90 % yield.

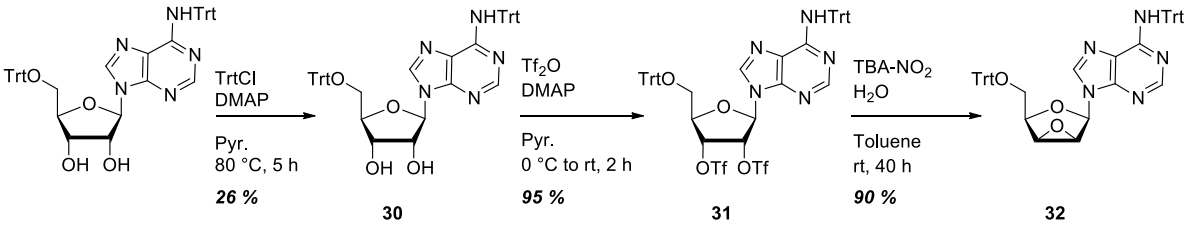

Scheme 46: Synthetic route leading to the *lyxo*-epoxide of adenosine

This epoxide could then be reacted with nucleophiles for opening.

2.2.2. Nucleophilic opening of the *lyxo*-epoxide.

The *lyxo*-epoxide was reacted in presence of various fluoride sources in several solvents, as described in **Table 3**.

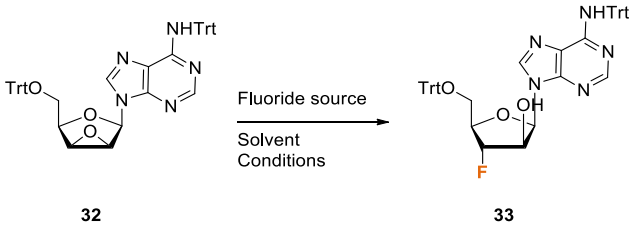

Entry	Fluoride source	Solvent	Conditions	Outcome
1	NaF	DMF	Rt, overnight	SM
2	NaF	DMF	Rt to reflux, overnight	SM + degradation
3	CsF	DMF	Rt, overnight	SM
4	CsF	DMF	Rt to reflux, overnight	SM + degradation
5	KHF_2	DMF	Rt, overnight	SM
6	KHF_2	DMF	Rt to reflux, overnight	SM + degradation
7	AgF	DMF	Rt, overnight	SM
8	AgF	DCM	Rt, overnight	SM
9	TBAF	THF	Rt, overnight	SM
10	TBAF	THF	Reflux, overnight	SM, degradation, traces of **33**
11	TBAF	THF, DCM	Reflux, overnight	SM
12	KHF_2	Ethylene glycol	Reflux, 24 h	Degradation
13	NaH, KHF_2	Ethoxyethanol	Reflux, 24 h	**33**, 45 % yield
14	NaH, KHF_2	Methoxyethanol	Reflux, 24 h	SM, Degradation
15	TBAF	MeCN, THF	Rt, overnight	SM

16	TBAF	MeCN, THF	Reflux, overnight	Degradation
17	TBAF	MeCN, THF	Reflux, 6 h	**33**, 67 % yield

Table 3: Reaction conditions used for fluoride-mediated opening of the *lyxo*-epoxide.

In the first approaches, described in entries 1 to 11, the screened fluoride sources were NaF, CsF, AgF, TBAF, KHF_2 and the solvents DCM, THF, and DMF depending on the solubility of the reagents. No more than traces of the desired compounds could be obtained. In those attempts, little conversion of the starting material was observed by TLC-monitoring. Increased reaction time or temperature led to degradation.

Similar examples to our case were reported in the literature. Miyai *et al*. described the use of KHF_2 in ethylene glycol at reflux allowed the fluorinated compound with a 41 % yield with the unprotected *lyxo*-epoxide of adenosine.[219] Those conditions gave no result in our case for two reasons: the ditritylated compound **32** was almost insoluble in ethylene glycol, and reflux of ethylene glycol (boiling point of 197 °C) led to a mixture of detritylated compounds (entry 12).

A conclusive result was obtained with adapted conditions from Srivastav *et al.*: the use of a mixture of KHF_2 and NaF in 2-ethoxyethanol at reflux (bp = 135 °C) for one day.[218] We applied these conditions to compound **32** and obtained compound **33** with a 45 % yield (**Method 1** in **Scheme 47**). A clear regioselectivity in favor of the 3' opening was observed by NMR, with a 3 to 1 ratio. Over the course of this study, the same results were reported in very similar conditions,[207] confirming our approach. However, drawbacks of this strategy emerged: the very similar polarity of **33** and **32** and the presence of residual 2-ethoxyethanol make purification extremely difficult. The solvent, 2-ethoxyethanol, has a high boiling point and is miscible with most organic solvent and is thus hard to remove for several synthetic steps. Its NMR signals overlap with the 5' protons of nucleosides and make analysis difficult. Attempts to replace it with 2-methoxyethanol failed, presumably because of lesser solubility of **32**.

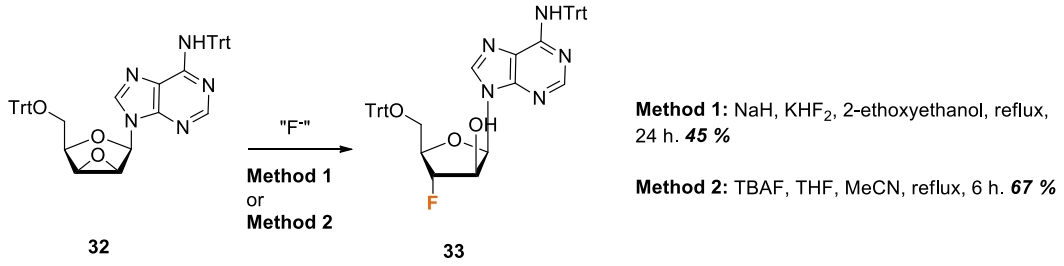

Scheme 47: Best results for fluoride-mediated opening of the *lyxo*-epoxide of adenosine

A second result was obtained with TBAF as a fluoride source and acetonitrile as a co-solvent, as reported in a patent by Cook.[220] The use of TBAF in a THF/MeCN mixture at reflux for 6 hours allowed

to obtain compound **35** in 67 % yield (**Method 2** in **Scheme 47**). However, scale-up of the reaction was difficult as the yield decreases importantly for amounts superior to 100 mg.

Despite these difficulties, we were able to pursue the synthetic scheme. The 2'-hydroxyl group of compound **33** could then be activated by triflic anhydride and undergo azidation to yield compound **35** (88 %) (**Scheme 48**).

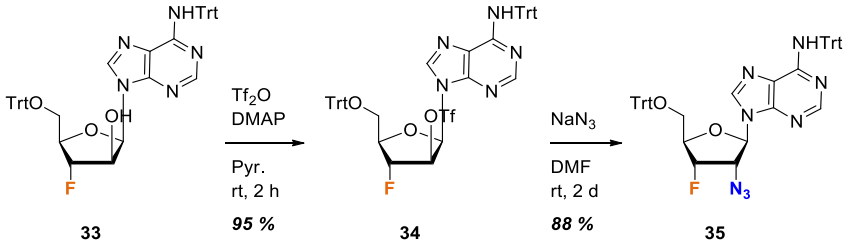

Scheme 48: Synthesis of the desired azido-fluoro **35** from **33**

Overall, though compound **33** could be isolated with acceptable yields, the disadvantages were significant: the low nucleophilic character of fluoride causes low conversion of the starting material, and long reaction times and high temperature tend to degrade the starting material; the close polarity of **32** and **33** makes monitoring of the reaction hard and purification time-consuming. These drawbacks limit the interest of this synthetic pathway despite it being more rationalized regarding regioselectivity. As a result, we explored the alternative strategy of azide-mediated opening of the *lyxo*-epoxide.

The reported conditions were the use of sodium azide and ammonium chloride in a water/DMF mixture at reflux during 90 minutes, and majorly led to 3'-azido.[108] Reasoning that the regioselectivity of epoxide-opening is influenced by the acidity of the medium, we removed ammonium chloride in our conditions. The use of sodium azide in DMF at 80 °C overnight led to the 3'-azido and 2'-azido compounds in a 1 to 1 ratio. The 2'-azido regioisomer **36** could be isolated with a 44 % yield (**Scheme 49**). Subsequent fluorination of this compound was performed in chloroform with diethylaminosulfur trifluoride (DAST) as a fluorinating agent and yielded compound **37** (54 %).

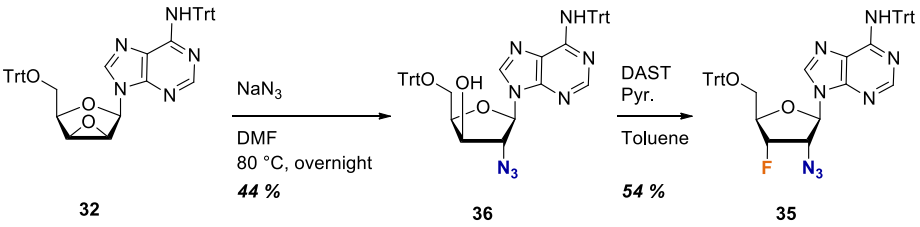

Scheme 49: Azide-mediated opening of the *lyxo*-epoxide and fluorination

Overall reproducibility and easy scale-up of this strategy makes it preferable to access compound **35**, despite the lack of 2'-regioselectivity during the epoxide opening.

2.2.3. Adequate protection

The synthesis of **38**, compatible with the SPS process, proceeds in two steps (**Scheme 50**): **35** is detritylated by trifluoroacetic acid (TFA) in DCM, and dimethoxytritylation is carried out in pyridine with *N,N*-dimethylaminopyridine (DMAP) to lead to the final compound **38**. The nucleobase is purposely left unprotected as it will be the attachment point for the solid support. Indeed, because both the 2' and 3' are functionalized, the solid support cannot be attached at those positions.

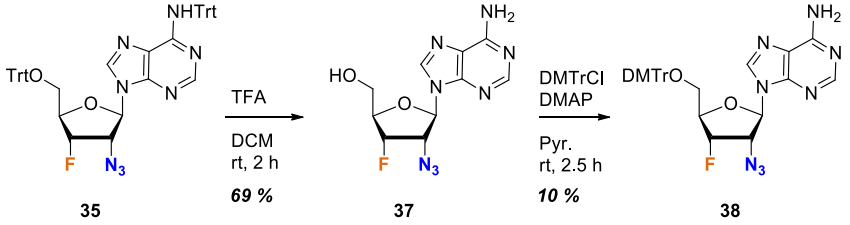

Scheme 50: Change of protecting groups for the *ribo*-configured compound

A major difficulty that arose in those steps was that compound **37** was obtained as a TFA salt. Several treatments with organic or inorganic bases were able to obtain **37** as a free base, but did not allow to improve significantly the yield of the dimethoxytritylation step, for which only poor yields up to 10 % were obtained.

Alternative deprotection methods were tested to overcome this issue, notably by using a Lewis acid instead of a Bronsted acid. Detritylation using $BF_3.Et_2O$ have been reported,[221] but in our case, only 5'-detritylation was observed. In the case of nucleosides, it was reported that the assistance of the cyclic oxygen of ribose is necessary for detritylation by Lewis acids.[222]

Despite this, **38** was isolated and characterized. Overall, both strategies were optimized and allowed to obtain the desired compounds. Attempts to graft it onto the solid support could be carried out.

In order to monitor the influence of the fluorine atom on conformation, we used the empirical method allowing to deduce the *North/*South relative populations from the value of the scalar coupling constant between H1' and H2'. For compound **38**, The coupling constant $J_{H1'-H2'}$ on the NMR spectrum in chloroform has a value of 7.9 Hz, suggesting a 79 % proportion of *South* conformation, consistent with what was expected. The azido group does not appear to impact the effect of the fluorine atom.

3. Synthesis of the *xylo* monomer

3.1. Retrosynthetic analysis

Very few examples of *xylo*-3'-fluoro-2'azido bisfunctionalization are reported in the literature. Both the fluorination and azidation steps proceed through SN2 mechanisms, so starting from the

commercially available adenosine, a 2'-inversion of configuration is necessary. Two strategies can be envisioned depending on the order of functionalization (**Scheme 51**). In a first strategy, the desired compound **H** could be obtained from 2'-azido **G**. Such a compound has been previously obtained and described in this manuscript (*cf* Chapter 1, 3.1., compound **8**). Such a strategy would require minimal optimization and would be efficient. In an alternative strategy, **H** could be obtained by azidation of *lyxo*-3'-fluoro **J**. **J** could be obtained from the *xylo*-3'-fluoro compound **I**, and such a compound has been previously described in our laboratory.[215] This strategy would require a larger number of steps and more optimization.

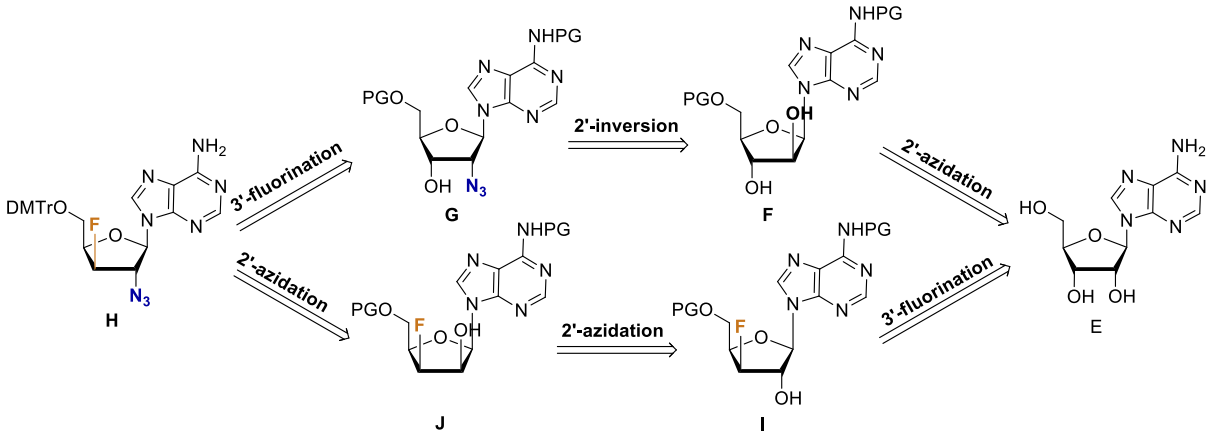

Scheme 51: Retrosynthetic scheme for the *xylo*-configured compound

3.2. Synthetic results

Compound **8** was synthesized according to the previously described procedure in an eight-step synthesis (Chapter 1, part 3.1.). A two-steps synthesis was envisioned to obtain the desired compound **H** (**Scheme 52**): first a fluorination step to convert the 3'-hydroxyl into 3'-fluoro with configuration inversion of carbon 3', and then a deprotection step on the nucleobase to remove the benzoyl group and let it free for grafting onto the solid support.

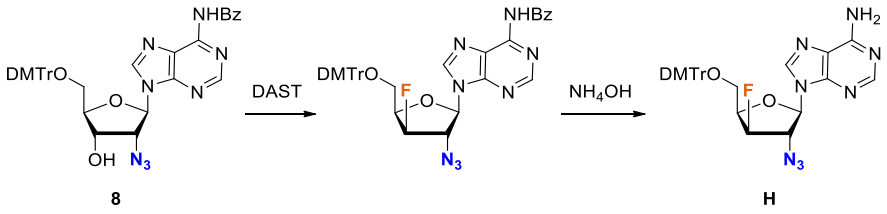

Scheme 52: Envisioned synthesis for the *xylo*-configured compound from compound **8.**

Unfortunately, the fluorination step never allowed to obtain more than traces of the desired compound. Instead, the elimination by-product was obtained with good yields. Multiple attempts were

made, from the 3'-hydroxyl, or by activating it in the form of a mesylate or a triflate, and with various fluoride sources: DAST, CsF, AgF, NaF, KHF_2 (**Table 4**).

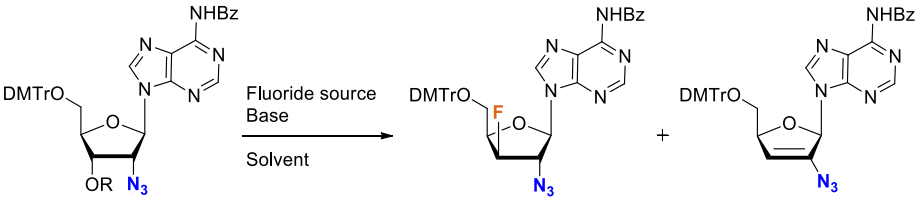

Entry	R	Fluoride source	Solvent, Base	Conditions	Outcome
1	H	DAST	DCM, Pyr.	0 °C to rt, 2 h	**41**, **40** (traces)
2	H	DAST	DCM	0 °C to rt, 2 h	**41**, **40** (traces)
3	H	DAST	$CHCl_3$	0 °C to rt, 2 h	**41**, **40** (traces)
4	H	DAST	DCM	-78 °C to rt	**41**, **40** (traces)
5	H	DAST	Dioxane	0 °C to rt	**41**, **40** (traces)
6	Ms	KHF_2	DMF, Pyr.	0 °C to rt	**41**, **40** (traces)
7	Ms	CsF	DMF	-78 °C to rt	**41**, **40** (traces)
8	Ms	AgF	DCM	-78 °C to rt	**41**, **40** (traces)
9	Tf	CsF	DMF	-78 °C to rt	**41**, **40** (traces)
10	Tf	AgF	DCM	-78 °C to rt	**41**, **40** (traces)

Table 4: Fluorination attempts on compound **8**

Efforts were made to favor the substitution product **40** over the elimination product **41** by decreasing the temperature, but were unsuccessful. Only traces of the desired compound could be isolated thanks to this method. Overall, this suggests that the elimination reaction is driven by the stability of the resulting vinyl-azide. For this reason, the alternative strategy in which the azide group is introduced after the fluorine atom has then been explored.

In this strategy, the first steps consist in introducing the fluorine atom in the 3'-position in the *xylo* configuration, as previously reported in our group (**Scheme 53**).[215] Adenosine was first tritylated and compound **42** was obtained in a 50 % yield. DAST-mediated fluorination can proceed to lead to the fluorinated compound **43** in a 50 % yield. Deprotection using TFA in DCM led to the desired fluorinated and unprotected compound **44**.

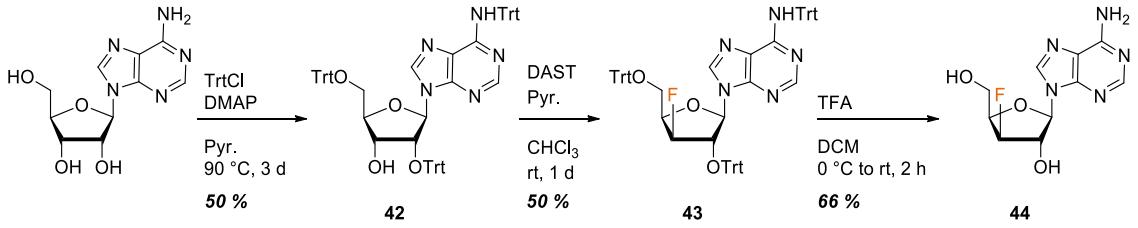

Scheme 53: Introduction of the 3'-fluorine atom in the *xylo* configuration

For the next steps, protection of the 5'-OH and the nucleobase was necessary. First, benzoylation lead to compound **45** (**Scheme 54**). The 5'-OH could then be protected using dimethoxytrityl chloride in a 92 % yield to lead to compound **46**.

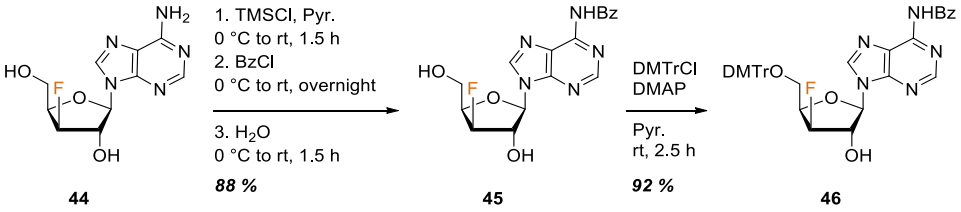

Scheme 54: Adequate protection steps for 2'-azidation

Alcohol **46** was oxidized using Dess-Martin periodinane to yield ketone **47** (71 %) (**Scheme 55**). Oxidation with DMP must be carried out at 0 °C to prevent DMTr cleavage. Reduction by sodium borohydride shows good conversion and good stereoselectivity and leads to compound **48**.

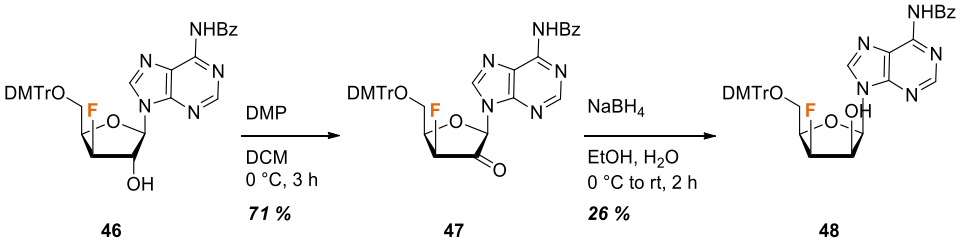

Scheme 55: Configuration inversion of the C2' of the *xylo*-configured 3'-fluorinated compound

Eventually, the azido group could be introduced by triflate activation of the 2'-hydroxyl followed by treatment with sodium azide (**Scheme 56**). Debenzoylation to yield the final compound was carried out in an ammonia/ethanol mixture at 55 °C for 2 hours, and compound **50** could be obtained in a 51 % yield.

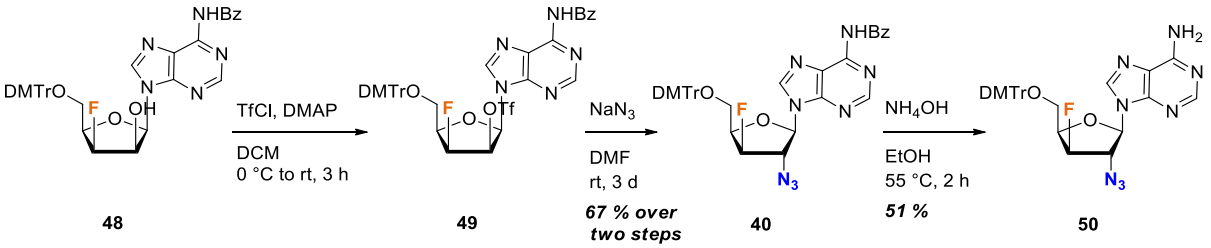

Scheme 56: 2'-azidation process leading to final compound **48**.

The final compound **50** could then, along with diastereoisomer **38**, undergo attempts to solid-support attachment.

Evaluation of the influence of the fluorine atom on the conformation of compound 50 was again performed by NMR. The coupling constant $J_{H1'-H2'}$ on the NMR spectrum in chloroform has a value of 1.6 Hz, suggesting an 84 % proportion of *North* conformation, consistent with what was expected. Again, the azido group does not prevent the fluorine atom to favor one conformation.

4. Attachment to the solid support

Usual conditions for attachment to the solid support were tested on **38** and **50**. The amino resin was first activated by succinic anhydride in pyridine for 20 h. Grafting of the nucleoside was attempted in the presence of a coupling reagent, dicyclohexylcarbodiimide (DCC), in usual conditions for such reactions (**Scheme 57**).

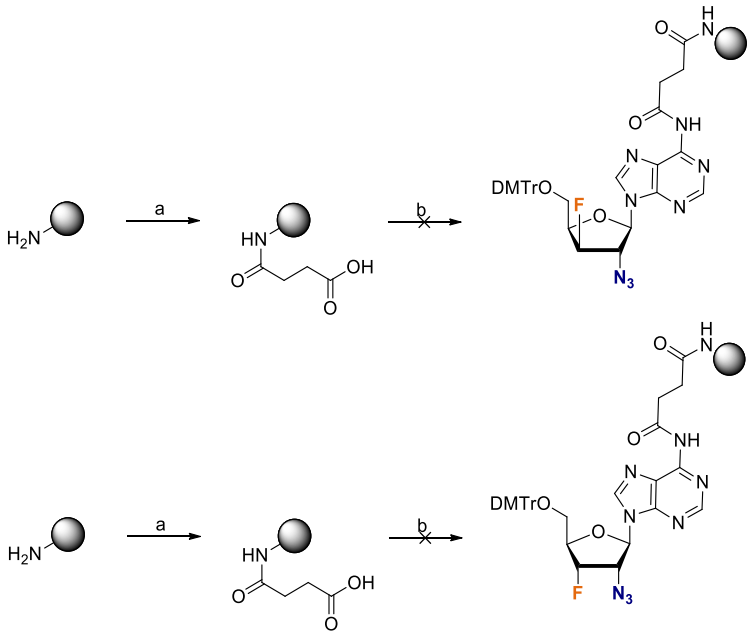

Scheme 57: Attempts of grafting compounds 38 and 50 onto a solid support. a) succinic anhydride, DIPEA, Pyr., rt, 20 h. b) **38** or **50**, DCI, DMAP, Pyr., rt, 20 h.

These conditions did not allow any loading, as determined by measurement of the optical density of the cleaved DMTr group. The syntheses of compounds **38** and **50** allowed to isolate amounts of 6 and 12 mg, respectively. Those small amounts can be responsible for this inconclusive result. New batches of **38** and **48** are currently being synthesized. Further optimization of the attachment to the resin will be carried out. The conditions reported by Micura and coworkers[113] will be tested. An alternative strategy can also be investigated, in which the linker is introduced on the nucleoside and then attached to the resin by peptidic coupling, instead of the other way around.

These two functionalized solid-support will then be able to undergo solid-phase synthesis and post-functionalization and be used as tools for the studies of FemX.

5. Remaining steps and outlooks

Both monomers will then be taken through the following steps (**Scheme 58**): attachment to a solid-support and solid-phase synthesis; CuAAC ligation of the analog of UM5K yielding crystallizable bi-substrates analogs; co-crystallization with FemX and resolving of the structure.

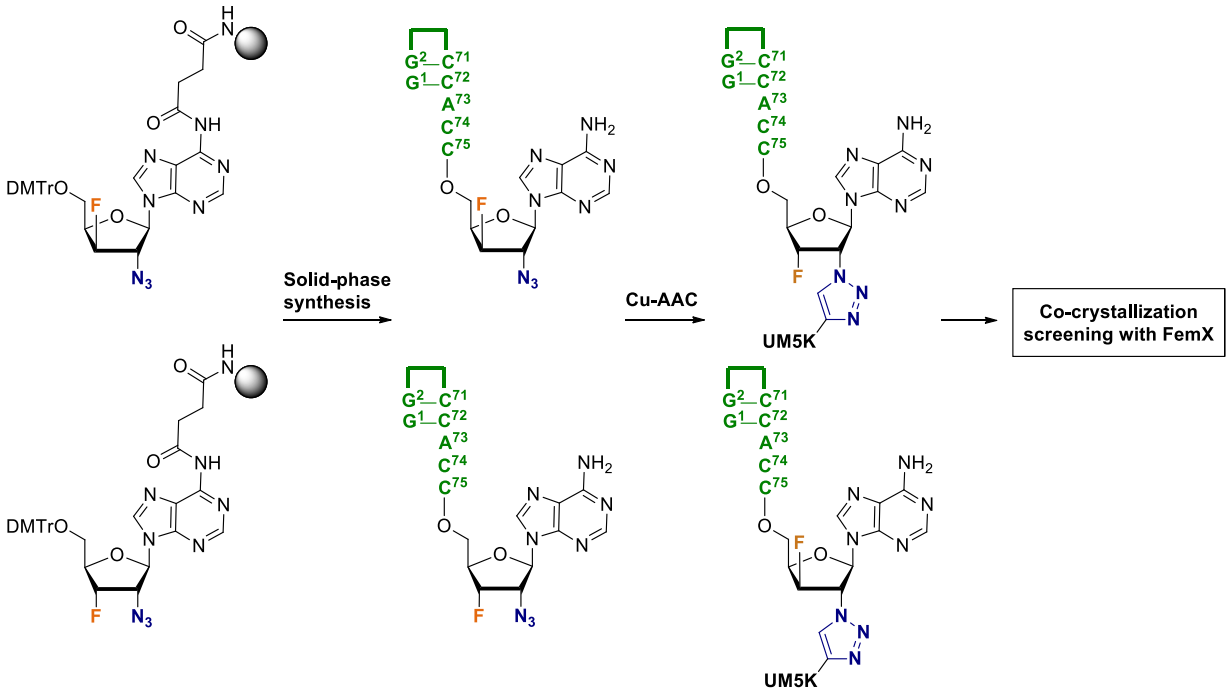

Scheme 58: Remaining steps to complete the synthesis of the targeted fluorinated bi-substrates compounds

Further steps have already been optimized in previous work. The CuAAC and the synthesis of alkyne-bearing UM5K have been used repeatedly and should proceed smoothly. The crystallization conditions allowing the co-crystallization of FemX with non-fluorinated compound will be the starting point of the crystallization screenings. Since our targeted fluorinated bi-substrate analogs only differ from the

previously synthesized non-fluorinated analog by the presence of the fluorine atom, co-crystallization should be successful.

6. Conclusion

In this chapter, the syntheses of 2',3'-bifunctionalized adenosine monomers have been investigated. Both *ribo* and *xylo* configured 2'-azido-2',3'-dideoxy-3'-fluoroadenosine SPS-compatible monomers have been obtained, and their syntheses were optimized while managing the control of the stereocenters and the protecting strategies.

These monomers will now be precursors for tools to study the influence of the fluorine atom on FemX recognition and possibly to detect and identify a conformational preference for Fem-transferases.

Part 2

Goals, results, and discussion

Chapter 3

Synthesis of tRNA analogs and RNA conjugates for inhibition and study of *S. aureus* FmhB

1. Introduction

1.1. FemABX family members present in *S. aureus*

Bacteria belonging to the genus *Staphylococcus* are common pathogenic infectious agents, both in the hospital and in the community. Among them, *Staphylococcus aureus* is particularly important: it is the first causal agent of nosocomial infections, , along with *Escherichia coli*.[223] Naturally carried healthily by 30 to 50 % of the population, it is responsible for an increasing number of infections, and a growing proportion of *S. aureus* strains exhibits resistance to multiple antibiotics.[223,224] For these reasons, it is crucial to look for new molecular targets and new antibiotics efficient on *S. aureus*.

The work presented in this chapter focused on the synthesis of aa-tRNA analogs for studying the enzyme FmhB of the bacterium *Staphylococcus aureus*, a good candidate for the development of antimicrobials.

As previously stated (*cf* Part 1, 3.3.), in *S. aureus*, the biosynthesis of the pentaglycine peptide interbridge of the peptidoglycan is done by three aminoacyl-transferase from the FemABX family (**Scheme 59**):[71]

- FmhB (anciently referred to as FemX), responsible for the addition of the first glycyl residue.
- FemA, responsible for the addition of the second and third glycyl residues.
- FemB, responsible for the addition of the fourth and fifth glycyl residues.

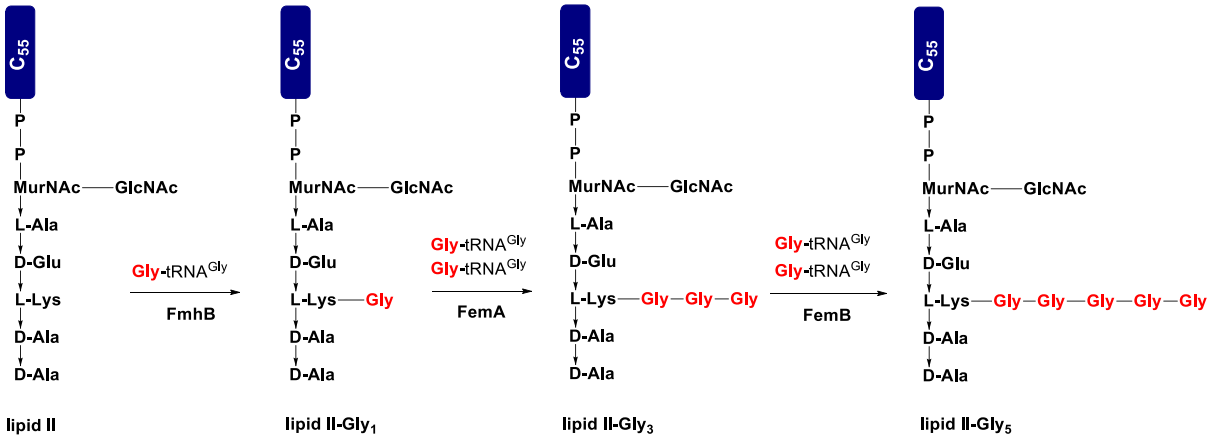

Scheme 59: Biosynthesis of the peptide interbridge by Fem-transferases in *S. aureus*

Inactivation of the *fmhB* and *femA* genes showed that they both are required for bacterial survival, whereas *femB* is reported to be unessential to bacterial viability.[225,226] All three of them are also crucial for the expression of methicillin resistance, though, again, *femB* is less crucial.[33,31] The reason of this is that the resistance is mediated by the penicillin-binding protein PBP2a. This transpeptidase requires a

full pentaglycine bridge to function, and inactivation of the FemABX genes leads to restoring the susceptibility to methicillin.

It is also interesting to note that the branched lipid II-Gly_x has been shown to be a substrate in sortase-catalyzed reaction: anchoring of surface proteins can occur on the N-termini of the Gly residues of the branched lipid II.[227] Thus, inhibition of the activity of FmhB/FemA/FemB could impact the anchoring of surface proteins which is an important phenomenon for the establishment of infection by Gram-positive bacteria.[228]

The structure of FemA as an apoenzyme has been resolved in 2002,[25] but not in complex with the $tRNA^{Gly}$ substrate nor the lipid II substrate. No structure has been resolved for neither FmhB nor FemB.

Because of our previous studies on FemX of *Weissella viridescens,* we focused on FmhB. Little structural data is known, and, compared to FemB, it is essential for bacterial survival. It has functional similarity with $FemX_{Wv}$ as they both catalyze the addition of the first amino acid of the peptide interbridge. For this reason, part of the work presented here consisted in applying the methods developed for FemX to FmhB in order to obtain $tRNA^{Gly}$ analogs and to gain insight into the mode of recognition of FmhB toward its substrates as well as to promote co-crystallization with FmhB to gather structural data on this crucial enzyme.

1.2. FmhB: an aa-tRNA-dependent glycyl-transferase.

FmhB catalyzes the transfer of a glycyl residue from a Gly-$tRNA^{Gly}$ onto the lipid II, a peptidoglycan precursor bound to the membrane (**Scheme 60**).

It has been shown that FmhB recognize as a substrate the lipid II and no other peptidoglycan precursor.[229] The lipid II is the latest peptidoglycan cytoplasmic precursor. It consists in MurNAc-pentapeptide, with a GlcNAc linked to the MurNAc *via* a beta-1→4 osidic linkage, and with an undecaprenyl(C_{55})-diphosphate moiety attached to the position 1 of the MurNAc.

The recognition of the tRNA substrate is more complex than in our previous model *Weissella viridescens*. Five $tRNA^{Gly}$ isoacceptors has been identified in *S. aureus*.[23,71] The ability of FmhB to recognize one, several or all of these isoacceptors is to be addressed. The multiplicity of isoacceptors has led to the hypothesis that some of them are dedicated to the translation process while the other ones are only involved in the peptidoglycan biosynthesis.[230] Such a system would allow the bacterium to have different and sufficient pools of $tRNA^{Gly}$ for these two processes and ensure that they were not in competition between the translation process and cell-wall synthesis.

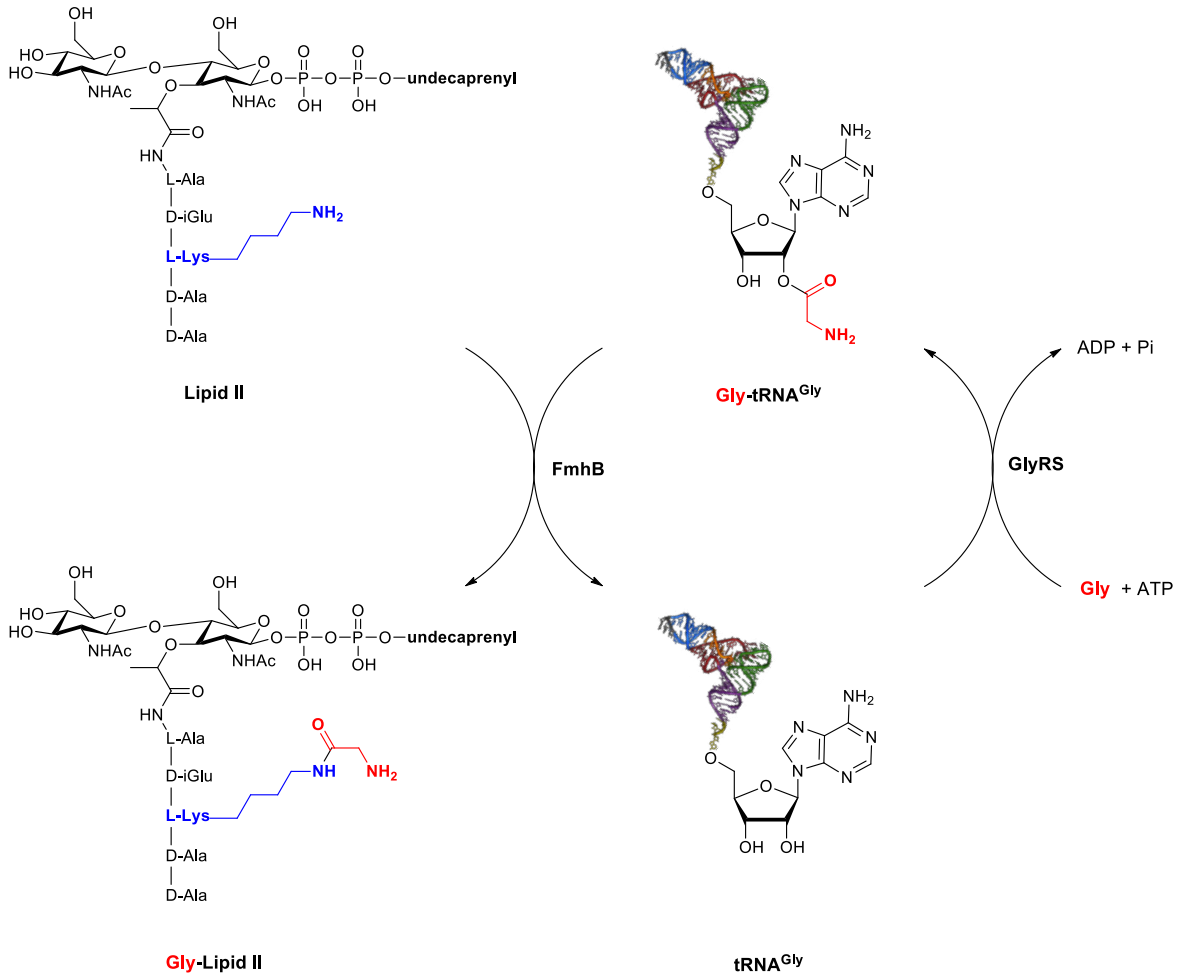

Scheme 60: Reaction catalyzed by FmhB. The glycyl residue is transferred from a Gly-tRNA^{Gly} onto the lipid II. Gly-tRNA^{Gly} is synthesized from Gly, tRNA^{Gly} and ATP by GlyRS.

All five of these tRNA possess the required identity elements for tRNA^{Gly} and are thus recognized and correctly aminoacylated by Gly-RS.[23] Consistently, NMR studies have established that they possess overall structural similarity.[231] Still, despite these common characteristics, they can be separated into two categories, according to some major structural and functional differences: the “proteogenic” and “non-proteogenic” tRNA^{Gly} isoacceptors. (**Figure 25**).[23,71]

The “proteinogenic” (P) tRNA^{Gly}, referred to as P1-GCC and P2-UCC. They show good affinity with the bacterial elongation factor EF-Tu. This is consistent with them possessing the key G^{49}-U^{65} and G^{51}-C^{63} base-pairings in the T-loop, considered recognition elements for EF-Tu. They also exhibit a GG sequence at positions 18 and 19.

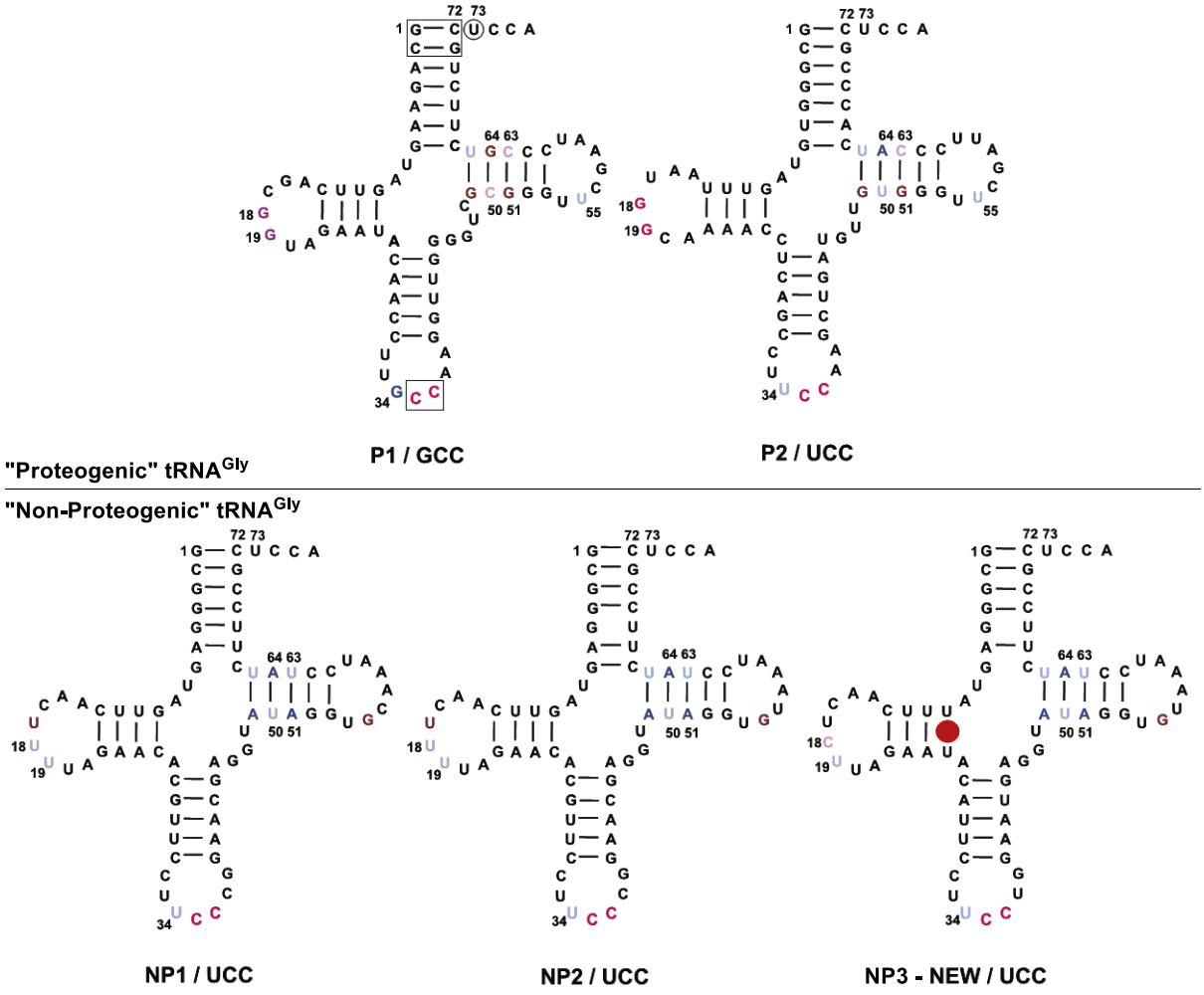

Figure 25: Proteogenic and Non-Proteogenic $tRNA^{Gly}$ isoacceptors in *Staphylococcus aureus* as described by Giannouli *et al.*[23]

The "non-proteinogenic" (NP) $tRNA^{Gly}$, referred to as NP1-UCC and NP2-UCC. The fifth $tRNA^{Gly}$, identified more recently, has been referred to in the literature as NEW-UCC. They show a lesser affinity with EF-Tu, and do not possess the abovementioned base-pairings. Instead, the G bases at positions 49 and 51 in the T-loop are replaced by A bases. The GG sequence at positions 18 and 19 is replaced by either CU or UU.

Those non-proteinogenic $tRNAs^{Gly}$ can thus be considered as good candidates to form a pool of $tRNA^{Gly}$ dedicated to cell-wall synthesis. The coincidental fact that there are three non-proteinogenic isoacceptor susceptible to be involved in the pentaglycine bridge biosynthesis and three Fem-transferases responsible for this process led to the hypothesis that each Fem utilizes its specialized isoacceptor.[229] To this day, there is no experimental evidence of such specificity.

Finally, it is interesting to note that FmhB, when expressed in *Enterococcus faecalis*, is able to transfer a Gly residue in the peptidoglycan as it does in *Staphylococcus aureus*, using the $tRNA^{Gly}$ pool present

in *E. faecalis*.[232] This would suggest that FmhB can also be tolerant toward $tRNA^{Gly}$ and is not in favor of a strict specificity between FmhB and $tRNA^{Gly}$ isoacceptors.

In light of these elements, we focused on the synthesis of compounds able to help to improve the understanding of FmhB recognition mode toward its substrates, to inhibit its action, and to gain structural insight.

1.3. Targeted compounds

The first objective was the synthesis of analogs of the acceptor arm of the $tRNA^{Gly}$ substrate with the same logic previously used for $FemX_{Wv}$. Such compounds should exhibit an RNA sequence mimicking the acceptor arm of $tRNA^{Gly}$ (**Figure 26**): long sequences should provide the better affinity, and short sequences, because of lower flexibility, should provide better chances of co-crystallization with FmhB. Variations in the sequence (length, nucleotide replacements) can help to understand the important features for recognition at the 3'-end of the tRNA. The 2'-position of the terminal adenosine should be either a non-transferable functional group or, better, an analog for the lipid II substrate. Such "bi-substrate" compounds showed the better results for both high-affinity inhibition and co-crystallization in previous studies with $FemX_{Wv}$. The synthesis of such compounds is presented in parts 2 and 3 of this chapter.

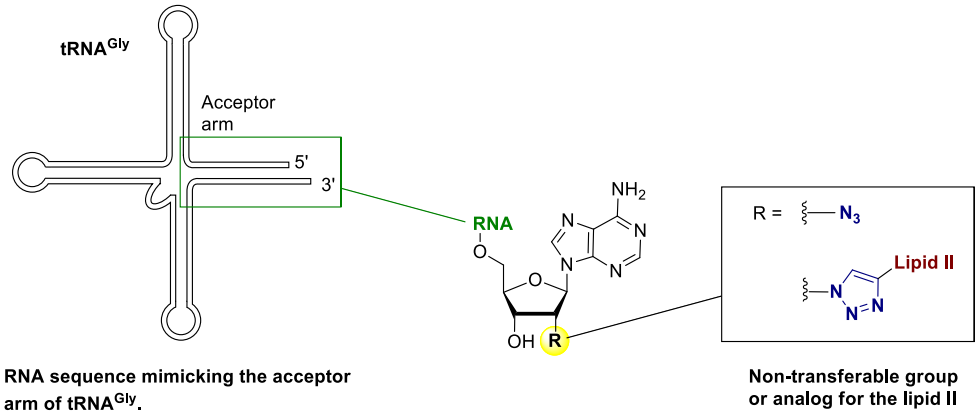

Figure 26: Structure of the targeted inhibitors of FmhB

A second objective was to synthesize tools to try and understand the key elements for recognition between $tRNA^{Gly}$ and FmhB. Because the FmhB system is more complex than the $FemX_{Wv}$ system, two issues were addressed: the recognition elements between FmhB and the five different $tRNA^{Gly}$ isoacceptors present in *S. aureus*; and the interaction of the $tRNA^{Gly}$ with the coiled-coil domain of FmhB which is thought to be the major different structural element. For the former issue, efforts were made to synthesize tRNA analogs exhibiting a standard recognized element by FmhB and variations in the RNA sequence (**Figure 27A**).

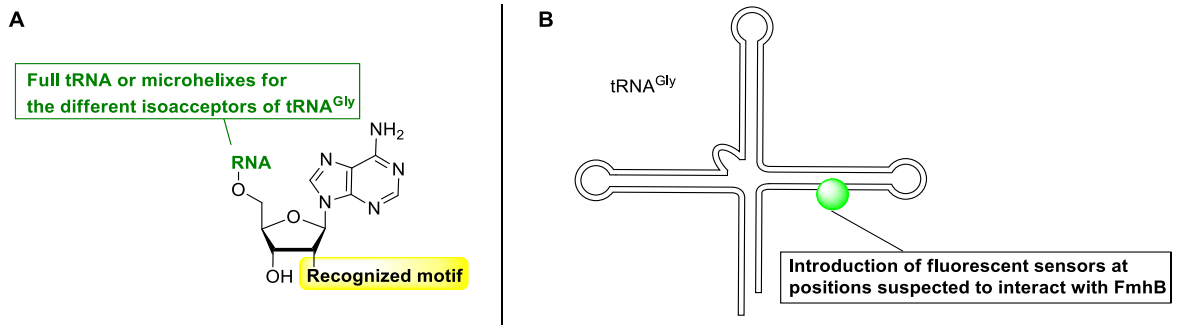

Figure 27: Structure of the targeted molecular tools for the study of the interactions between FmhB and $tRNA^{Gly}$ isoacceptors **(A)** or between $tRNA^{Gly}$ and the coiled-coil domain of FmhB **(B)**.

For the latter issue, in collaboration with the group of Alain Burger (Nice University, France), oligos bearing original fluorophores[233,234] have been investigated as precursors of tRNA comprising sensors for protein interaction (**Figure 27B**). Those fluorophores possess the ability to exhibit different fluorescence properties whether they interact with a protein or not. By placing them at the positions suspected to interact with the coiled-coil domain of FmhB, we could hopefully identify the nucleotides responsible for the interaction with the coiled-coil domain. Preliminary results concerning this approach are presented in parts 4 and 5 of this chapter.

2. Synthesis of duplexes mimicking $tRNA^{Gly}$

For the synthesis of duplexes mimicking the acceptor arm of $tRNA^{Gly}$, we chose to use the functionalized solid-support **9** exhibiting an azido group at the 2'-position. It is a non-transferable functional group; it is different from a 2'-hydroxy group that promotes substrate release in the natural substrate; finally, it can be functionalized through CuAAC and is thus a precursor to "bi-substrate" compounds.

The synthesis of the modified solid-support **9** is detailed in the first chapter of this thesis (*cf* Part 2, 3.1. and 3.2.). Solid-phase synthesis using this azido-bearing monomer allowed to obtain duplexes **51** to **58** mimicking the acceptor arm of $tRNA^{Gly}$ (**Scheme 61**). The common sequence of the acceptor arm of non-proteinogenic $tRNA^{Gly}$ isoacceptors was used for oligos **51** to **56**. Compound **57** exhibits the sequence of proteinogenic $tRNA^{Gly}$ isoacceptor P1. **58** exhibits a single-nucleotide modification at position 73.

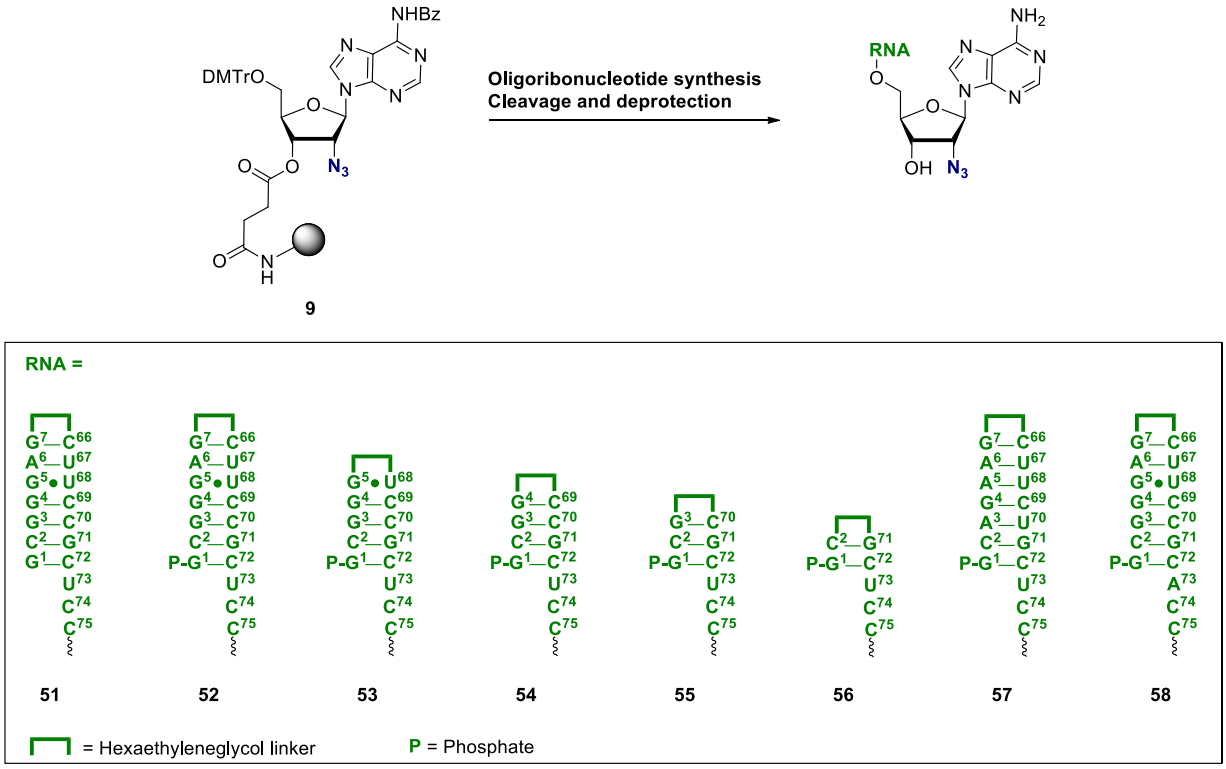

Scheme 61: Solid-phase synthesis of $tRNA^{Gly}$ analogs **51** to **58** from the 2'-azido solid support **9**

Those duplexes are analogs of $tRNA^{Gly}$. They were tested as inhibitors of FmhB and gave out IC_{50} values between 1 and 100 µM (**Table 5**).

51	52	53	54	55	56	57	58
7.1 µM	9.4 µM	22.2 µM	N.D.	59.6 µM	N.D.	≈ 10 µM	11.6 µM

Table 5: Biological evaluation of oligo **51** to **58**. The IC_{50} is indicated for each compound.

As well as what had been observed for FemX,[30] the number of base-pairings mimicking the acceptor arm of $tRNA^{Gly}$ is correlated with the affinity for FmhB. The presence of a 5'-terminal phosphate did not show a significant impact of the affinity, whereas it was responsible for a 4-fold increase in the case of $FemX_{Ww}$. The presence of an A at position 73 does not seems to impact the affinity, as well as the presence of A, A, and U at position 3, 5 and 70, respectively. These last modifications correspond to the sequence of the proteogenic $tRNA^{Gly}$ isoacceptor P1. This preliminary result suggests that either FmhB does not discriminate P1 and NP $tRNA^{Gly}$ isoacceptor or it discriminates them based on recognition elements situated away from the acceptor arm.

Overall, the observed IC_{50} for FmhB are higher than homologous compounds for $FemX_{Wv}$.This could suggest that recognition elements between FmhB and $tRNA^{Gly}$ are located out of the acceptor arm of $tRNA^{Gly}$ in a greater proportion than the recognition elements between $FemX_{Wv}$ and $tRNA^{Ala}$.

These azido-bearing $tRNA^{Gly}$-mimicking oligos could then undergo CuAAC in order to yield bi-substrate analogs.

3. Synthesis of lipid II-RNA conjugates for FmhB

Two oligos were investigated for "Click"-chemistry: the 18-mer **51**, which exhibited the best affinity; and the 8-mer **56**, which is expected to have the best chance to co-crystallize with FmhB.

Beforehand, the synthesis of an alkyne-bearing lipid II analog was carried out by our collaborators from the group of Dr Dominique Mengin-Lecreulx (Paris Sud University) and the group of Dr Michel Arthur (Centre de Recherche des Cordeliers). They followed a chemo-enzymatic synthetic route (**Scheme 62**):

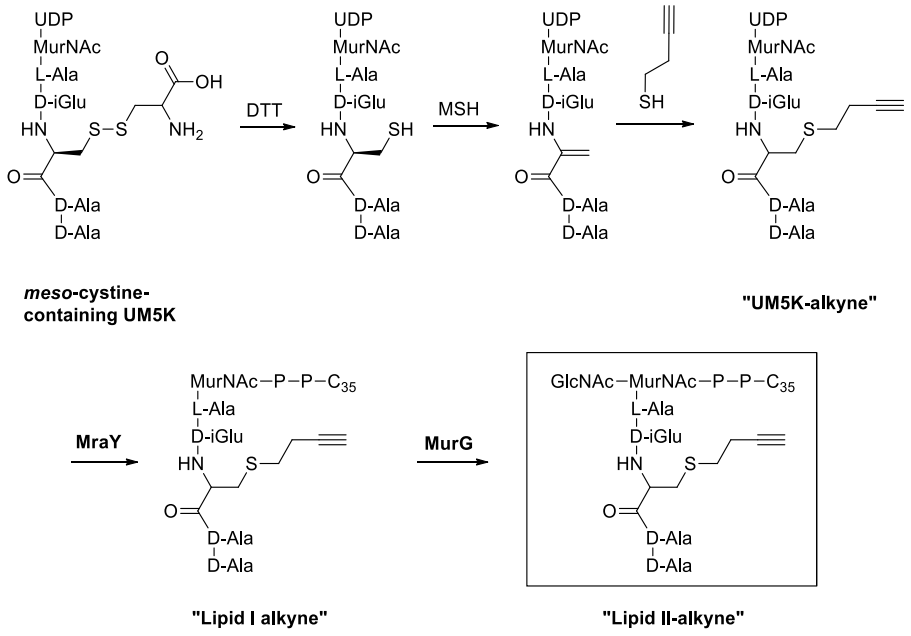

Scheme 62: Chemo-enzymatic synthesis of the lipid II-alkyne.

Using Mur enzymes, a modified UDP-MurNAc-pentapeptide was synthesized with a mesocystine instead of the natural lysine at position 3.[123] Reduction of the mesocystine residue and subsequent action of *O*-(Mesitylenesulfonyl)hydroxylamine (MSH) – as previsouly described on proteins[194] – led to a dehydroalanine residue, that could then react with but-3-ynethiol. The subsequent alkyne-bearing UM5K analog was then processed by enzymes MraY and MurG in order to, respectively, be attached to the lipidic motif C_{35} and to the GlcNAc moiety, leading to an alkyne-lipid II analog.

This alkyne-lipid II could then be reacted with oligos **51** for CuAAC (**Scheme 63**). The resulting compound **59** is a complex biomolecule conjugate comprising RNA, disaccharide, peptide, and lipid moieties (**Figure 28**). The same conditions, applied to **56**, have not yet yielded the corresponding conjugate as the purification of such conjugate exhibiting amphiphilic properties is challenging.

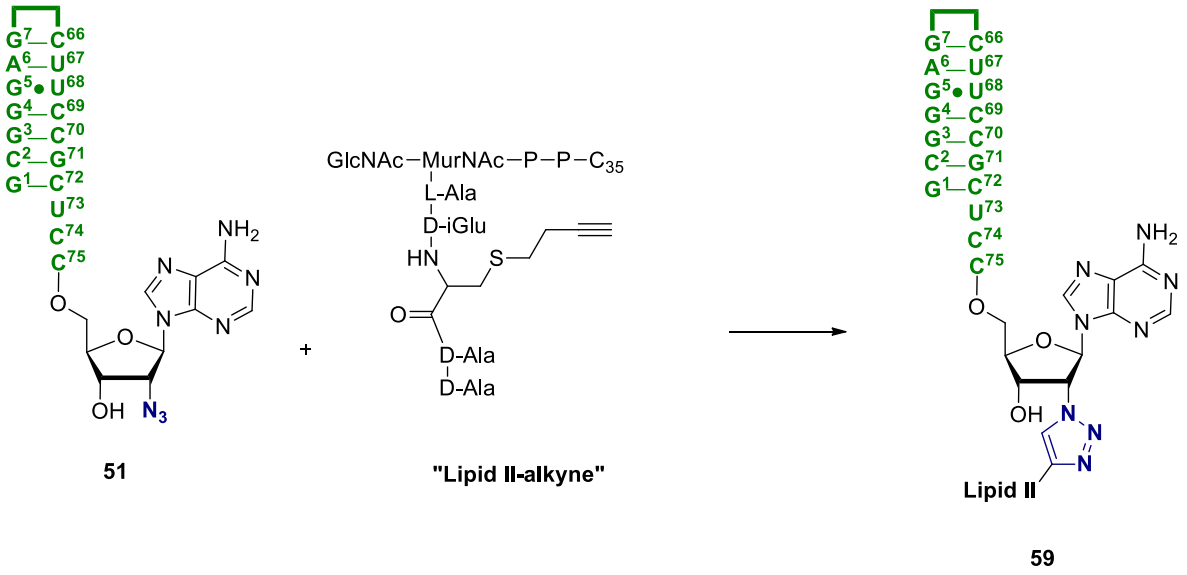

Scheme 63: CuAAC-mediated synthesis of RNA-lipid II conjugate **59**.

Conjugate **59** was tested as a competitive inhibitor of FmhB. The measured inhibition constant IC_{50} was 5 +/- 3 nM. The ligation of the lipid II analog to the oligo allowed more than a 1000-fold increase in affinity, confirming the validity of the bi-substrate approach for the design of compounds exhibiting high affinity for FmhB.

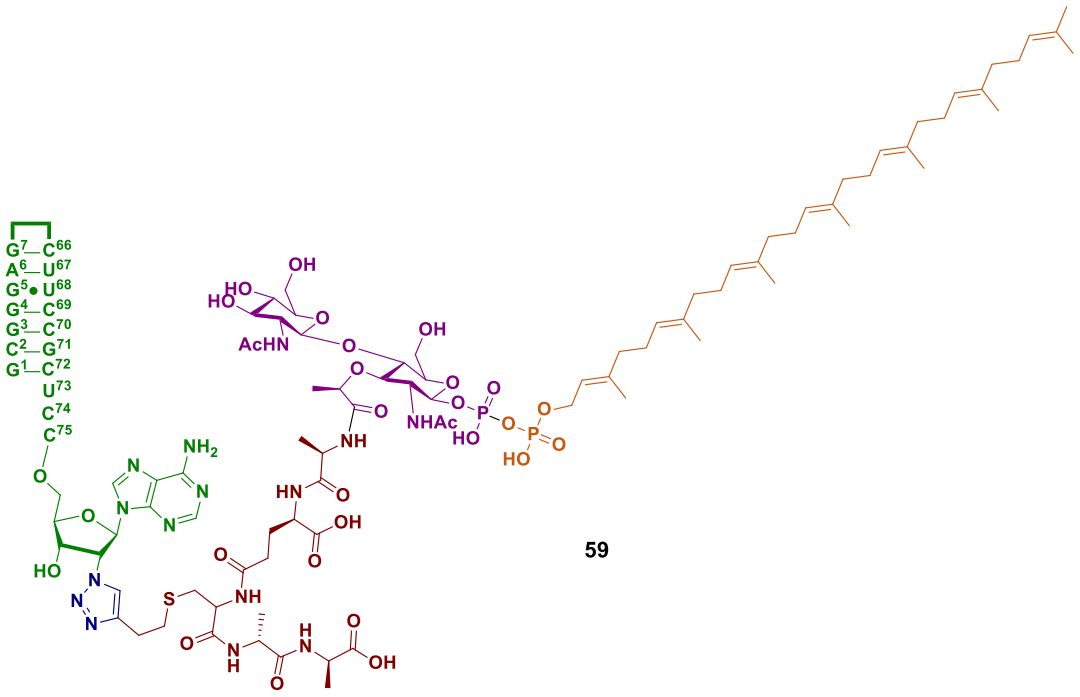

Figure 28: Structure of conjugate **59**. In green: RNA moiety; In blue: triazole linker; in maroon: peptide moiety; in purple: disaccharide moiety; in orange: lipid moiety

The conjugate between lipid II alkyne and oligo **56**, when properly obtained and characterized, will be used in crystallography studies with our collaborators from the group of Prof. Herman Van Tilbeurgh (Paris Sud University). Conditions allowing the crystallization of FmhB alone have been screened. Diffracting crystals have already been obtained but no structure could be resolved from them. Further screenings using FmhB incorporating selenomethionine reisudes to aid the elucidation of the structure are currently being carried out. The conjugate will be used in the screened conditions might allow to obtain co-crystals with FmhB and gain structural insight into FmhB recognition towards both its substrates.

After having focused on the terminal adenosine 76 and the acceptor arm of $tRNA^{Gly}$, we then moved on to the synthesis of tools to study the role of the other parts of $tRNA^{Gly}$.

4. Tools to study FmhB's preference between $tRNA^{Gly}$ isoacceptors

Preliminary results obtained by our collaborators (Dr Matthieu Fonvielle, group of Dr Michel Arthur, Centre de Recherche des Cordeliers, Paris, France) tend to show that even though FmhB can utilize all five aminoacylated isoacceptors of $tRNA^{Gly}$ as substrates, it does it with variable catalytic efficiency (**Table 6**).

$tRNA^{Gly}$ isoacceptor	**Catalytic efficiency ($min^{-1}.\mu M^{-1}$)**	**% compared to NP1**

$tRNA^{Gly}$ P1	34	22 %
$tRNA^{Gly}$ P2	84	54 %
$tRNA^{Gly}$ NP1	156	100 %
$tRNA^{Gly}$ NP2	131	84 %
$tRNA^{Gly}$ NP3-NEW	154	99 %

Table 6: FmhB's utilization of the different $tRNA^{Gly}$ isoacceptors.

Overall, the three non-proteinogenic $tRNA^{Gly}$ (NP1, NP2 and NP3-NEW) are used similarly by FmhB. The two proteinogenic $tRNA^{Gly}$ (P1, P2) are not as well processed: compared to the catalytic efficiency found with NP1, FmhB uses P2 and P1 with less efficiency, 54 % and 22 % respectively. These preliminary results tend to confirm that the segregation of $tRNA^{Gly}$ isoacceptors into two groups – proteinogenic and non-proteinogenic, but it disproved the hypothesis that FmhB would have its own specific isoacceptor, as would have FemA and FemB.

To further explore this issue, analogs were synthesized with variations in the RNA moiety to understand the recognition elements present on the $tRNA^{Gly}$ isoacceptors responsible for their different interaction with FmhB. To allow the introduction of molecular diversity with long RNA moiety, we chose to introduce them by enzymatic ligation. Starting from 2'-azido-2'-deoxyadenosine **6**, selective 5'-desilylation yielded **61** (97 %). Dinucleotide **62** was synthesized through phosphoramidite coupling in solution with a dC phosphoramidite monomer in an 82 % yield (**Scheme 64**).

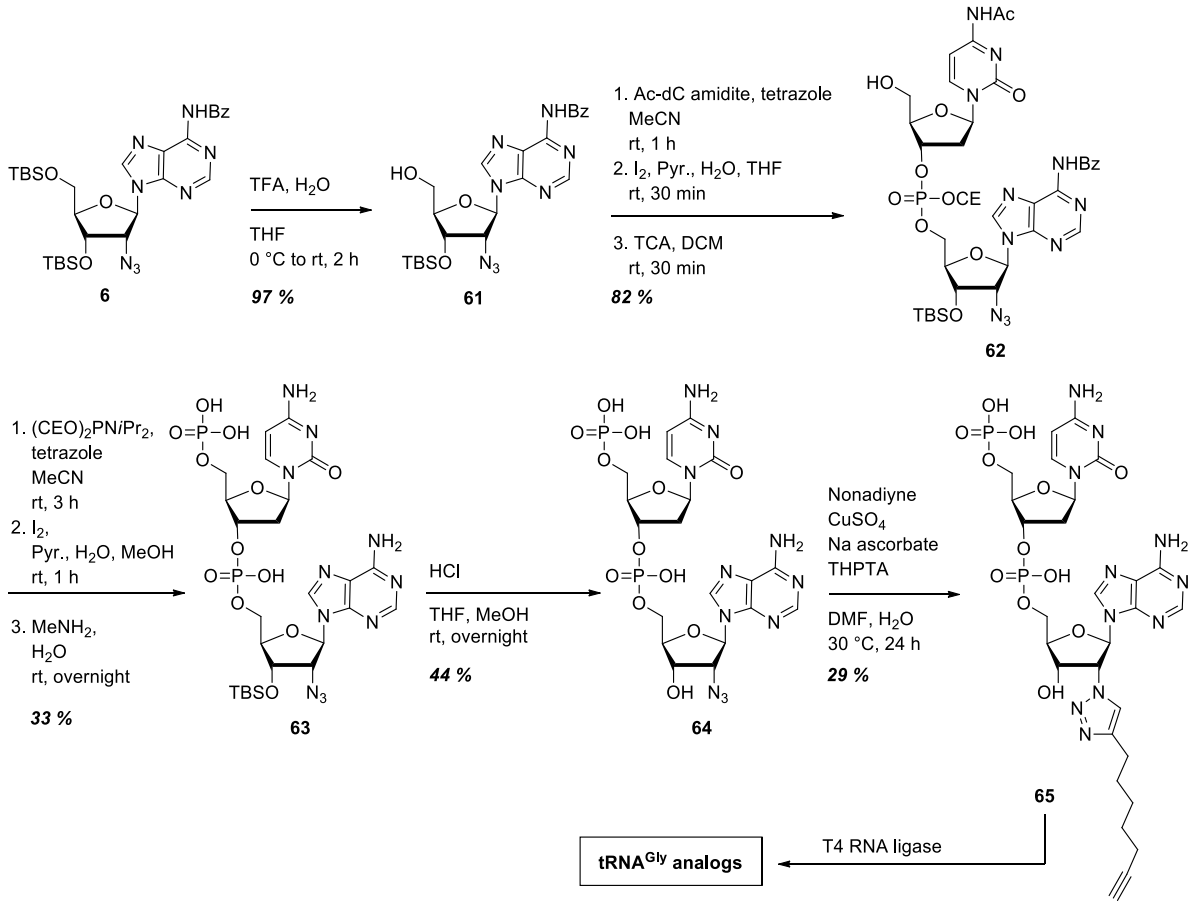

Scheme 64: Synthesis of dinucleotide **65**, precursor of $tRNA^{Gly}$ analogs.

Phosphorylation and deprotection led to azido-dinucleotide **64** in a 15 % yields over three steps and two reversed-phase HPLC purifications. CuAAC with nonadiyne yielded 2'-functionalized phosphorylated dinucleotide **65** which was used by our collaborators as a precursor towards several $tRNA^{Gly}$ analogs exhibiting various RNA moieties. The nonadiyne motif was serendipitously discovered to be well-recognized by $FemX_{Wv}$ and FmhB during previous optimization of the CuAAC on deprotected dinucleotides in which nonadiyne served as an easily available alkyne.

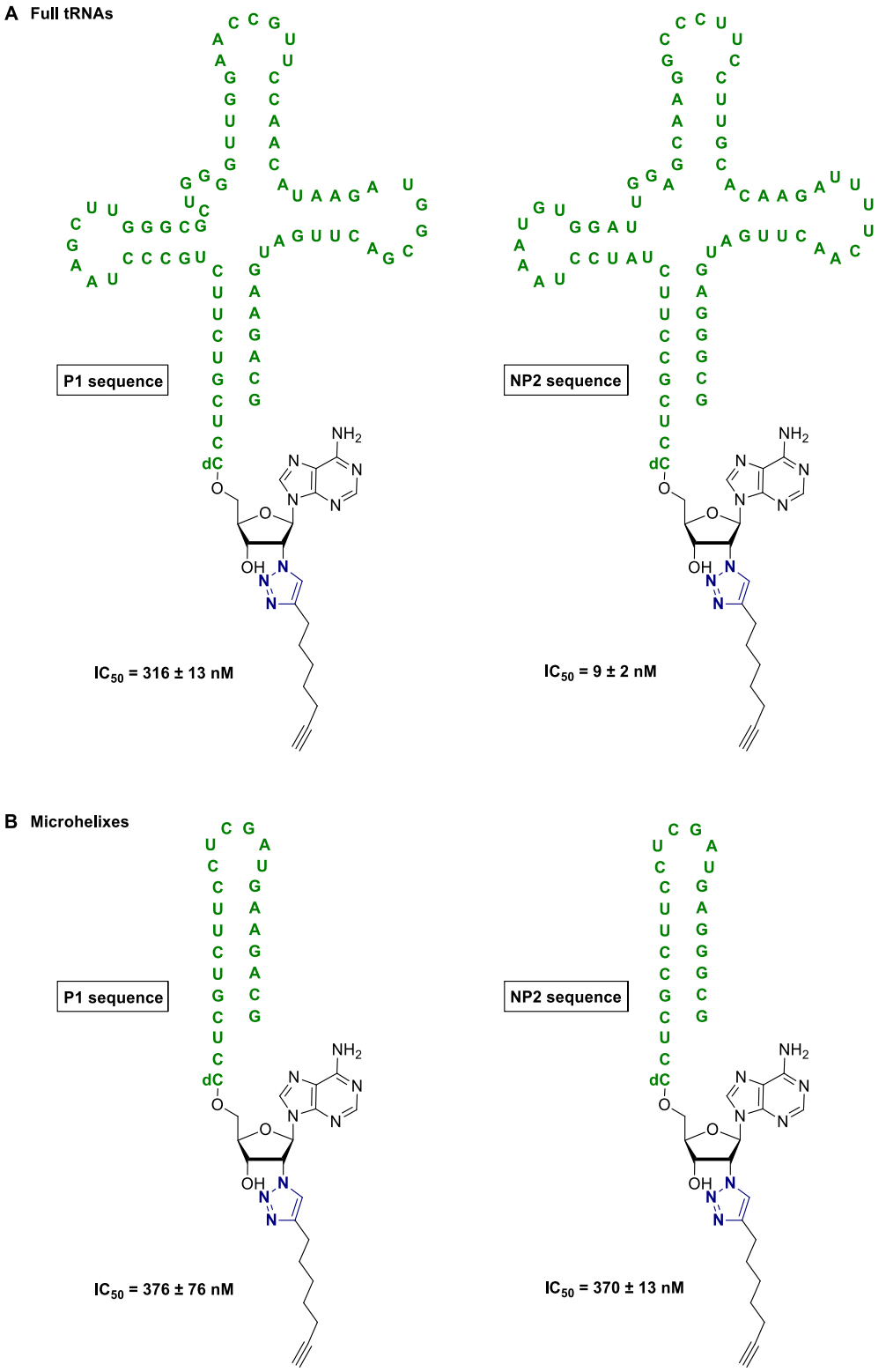

Figure 29: Structure and measured IC_{50} of $tRNA^{Gly}$ analogs obtained by enzymatic ligation of P1 and NP2 sequences on dinucleotide **65**.

Only preliminary results can be presented here. So far, four compounds have been obtained through enzymatic ligation with full tRNA sequences for both P1 and NP2 as well as microhelixes mimicking the

acceptor arm of P1 and NP2 (**Figure 29**). They were evaluated as competitive inhibitors of FmhB. The compound containing the NP2 sequence is a better inhibitor than the one containing the P1 sequence, with a 30-fold difference. This is consistent with the previous results which showed that NP2 is used more efficiently than P1 by FmhB, and further validates the hypothesis that NP2 is likely to be dedicated to cell-wall synthesis and P1 to the translation process.

Both of the compounds containing microhelixes instead of full tRNA sequences are poorer inhibitors and microhelixes corresponding to P1 and NP2 show no differences in affinity. This tends to confirm that a significant number of recognition elements of the $tRNA^{Gly}$ isoacceptors for FmhB are located out of the acceptor arm of $tRNA^{Gly}$. This differs from previous studies on $FemX_{Wv}$.[27]

Because the main structural difference between $FemX_{Wv}$ and FmhB is the absence of a coiled-coil domain in the former, one hypothesis could be that the interactions between the coiled-coil domain of FmhB with $tRNA^{Gly}$ are responsible for the better recognition of non-proteinogenic $tRNA^{Gly}$. Thus, future studies are planned to be developed in our group to synthesize tools to study this interaction.

5. Outlooks: tools to study the interaction between FmhB coiled-coil domain and $tRNA^{Gly}$

The results of the biological evaluation of duplexes **51** to **58** and conjugate **59** on FmhB differs from the results obtained with analogous compounds for $FemX_{Wv}$.[30,123] The main structural difference between $FemX_{Wv}$ and FmhB is thought to be the presence of a coiled-coil domain in FmhB. Thus, this domain is suspected to be responsible for the observed differences in biological evaluation because of its interacting with the $tRNA^{Gly}$ substrate. Using the homology between FemA and FmhB and the structural data from the crystallographic structure of FemA, molecular modeling could be done to investigate the interaction between FmhB and $tRNA^{Gly}$ (**Figure 30**).

These data could suggest that the coiled-coil of FmhB would be well-positioned to interact with nucleotides close to position 17. In order to investigate the interaction between the $tRNA^{Gly}$ substrate and the coiled-coil domain of FmhB, the objective was set on the synthesis of a $tRNA^{Gly}$ bearing at position 17 a sensor of the interaction with FmhB.

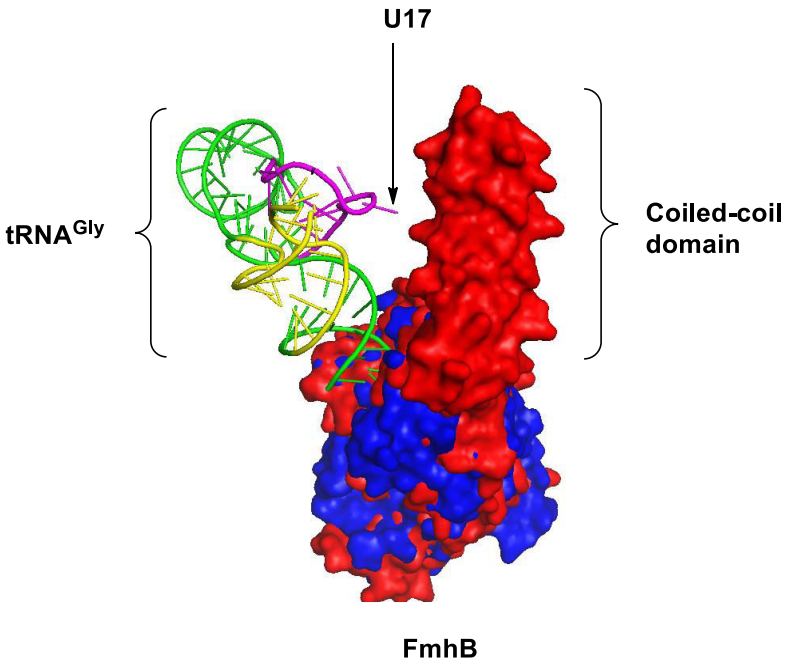

Figure 30: Molecular modeling of the interaction between FmhB and $tRNA^{Gly}$, estimated from the structural data of FemA and the homology between FemA and FmhB.

The group of Dr Alain Burger recently reported the synthesis and use of a modified deoxyuridine monomer bearing a 3-hydroxychromone scaffold acting as probe to detect interaction of the modified oligo with other DNA or with protein (**Figure 31**).[233] Depending on its hydration, the 3-hydroxychromone motif emits differently. Because the hydration state is modified when the fluorophore interacts with protein, a change in fluorescence emission can be measured to monitor the interaction. Such a nucleoside can then act as a sensor of interactions with proteins.

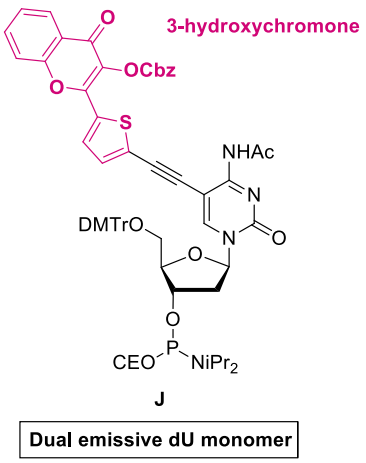

Figure 31: Structure of the dual-emissive dU monomer J exhibiting a 3-hydroxychromone scaffold, from Barthes *et al.*[233]

First, in order to establish a proof of concept on Fem-enzymes, three compounds are intended to be synthesized: two known bi-substrate inhibitors of $FemX_{Wv}$ and one inhibitor of FmhB (**Figure 32**).

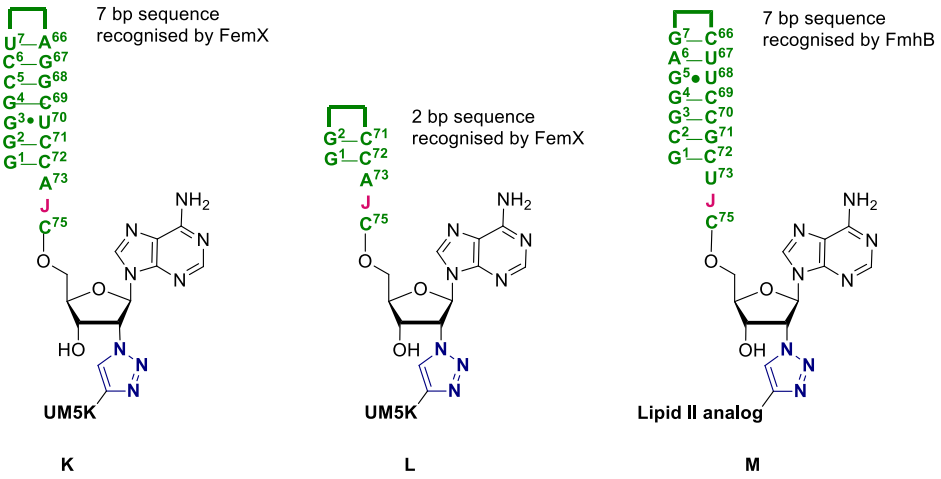

Figure 32: Structure of the targeted bi-substrates analogs with the fluorescent nucleoside **J**

Targeted compound **K** is expected to have a high affinity with $FemX_{Wv}$ since the unmodified version (without the fluorescent nucleoside **J**) exhibited a subnanomolar inhibition constant[30]. By the same logic, targeted compound **L** is expected to exhibit micromolar inhibition of $FemX_{Wv}$. Previous crystallographic of the unmodified version of **L** ensures that the modified position is positioned to interact with $FemX_{Wv}$.

Targeted compound **M** would allow to have a proof of concept on FmhB and to optimize the fluorescence experiment with FmhB.

Secondly, in order to achieve monitoring of the suspected interaction of U17 with the coiled-coil domain of FmhB, the synthesis of a version of the NP1 $tRNA^{Gly}$ isoacceptor bearing the fluorescent nucleoside **J** is necessary (**Scheme 65**). Introduction of fluorescent amidite **J** in the SPS could lead to a fluorescent oligo corresponding to the 5'-end of the desired $tRNA^{Gly}$. The 3'-fragment of the $tRNA^{Gly}$ would then be introduced by enzymatic ligation to yield the fluorescent sensor $tRNA^{Gly}$ **N**.

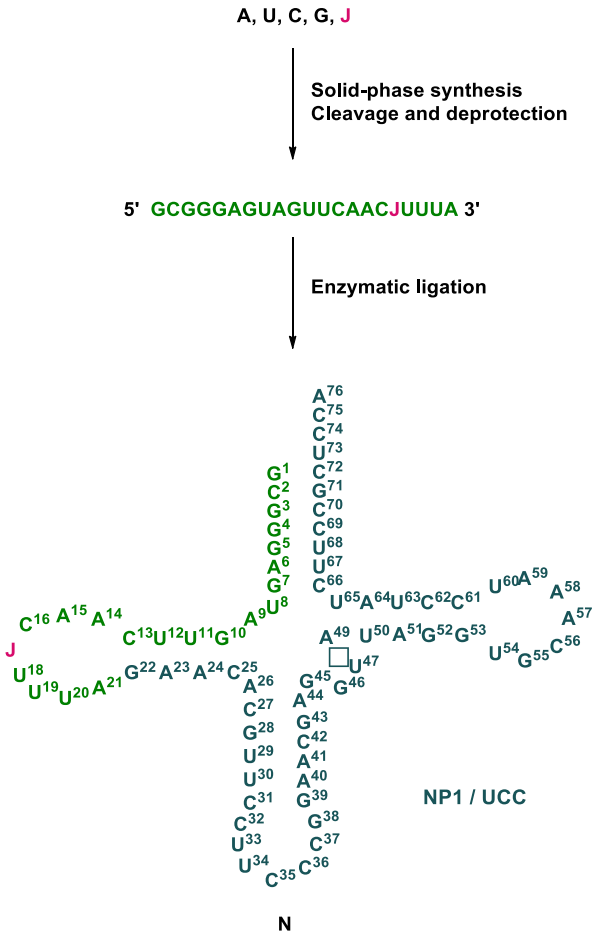

Scheme 65: Envisioned strategy to obtain fluorescent sensor $tRNA^{Gly}$

First attempts to synthesize the precursor oligos for **K**, **L**, **M** and **N** were unsuccessful. A reason for this inconclusive result is the use of 2-thiomorpholine-4-carbothioate (TC) protection at the 2'-position. The ethylenediamine-mediated deprotection step is not mild and might be incompatible with the 3-hydroxychromone motif. Synthesis with 2-silylated protecting groups is currently under investigation.

6. Conclusion

In this chapter have been presented our first approach to synthesize inhibitors of FmhB and tools to study its structure and its interactions with its substrates.

Duplexes mimicking the acceptor arm bearing an azido group allowed to achieve micromolar inhibition of FmhB and to identify the similarities and differences in recognition of the tRNA substrate from the $FemX_{Wv}$ model.

Conjugation of such duplexes with a lipid II analog allowed to achieve nanomolar inhibition of FmhB and to start co-crystallization screenings in order to obtain the crucial structural data of this important enzyme.

Because of the complexity of the FmhB system, new approaches had to be investigated to explore the issue of the different $tRNA^{Gly}$ isoacceptors as well as the interaction of the tRNA substrate with the coiled-coil domain of FmhB. For these purpose, preliminary results include the synthesis of functionalized dinucleotides as precursors of tools to study the recognition elements between FmhB and the different $tRNA^{Gly}$ isoacceptors. The synthesis of fluorescent analogs to study the interaction between FmhB's coiled-coil domain and the D-arm of $tRNA^{Gly}$ has been started and is still under investigation.

Part 2

Goals, results, and discussion

Chapter 4

Synthesis of aa-tRNA analogs for the study of Cyclodipeptide-synthases.

1. Cyclodipeptides synthases are aa-tRNA-dependent enzymes

Among all the biological roles of aa-tRNAs, their involvement in the synthesis of cyclodipeptides was recently discovered. In 2009, Muriel Gondry *et al.* reported that a class of enzymes called Cyclodipeptide-synthases (CDPSs) catalyze the formation of cyclodidpeptides in an ATP-independent manner through the use of aa-tRNAs as sources of activated amino acids.[74]

Cyclodipeptides (CDPs) are cyclic peptides synthesized in many organisms as precursors of diketopiperazines (DKP), with which they form a large class of secondary metabolites. A large number of them exhibit interesting features, such as antibacterial,[235] antifungal,[236] immunosuppressive[237] activities, among many others. For these reasons, the biosynthetic pathways responsible for their formation has been investigated. In most cases, the enzymes involved in their synthesis are non-ribosomal peptides synthetases (NRPSs).[74] These large enzymes often consist of multiples modules, each of them able to select, activate and incorporate an amino acid. Activation of the free amino acids by NRPSs proceeds through ATP-mediated adenylation. CDPs are synthesized by NRPSs either as a result of truncated side products during the synthesis of longer peptide or by condensation between two activated amino acids bound to adjacent modules.

During their study of the biosynthesis of albonoursin – an antibacterial DKP found in *Streptomyces noursei*, the group of Pernodet reported the first DKP biosynthetic pathway to proceed in an ATP-independent fashion.[238] The enzyme responsible for the formation of cyclo(L-Phe-L-Leu) (cFL), the CDP precursor of albonoursin, is AlbC, a small protein unrelated to NRPSs (239 residues, 27 kDa). Such a small enzyme cannot possess adenylation modules, and must then use activated amino acids as substrates. Gondry *et al*. established that AlbC uses aa-tRNAs as sources of activated amino acids.[74] They showed that seven other proteins showing similarity to AlbC use aa-tRNAs to form CDPs as well, and that together they form a class of enzymes that they called cyclodipeptide-synthases (CDPSs) (**Scheme 66**). Finally, their results suggest that the genes coding for CDPSs are clustered with those coding for enzymes responsible for the modification of the CDPs synthesized by CDPS, thus forming consistent biosynthetic units for DKPs.

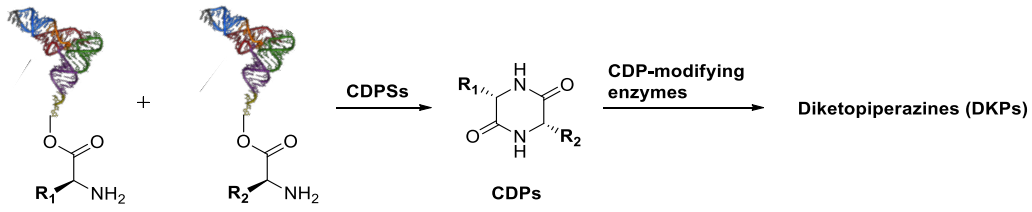

Scheme 66: Biosynthetic pathway of DKPs involving CDPSs

2. The AlbC enzyme from *S. noursei*.

In the bacterium *Streptomyces noursei*, AlbC catalyzes the synthesis of the cFL cyclodipeptide from Leu-tRNA^{Leu} and Phe-tRNA^{Phe} (**Scheme 67**). The cFL cyclodipeptide is later converted into albonoursin, known to have antibacterial properties, by cyclodipeptide-oxidase (CDO), a tailoring enzyme.[238,238]

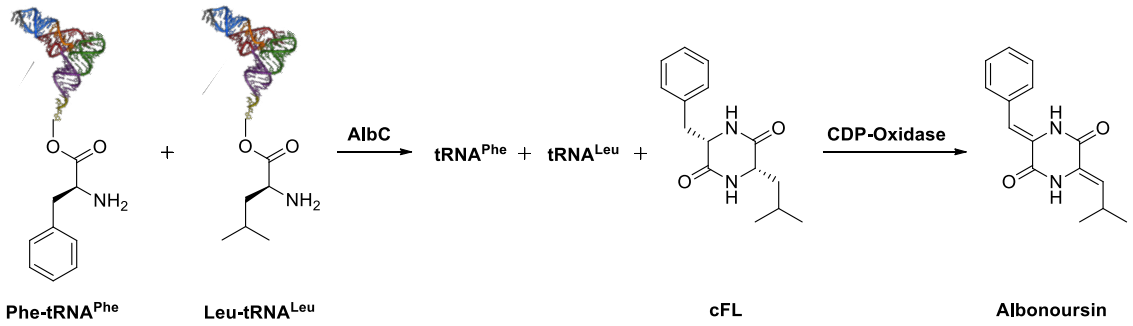

Scheme 67: Biosynthesis of albonoursin, catalyzed by AlbC and CDO

Its crystallographic structure was resolved in 2011[239] (**Figure 33**) and shows similarity to the one of class I aminoacyl-tRNA-synthetases (aaRSs). However, AlbC lacks the domains of class I aaRSs interacting with ATP, confirming that AlbC uses already formed aa-tRNA as substrates. The analysis of the structural data suggested that the recognition mode of the tRNA moiety of aa-tRNA is different from aaRSs, but this issue remains to be investigated.

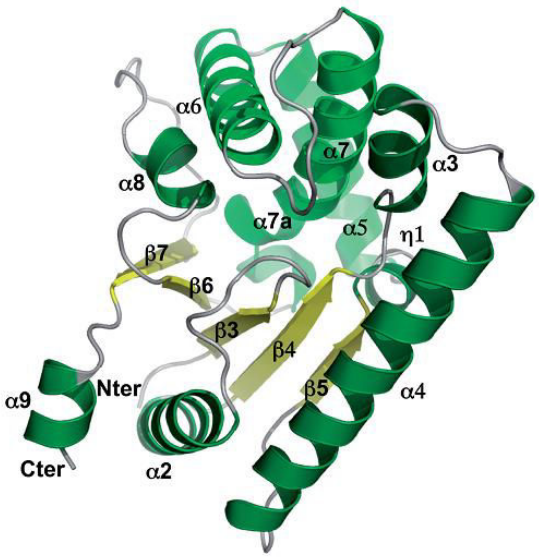

Figure 33: Overall crystallographic structure of AlbC, from Sauguet *et al.*. Alpha-helixes are shown in green, beta-strands in yellow and loops in grey.

AlbC does not possess interaction sites for both aa-tRNA substrates. The existence of a functional homodimer of AlbC is not consistent with the structural data. Instead, the proposed mechanism for

the AlbC-catalyzed reaction is the following: Phe-tRNA^{Phe} interacts with AlbC and the catalytic Ser 37 forms a covalent adduct with the Phe residue. TRNA^{Phe} exists and the formed Phe-AlbC adduct reacts with Leu-tRNA^{Leu} to form the cFL cyclodipeptide (**Scheme 68**).[239]

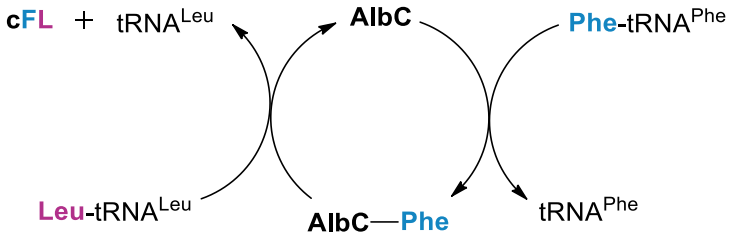

Scheme 68: Proposed catalytic mechanism for the AlbC-catalyzed cFL formation, involving an AlbC-Phe covalent adduct.

Even though the existence of the Phe-AlbC covalent adduct was proven, a detailed mechanism remains to be established, especially the events allowing the activation of Ser 37. No neighboring amino acid residue can be suspected of being able to deprotonate Ser 37. A possible explanation could be a concerted mechanism involving the vicinal 2' and 3' hydroxyl groups of the terminal A76 of Phe-tRNA^{Phe}, similarly to what was proposed for the catalytic mechanism of FemX$_{Wv}$.

In order to study both the recognition mode of the aa-tRNA substrates of AlbC and the detailed mechanism of the formation of cFL catalyzed by AlbC, analogs of the Phe-tRNA^{Phe} and Leu-tRNA^{Leu} substrates were investigated.

3. Synthesis of Phe-tRNA^{Phe} and Leu-tRNA^{Leu} analogs for the study of AlbC

The synthesis of stable analog of the aa-tRNAs substrates of AlbC could help to study this enzyme. Previous studies on FemX$_{Wv}$[121,123,30] and the results presented in chapter 1 and chapter 3 of this work showed that replacing the natural ester bond present between the amino acid and the tRNA moieties of aa-tRNAs by a triazole ring allows access to non-hydrolyzable and non-isomerizable analogs of aa-tRNAs. Such compounds could help to gain structural and mechanistic insight into the activity of AlbC. Phe-tRNA^{Phe} and Leu-tRNA^{Leu} analogs in the form of triazoyl-dinucleotides, -tRNA or -microhelixes mimicking the acceptor arm of tRNAs were synthesized (**Figure 34**). The results of this work are presented in the enclosed publication in *Bioorganic and Medicinal Chemistry Letters*.[240]

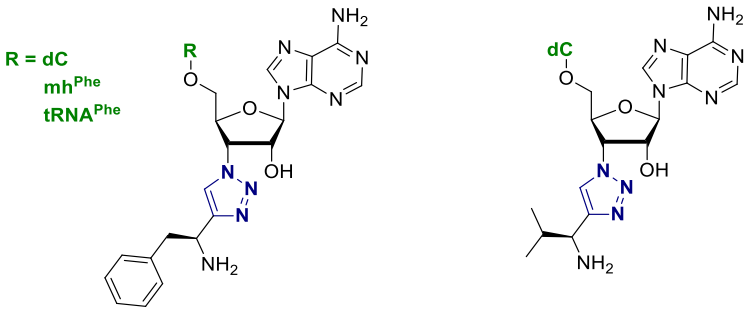

Figure 34: Structure of the synthesized Phe-tRNA^{Phe} and Leu-tRNA^{Leu} analogs

Those compounds are now under study with AlbC by our collaborators from the group of Muriel Gondry (Commissariat à l'énergie atomique et aux énergies alternatives, Saclay, France).

Bioorganic & Medicinal Chemistry Letters 24 (2014) 3231–3233

Contents lists available at ScienceDirect

Bioorganic & Medicinal Chemistry Letters

journal homepage: www.elsevier.com/locate/bmcl

Synthesis of 3′-triazoyl-dinucleotides as precursors of stable Phe-tRNA^{Phe} and Leu-tRNA^{Leu} analogues

Marco Santarem [a], Matthieu Fonvielle [b], Nicolas Sakkas [c], Guillaume Laisné [c], Maryline Chemama [a], Jean-Philippe Herbeuval [c], Emmanuelle Braud [c], Michel Arthur [b], Mélanie Etheve-Quelquejeu [c,*]

[a] Institut Parisien de Chimie Moléculaire, CNRS UMR 7201, Université Pierre et Marie Curie Paris 6, 4, place Jussieu, 75005 Paris, France
[b] Centre de Recherche des Cordeliers, LRMA, Equipe 12, INSERM UMR S 1138, Université Pierre et Marie Curie–Paris 6, UMR S 1138, Paris F-75006, France; Université Paris Descartes, Sorbonne Paris Cité, UMR S 1138, Paris F-75006 France
[c] Chemistry & Biology Nucleo(s)tides & Immunology for Therapy (CBNIT), CNRS UMR8601, Université Paris Descartes, PRES Sorbonne Paris Cité, 45 rue des Saints-Pères, 75270 Paris Cedex 06, France

ARTICLE INFO

Article history:
Received 28 May 2014
Revised 9 June 2014
Accepted 10 June 2014
Available online 19 June 2014

Keywords:
Aminoacyl-tRNA
Click chemistry
Cyclodipeptides synthases
Dinucleotides
Cycloaddition

ABSTRACT

We report here the synthesis of stable Phe-tRNA^{Phe} and Leu-tRNA^{Leu} analogues containing a 1,2,3-triazole ring instead of the ribose-amino acid ester bond. The 1,2,3-triazole ring is generated by dipolar cycloaddition of alkyne Phe and Leu analogues to 3′-azido-3′-deoxyadenosine via the Cu^{I}-catalysed Huisgen, Meldal, Sharpless 1,3-cycloaddition. The corresponding triazoyl pdCpA dinucleotides, obtained by classical phosphoramidite chemistry, were enzymatically ligated to 22-nt or 74-nt RNA generating stable Phe-tRNA^{Phe} analogues containing the acceptor stem or full tRNA moieties, respectively. These molecules represent useful tools to study the contribution of the RNA and amino acid moieties in stabilization of aminoacyl-tRNA/protein complexes.

Aminoacyl-tRNAs have important roles in a variety of biological processes in addition to protein synthesis by ribosomes.[1] Recently, cyclodipeptide synthases (CDPSs) were shown to use aminoacyl-tRNAs as substrates to catalyze the formation of the two peptide bonds of various cyclodipeptides[2] (Fig. 1). The cyclodipeptides form the diketopiperazine (DKP) scaffold of a variety of natural products with interesting biological properties, including antibacterial,[3] antiviral,[4] antitumoral,[5] immunosuppressive[6] and anti-inflammatory[7] activities. The first member of the CDPS family to be identified was AlbC from *Streptomyces noursei*, which has been showed to use mainly Phe-tRNA^{Phe} and Leu-tRNA^{Leu} as substrates to preferentially synthesize cyclo(L-Phe-L-Leu)[2]. The crystal structures of AlbC, YvmC-Blic, and Rv2275 CDPSs revealed a compact α/β structure containing a Rossman-fold domain[8] and similarities with aminoacyl-tRNA synthases (aaRS). These findings suggest that all CDPSs share a common aaRS-like architecture and catalytic mechanism. Moreover, biochemical data indicated that YvmC-Blic binds tRNA and generates cyclo(L-Leu-L-Leu) via formation of an aminoacyl-enzyme intermediate.[8c] However, recognition mode of

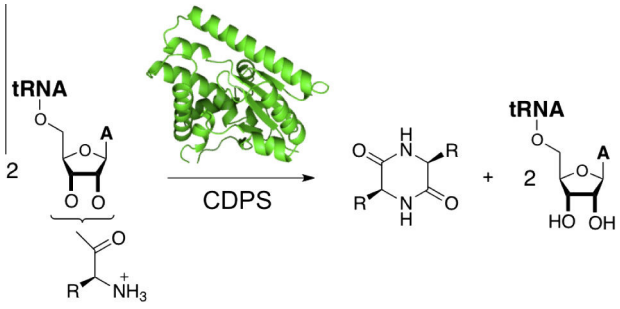

Figure 1. Synthesis of cyclodipeptides by CDPS. R = Phe and Leu for AlbC from *Streptomyces noursei*; A = Adénosine.

the RNA moiety of the substrates remains elusive since no crystal structures of CDPS in complexes with aminoacyl-tRNAs have been resolved. In such substrates, the ester bond connecting the amino acid residue to the 2′ or 3′ position of the terminal nucleotide is labile with half-lives from 10 min to 1 h at neutral pH.[9] *Trans*-esterification between the 2′ and 3′ positions occurs in the absence of enzyme with a rate and thermodynamic equilibrium constant of 5 s^{-1} and 1, respectively.[10] We have shown that triazole rings act

* Corresponding author. Tel.: +33 0142864026.
E-mail address: melanie.etheve-quelquejeu@parisdescartes.fr (M. Etheve-Quelquejeu).

http://dx.doi.org/10.1016/j.bmcl.2014.06.027
0960-894X/

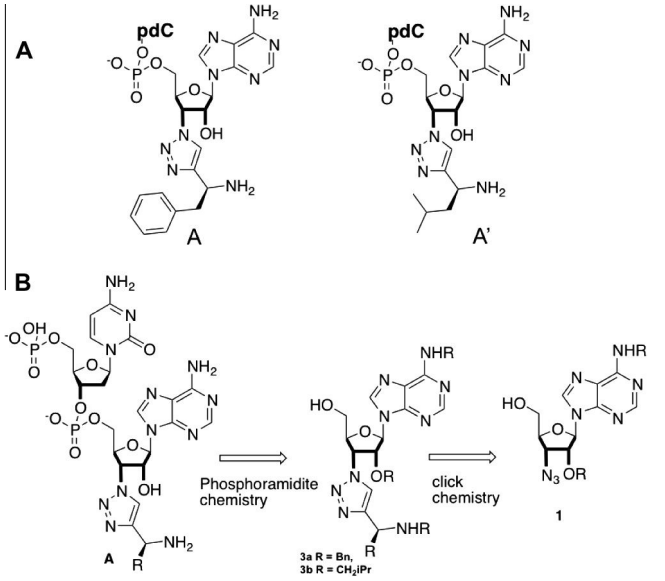

Figure 2. Structure of stable Phe-tRNA^{Phe} and Leu-tRNA^{Leu} analogues (A) and retrosynthesis (B).

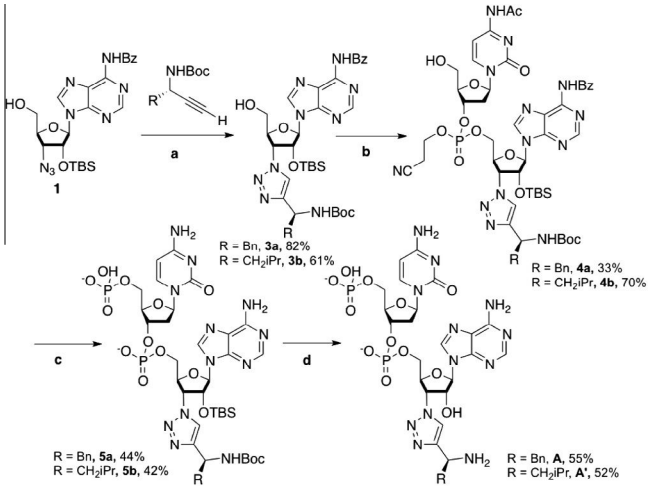

Scheme 2. Synthesis of 3′-triazoyl-dinucleotides **A** and **A′**. (a) $CuSO_4$, sodium ascorbate, THF/H_2O, rt, 24 h; (b) (i) Ac-dC-PCNE, tetrazole, rt, 1 h, CH_3CN, (ii) I_2, H_2O/pyr/THF, rt, 30 min, (iii) TCA, CH_2Cl_2, rt, 30 min; (c) (i) $iPr_2NP(OCH_2CH_2CN)_2$, tetrazole, CH_3CN, rt, 1 h, (ii) I_2, H_2O/pyr/THF, rt, 30 min, (iii) $MeNH_2$, rt, 24 h; (d) HCl/THF/MeOH (1:2:1), rt, 24 h.

as surrogates of the ester bond and provide non-hydrolysable and non-isomerisable analogues of Ala-tRNA^{Ala}.[11] These analogues are good candidates for crystallization of enzyme/aminoacyl-tRNA complexes and for the investigation of catalytic mechanisms, as recently shown for the Fem transferases involved in bacterial cell wall synthesis.[12]

We describe here the synthesis of triazoyl-dinucleotides **A** and **A′**, mimicking the terminal sequence pCpA of Phe-tRNA^{Phe} and Leu-tRNA^{Leu} (Fig. 2A). The general strategy for the preparation of the target compounds **A** and **A′** is outlined in Figure 2B. We planned to synthesize dinucleotides by coupling monomers **3a** and **3b** with Ac-dC-CE phosphoramidite. The key step to obtain monomers **3a** and **3b** was the cycloaddition of alkyne amino acids with azido-adenosine **1**. Knowing that AlbC catalyzes essentially the synthesis of cyclodipeptide Phe-Phe and Phe-Leu, we focused our attention on the synthesis of alkynes **2a** and **2b** (Scheme 1) providing mimics of Phe and Leu. Conversion of N-Boc-aminomethylesters into the corresponding alkynes **2** was achieved by a Seyferth–Gilbert homologation of the α-amino aldehydes using the Bestmann-Ohira reagent.[13] Alkynes **2a**[14] and **2b**[14b] were obtained in 73% and 45% yields, respectively, (Scheme 1).

Cycloaddition of organic azides and alkynes is the most direct route to 1,2,3-triazoles.[15] The use of Cu^{I} as a catalyst has the advantage of providing exclusively the 1,4-disubstitued 1,2,3-triazole regioisomers. Alkynes **2a** and **2b** reacted with the known 3′-azido-2′-O-(*tert*-butyldimethylsilyl)-3′-deoxyadenosine **1**[11a] in presence of copper(II) sulfate and sodium ascorbate. The 3′-triazoyl deoxyadenosine **3a** and **3b** were obtained in 82% and 61% yields, respectively, (Scheme 2). From nucleosides **3a** and **3b**, the phosphoramidite approach was used to obtain the corresponding dinucleotides **A** and **A′** (Scheme 2). For the latter transformation, commercially available deoxycytidine phosphoramidite is mixed with nucleosides **3a** or **3b** and tetrazole in acetonitrile to form the corresponding phosphite triester intermediates. The crude products were oxidized with a solution of iodine and treated with trichloroacetic acid to afford compounds **4a** and **4b** in 33% and 70% yields, respectively. A phosphorylation step in 5′-position of **4a** and **4b** was necessary because T4 RNA ligase catalyzes the ligation of a 5′-phosphate-dinucleotide to the 3′-OH extremity of an incomplete tRNA (see below). In order to obtain the two protected dinucleotides, compounds **4a** and **4b** were mixed with the phosphitylation reagent bis(2-cyanoethyl) diisopropylphosphoramidite in the presence of tetrazole. Removal of acetyl, cyanoethyl and benzoyl groups with a solution of methylamine afforded the desired compounds **5a** and **5b** in 44% and 42% yields, respectively. Eventually, the TBS and *N*-Boc protecting groups were removed by stirring with a solution of HCl during 24 h, producing the deprotected dinucleotides **A** and **A′** in 55% and 52% yields, respectively.

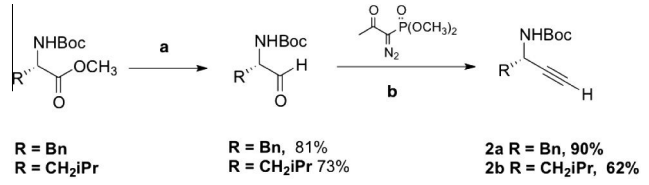

Scheme 1. Synthesis of alkynes **2a** and **2b**. (a) DIBAL-H, CH_2Cl_2, −78 °C, 1 h; (b) K_2CO_3, MeOH, 0 °C 1 h, then rt, 24 h.

The Phe-tRNA^{Phe} analogues were obtained by enzymatic ligation of dinucleotides **A** with 74- and 22-nt RNA molecules (Fig. 3). Addition of pdCpA to these RNAs generate the sequence of the full tRNA^{Phe} or its acceptor arm, respectively. The ligation reaction is catalyzed by T4 RNA ligase, which tolerates a wide range of modifications of the adenosine, including a triazole ring in 2′ or 3′ position.[11a] The ligation was performed in HEPES buffer containing the 74- and 22-nt RNAs, compound **A**, T4 RNA ligase, ATP and $MgCl_2$. After two hours, the Phe-tRNA^{Phe} analogues were purified by anion-exchange chromatography and analyzed by denaturating polyacrylamide gel electrophoresis (Fig. 3).

In summary, we synthesised two dinucleotides pdCpA, containing a 3′-terminal triazoyl-deoxyadenosine mimicking the 3′-terminal sequence of Phe-tRNA^{Phe} and Leu-tRNA^{Leu}. These molecules are stable analogues of aminoacyl-tRNAs because the triazole rings act as bio-isoster of the ester bond and provide non-hydrolysable and non-isomerisable analogues of Phe-tRNA^{Phe} and Leu-tRNA^{Leu}. Dinucleotide **A** underwent enzymatic ligation to a 22nt-microhelix and to a 74nt-RNA to afford two Phe-tRNA^{Phe} analogues. These compounds are currently investigated as ligands for co-crystallization with cyclodipeptide synthetase AlbC.

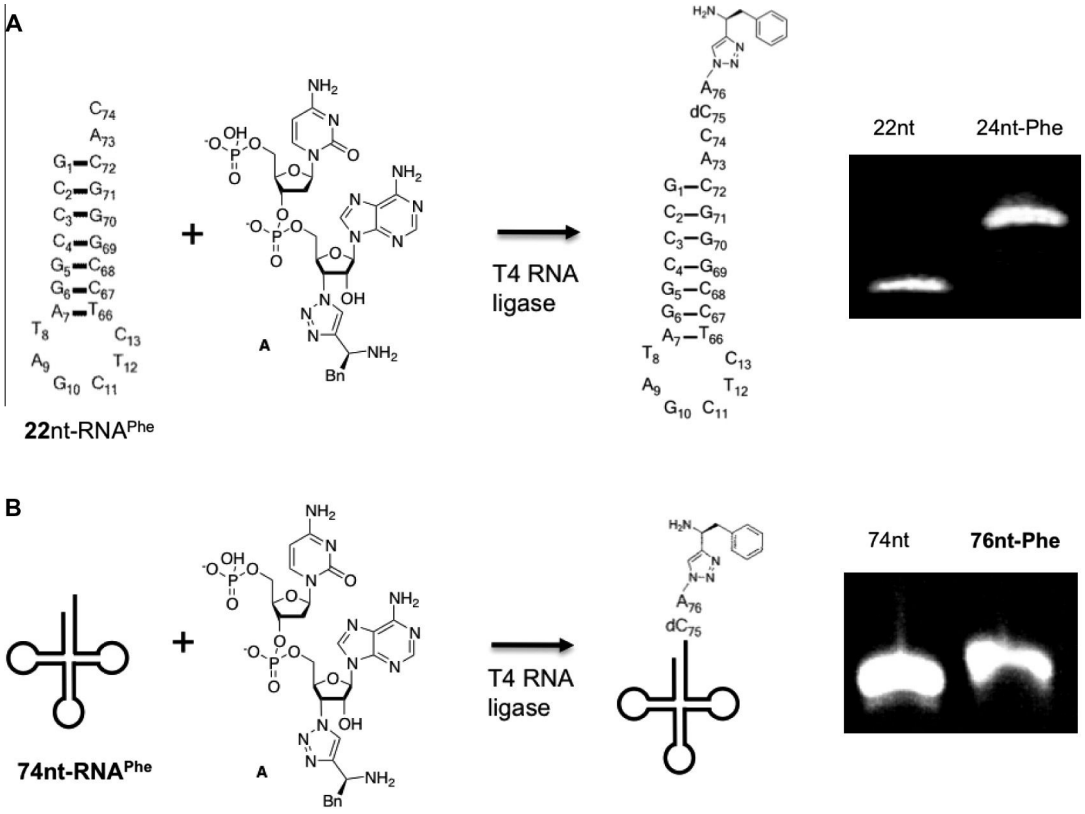

Figure 3. Ligation of **A** to 22-nt by T4 RNA ligase (A); Ligation of **A** to 74-nt by T4 RNA ligase (B).

Acknowledgments

The ANR CyDiPepS and MimictRNA supported this work.

Supplementary data

Supplementary data (experimental details for the preparation of nucleosides and nucleotides) associated with this article can be found, in the online version, at http://dx.doi.org/10.1016/j.bmcl.2014.06.027.

References and notes

1. (a) von Dohren, H. *Nat. Chem. Biol.* **2009**, *5*, 374; (b) Shepherd, J.; Ibba, M. *FEBS Lett.* **2013**, *587*, 2895.
2. Gondry, M.; Sauguet, L.; Belin, P.; Thai, R.; Amouroux, R.; Tellier, C.; Tuphile, K.; Jacquet, M.; Braud, S.; Courcon, M.; Masson, C.; Dubois, S.; Lautru, S.; Lecoq, A.; Hashimoto, S.; Genet, R.; Pernodet, J. L. *Nat. Chem. Biol.* **2009**, *5*, 414.
3. Cain, C. C.; Lee, D. H.; Waldo, R. H.; Henry, A. T.; Casida, E. J.; Wani, M. C.; Wall, M. E.; Oberlies, N. H.; Falkinham, J. O. *Antimicrob. Agents Chemother.* **2003**, *47*, 2113.
4. Rodriguez, P. L.; Carrasco, L. *J. Virol.* **1992**, *66*, 1971.
5. Jia, J. M.; Ma, X. C.; Wu, C. F.; Wu, L. J.; Hu, G. S. *Chem. Pharm. Bull. (Tokyo)* **2005**, *53*, 582.
6. Waring, P.; Beaver, J. *Gen. Pharmacol.* **1996**, *27*, 1311.
7. Minelli, A.; Grottelli, S.; Mierla, A.; Pinnen, F.; Cacciatore, I.; Bellezza, I. *Int. J. Biochem. Cell. B* **2012**, *44*, 525.
8. (a) Sauguet, L.; Moutiez, M.; Li, Y.; Belin, P.; Seguin, J.; Le Du, M. H.; Thai, R.; Masson, C.; Fonvielle, M.; Pernodet, J. L.; Charbonnier, J. B.; Gondry, M. *Nucleic Acids Res.* **2011**, *39*, 4475; (b) Vetting, M. W.; Hegde, S. S.; Blanchard, J. S. *Nat. Chem. Biol.* **2010**, *6*, 797; (c) Bonnefond, L.; Arai, T.; Sakaguchi, Y.; Suzuki, T.; Ishitani, R.; Nureki, O. *Proc. Natl. Acad. Sci. U.S.A.* **2011**, *108*, 3912.
9. Hentzen, D.; Mandel, P.; Garel, J. P. *Biochim. Biophys. Acta* **1972**, *281*, 228.
10. Taiji, M.; Yokoyama, S.; Miyazawa, T. *Biochemistry* **1983**, *22*, 3220.
11. (a) Chemama, M.; Fonvielle, M.; Arthur, M.; Valery, J. M.; Etheve-Quelquejeu, M. *Chem.-Eur. J.* **2009**, *15*, 1929; (b) Fonvielle, M.; Chemama, M.; Lecerf, M.; Villet, R.; Busca, P.; Bouhss, A.; Etheve-Quelquejeu, M.; Arthur, M. *Angew. Chem., Int. Ed.* **2010**, *49*, 5115.
12. (a) Fonvielle, M.; de La Sierra-Gallay, I. L.; El-Sagheer, A. H.; Lecerf, M.; Patin, D.; Mellal, D.; Mayer, C.; Blanot, D.; Gale, N.; Brown, T.; van Tilbeurgh, H.; Etheve-Quelquejeu, M.; Arthur, M. *Angew. Chem., Int. Ed.* **2013**, *52*, 7278; (b) Fonvielle, M.; Mellal, D.; Patin, D.; Lecerf, M.; Blanot, D.; Bouhss, A.; Santarem, M.; Mengin-Lecreulx, D.; Sollogoub, M.; Arthur, M.; Etheve-Quelquejeu, M. *Chem.-Eur. J.* **2013**, *19*, 1357.
13. (a) Ohira, S. *Synth. Commun.* **1989**, *19*, 561; (b) Roth, G. J.; Liepold, B.; Muller, S. G.; Bestmann, H. J. *Synthesis-Stuttgart* **2004**, 59.
14. (a) Proteau-Gagne, A.; Rochon, K.; Roy, M.; Albert, P. J.; Guerin, B.; Gendron, L.; Dory, Y. L. *Bioorg. Med. Chem. Lett.* **2013**, *23*, 5267; (b) Detz, R. J.; Abiri, Z.; le Griel, R.; Hiemstra, H.; van Maarseveen, J. H. *Chem.-Eur. J.* **2011**, *17*, 5921.
15. (a) Rostovtsev, V. V.; Green, L. G.; Fokin, V. V.; Sharpless, K. B. *Angew. Chem., Int. Ed.* **2002**, *41*, 2596; (b) Tornoe, C. W.; Christensen, C.; Meldal, M. *J. Org. Chem.* **2002**, *67*, 3057.

General Conclusion

General conclusion

Among the potential new targets for the development of antimicrobials are transferases from the FemABX family. They are non-ribosomal aminoacyl-transferases responsible for the biosynthesis of the peptide interbridge in many Gram-positive bacteria, and some pathogenic Gram-negative bacteria. They use, as source of activated amino acids, aminoacyl-tRNAs. In this work have been presented the syntheses of aminoacyl-tRNA analogs able to study and inhibit two Fem-transferases: $FemX_{Wv}$ in *Weissella viridescens*, used as a model in our studies, and FmhB in *Staphylococcus aureus*, a crucial pathogenic germ. Both of these enzymes are essential to bacterial survival.

The context of this work was presented in the first part of this thesis as a bibliographical study which reviewed the peptidoglycan, as the studied bacterial process, Fem-transferases, as molecular targets of our investigations, and tRNAs and aminoacyl-tRNAs, as scaffolds for the development of our compounds. In particular, the state of the art regarding the synthesis of aminoacyl-tRNAs analogs was presented.

The second part of this thesis presented the results and discussions, organized in four chapters.

The first chapter deals with the synthesis of electrophilic tRNA analogs able to form covalent adducts with Fem-transferases. For this purpose, a maleimide-bearing RNA was first synthesized and showed the ability to form covalent adducts with $FemX_{Wv}$, but without any selectivity toward one particular amino acid within FemX, or toward FemX among other enzymes. Second, RNA-squaramates were synthesized with the idea that the squaryl ring, being a lysine-specific, moderate electrophile, could help us to reach our goal. Site-specific and enzyme-specific labeling of $FemX_{Wv}$ was achieved through the use of these RNA-squaramates. These results open the way to the use of similar RNA-squaramates to react, characterize or perhaps identify other transferases of the FemABX family, or other aminoacyl-tRNA-dependents enzymes. Finally, in parallel to this goal, efforts were made to optimize the traceless Staudinger ligation method to introduce amide bonds in post-functionalization steps on RNA. This method was successfully applied on an oligoribonucleotide, and will, in the future, investigated to incorporate electrophilic motifs and tags into RNA.

The second chapter presents the synthesis of 2',3'-bisfunctionalized nucleosides as precursors of fluorinated tRNA analogs and fluorinated RNA-peptide conjugates. The optimization of the syntheses of both the *xylo* and *ribo*-configurated analog of 2'-azido-2',3'-dideoxy-3'-fluoroadenosine has been successfully realized and is presented in chapter 2. Such nucleosides will soon be used to synthesize

fluorinated analogs in order to investigate the role of the 3'-terminal hydroxyl groups of aa-tRNAs in FemABX-catalyzed processes, as well as a potential conformational preference of Fem-transferases.

The third chapter concerns the application of the knowledge regarding the synthesis of aa-tRNAs analogs for $FemX_{Wv}$ to FmhB, an essential Fem-transferase found in *S. aureus*. Duplexes exhibiting micromolar inhibition potency on FmhB were obtained. Conjugate of the best duplex with an analog for the lipid II led to a complex RNA-peptide-disaccharide-lipid conjugate exhibiting nanomolar inhibition of FmhB. Derivatives of these compounds will also be used in structural studies of FmhB. Finally, preliminary results concerning the synthesis of tools to study other aspects of FmhB are presented: compounds to investigate how FmhB uses and discriminates between all five $tRNA^{Gly}$ isoacceptors present in *S. aureus*; compounds to explore what role the coiled-coil domain of FmhB plays in its interaction with the Gly-$tRNA^{Gly}$ substrate. These compounds will allow to explore new aspects of FmhB's mode of recognition and structure for the development of inhibitors.

The fourth chapter presents the results obtained in a side-project in which similar triazole-containing aa-tRNA anlogs were synthesized for the study of cyclodipeptide-synthases. Analogs of Phe-$tRNA^{Phe}$ and Leu-$tRNA^{Leu}$ were obtained and are currently in the hands of our collaborators for structural and mechanistical studies of AlbC, a CDPS involved in the biosynthesis of albonoursin, an antibacterial metabolite found in *Streptomyces noursei*.

During this work, I was involved in the solution-phase synthesis of modified nucleosides, the solid-phase synthesis of oligoribonucleotides (in the laboratory of Prof. Tom Brown, University of Oxford, UK) as well as the post-functionalization on RNA compounds. Thanks to our collaborators from the group of Dr Michel Arthur (Centre de Recherche des Cordeliers, Paris, France), functionalized RNA could be used for enzymatic ligation, cross-linking with Fem-transferases and evaluated as inhibitors of Fem-transferases. Our close collaboration allowed us to deepen our studies on the model Fem-transferase $FemX_{Wv}$ and to pave the way for similar studies on the therapeutically relevant FmhB enzyme in the future.

List of communications

Publications

Electrophilic RNA for Peptidyl-RNA Synthesis and Site-Specific Cross-Linking with tRNA-Binding Enzymes.

Matthieu Fonvielle,[+] Nicolas Sakkas,[+] Laura Iannazzo, Chloé Le Fournis, Delphine Patin, Dominique Mengin-Lecreulx, Afaf El-Sagheer, Emmanuelle Braud, Sébastien Cardon, Tom Brown, Michel Arthur*, Mélanie Etheve-Quelquejeu*.

Angewandte Chemie, International Edition. In press. DOI: 10.1002/anie.201606843R1.

+: These authors contributed equally to this work.

Synthesis of 3'-triazoyl-dinucleotides as precursors of stable Phe-tRNA^{Phe} and Leu-tRNA^{Leu} analogues. Marco Santarem, Matthieu Fonvielle, Nicolas Sakkas, Guillaume Laisné, Maryline Chemama, Jean-Philippe Herbeuval, Emmanuelle Braud, Michel Arthur, Mélanie Etheve-Quelquejeu*.

Bioorganic & Medicinal Chemistry Letters, **2014**, *24* (15), 3231–3233 DOI: 10.1016/j.bmcl.2014.06.027.

Oral communications

RNA-Squaramates as aminoacyl-tRNA analogs.

Scientific days of the Graduate School "Medicines, Toxicology, Chemistry and Imaging", 23-24/06/2016, Paris, France. **Prize for best oral communication.**

Poster communications

Oligonucleotide-squaramates as aminoacyl-tRNA analogs: application to the essential FemX of Weissella viridescens.

20ème journée de chimie organique et chimie organique biologique de la montagne Sainte-Geneviève.

Oligonucleotide-squaramates as aminoacyl-tRNA analogs: application to bacterial FemX-transferase.

22th International Round Table on Nucleosides, Nucleotides and Nucleic Acids (XXII IRT), 18-22/07/2016, Paris, FRANCE. **IS3NA A. Holy IRT Poster Award**

Experimental Part

1. General experimental methods

Reactions were carried out under an argon atmosphere. They were monitored by thin-layer chromatography with precoated silica on aluminium foil (Merck KGaA). Solvents were purified as such: CH_2Cl_2, DMF, pyridine, chloroform and NEt_3 were distilled over calcium hydride, THF was distilled over sodium and benzophenone. Flash chromatography was performed with silica gel 60 (Merck 40-63 μm); Spectroscopic ^{1}H, ^{13}C, ^{19}F, ^{31}P NMR, MS and/or analytical data were obtained using chromatographically homogeneous samples. ^{1}H NMR (500 MHz) ^{19}F (471 MHz) and ^{13}C NMR (125 MHz) spectra were recorded on a Bruker Avance II spectrometer, unless specified otherwise. The chemical shifts (δ) are reported in ppm, referenced to the residual proton resonance of the solvents (7.26 for $CDCl_3$; 2.50 for DMSO and 3.31 for MeOD, 2.09 for acetone-d6, 4.80 for D_2O), to the carbon resonance of the solvent (77.16 for $CDCl_3$; 39.52 for DMSO and 49.00 for MeOD). and the coupling constants are given in Hz. The terms m, s, d, t, q, quint, refer to multiplet, singlet, doublet, triplet, quartet, quintet; bs means broad signal. When possible, NMR signals were assigned on the basis of COSY, HSQC, HMBC, DEPT-135 experiments. Mass spectra (MS) were recorded with an ion trap mass analyzer under electrospray ionization (ESI) in positive ionization – unless specified otherwise – mode detection or atmospheric pressure chemical ionization (APCI) on a LCQ Advantage Finnigan spectrometer. High resolution mass spectra (HRMS) were recorded with a TOF mass analyzer under electrospray ionization (ESI) in positive ionization – unless specified otherwise – mode detection, atmospheric pressure chemical ionization or atmospheric pressure photoionization (APPI).

2. Solid-phase synthesis, cleavage and deprotection of oligoribonucleotides.

The building blocks for the RNA analogues were prepared using 2'-TBS protected RNA phosphoramidite monomers with t-butylphenoxyacetyl protection of the A, G and C nucleobases and unprotected U (Sigma-Aldrich). Hexaethylene glycol phosphoramidite monomers were purchased from Link Technologies Ltd (Glasgow). A solution of 0.3 M benzylthiotetrazole in acetonitrile (Link Technologies) was used as the coupling agent, t-butylphenoxyacetic anhydride as the capping agent and 0.1 M iodine as the oxidizing agent (Sigma-Aldrich). All phosphoramidite monomers were dissolved in anhydrous acetonitrile to a concentration of 0.1 M immediately prior to use, and the coupling time for all monomers was 6 min. Stepwise coupling efficiencies were determined by automated trityl cation conductivity monitoring and in all cases were >97%. Cleavage of oligonucleotides from the solid support and deprotection were achieved by exposure to concentrated aqueous ammonia/ethanol (3/1 v/v) for 2 h at room temperature followed by heating in a sealed tube for 45 min at 55 °C.

After cleavage from the solid support and deprotection of the nucleobases and phosphodiesters, oligonucleotides were concentrated to a small volume in vacuo, transferred to 15 mL plastic tubes and freeze dried. The residue was dissolved in DMSO (300 μL) and triethylamine trihydrofluoride (300 μL)

was added after which the reaction mixtures were kept at 65 °C for 2.5 hr. Sodium acetate (3 M, 50 µL) and butanol (3 mL) were added with vortexing and the samples were kept at -80 °C for 30 min then centrifuged at 4 °C at 13,000 rpm for 10 min. The supernatant was decanted and the precipitate was washed twice with ethanol (0.75 mL) then dried under vacuum.

3. Synthesized compounds

Protocols and characterizations of the synthesized compounds are indicated according to the following numbering of atoms:

Adenosine derivatives

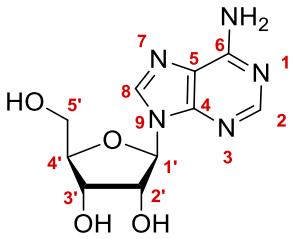

Benzoyl groups

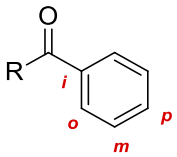

Dimethoxytrityl groups

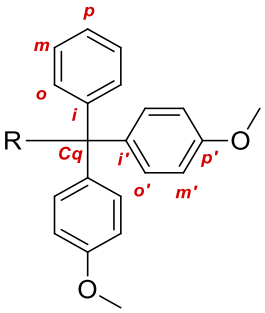

(1) (2R,3R,4S,5R)-2-(6-amino-9H-purin-9-yl)-4-((tert-butyldimethylsilyl)oxy)-5-(((tert-butyldimethylsilyl)oxy)methyl)tetrahydrofuran-3-ol

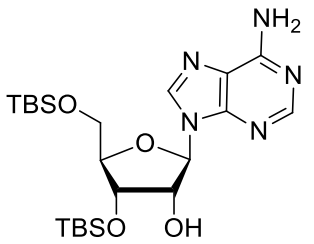

1

Chemical Formula: $C_{22}H_{41}N_5O_4Si_2$
Molecular Weight: 495,7630

Adenosine (4.00 g, 15.0 mmol) and TBDMSCl (7.02 g, 46.6 mmol) were added to a suspension of DABCO (10.4 g, 93.1 mmol) and $AgNO_3$ (7.92 g, 46.6 mmol) in THF (210 mL) previously stirred for 30 min. The reaction mixture was vigorously stirred at rt for 4 h then filtered over silica gel. The filtrate was concentrated, and the residue was partitioned between DCM and brine. The phases were separated and the aqueous phase was extracted twice with DCM. The combined organic layers were dried over sodium sulfate and concentrated. Flash chromatography of the residue (Cyclohexane/AcOEt 4/6) yielded **1** as a white amorphous solid (4.80 g, 65 %).

^{1}H NMR (250 MHz, $CDCl_3$) δ 8.29 (s, 1H, H2 or H8), 8.07 (s, 1H, H2 or H8), 6.26 (bs, 2H, NH_2), 6.03 (d, *J* = 2.5 Hz, 1H, H1'), 4.56-4.54 (m, 2H, H2'/ H3'), 4.11 (d, *J* = 2.5 Hz, 1H, H4'), 3.91 (dd, *J* = 2.5, 27.5 Hz, 1H, H5'a), 3.75 (dd, *J* = 2.5, 27.5 Hz, 1H, H5'b), 0.92 (s, 9H, *t*Bu^{TBS}), 0.87(s, 9H, *t*Bu^{TBS}), 0.15 (s, 6H, 2 x Me^{TBS}), 0.06 (s, 3H, Me^{TBS}), 0.04 (s, 3H, Me^{TBS}).

^{13}C NMR (63 MHz, $CDCl_3$) δ 155.8, 153.1 (C2 or C8), 149.8 (Cq^{Ad}), 139.1 (C2 or C8), 120.0 (Cq^{Ad}), 88.9 (C1'), 85.6 (C4'), 75.3 (C2'), 71.8 (C3'), 62.5 (C5'), 26.0, 25.9 (2 x *t*Bu^{TBS}), 18.5, 18.2 (2 x Cq^{TBS}), -4.6, -4.7, -5.3, -5.4 (4 x Me^{TBS}).

Hakimelahi, G. H., Proba, Z. A., & Ogilvie, K. K. (1982). New catalysts and procedures for the dimethoxytritylation and selective silylation of ribonucleosides. *Canadian Journal of Chemistry*, *60*(9), 1106-1113.

(2) N-benzoyl-N-(9-((2R,3R,4S,5R)-4-((tert-butyldimethylsilyl)oxy)-5-(((tert-butyldimethylsilyl)oxy)methyl)-3-hydroxytetrahydrofuran-2-yl)-9H-purin-6-yl)benzamide

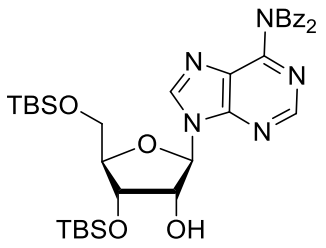

2

Chemical Formula: $C_{36}H_{49}N_5O_6Si_2$
Molecular Weight: 703,9752

To a solution of **1** (2.50 g, 5.04 mmol) in pyridine (30 mL), trimethylsilyl chloride (2.56 mL, 20.2 mmol) was added at 0 °C. The reaction mixture was stirred at rt for 1.5 h. Benzoyl chloride (2.93 mL, 25.2 mmol) was added at 0 °C and the reaction mixture was stirred overnight. Water (35 mL) was added at 0 °C, and the reaction mixture was stirred for 1.5 h. Toluene (30 mL) was added and the mixture was concentrated. The residue was partitioned between AcOEt and brine, and the phases were separated. The aqueous phase was extracted twice with AcOEt. The combined organic layers were dried over sodium sulfate and concentrated. Flash chromatography of the residue (Cyclohexane/AcOEt 7/3) quantitatively yielded **2** as a white foam.

^{1}H NMR (250 MHz, $CDCl_3$) δ 8.65 (s, 1H, H2 or H8), 8.32 (s, 1H, H2 or H8), 7.88-7.86 (m, 4H, H^{Bz}), 7.47-7.46 (m, 2H, H^{Bz}), 7.36-7.34 (m, 4H, H^{Bz}), 6.07 (d, *J* = 5.0 Hz, 1H, H1'), 4.64-4.62 (m, 2H, H2'/H3'), 4.12-4.09 (m, 1H, H4'), 3.92 (dd, *J* = 3.5, 11.5 Hz, 1H, H5'a), 3.78 (dd, *J* = 3.5, 11.5 Hz, 1H, H5'b), 0.96 (s, 9H, *t*Bu^{TBS}), 0.88 (s, 9H, *t*Bu^{TBS}), 0.18 (s, 6H, 2 x Me^{TBS}), 0.07 (s, 3H, Me^{TBS}), 0.03 (s, 3H, Me^{TBS}).

^{13}C NMR (63 MHz, $CDCl_3$) δ 172.4 (2 x $C{=}O^{Bz}$), 153.0 (Cq^{Ad}), 152.25 (C2 or C8), 151.9 (Cq^{Ad}), 143.7 (C2 or C8), 151.9 (Cq^{Ad}), 134.1 (Cq^{Bz}), 133.0, 129.6, 128.8 (10 x CH^{Bz}), 128.3 (Cq^{Ad}), 89.1 (C1'), 85.7 (C4'), 74.9 (C2'), 71.7 (C3'), 62.4 (C5'), 26.0, 25.8 (2 x *t*Bu^{TBS}), 18.5, 18.2 (2 x Cq^{TBS}), - 4.5, -4.7, -5.3, -5.4 (4 x Me^{TBS}).

Chatgilialoglu, C., Duca, M., Ferreri, C., Guerra, M., Ioele, M., Mulazzani, Q. G., ... & Giese, B. (2004). Selective generation and reactivity of 5′-adenosinyl and 2′-adenosinyl radicals. *Chemistry–A European Journal*, *10*(5), 1249-1255.

(3) N-benzoyl-N-(9-((2R,4R,5R)-4-((tert-butyldimethylsilyl)oxy)-5-(((tert-butyldimethylsilyl)oxy)methyl)-3-oxotetrahydrofuran-2-yl)-9H-purin-6-yl)benzamide

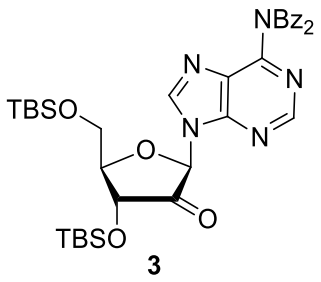

3

Chemical Formula: $C_{36}H_{47}N_5O_6Si_2$
Molecular Weight: 701,9593

To a solution of **2** (2.61 g, 3.71 mmol) in DCM (60 mL), Dess-Martin Periodinane (4.72 g, 11.1 mmol) in solution in DCM (60 mL) was added dropwise at 0 °C. The reaction mixture was stirred at rt for 4 h. The reaction was stopped by the addition of a 1/1 mixture of saturated aqueous sodium hydrogenocarbonate and sodium metabisulfite solutions at 0 °C. The phases were separated. The aqueous phase was extracted twice with DCM. The combined organic layers were dried over sodium sulfate and concentrated. Flash chromatography of the residue (Cyclohexane/AcOEt 8/2) yielded **3** as a white foam (2.31 g, 89 %).

---

^{1}H NMR (250 MHz, $CDCl_3$) δ 8.55 (s, 1H, H2 or H8), 8.09 (s, 1H, H2 or H8), 7.88-7.85 (m, 4H, H^{Bz}), 7.50-7.48 (m, 2H, H^{Bz}), 7.37-7.35 (m, 4H, H^{Bz}), 5.84 (s, 1H, H1'), 5.21 (d, *J* = 7.1 Hz, 1H, H3'), 4.05-4.03 (m, 2H, H4'/H5'a), 3.92 (dd, *J* = 3.5, 12.4 Hz, 1H, H5'b), 0.95 (s, 9H, *t*Bu^{TBS}), 0.78 (s, 9H, *t*Bu^{TBS}), 0.24 (s, 3H, Me^{TBS}), 0.20 (s, 3H, Me^{TBS}), 0.01 (s, 3H, Me^{TBS}), -0.13 (s, 3H, Me^{TBS}).

^{13}C NMR (63 MHz, $CDCl_3$) δ 207.0 (C=OC2'), 172.3 ($C=O^{Bz}$), 152.4 (C2 or C8), 152.3, 152.2 (2 x Cq^{Ad}), 144.3 (C2 or C8), 134.0 (Cq^{Bz}), 133.1, 129.6, 128.9 (10 x CH^{Bz}), 127.3 (Cq^{Ad}), 80.4 (C4'), 80.1 (C1'), 71.7 (C3'), 61.0 (C5'), 25.8, 25.7 (2 x *t*Bu^{TBS}), 18.3 (2 x Cq^{TBS}), -4.2, -5.1, -5.3, -5.4 (4 x Me^{TBS}).

Chatgilialoglu, C., Duca, M., Ferreri, C., Guerra, M., Ioele, M., Mulazzani, Q. G., ... & Giese, B. (2004). Selective generation and reactivity of 5′-adenosinyl and 2′-adenosinyl radicals. *Chemistry–A European Journal*, *10*(5), 1249-1255.

(4) N-benzoyl-N-(9-((2R,3R,4S,5R)-4-((tert-butyldimethylsilyl)oxy)-5-(((tert-butyldimethylsilyl)oxy)methyl)-3-hydroxytetrahydrofuran-2-yl)-9H-purin-6-yl)benzamide

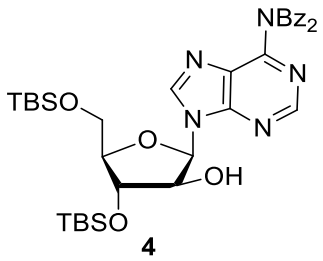

4

Chemical Formula: $C_{36}H_{49}N_5O_6Si_2$
Molecular Weight: 703,9752

To a solution of **3** (2.31 g, 3.29 mmol) in a 15/1 EtOH/water mixture (18 mL, 1.2 mL), sodium borohydride (224 mg, 5.92 mmol) was added at 0 °C. The reaction mixture was stirred at rt for 2 h. The reaction mixture was partitioned between AcOEt and brine, and the phases were separated. The aqueous phase was extracted twice with AcOEt. The combined organic layers were dried over sodium sulfate and concentrated. Flash chromatography of the residue (Cyclohexane/AcOEt 8/2) yielded **4** as a white foam (1.25 g, 54 %).

---

^{1}H NMR (250 MHz, $CDCl_3$) δ 8.64 (s, 1H, H2 or H8), 8.57 (s, 1H, H2 or H8), 7.87-7.85 (m, 4H, ^{Bz}), 7.49-7.47 (m, 2H, H^{Bz}), 7.36-7.34 (m, 4H, H^{Bz}), 6.43 (d, *J* = 2.4 Hz, 1H, H1'), 4.75 (bs, 1H, OH), 4.33 (s, 1H, H3'), 4.11 (s, 1H, H2'), 4.05 (d, *J* = 7.1 Hz, 1H, H4'), 3.96 (dd, *J* = 2.2, 11.3 Hz, 1H, H5'a), 3.82 (dd, *J* = 1.8, 11.3 Hz, 1H, H5'b), 0.93 (s, 9H, *t*BuTBS), 0.88 (s, 9H, $t\text{Bu}^{TBS}$), 0.15 (s, 3H, Me^{TBS}), 0.14 (s, 3H, Me^{TBS}) , 0.13(s, 3H, Me^{TBS}); 0.12 (s, 3H, Me^{TBS}).

^{13}C NMR (63 MHz, $CDCl_3$) δ 172.3 (2 x $C{=}O^{Bz}$), 153.2 (Cq^{Ad}), 152.1 (C2 or C8), 151.5 (Cq^{Ad}), 144.8 (C2 or C8), 134.1 (Cq^{Bz}), 133.0, 129.5, 128.7 (10 x CH^{Bz}), 127.0 (Cq^{Ad}), 86.5 (C2'), 85.2 (C1'), 78.2 (C3'), 76.1 (C4'), 63.5 (C5'), 25.9, 25.8 (2 x $t\text{Bu}^{TBS}$), 18.4, 18.1 (2 x Cq^{TBS}), -4.6, -4.8, -5.4, -5.7 (4 x Me^{TBS}).

Fonvielle, M., Chemama, M., Lecerf, M., Villet, R., Busca, P., Bouhss, A., ... & Arthur, M. (2010). Decoding the Logic of the tRNA Regiospecificity of Nonribosomal $FemX_{Wv}$ Aminoacyl Transferase. *Angewandte Chemie International Edition*, *49*(30), 5115-5119.

(5) (2R,3R,4R,5R)-2-(6-(N-benzoylbenzamido)-9H-purin-9-yl)-4-((tert-butyldimethylsilyl)oxy)-5-(((tert-butyldimethylsilyl)oxy)methyl)tetrahydrofuran-3-yl trifluoromethanesulfonate

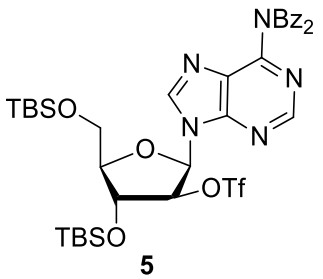

5

Chemical Formula: $C_{37}H_{48}F_3N_5O_8SSi_2$
Molecular Weight: 836,0369

To a solution of **4** (1.25 g, 1.78 mmol) in DCM (18 mL), DMAP (651 mg, 5.33 mmol) and fresh trifluoromethylsulfonate chloride (369 µL, 3.55 mmol) were added at 0 °C. The reaction mixture was stirred at rt for 2 h. The mixture was diluted in DCM and brine. The phases were separated. The aqueous phase was extracted twice with DCM. The combined organic layers were dried over sodium sulfate and concentrated to quantitavely yield **5** without further purification as a white amorphous solid.

^{1}H NMR (250 MHz, $CDCl_3$) δ 8.66 (s, 1H, H2 or H8), 8.24 (s, 1H, H2 or H8), 7.86-7.77 (m, 4H, H^{Bz}), 7.49-7.39 (m, 2H, H^{Bz}), 7.35-7.25 (m, 4H, H^{Bz}), 6.62 (d, *J* = 3.8 Hz, 1H, H1'), 5.22 (dd, *J* = 2.5, 3.3 Hz, 1H, H2'), 4.83-4.77 (m, 1H, H3'), 4.10-4.02 (m, 1H, H4'), 3.89-3.87 (m, 2H, H5'a/H5'b), 0.94 (s, 9H, *t*Bu^{TBS}), 0.92 (s, 9H, *t*Bu^{TBS}), 0.18 (s, 3H, Me^{TBS}), 0.17 (s, 3H, MeTBS), 0.10 (s, 3H, MeTBS), 0.09 (s, 3H, MeTBS).
^{13}C NMR (63 MHz, $CDCl_3$) δ 172.2 (2 x $C{=}O^{Bz}$), 152.6 (C2 or C8), 152.3 (Cq^{Ad}), 152.2 (Cq^{Ad}), 143.2 (C2 or C8), 134.0 (Cq^{Bz}), 133.1, 129.6, 128.8 (10 x CH^{Bz}), 127.6 (Cq^{Ad}), 88.3 (C2'), 85.7 (C4'), 83.1 (C1'), 75.5 (C3'), 61.6 (C5'), 26.0, 25.7 (2 x *t*Bu^{TBS}), 18.5, 17.9 (2 x Cq^{TBS}), -4.8, -5.3 (4 x Me^{TBS}).

Fonvielle, M., Chemama, M., Lecerf, M., Villet, R., Busca, P., Bouhss, A., ... & Arthur, M. (2010). Decoding the Logic of the tRNA Regiospecificity of Nonribosomal $FemX_{Wv}$ Aminoacyl Transferase. *Angewandte Chemie International Edition*, *49*(30), 5115-5119.

(6) N-(9-((2R,3R,4S,5R)-3-azido-4-((tert-butyldimethylsilyl)oxy)-5-(((tert-butyldimethylsilyl)oxy)methyl)tetrahydrofuran-2-yl)-9H-purin-6-yl)benzamide

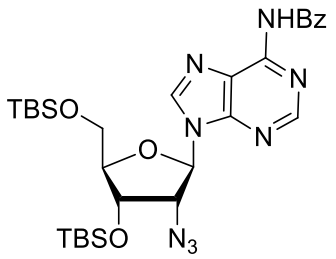

6

Chemical Formula: $C_{29}H_{44}N_8O_4Si_2$
Molecular Weight: 624,8819

To a solution of **5** (1.67 g, 1.99 mmol) in DMF (9.5 mL), sodium azide (1.30 g, 19.9 mmol) was added. The reaction mixture was stirred at rt for 48 h. The mixture was concentrated and the residue was partitioned between AcOEt and brine. The phases were separated. The aqueous phase was extracted twice with AcOEt. The combined organic layers were dried over sodium sulfate and concentrated. Flash chromatography of the residue (Cyclohexane/AcOEt 6/4) yielded **6** as a white foam (811 mg, 65 %).

^{1}H NMR (250 MHz, $CDCl_3$) δ 9.33 (bs, 1H, NH), 8.72 (s, 1H, H2 or H8), 8.25 (s, 1H, H2 or H8), 8.02-7.92 (m, 2H, H^{Bz}), 7.60-7.37 (m, 3H, H^{Bz}), 6.18 (d, *J* = 5.5 Hz, 1H, H1'), 4.68 (dd, *J* = 4.5, 9.1 Hz, 1H, H2'), 4.44 (t, *J* = 5.2 Hz, 1H, H4'), 4.14 (d, *J* = 3.6 Hz, 1H, H3'), 3.92 (dd, *J* = 3.6 ,11.5 Hz, 1H, H5'a), 3.74 (dd, *J* = 2.8, 11.6 Hz, 1H, H5'b), 0.93 (s, 9H, *t*Bu^{TBS}), 0.85 (s, 9H, *t*Bu^{TBS}), 0.16 (s, 3H, Me^{TBS}), 0.14 (s, 3H, Me^{TBS}), 0.04 (s, 3H, Me^{TBS}), 0.03 (s, 3H, Me^{TBS}).

^{13}C NMR: (63 MHz, $CDCl_3$) δ 164.9 ($C=O^{Bz}$), 152.9 (C2 or C8), 151.7 (Cq^{Ad}), 149.8 (Cq^{Ad}), 141.7 (C2 or C8), 133.7 (Cq^{Bz}), 133.9, 128.9, 128.0 (5 x CH^{Bz}), 123.5 (Cq^{Ad}), 86.2 (C1'), 86.0 (C4'), 72.6 (C3'), 65.3 (C2'), 62.1 (C5'), 26.0, 25.8 (*t*Bu^{TBS}), 18.5, 18.2 (Cq^{TBS}), -4.6, -4.9, -5.3, -5.4 (Me^{TBS}).

Fonvielle, M., Chemama, M., Lecerf, M., Villet, R., Busca, P., Bouhss, A., ... & Arthur, M. (2010). Decoding the Logic of the tRNA Regiospecificity of Nonribosomal FemXWv Aminoacyl Transferase. *Angewandte Chemie International Edition*, *49*(30), 5115-5119.

(7) N-(9-((2R,3R,4S,5R)-3-azido-4-hydroxy-5-(hydroxymethyl)tetrahydrofuran-2-yl)-9H-purin-6-yl)benzamide

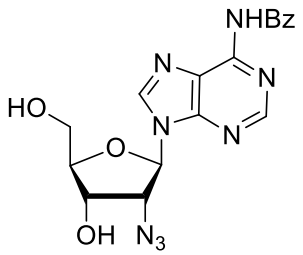

Chemical Formula: $C_{17}H_{16}N_8O_4$
Molecular Weight: 396,3601

7

To a solution of **6** (50 mg, 0.08 mmol) in THF (590 µL), TBAF in a 1 M solution in THF (240 µL, 0.24 mmol) was added at 0 °C. The reaction mixture was stirred at rt overnight. A saturated sodium hydrogenocarbonate aqueous solution was added, and the mixture was partitioned between AcOEt and brine. The phases were separated. The aqueous phase was extracted twice with AcOEt. The combined organic layers were dried over sodium sulfate and concentrated. Flash chromatography of the residue (DCM/MeOH 9/1) yielded **7** as a white foam (30 mg, 93 %).

^{1}H NMR (250 MHz, CD_3OD) δ 8.68 (s, 2H, H-2 and H-8), 8.06 (m, 2H, HBz), 7.56 (m, 3H, HBz), 6.20 (d, J = 4 Hz, 1H, H-1'), 4.68 (m, 2H, H-2'/H-3'), 4.23 (m, 1H, H-4'), 3.88 (m, 2H, H-5')

^{13}C NMR (63 MHz, CD_3OD) δ 168.2 (C=O), 153.3 (C-2 or C-8), 153.2 (Cq^{Ad}), 151.0 (Cq^{Ad}), 144.4 (C-2 or C-8), 134.9 (Cq^{Bz}), 134.0 (C^{Bz}), 129.8 (C^{Bz}), 129.5 (C^{Bz}), 125.4 (Cq^{Ad}), 88.6 (C-1'), 87.6 (C-4'), 72.7 (C-3'), 67.3 (C-2'), 62.4 (C-5')

Fonvielle, M., Li de La Sierra-Gallay, I., El-Sagheer, A. H., Lecerf, M., Patin, D., Mellal, D., ... & van Tilbeurgh, H. (2013). The Structure of $FemX_{Wv}$ in Complex with a Peptidyl-RNA Conjugate: Mechanism of Aminoacyl Transfer from Ala-$tRNA^{Ala}$ to Peptidoglycan Precursors. *Angewandte Chemie International Edition*, *52*(28), 7278-7281.

(8) N-(9-((2R,3R,4S,5R)-3-azido-5-((bis(4-methoxyphenyl)(phenyl)methoxy)methyl)-4-hydroxytetrahydrofuran-2-yl)-9H-purin-6-yl)benzamide

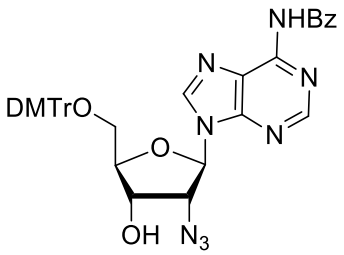

Chemical Formula: $C_{38}H_{34}N_8O_6$
Molecular Weight: 698,7266

8

To a solution of **7** (570 mg, 1.44 mmol) in pyridine (10.3 mL), dimethoxytrityl chloride (536 mg, 1.58 mmol) and DMAP (176 mg, 1.44 mmol) were added. The reaction mixture was stirred at rt for 2 h, before the second addition of DMTrCl (536 mg, 1.58 mmol). After being stirred another 2 h, the reaction mixture was diluted in MeOH, and concentrated. The residue was partitioned between DCM and brine, and the phases were separated. The aqueous phase was extracted twice with DCM. The combined organic layers were dried over sodium sulfate and concentrated. Flash chromatography of the residue (Cyclohexane/AcOEt 5/5 to 0/10) yielded **8** as a white foam (654 mg, 65 %).

^{1}H NMR (400 MHz, $CDCl_3$) δ 9.0 (bs, 1H, NHBz), 8.72 (s, 1H, H2 or H8), 8.18 (s, 1H, H-2 or H-8), 8.04 (d, J = 7 Hz, 2H, H^{Bz}), 7.53 (m, 3H, H^{Bz}), 7.37 (m, 2H, H^{DMTr}), 7.26 (m, 6H, H^{DMTr}), 6.79 (m, 4H, H^{DMTr}), 6.10 (d, J = 5 Hz, 1H, H-1'), 5.04 (t, J = 5.5 Hz, 1H, H-2'), 4.69 (t, J = 5 Hz, 1H, H-3'), 4.24 (dd, J = 8 Hz, J = 4 Hz, 1H, H-4'), 3.77 (s, 6H, Me^{DMTR}), 3.71 (q, J = 7 Hz, 1H, H-5')

^{13}C NMR (100 MHz, $CDCl_3$) δ 164.5 (C=O), 158.6 (Cq^{OMe}), 152.8 (C-2 or C-8), 151.4 (Cq^{Ad}), 149.7 (Cq^{Ad}), 144.3 (C-2 or C-8), 141.8 (Cq^{DMTr}), 135.4 (Cq^{DMTr}), 133.5 (C^{Bz}), 132.8 (C^{Bz}), 129.9 (C^{Bz}), 128.8 (C^{Bz}), 128.0 (C^{Bz}), 127.9 (C^{DMTr}), 127.8 (C^{DMTr}), 127.0 (C^{DMTr}), 123.5 (Cq^{DMTr}), 113.2 (C^{DMTr}), 87.2 (C-1'), 86.8 (Cq^{DMTr}), 83.9 (C-4'), 71.9 (C-3'), 65.6 (C-2'), 62.8 (C-5'), 55.2 (C^{OMe})

Fonvielle, M., Li de La Sierra-Gallay, I., El-Sagheer, A. H., Lecerf, M., Patin, D., Mellal, D., ... & van Tilbeurgh, H. (2013). The Structure of $FemX_{Wv}$ in Complex with a Peptidyl-RNA Conjugate: Mechanism of Aminoacyl Transfer from Ala-$tRNA^{Ala}$ to Peptidoglycan Precursors. *Angewandte Chemie International Edition*, *52*(28), 7278-7281.

(9) 2'-azido-2'-deoxyadenosine-functionalized solid-support

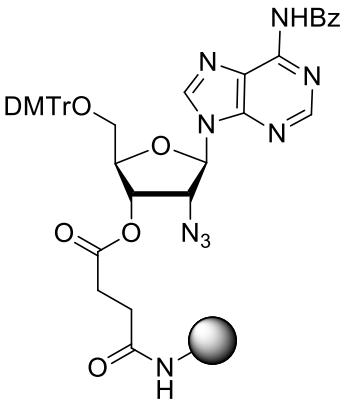

9

Amino-SynBase resin 1000/100 (Link Technologies, Glasgow, UK) (1000 Å pore size, loading 59 mole/g, 1.5) was treated with 3% trichloroacetic acid (TCA) in dichloromethane (CH_2Cl_2) for 4 h in a stoppered glass vessel. The solvents were removed by filtration and the resin was washed with triethylamine:di-isopropylethylamine (9:1), CH_2Cl_2 and diethyl ether, dried under vacuum, and soaked in dry pyridine for 10 min. Succinic anhydride (7.5 mmol) and DMAP (0.62 mmol) in dry pyridine (15 mL) were added and the vessel was rotated for 20 h. The resin was washed with pyridine, CH_2Cl_2 and diethyl ether, dried, and soaked in pyridine for 10 min. Ethyldimethylaminopropylcarbodiimide hydrochloride (1.5 mmole), DMAP (0.098 mmol), and triethylamine (60 µL) in dry pyridine (5 mL) were added to the resin followed by compound **5** (0.072 mmol) in dry pyridine (2 mL). The reaction was rotated for 20 h at room temperature, pentachlorophenol (0.13 mmol) was added, and the vessel was rotated for a further 3 h. The resin was filtered and washed with pyridine, CH_2Cl_2, and diethyl ether. Piperidine (10% in DMF, 10 mL) was added and the resin was washed after 1 min at room temperature with CH_2Cl_2 and diethyl ether. Capping reagent (oligonucleotide synthesis grade, acetic anhydride/pyridine/tetrahydrofuran: *N*-methyl imidazole in tetrahydrofuran, 1:1, 10 mL, Applied Biosystems) was added and the vessel was rotated for 1 h. The resin was washed with pyridine, CH_2Cl_2, diethyl ether, and dried under vacuum overnight. The loading of (**9**) on the resin was 29 mol/g as determined from the cleaved DMTr groups.

Fonvielle, M., Li de La Sierra-Gallay, I., El-Sagheer, A. H., Lecerf, M., Patin, D., Mellal, D., ... & van Tilbeurgh, H. (2013). The Structure of $FemX_{Wv}$ in Complex with a Peptidyl-RNA Conjugate: Mechanism of Aminoacyl Transfer from Ala-$tRNA^{Ala}$ to Peptidoglycan Precursors. *Angewandte Chemie International Edition*, *52*(28), 7278-7281.

(10) (11) (12) (14) 2'-azido-oligoribonucleotides.

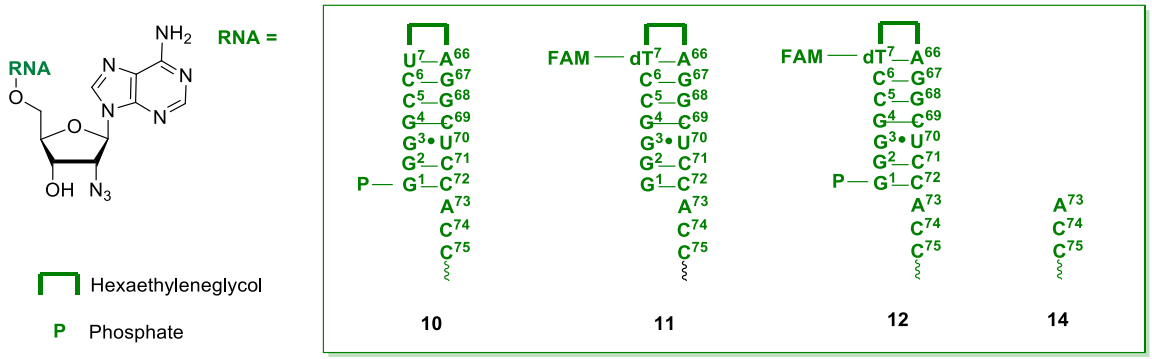

10, 11, 12 and **14** were synthesized according to the general solid-phase synthesis procedure.

The fully deprotected oligonucleotides **10, 11, 12** and **14** were purified by reversed-phase HPLC on a Gilson system using a Luna 10µ C8 100 Å pore Phenomenex column (10 x 250 mm) with a gradient of acetonitrile in triethylammonium acetate (0% to 50% buffer B over 20 min, flow rate 4 mL/min), (buffer A: 0.1 M triethylammonium acetate, pH 7.0, buffer B: 0.1 M triethylammonium acetate, pH 7.0, with 50% acetonitrile). Elution was monitored by UV absorption at 295 nm. After HPLC purification, oligonucleotides **10, 11, 12** and **14** were desalted using NAP-25 then NAP-10 columns (GE Healthcare).

Compound **10**: **MS** Calcd. for [M+H]: 6193; found: 6194.

Analytic anion exchange-HPLC chromatograms for compound **11**, **12, 14**:

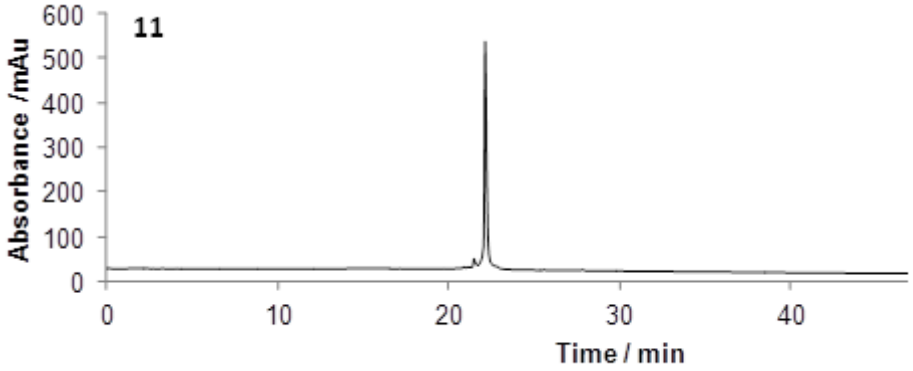

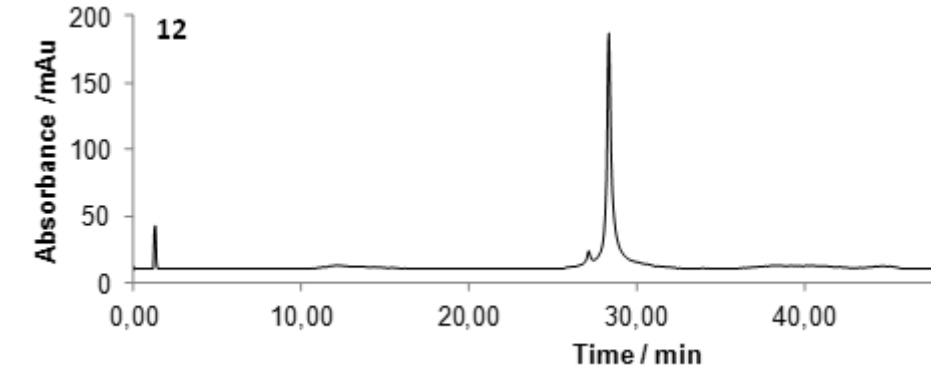
12
Absorbance /mAu
200
150
100
50
0
0,00
10,00
20,00
30,00
40,00
Time / min

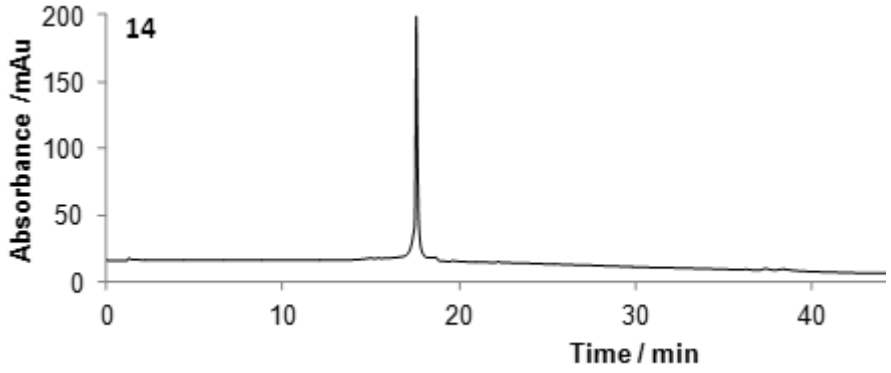
14
Absorbance /mAu
200
150
100
50
0
0
10
20
30
40
Time / min

(13) 1-(prop-2-yn-1-yl)-1H-pyrrole-2,5-dione

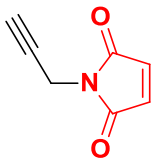

13

Maleic anhydride (2.00 g, 20.3 mmol) and propargylamine (1.3 mL, 20.3 mmol) were dissolved in acetone (10 mL). The reaction mixture was stirred at reflux for 1 h, and concentrated, to yield the intermediate alkyne (1.40 g, 45 %), which was then dissolved in acetic anhydride (10 mL). Sodium acetate (824 mg, 10.0 mmol) was added and the reaction mixture was stirred at 65 °C for 2 h, then distilled under vacuum. Flash chromatography of the distillate yielded **13**

^{1}H NMR (500 MHz, $CDCl_3$): δ 6.73 (s, 2H, CH=CH), 4.24 (s, 2H, CH_2), 2.18 (s, CH)

^{13}C NMR (126 MHz, $CDCl_3$): δ 169.3 (C=O), 134.5 (2C, HC=CH), 77.1 (≡C-), 71.6 (≡C-), 26.9 (CH_2).

Park, K. D., Liu, R., & Kohn, H. (2009). Useful tools for biomolecule isolation, detection, and identification: acylhydrazone-based cleavable linkers. *Chemistry & biology*, *16*(7), 763-772.

(15)

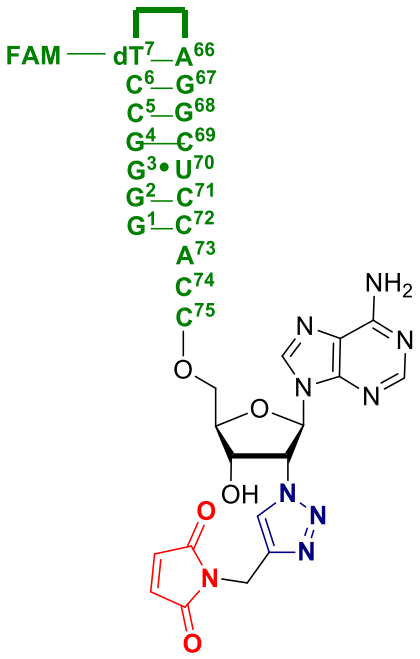

15

Oligo **11** (final concentration 20 µM) reacted with the alkyne-maleimide **13** (final concentration 50 mM) in the presence of THPTA (3.5 mM), $CuSO_4$ (0.5 mM), sodium ascorbate (5 mM), a phosphate buffer pH8 (100 mM) in a DMF/Water mixture (10 % DMF, total volume 10 µL). The reaction mixture was let at 37 °C overnight. **15** was purified by precipitation in EtOH.

Because of the low obtained amounts and overall instability, **15** was extemporaneously used for cross-linking experiments.

---

(16) (17)

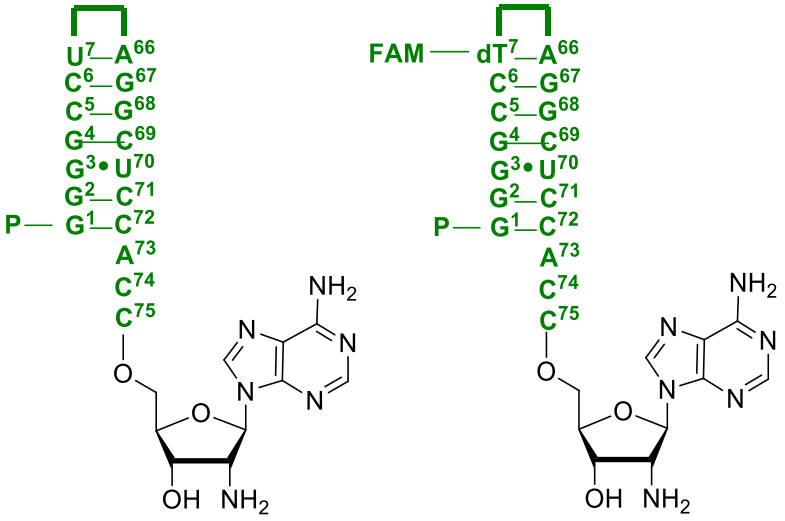

16 **17**

To an aqueous solution of TCEP (2.5 µmol, final concentration 500 µM) in Tris-HCl buffer pH 8.0 (100 mM) was added 3'-azido-RNA **10** or **12** (100 nmol, final concentration 20 µM) and the reaction mixture was kept at -20 °C for 12 h. Final product was purified by DNAPac-HPLC semi preparative DNAPac-HPLC (0% for 7 min then 0% to 10% buffer B in 3 min then 10% to 50% buffer B in 37 min at 3 mL.min^{-1}; RT = 30.7 min for **16**; 0% for 7min then 0% to 30% Buffer B in 3 min then 10% to 70% Buffer B in 30 min at 3 mL.min^{-1}; RT = 20.8 min for **17**).The amino oligonucleotides **16** and **17** were lyophilized, taken in water and concentrations were determined spectrophotometrically at 260 nm (ε^{260nm} = 170 000 M^{-1}.cm^{-1}). 47 and 22 nmol were obtained (yields = 47 % and 22 %, respectively).

Analytical DNAPac-HPLC: RT(**16**) = 25.20 min; RT(**17**)= 27.84 min

16: **HRMS:** *m/*z calcd. for $C_{183}H_{242}N_{71}O_{134}P_{19}$: 6165.9319 [*M*]; found: 6165.8095.

17: **MS:** *m/*z calcd. for $C_{213}H_{268}N_{73}O_{140}P_{19}$: 6679.4 [*M*]; found: 6679.3.

Analytic anion exchange-HPLC chromatograms for compound **16** and **17**:

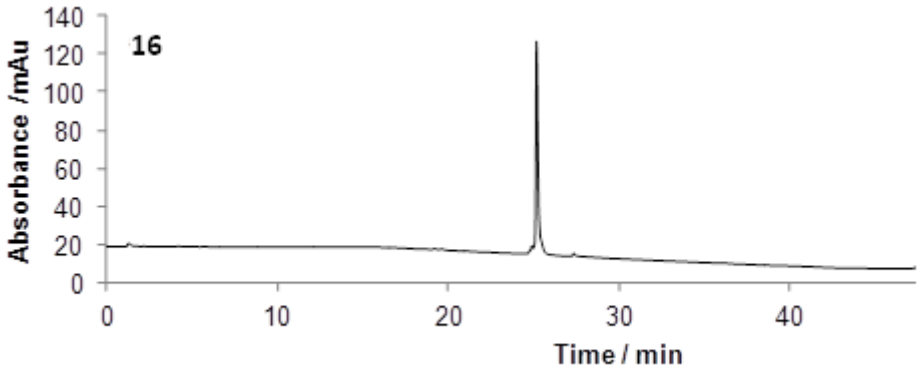
16
Absorbance /mAu
140
120
100
80
60
40
20
0
0
10
20
30
40
Time / min

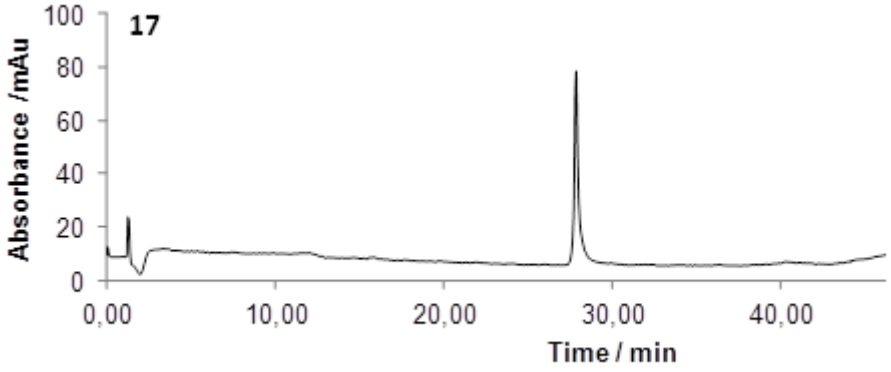
17
Absorbance /mAu
100
80
60
40
20
0
0,00
10,00
20,00
30,00
40,00
Time / min

(18)

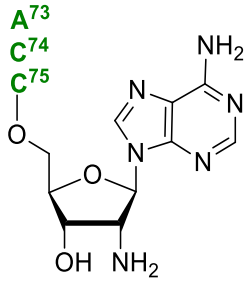

18

To an aqueous solution of TCEP (500 µM) in Tris.HCl buffer pH 8.0 (100 mM) was added 2'-azido-RNA **14** (63 nmol, 20 µM). The reaction mixture was kept at -20 °C for 12 h and ACCA-2'-amino oligonucleotide **18** was purified with the semi-preparative DNAPac PA100 column (ThermoFisher) (0% for 8.5 min then 0% to 45% buffer B in 37 min at 3 mL.min^{-1}; RT= 17.4 min.) The recovered product was lyophilized, dissolved in 60 µL of free RNAse water. Final concentration was determined spectrophotometrically at 260 nm (ε^{260nm} = 37 200 M^{-1}.cm^{-1}). Yield 51 % (32 nmol).

Analytical DNAPac-HPLC: RT= 17.02 min

HRMS: *m/*z calcd. for $C_{38}H_{50}N_{17}O_{23}P_3$: 1205.2478 [*M*]; found: 1205.2230

---

(19) N-(9-((2R,3R,4S,5R)-3-amino-4-((tert-butyldimethylsilyl)oxy)-5-(((tert-butyldimethylsilyl)oxy)methyl)tetrahydrofuran-2-yl)-9H-purin-6-yl)benzamide

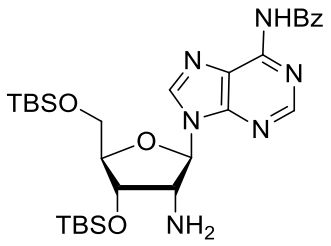

Chemical Formula: $C_{29}H_{46}N_6O_4Si_2$
Molecular Weight: 598,8843

19

To a solution of **6** (1.94 g, 3.11 mmol) in MeOH (20 mL), activated palladium on charcoal (66 mg, 0.62 mmol) was added. The reaction mixture was stirred at rt for 60 h under a hydrogen atmosphere. The mixture was then filtered over silica and the filtrate was concentrated. Flash chromatography of the residue (Cyclohexane/AcOEt 3/7) yielded **19** as a white foam (1.15 g, 62 %).

^{1}H NMR (250 MHz, $CDCl_3$) δ 9.16 (s, 1H, NH^{Bz}), 8.77 (s, 1H, H2 or H8), 8.28 (s, 1H, H2 or H8), 8.07-7.92 (m, 2H, H^{Bz}), 7.66-7.38 (m, 3H, H^{Bz}), 5.97 (d, *J = 7.3 Hz*, 1H, H1'), 4.34 (d, *J = 7.5 Hz*, 1H, H3'), 4.18-4.12 (m, 1H, H4'), 4.07-3.94 (m, 1H, H2'), 3.93-3.83 (m, 1H, H5'a), 3.81-3.74 (m, 1H, H5'b), 2.12 (bs, 2H, NH_2), 0.96 (s, 9H, *t*Bu^{TBS}), 0.91 (s, 9H, *t*Bu^{TBS}), 0.16 (bs, 6H, 2 x Me^{TBS}), 0.10 (bs, 6H, 2 x Me^{TBS}).

^{13}C NMR: (63 MHz, $CDCl_3$) δ 165.8 ($C=O^{Bz}$), 152.7 (C2 or C8), 152.4 (Cq^{Ad}), 150.3 (Cq^{Ad}), 141.7 (C2 or C8), 134.2 (Cq^{Bz}), 132.8, 128.4, 128.0 (5 x CH^{Bz}), 124.0 (Cq^{Ad}) 89.9 (C1'), 87.2 (C4'), 74.1 (C3'), 63.5 (C5'), 59.4 (C2'), 26.3, 25.9 (2 x *t*Bu^{TBS}), 18.5, 18.3 (Cq^{TBS}), -4.2, -4.4, -5.0, -5.1 (4 x Me^{TBS}).

Mellal, D., Fonvielle, M., Santarem, M., Chemama, M., Schneider, Y., Iannazzo, L., ... & Etheve-Quelquejeu, M. (2013). Synthesis and biological evaluation of non-isomerizable analogues of Ala-tRNA Ala. *Organic & biomolecular chemistry*, *11*(36), 6161-6169.

(20) N-(9-((2R,3R,4S,5R)-4-((tert-butyldimethylsilyl)oxy)-5-(((tert-butyldimethylsilyl)oxy)methyl)-3-((2-ethoxy-3,4-dioxocyclobut-1-en-1-yl)amino)tetrahydrofuran-2-yl)-9H-purin-6-yl)benzamide

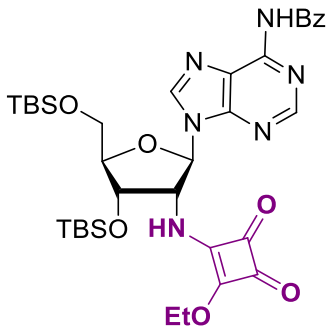

Chemical Formula: $C_{35}H_{50}N_6O_7Si_2$
Molecular Weight: 722,9785

20

To a solution of **19** (150 mg, 0.25 mmol) in EtOH (1.5 mL) were added DIPEA (22 µL, 0.13 mmol) and diethylsquarate (42 µL, 0.37 mmol). The reaction mixture was stirred at rt for 45 min then concentrated. Flash chromatography (Cyclohexane/AcOEt 4/6) of the residue yielded squaramate **20** (145 mg, 80 %) as a white foam.

^{1}H NMR (250 MHz, Acetone) δ 8.68 (s, 1H, H2 or H8), 8.53 (s, 1H, H2 or H8), 8.17 (d, *J* = 7.1 Hz, 2H, CH^{Bz}), 7.72 – 7.35 (m, 3H, CH^{Bz}), 6.53 (d, *J* = 7.5 Hz, 1H, H1'), 4.83 (d, *J* = 3.7 Hz, 1H, H3'), 4.59 (s, 2H, CH_2), 4.33 (s, 1H, H4'), 4.10 (m, 1H, H5'), 3.98 (dd, *J* = 11.3, 3.5 Hz, 1H, H5'), 3.04 (s, 3H, CH_3), 1.02 (s, 9H, *t*Bu^{TBS}), 0.99 (s, 9H, *t*Bu^{TBS}), 0.26 (s, 3H, Me^{TBS}), 0.23 (s, 3H, Me^{TBS}), 0.19 (s, 6H, 2 Me^{TBS}).

^{13}C NMR (63 MHz, Acetone) δ 173.4, 164.8, 152.7, 151.3, 143.2, 134.8, 133.1, 129.3, 129.1, 125.8, 87.6, 73.8, 70.0, 63.8, 60.4, 26.1, 26.4, 19.0, 18.7, 16.0, -4.4, -4.6, -5.2.

HRMS: *m/z* calcd. for $C_{35}H_{51}N_6O_7Si_2$: 723.3358 [*M*+H]; Found: 723.3325.

---

(21) 6-((2-(((2R,3R,4S,5R)-2-(6-amino-9H-purin-9-yl)-4-((tert-butyldimethylsilyl)oxy)-5-(((tert-butyldimethylsilyl)oxy)methyl)tetrahydrofuran-3-yl)amino)-3,4-dioxocyclobut-1-en-1-yl)amino)-2-((tert-butoxycarbonyl)amino)hexanoic acid

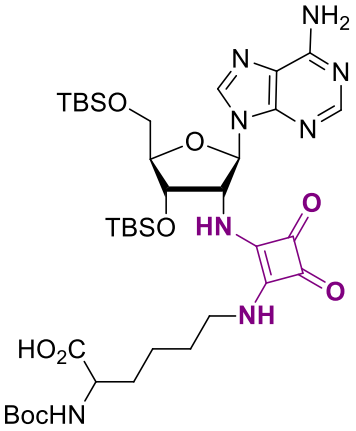

Chemical Formula: $C_{37}H_{62}N_8O_9Si_2$
Molecular Weight: 819,1074

21

To a solution of **20** (40 mg, 0.055 mmol) in EtOH (1 mL) were added DIPEA (5 µL, 0.029 mmol, 0.5 eq) and Boc-Lys-OH (14 mg, 0.055 mmol). The reaction mixture was stirred at 40 °C for 24 h then concentrated. Flash chromatography (DCM/MeOH 96/4 to 90/10) of the residue yielded squaramide **21** (33 mg, 73 %) as a white foam.

^{1}H NMR (250 MHz, DMSO) δ 8.32 (s, 1H, H2 or H8), 8.15 (s, 1H, H2 or H8), 7.35 (s, 1H, NH), 6.15 (m, 1H, H1'), 5.41 (s, 1H), 4.58 (s, 1H), 4.07 (s, 1H), 3.92-3.86 (m, 1H), 3.74-3.71 (m, 2H), 3.41 (s, 8H, CH_2), 1.32 (s, 9H, tBu^{Boc}), 0.87 (s, 9H, tBu^{TBS}), 0.85 (s, 9H, tBu^{TBS}), 0.08 (m, 6H, Me^{TBS}), 0.005 (m, 6H, Me^{TBS}).

HRMS: *m/z* calcd. for $C_{37}H_{63}N_8O_9Si_2$: 819.4257 [*M*+H]; Found: 819.4313.

---

(22)

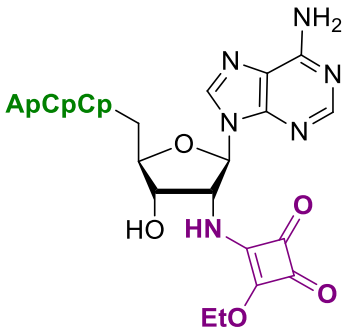

22

To an aqueous solution of oligo **18** (67 nmol, final concentration 100 µM) in a 100 mM HEPES buffer pH 7.5, was added a 5 mM solution of diethylsquarate in DMF (final concentration 1 mM). The reaction mixture was kept at rt for 12 h and ACCA-2'-NH-Sq-OEt squaramate **22** was purified using semi-preparative DNAPac PA100 column (ThermoFisher) (0% for 12.5 min then 0% to 30% buffer B in 37 min at 3 mL.min^{-1}; RT = 23.6 min). The recovered product was lyophilized, dissolved in 27 µL of free RNAse water and its final concentration was determined spectrophotometrically at 260 nm (ε^{260nm} = 37 200 M^{-1}.cm^{-1}). Yield: 79 % (53 nmol).

Analytical DNAPac-HPLC: RT = 17.12 min

HRMS: *m/*z calcd. for $C_{44}H_{54}N_{17}O_{26}P_3$: 1329.2639 [*M*]; found: 1329.2406

---

(23) (23b) (24)

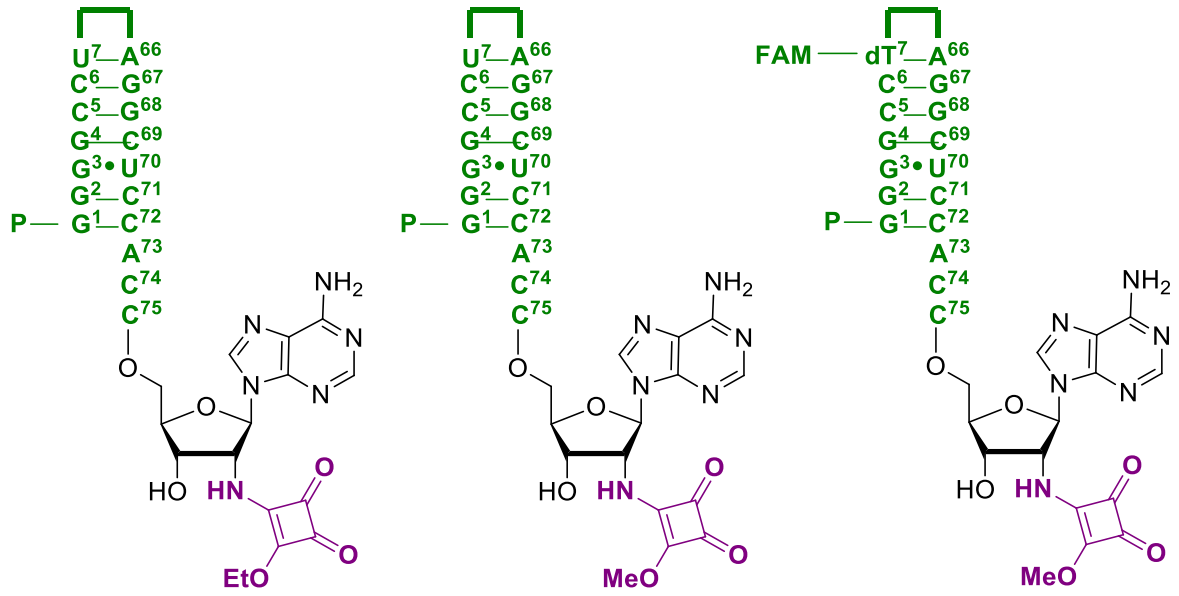

23 **23b** **24**

To an aqueous solution of oligo **16** or **17** (20 nmol for **16** and 35 nmol for **18**, final concentration 100 µM) in a 100 mM HEPES buffer pH 7.5, was added a 50 mM solution of diethyl- or dimethyl-squarate in DMF (80 µL, 4 µmol, final concentration 10 mM). The reaction mixture was kept at 37 °C for 12 h. Squaramide RNAs were purified by semi preparative DNAPac-HPLC (0% for 14 min then 0% to 10% buffer B in 3 min then 10% to 50% buffer B in 37 min at 3 mL.min^{-1} ; RT = 40.0 min for OEt squaramide **23** and 35.0 min for OMe squaramide **23b;** 0% for 12min then 0% to 10% buffer B in 3 min then 10% to 43% buffer B in 30 min then 43% to 61% buffer B in 7min at 3 mL.min^{-1}; RT = 52.1 min for **24**). Oligonucleotide-squaramides **23, 23b** and **24** were lyophilized, dissolved in water and concentrations were determined spectrophotometrically at 260 nm (ε^{260nm} = 170 000 M^{-1}.cm^{-1}). 14.7 nmol were obtained for ethylsquaramate **23** (yield = 74%), 15.8 nmol for methylsquaramate **23b** (yield=79%) and 13.4 nmol for **24** (yield=38%).

Compound **23**:

HRMS: *m/*z calcd. for $C_{189}H_{246}N_{71}O_{137}P_{19}$: 6289.9480 [*M*]; found: 6291.0191

Analytical DNAPac-HPLC: RT= 25.28 min

Compound **23b**:

HRMS: *m/*z calcd. for $C_{188}H_{244}N_{71}O_{137}P_{19}$: 6275.9323 [*M*]; found: 6275.9852

Analytical DNAPac-HPLC: RT= 25.61 min

Compound **24:**

MS: *m/*z calcd. for $C_{218}H_{270}N_{73}O_{143}P_{19}$: 6789.4 [*M*]; found: 6789.1

Analytical DNAPac-HPLC: RT= 26.87 min

Analytic anion exchange-HPLC chromatograms:

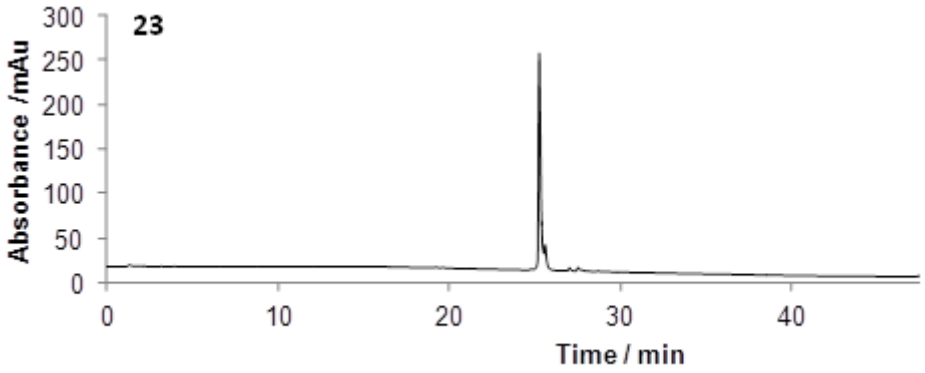

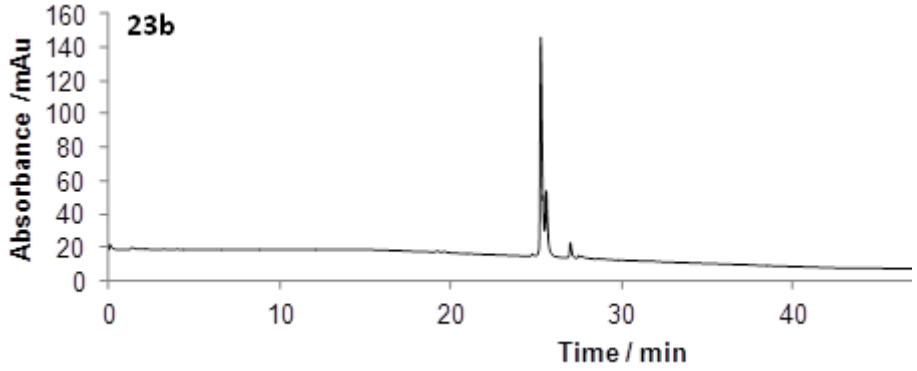

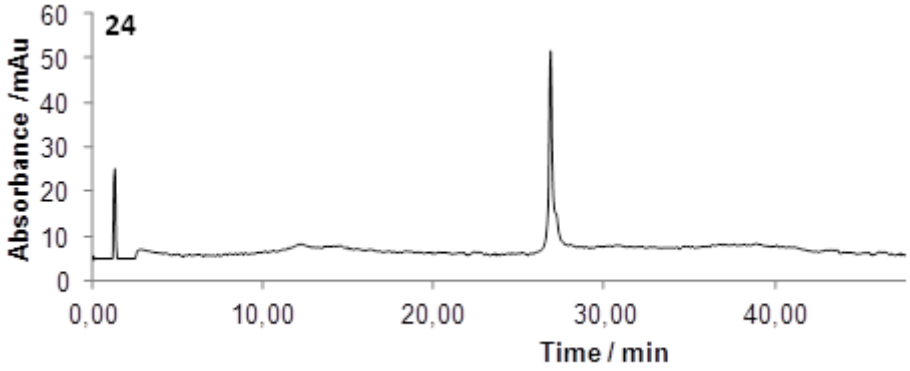

(25)

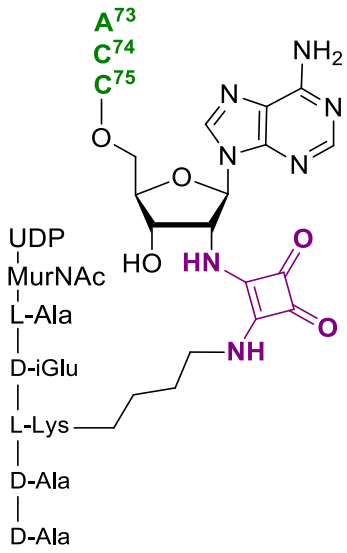

25

Oligo **22** (20 nmol) and UDP-MurNAc-pentapeptide (200 nmol) were lyophilized and dissolved in 10 µL of a 500 mM borate buffer pH 9.2 containing 10% DMF. The reaction mixture was kept at 37°C for 72 h. ACCA-2'-bis-squaramide-UDP-MurNAc-pentapepide **25** was purified using semi-preparative DNAPac PA100 column (ThermoFisher) (0% for 14 min then 0% to 30% buffer B in 37 min at 3 mL.min^{-1}; RT = 41.8 min). The recovered product was lyophilized, dissolved in 100 µL of free RNAse water and its final concentration was determined spectrophotometrically at 260 nm (ε^{260nm} = 47 200 M^{-1}.cm^{-1}). Yield 22 % (2.24 nmol).

Analytical DNAPac-HPLC: RT= 19.38 min

HRMS: *m/z* calcd. for $C_{82}H_{113}N_{26}O_{51}P_5$: 2432.5736 [*M*]; found: 2432.6277

Analytic anion exchange-HPLC chromatogram:

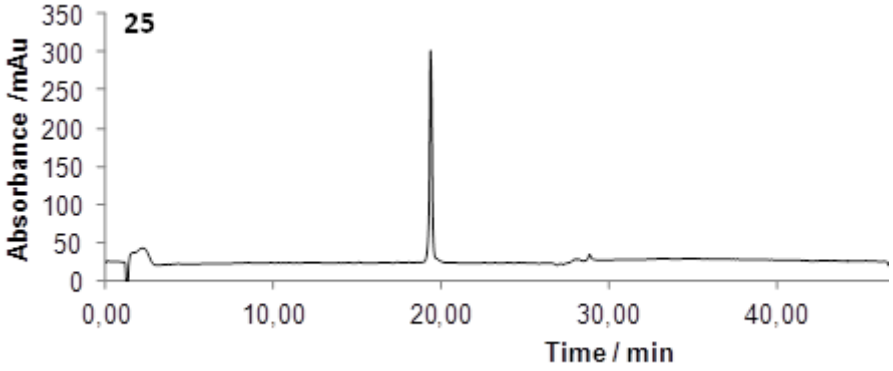

---

(26)

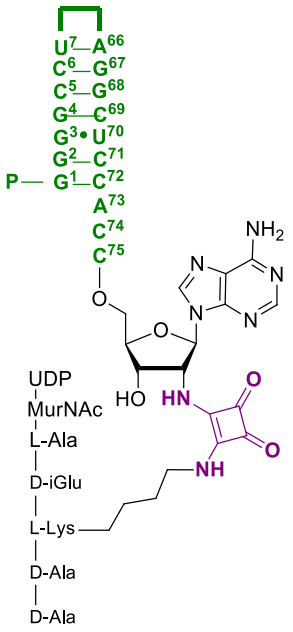

26

Oligo **23** (11 nmol) and UDP-MurNAc-pentapeptide (110 nmol) were lyophilized and dissolved in 10 µL of a 500 mM borate buffer pH 9.2 containing 10% DMF. The reaction mixture was kept at 37 °C for 72 h. Compound **26** was purified using semi-preparative DNAPac-HPLC (ThermoFisher) (0% for 14 min then 0% to 50% buffer B in 37 min at 3 mL.min^{-1} ; RT = 41.9 min). The recovered product was lyophilized, taken in 100 µL of free RNAse water and final concentration was determined spectrophotometrically at 260 nm (ε^{260nm} = 180 000 M^{-1}.cm^{-1}). Yield 45 % (5 nmol).

Analytical DNAPac-HPLC: RT= 23.74 min

MS: *m/z* calcd. for $C_{227}H_{305}N_{80}O_{162}P_{21}$: 7396.8 [*M*]; found: 7396.6

Analytic anion exchange-HPLC chromatogram:

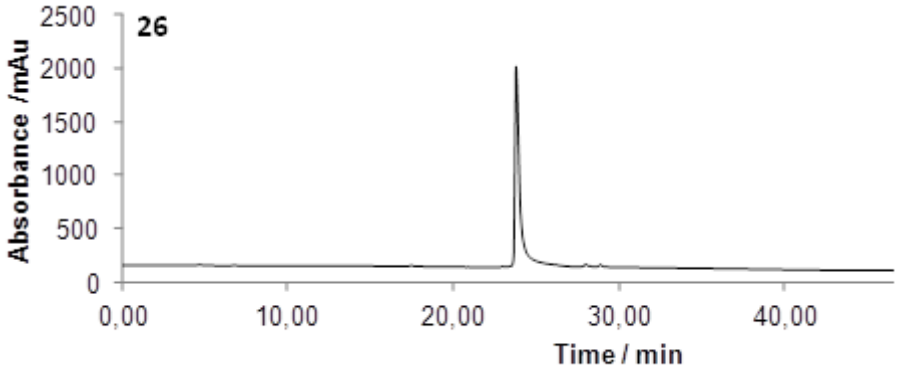

---

(27) 2-(diphenylphosphino)phenyl acetate

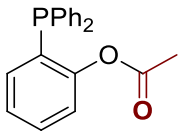

Chemical Formula: $C_{20}H_{17}O_2P$
Molecular Weight: 320,3215

27

To a solution of (2-hydroxyphenyl)diphenylphosphine (150 mg, 0.539 mmol) and DIPEA (89 µL, 0.461 mmol) in DCM (4.5 mL), a solution of acetic acid (185 µL, 3.23 mmol), EDC (619 mg, 3.23 mmol) and DIPEA (535 µL, 2.76 mmol) in DCM (4.5 mL) was added. The mixture was stirred at rt overnight and partitioned between DCM and brine. The phases were separated. The aqueous phase was extracted twice with DCM. The combined organic layers were dried over sodium sulfate and concentrated. Flash chromatography of the residue (Cyclohexane/AcOEt 9/1) yielded **27** as a white amorphous solid (129 mg, 71 %).

^{1}H NMR (500 MHz, $CDCl_3$) δ 7.22 (m, 11H), 7.04 – 6.98 (m, 2H), 6.75 (ddd, *J* = 7.6, 4.4, 1.5 Hz, 1H), 1.85 (s, 3H).

Bianchi, A., & Bernardi, A. (2006). Traceless Staudinger ligation of glycosyl azides with triaryl phosphines: Stereoselective synthesis of glycosyl amides.*The Journal of organic chemistry*, *71*(12), 4565-4577.

(28) N-(9-((2R,3R,4S,5R)-3-acetamido-4-hydroxy-5-(hydroxymethyl)tetrahydrofuran-2-yl)-9H-purin-6-yl)benzamide

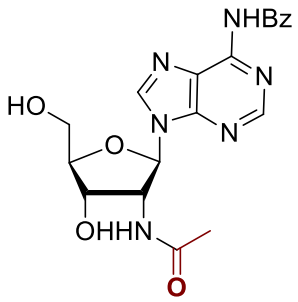

Chemical Formula: $C_{19}H_{20}N_6O_5$
Molecular Weight: 412,3993

28

To a solution of **7** (40 mg, 0.101 mmol) in DMF (2.9 mL), **27** (40 mg, 0.125 mmol) was added. Water (300 µL) was added and the reaction mixture was stirred at rt for 20 h, then at 75 °C for 4 h. The reaction mixture was concentrated. Flash chromatography of the residue (DCM/MeOH 99/1 to 90/10) yielded **28** as a white foam (31 mg, 74 %).

^{1}H NMR (250 MHz, $CDCl_3$) δ 8.67 (s, 1H, H2 or H8), 8.59 (s, 1H, H2 or H8), 8.08 – 7.95 (m, 2H, CH^{Bz}), 7.69 – 7.42 (m, 3H, CH^{Bz}), 6.15 (d, *J* = 8.3 Hz, 1H, H1'), 5.16 (dd, *J* = 8.2, 5.4 Hz, 1H, H2'), 4.38 (d, *J* = 5.3 Hz, 1H, H3'), 4.19 (d, *J* = 1.3 Hz, 1H, H4'), 3.81 (qd, *J* = 12.3, 3.1 Hz, 2H, H5'), 1.85 (s, 3H, CH_3^{Ac}).

MS: *m/*z calcd. for $C_{19}H_{21}N_6O_5$: .413.2 [*M+H*]; found: 413.3

---

(29)

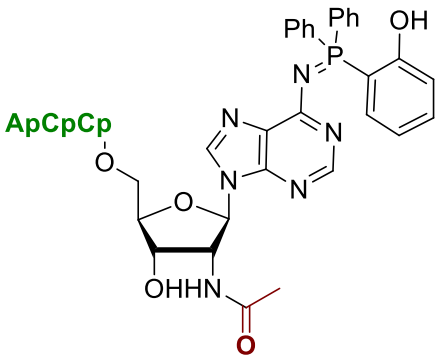

29

Oligo **14** (final concentration 100 µM) and phosphine **27** (final concentration 30 mM) are reacted in a 9/1 DMF/water mixture at 37 °C overnight in a sealed eppendorf. The mixture was cooled down to rt, and diluted in water to reach a DMF proportion inferior to 1 %. The troubled mixture was centrifugated (12000 rpm during 5 min). The supernatant was purified by rp-HPLC on a semi-preparative C18 column (Buffer A: ammonium acetate pH7.4; Buffer B: 50 % buffer A, 50 % MeCN; gradient from 0 % to 100 % of buffer B in 30 minutes, 100 % B for 5 minutes; retention time 33.3 min) to yield **29**.

HRMS: *m/z* calcd. for $C_{58}H_{65}N_{17}O_{25}P_4$: 1523.3288 [*M*]; found: 1523.3149.

---

(30) (2R,3R,4S,5R)-2-(6-(tritylamino)-9H-purin-9-yl)-5-((trityloxy)methyl)tetrahydrofuran-3,4-diol

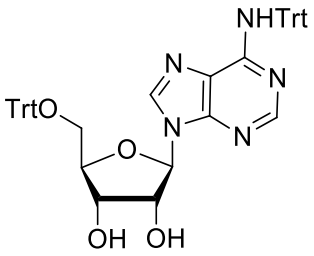

Chemical Formula: $C_{48}H_{41}N_5O_4$
Molecular Weight: 751,8702

30

To a solution of adenosine (3.00 g, 11.2 mmol) in pyridine (150 mL), were added trityl chloride (10.93 g, 39.29 mmol) and DMAP (1.10 g, 8.98 mmol). The reaction mixture was stirred for 4 h at 80 °C and was then cooled down to rt. Ethanol (50 mL) was added, and the reaction mixture was concentrated. The residue was filtered over silica gel (AcOEt), and the filtrate was concentrated. Flash chromatography of the residue (Cyclohexane/AcOEt 6/4) yielded **30** (2.17 g, 26 %) as a white foam.

^{1}H NMR (250 MHz, $CDCl_3$) δ 8,08 (s,1H,H2 or H8), 7.99 (s, 1H, H2 or H8), 7.26 (m, 30H, CH^{Bz}), 6,61 (s, 1H, NH), 5,91 (d, *J* = 6,5 Hz, 1H, H1'), 4,77 (t, *J* = 1.0 Hz, 1H, H2'), 4,44 (s, 1H, H4'), 4,31 (d, *J* = 5.0 Hz, 1H, H3'), 3,49 (dd, *J* = 10,75 Hz, *J* = 3,5 Hz, 1H, H5'a), 3,20 (dd, *J* = 10,5 Hz, *J* = 3.0 Hz, 1H, H5'b)

Charafeddine, A., Dayoub, W., Chapuis, H., & Strazewski, P. (2007). First Synthesis of 2'-Deoxyfluoropuromycin Analogues: Experimental Insight into the Mechanism of the Staudinger Reaction. *Chemistry–A European Journal*,*13*(19), 5566-5584.

(31) (2R,3R,4R,5R)-2-(6-(tritylamino)-9H-purin-9-yl)-5-((trityloxy)methyl)tetrahydrofuran-3,4-diyl bis(trifluoromethanesulfonate)

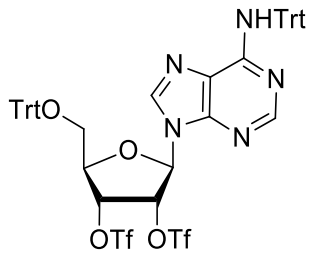

Chemical Formula: $C_{50}H_{39}F_6N_5O_8S_2$
Molecular Weight: 1015,9938

31

To a solution of **30** (1.70 g, 2.26 mmol) and DMAP (690 mg, 5.65 mmol) in pyridine (53 mL), triflic anhydride (2.96 mL, 18.1 mmol) was added slowly at 0 °C. The reaction mixture was stirred at rt for 3 h. Methanol (10 mL) was added and the reaction mixture was concentrated. The residue was partitioned between DCM and brine. The phases were separated and the aqueous layer was extracted twice by DCM. The combined organic layers were dried over sodium sulfate and concentrated. Flash chromatography of the residue (Cyclohexane/AcOEt 7/3) yielded **31** (2.18 g, 95 %).

^{1}H NMR (250 MHz, $CDCl_3$) δ 7,89 (s, 1H, H2 or H8), 7,84 (s, 1H, H2 or H8), 7,31 (m, 30H, CH^{Trt}), 7,28 (s, 1H, NH), 6,46 (t, *J* = 5,5 Hz, 1H, H2'), 6,20 (d, *J* = 6 Hz, 1H, H1'), 5.84 (t, *J* = 3,5 Hz, 1H, H3'), 4,90 (d, *J* = 3,5 Hz, 1H, H4'), 3,70 (dd, *J* = 11,25 Hz, *J* = 4 Hz, 1H, H5'), 3,40 (dd, *J* = 11 Hz, *J* = 3,75 Hz, 1H, H5'b)

Charafeddine, A., Dayoub, W., Chapuis, H., & Strazewski, P. (2007). First Synthesis of 2'-Deoxyfluoropuromycin Analogues: Experimental Insight into the Mechanism of the Staudinger Reaction. *Chemistry–A European Journal*,*13*(19), 5566-5584.

(32) N-trityl-9-((1S,2R,4R,5S)-4-((trityloxy)methyl)-3,6-dioxabicyclo[3.1.0]hexan-2-yl)-9H-purin-6-amine

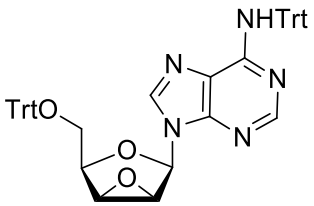

Chemical Formula: $C_{48}H_{39}N_5O_3$
Molecular Weight: 733,8550

32

To a solution of **31** (2.19 g, 2.16 mmol) and tetrabutylammonium nitrite (2.78 g, 9.65 mmol) in toluene (47 mL), water (5.8 mL) was added. The reaction mixture was stirred at rt for 40 h, then diluted in diethyl ether. The phases were separated, and the aqueous layer was extracted twice by diethyl ether. The combined organic layers were dried over sodium sulfate and concentrated. Flash chromatography of the residue (Cylohexane/AcOEt 7/3) yielded **32** (1.42 g, 90 %) as a yellowish solid.

^{1}H NMR (250 MHz, $CDCl_3$) δ 8,05 (s, 1H, H2 or H8), 8,03 (s, 1H, H2 or H8), 7,34 (m, 30H, CH^{Trt}), 7,30 (s, 1H, NH), 6,29 (s, 1H, H1'), 4,23 (t, *J* = 7,5 Hz, 1H, H4'), 4,03 (m, 2H, H2' et H3'), 3,51 (dd, *J* = 7,5 Hz, *J* = 5.0 Hz, 1H, H5'), 3,40 (dd, *J* = 10.0 Hz, *J* = 7,5 Hz, 1H, H5'b)

Charafeddine, A., Dayoub, W., Chapuis, H., & Strazewski, P. (2007). First Synthesis of 2'-Deoxyfluoropuromycin Analogues: Experimental Insight into the Mechanism of the Staudinger Reaction. *Chemistry–A European Journal*,*13*(19), 5566-5584.

(33) (2R,3R,4S,5R)-4-fluoro-2-(6-(tritylamino)-9H-purin-9-yl)-5-((trityloxy)methyl)tetrahydrofuran-3-ol

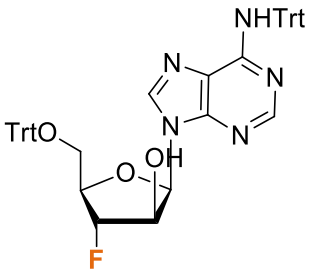

Chemical Formula: $C_{48}H_{40}FN_5O_3$
Molecular Weight: 753,8613

33

Method 1: To a solution of **32** (441 mg, 0.602 mmol) in 2-ethoxyethanol (4 mL), KHF_2 (329 mg, 4.21 mmol) and NaF (329 mg, 7.83 mmol) were added. The reaction mixture was stirred at reflux for 24 h, then concentrated. The residue was partitioned between DCM and brine. The phases were separated and the aqueous layer was extracted twice with DCM. The combined organic layers were dried over sodium sulfate and concentrated. Flash chromatography of the residue (Cyclohexane/AcOEt 3/1) yielded **33** (204 mg, 45 %) as a white solid.

Method 2: To a solution of **32** (50 mg, 0.068 mmol) in MeCN (1 mL), TBAF in a 1 M solution in THF (680 µL, 0.68 mmol) was added. The reaction mixture was stirred at reflux for 6 h. An aqueous solution of $NaHCO_3$ (2 mL) was added, and the mixture was concentrated. The residue was partitioned between DCM and brine. The phases were separated and the aqueous layer was extracted twice with DCM. The combined organic layers were dried over sodium sulfate and concentrated. Flash chromatography (Cyclohexane/AcOEt 3/1) of the residue yielded **33** (34 mg, 67 %) as a white solid.

^{1}H NMR (500 MHz, $CDCl_3$) δ 8.08 (s, 1H, H8), 7.95 (s, 1H, H2), 7.48-7.44 (m, 1H, -CH^{Trt}), 7.42 – 7.38 (m, 6H, *o*-$CH^{5'\text{-}OTrt}$), 7.34 (dt, *J* = 3.9, 2.1 Hz, 6H, *o*-$CH^{\text{-}NHTrt}$), 7.31 – 7.15 (m, 17H, -CH^{Trt}), 7.03 (bs, 1H, NH), 6.16 (t, *J* = 2.9 Hz, 1H, H1'), 5.39 (d, *J* = 8.0 Hz, 1H, -OH), 5.08 (dt, *J* = 51.7, 1.6 Hz, 1H, H3'), 4.58-4.52 (m, 1H, H2'), 4.30 (dtd, *J* = 29.1, 4.5, 1.5 Hz, 1H, H4'), 3.57 – 3.48 (m, 1H, H5'a), 3.41 (ddd, *J* = 28.3, 9.9, 5.7 Hz, 1H, H5'b).

^{13}C NMR (126 MHz, $CDCl_3$) δ 154.49 (C6), 152.10 (C2), 148.31 (C4), 144.98 (3C, C*i*$^{\text{-}NHTrt}$), 143.23 (3C, C*i*$^{5'\text{-}OTrt}$), 140.50 (C8), 129.13 (6C, *o*-$CH^{\text{-}NHTrt}$), 128.79 (6C, *o*-$CH^{5'\text{-}OTrt}$), 128.16 (6C, *m*-CH^{Trt}), 128.09 (6C, *m*-CH^{Trt}), 127.54 (3C, *p*-$CH^{5'\text{-}OTrt}$), 127.14 (3C, *p*-$CH^{\text{-}NHTrt}$), 121.05 (C5), 96.92 (d, *J* = 183.8 Hz, C3'), 88.01 ($Cq^{5'\text{-}OTrt}$), 86.33 (C1'), 81.83 (d, *J* = 26.0 Hz, C4'), 74.65 (d, *J* = 25.4 Hz, C2'), 71.67 ($Cq^{\text{-}NHTrt}$), 63.39 (d, *J* = 9.8 Hz, C5').

^{19}F NMR (471 MHz, $CDCl_3$) δ -181.45 (s).

Dawadi, S., Viswanathan, K., Boshoff, H. I., Barry III, C. E., & Aldrich, C. C. (2015), *The Journal of organic chemistry*, *80*(10), 4835-4850.

(34) (2R,3R,4R,5R)-4-fluoro-2-(6-(tritylamino)-9H-purin-9-yl)-5-((trityloxy)methyl)tetrahydrofuran-3-yl trifluoromethanesulfonate

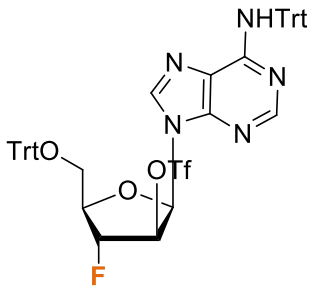

Chemical Formula: $C_{49}H_{39}F_4N_5O_5S$
Molecular Weight: 885,9231

34

To a solution of **33** (90 mg, 0.12 mmol) and DMAP (37 mg, 0.30 mmol) in pyridine (2.8 mL), triflic anhydride (170 µL, 0.18 mmol) was added at 0 °C. The reaction mixture was stirred at rt for 1 h. Methanol (2 mL) was added and the reaction mixture was concentrated. The residue was partitioned between DCM and brine, and the phases were separated. The aqueous layer was extracted twice with DCM. The combined organic layers were dried over sodium sulfate and concentrated. Flash chromatography of the residue (Cylohexane/AcOEt 7/3) yielded **34** (101 mg, 95 %) as a white solid.

^{1}H NMR (250 MHz, $CDCl_3$) δ=7.97 (s, 1H, H2 or H8), 7.90 (s, 1H, H2 or H8), 7.27 (m, 30H, CH^{Trt}), 7.00 (s, 1H, NH), 6.52 (d, *J* = 2,5 Hz, 1H, H1'), 5.60 (d, *J* = 30 Hz, 1H, H3'), 5.40 (d, *J* = 42,5 Hz, 1H, H2'), 4.30 (dtd, *J* = 29 Hz, 4,5 Hz, 2.0 Hz, 1H, H4'), 3.45 (dd, *J* = 10.0 Hz, *J* = 4,5 Hz, 1H, H5'a), 3.37 (dd, *J* = 10,5 Hz, 4.0 Hz, 1H, H5'b)

---

(35) 9-((2R,3S,4S,5R)-3-azido-4-fluoro-5-((trityloxy)methyl)tetrahydrofuran-2-yl)-N-trityl-9H-purin-6-amine

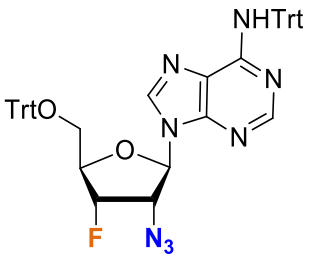

Chemical Formula: $C_{48}H_{39}FN_8O_2$
Molecular Weight: 778,8741

35

To a solution of **34** (33 mg, 0.037 mmol) in DMF (150 µL), sodium azide (24 mg, 0.37 mmol) was added. The reaction mixture was stirred at rt for 24 h, and was then partitioned between DCM and brine. The phases were separated and the aqueous phase was extracted twice with DCM. The combined organic layers were dried of sodium sulfate and concentrated. Flash chromatography of the residue (Cyclohexane/AcOEt 8/2) yielded **35** (26 mg, 88 %) as a white foam.

^{1}H NMR (500 MHz, $CDCl_3$) δ 7.88 (s, 1H, H2), 7.82 (s, 1H, H8), 7.38 (dd, *J* = 8.0, 1.4 Hz, 6H, *o*-$CH^{5'\text{-}OTrt}$), 7.36 – 7.31 (m, 6H, *o*-$CH^{\text{-}NHTrt}$), 7.29 – 7.18 (m, 18H, *m*- and *p*-CH^{Trt}), 6.99 (bs, 1H, NH), 5.99 (d, *J* = 7.8 Hz, 1H, H1'), 5.26 (ddd, *J* = 53.9, 4.5, 1.2 Hz, 1H, H3'), 5.23 – 5.14 (m, 1H, H2'), 4.44 (dt, *J* = 9.1, 4.9 Hz, 1H, H4'), 3.51 (dd, *J* = 10.7, 5.0 Hz, 1H, H5'a), 3.39 (dd, *J* = 10.7, 4.3 Hz, 1H, H5'b).

^{13}C NMR (126 MHz, $CDCl_3$) δ 154.33 (C6), 152.64 (C2), 148.95 (C4), 145.01 (3C, $Ci^{\text{-}NHTrt}$), 143.36 (3C, $Ci^{5'\text{-}OTrt}$), 139.43 (C8), 129.12 (6C, *o*-$CH^{\text{-}NHTrt}$), 128.71 (6C, *o*-$CH^{5'\text{-}OTrt}$), 128.11 (6C, *m*-CH^{Trt}), 128.05 (6C, *m*-CH^{Trt}), 127.49 (3C, *p*-$CH^{5'\text{-}OTrt}$), 127.10 (3C, *p*-$CH^{\text{-}NHTrt}$), 121.72 (C5), 92.64 (d, *J* = 187.4 Hz, C3'), 87.61 ($Cq^{5'\text{-}OTrt}$), 86.11 (C1'), 82.69 (d, *J* = 23.3 Hz, C4'), 71.59 ($Cq^{\text{-}NHTrt}$), 62.74 (d, *J* = 9.4 Hz, C5'), 61.93 (d, *J* = 16.1 Hz, C2').

^{19}F NMR ($CDCl_3$) δ -196.70 (s).

HRMS: Calcd. for Chemical Formula: $C_{48}H_{39}FN_8O_2$ [M+H]: 779.3258; Found: 779.3254

Charafeddine, A., Dayoub, W., Chapuis, H., & Strazewski, P. (2007). First Synthesis of 2'-Deoxyfluoropuromycin Analogues: Experimental Insight into the Mechanism of the Staudinger Reaction. *Chemistry–A European Journal*,*13*(19), 5566-5584.

(36) (2R,3R,4R,5R)-4-azido-5-(6-(tritylamino)-9H-purin-9-yl)-2-((trityloxy)methyl)tetrahydrofuran-3-ol

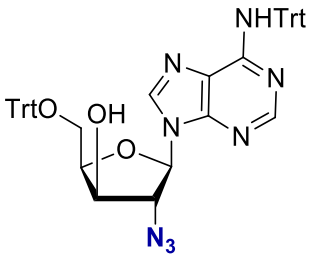

Chemical Formula: $C_{48}H_{40}N_8O_3$
Molecular Weight: 776,8830

36

To a solution of **32** (750 mg, 1.02 mmol) in DMF (7 mL) and water (0.5 mL), sodium azide (396 mg, 6.08 mmol) was added. The reaction mixture was stirred at 100 °C for 1.5 h, and was then partitioned between DCM and brine. The phases were separated. The aqueous phase was extracted twice with DCM. The combined organic layers were dried over sodium sulfate and concentrated. Flash chromatography of the residue (Cyclohexane/AcOEt 8/2) yielded **36** as a white foam (347 mg, 44 %).

^{1}H NMR (250 MHz, $CDCl_3$): δ = 7.92 (s, 1H, H2 or H8), 7.86 (s, 1H, H2 or H8), 7.49-7.19 (m, 30H, CH^{Trt}), 7.14 (s, 1H, NH^{Trt}), 5.64 (d, *J* = 2.0 Hz, 1H, H1'), 4.52 (d, 1H, *J* = 2.0 Hz, H2'), 4.29-4.19 (m, 2H, H3' and H4'), 3.58 (d, *J* = 5.25 Hz, 2H, H5').

Charafeddine, A., Dayoub, W., Chapuis, H., & Strazewski, P. (2007). First Synthesis of 2'-Deoxyfluoropuromycin Analogues: Experimental Insight into the Mechanism of the Staudinger Reaction. *Chemistry–A European Journal*,*13*(19), 5566-5584.

(37) ((2R,3S,4S,5R)-5-(6-amino-9H-purin-9-yl)-4-azido-3-fluorotetrahydrofuran-2-yl)methanol

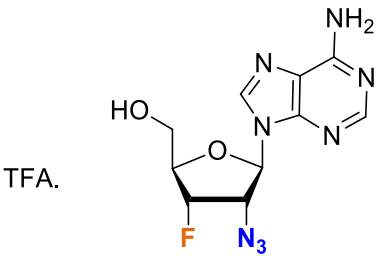

37

Free base:
Chemical Formula: $C_{10}H_{11}FN_8O_2$
Molecular Weight: 294,2451

TFA salt:
Chemical Formula: $C_{12}H_{12}F_4N_8O_4$
Molecular Weight: 408,2685

Compound **36** (155 mg, 0.199 mmol) was dissolved in DCM (1.7 mL), and TFA (198 µL, 2.59 mmol) was slowly added at 0 °C. The reaction mixture was stirred for 2 h, then was diluted with DCM. The mixture was washed with water three times. The combined aqueous layers were freezedried to yield compound **37** as a trifluoroacetate salt as a white solid (54 mg, 66 %).

^{1}H NMR (500 MHz, MeOD) δ 8.56 (s, 1H, H8), 8.37 (s, 1H, H2), 6.24 (d, *J* = 7.9 Hz, 1H, H1'), 5.45 (dd, *J* = 53.8, 3.9 Hz, 1H, H3'), 4.84 – 4.72 (m under MeOH, 1H, H2'), 4.48 (d, *J* = 26.4 Hz, 1H, H4'), 3.83 (s, 2H, H5').

^{13}C NMR (126 MHz, MeOD) δ 153.57 (C6), 150.06 (C4), 147.85 (C2), 143.15 (C8), 120.65 (C5), 94.61 (d, *J* = 185.1 Hz, C3'), 87.61 (C1'), 86.72 (d, *J* = 22.2 Hz, C4'), 65.77 (d, *J* = 15.7 Hz, C2'), 62.23 (d, *J* = 10.6 Hz, C5').

^{19}F NMR (471 MHz, MeOD) δ -196.06 (s)

HRMS: Calcd. for [M+H]: 295.1067; Found: 295.1061

---

(38) 9-((2R,3S,4S,5R)-3-azido-5-((bis(4-methoxyphenyl)(phenyl)methoxy)methyl)-4-fluorotetrahydrofuran-2-yl)-9H-purin-6-amine

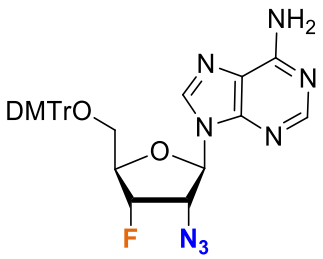

Chemical Formula: $C_{31}H_{29}FN_8O_4$
Molecular Weight: 596,6116

38

Compound **37** (50 mg, 0.12 mmol) was dissolved in pyridine (1 mL) with DMAP (0.7 mg, 0.006 mmol). DMTrCl (47 mg, 0.14 mmol) was added, and the reaction mixture was stirred at for 2 h. A second equivalent of DMTrCl (47 mg, 0.14 mmol) was added, and the reaction mixture was stirred overnight. The reaction mixture was partitioned between DCM and water. The organic layer was concentrated and flash chromatography (Cyclohexane/AcOEt 5/5 to 0/10) of the residue yielded 4 mg of compound **38**. The aqueous layer was freezedried, and the residue was reacted with DMTrCl, DMAP, and Pyr. In the same conditions. The reaction mixture was then concentrated and flash chromatography (Cyclohexane/AcOEt 5/5 to 0/10) of the residue yielded 3 mg of compound **38**. Pooling of the two samples allowed to recover **38** (7 mg, 10 %) as a white amorphous solid.

^{1}H NMR (500 MHz, $CDCl_3$) δ 8.22 (s, 1H, H2), 7.91 (s, 1H, H8), 7.42 – 7.38 (m, 2H, *o*-CH^{DMTr}), 7.32 – 7.28 (m, 4H, *o'*-CH^{DMTr}), 7.27-7.24 (m, *J* = 5, *m*-CH^{DMTr}), 7.23 (dt, *J* = 5.0, 2.0 Hz, 1H, *p*-CH^{DMTr}), 6.83 – 6.78 (m, 4H, *m'*-CH^{DMTr}), 6.07 (d, *J* = 7.9 Hz, 1H), 5.68 (s, 2H), 5.30 (ddd, *J* = 54.1, 4.5, 1.3 Hz, 1H), 5.18 (ddd, *J* = 23.1, 7.9, 4.4 Hz, 1H), 4.53 – 4.40 (m, 1H), 3.79 (s, 3H), 3.79 (s, 3H), 3.55 (dd, *J* = 10.7, 4.7 Hz, 1H), 3.40 (dd, *J* = 10.7, 3.9 Hz, 1H).

^{13}C NMR (126 MHz, $CDCl_3$) δ 158.87 (2C, *p'*-C^{DMTr}), 155.67 (C6), 153.44 (C2), 150.19 (C4), 144.39 (C*i*^{DMTr}), 139.92 (C8), 135.54 (C*i'*^{DMTr}), 135.44 (C*i'*^{DMTr}), 130.18 (2C, *o'*-CH^{DMTr}), 130.17 (2C, *o'*-CH^{DMTr}), 128.22 (2C, *o*-CH^{DMTr}), 128.13 (2C, *m*-CH^{DMTr}), 127.25 (*p*-CH^{DMTr}), 120.52 (C5), 113.44 (4C, *m'*-CH^{DMTr}), 92.74 (d, *J* = 187.2 Hz, C3'), 87.17 (Cq^{DMTr}), 85.99 (C1'), 82.88 (d, *J* = 23.4 Hz, C4'), 62.64 (d, *J* = 9.3 Hz, C5'), 62.40 (d, *J* = 15.8 Hz, C2'), 55.40 (2C, -OMe^{DMTr}).

^{19}F NMR (471 MHz, $CDCl_3$) δ -194.56 (s).

HRMS: Calcd. for $C_{31}H_{30}FN_8O_4$ [*M+H*]: 597.2374; Found: 597.2368

---

(40) N-(9-((2R,3S,4R,5R)-3-azido-5-((bis(4-methoxyphenyl)(phenyl)methoxy)methyl)-4-fluorotetrahydrofuran-2-yl)-9H-purin-6-yl)benzamide

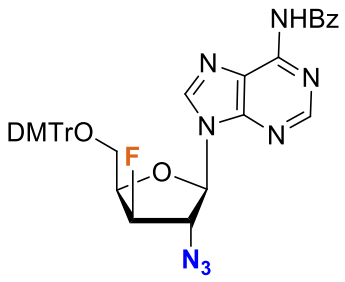

Chemical Formula: $C_{38}H_{33}FN_8O_5$
Molecular Weight: 700,7176

40

To a solution of crude compound **49** (90 mg) in DMF (520 µL), sodium azide (72 mg, 1.1 mmol) was added. The reaction mixture was stirred at rt for 48 h, and was then partitioned between DCM and brine. The phases were separated, and the aqueous layer was extracted twice with DCM. The combined organic layers were dried over $MgSO_4$ and concentrated. Flash chromatography of the residue (Cyclohexane/AcOEt 5/5) yielded **40** (32 mg, 67 % over two steps).

^{1}H NMR (500 MHz, $CDCl_3$) δ 9.03 (s, 1H, NH), 8.80 (s, 1H, H2), 8.04 (s, 1H, H8), 8.01 (d, *J* = 7.4 Hz, 2H, *o*-CH^{Bz}), 7.60 (t, *J* = 7.4 Hz, 1H, *p*-CH^{Bz}), 7.52 (t, *J* = 7.6 Hz, 2H, *m*-CH^{Bz}), 7.47 (d, *J* = 7.7 Hz, 2H, *o'*-CH^{DMTr}), 7.36 (dd, *J* = 8.9, 2.7 Hz, 4H, *o*-CH^{DMTr}), 7.31 (t, *J* = 7.6 Hz, 2H *m*-CH^{DMTr}), 7.24 (t, *J* = 7.3 Hz, 1H *p*-CH^{DMTr}), 6.85 (d, *J* = 8.7 Hz, 4H, *m'*-CH^{DMTr}), 6.29 (s, 1H, H1'), 5.11 (dd, *J* = 50.4, 1.8 Hz, 1H, H3'), 4.71 (d, *J* = 14.6 Hz, 1H, H2'), 4.49 (dtd, *J* = 29.9, 6.1, 2.5 Hz, 1H, H4'), 3.80 (s, 6H, -OMe^{DMTr}), 3.64 (dd, *J* = 9.1, 6.9 Hz, 1H, H5'a), 3.52 (dd, *J* = 9.9, 5.8 Hz, 1H, H5'b).

^{13}C NMR (126 MHz, $CDCl_3$) δ 164.65 (C=O), 158.86 (*p'*-C^{DMTr}), 158.83 (*p'*-C^{DMTr}), 153.08 (C2), 151.39 (C4), 149.64 (C6), 144.50 ($C1^{DMTr}$), 140.41 (d, *J* = 5.0 Hz, C8), 135.70 ($C1'^{DMTr}$), 135.52 ($C1'^{DMTr}$), 133.72 ($C1^{Bz}$), 132.96 (*p*-CH^{Bz}), 130.21 (2C, *o'*-CH^{DMTr}), 130.13 (2C, *o'*-CH^{DMTr}), 129.02 (2C, *m*-CH^{Bz}), 128.20 (2C, *o*-CH^{DMTr}), 128.10 (2C, *m*-CH^{Bz}), 128.00 (2C, *o*-CH^{Bz}), 127.19 (*p*-CH^{DMTr}), 123.39 (C5), 113.42 (2C, *m'*-CH^{DMTr}), 113.41 (2C, *m'*-CH^{DMTr}), 93.74 (d, *J* = 188.9 Hz, C3'), 88.61 (C1'), 86.96 (Cq^{DMTr}), 82.35 (d, *J* = 19.0 Hz, C4'), 69.43 (d, *J* = 27.5 Hz, C2'), 60.42 (d, *J* = 9.0 Hz, C5'), 55.38 (2C, -OMe^{DMTr}).

^{19}F NMR (471 MHz, $CDCl_3$) δ -197.04 (s).

HRMS: Calcd. for $C_{38}H_{34}FN_8O_5$ [*M+H*]: 701.2636; Found: 701.2642.

---

(41) N-(9-((2R,5S)-3-azido-5-((bis(4-methoxyphenyl)(phenyl)methoxy)methyl)-2,5-dihydrofuran-2-yl)-9H-purin-6-yl)benzamide

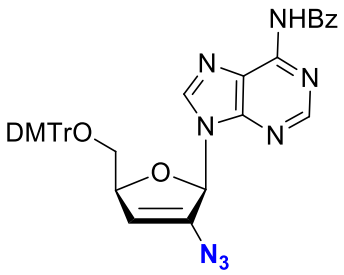

Chemical Formula: $C_{38}H_{32}N_8O_5$
Molecular Weight: 680,7113

41

To a solution of **8** (21 mg, 0.030 mmol) and pyridine (58 µL, 0.72 mmol) in chloroform (380 µL), DAST (18 µL, 0.138 mmol) was added at 0 °C. The reaction mixture was stirred at rt for 24 h and was then partitioned between DCM and an aqueous saturated hydrogenocarbonate solution. The phases were separated, and the aqueous layer was extracted twice with DCM. The combined organic layers were dried over sodium sulfate and concentrated. Flash chromatography (Cyclohexane/AcOEt 1/1 to 0/1) of the residue yielded **41** (10 mg, 50%).

^{1}H NMR (250 MHz, $CDCl_3$) δ 9.04 (s, 1H, H2 or H8), 8.76 (s, 1H, H2 or H8), 8.06 (m, 2H, CH^{Bz} or CH^{DMTr}), 7.54 (s, 3H, CH^{Bz} or CH^{DMTr}), 7.32 (m, 9H, CH^{Bz} or CH^{DMTr}), 6.82 (m, 4H, CH^{Bz} or CH^{DMTr}), 5.81 (s, 1H, H1'), 5.14 (s, 1H, H3'), 3.77 (s, 1H, H4'), 3.41 (m, 2H, H5'a and H5'b).

MS: calcd for $C_{38}H_{33}N_8O_5$ [*M+H*]: 681.2; found: 994.4306.

---

(42) (2R,3R,4R,5R)-5-(6-(tritylamino)-9H-purin-9-yl)-4-(trityloxy)-2-((trityloxy)methyl)tetrahydrofuran-3-ol

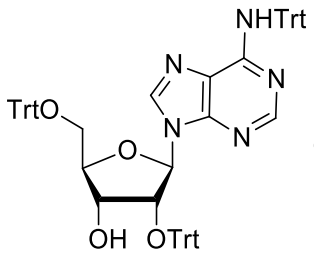

Chemical Formula: $C_{67}H_{55}N_5O_4$
Molecular Weight: 994,1847

42

A mixture of adenosine (2.67 g, 10.0 mmol), DMAP (1.00 g, 8.0 mmol) and TrtCl (13.9 g, 50.0 mmol) in pyridine (125 mL) was heated at 80 °C for three days. The reaction was quenched with EtOH, concentrated in vacuo and coevaporated with toluene. CH_2Cl_2 was added to the resulting orange foam, the mixture was washed with H_2O and the combined aqueous layers were then re-extracted with CH_2Cl_2. The combined organic layers were dried over Na_2SO_4, concentrated in vacuo and the crude residue was purified by chromatography using cyclohexane/EtOAc (9/1 then 8/2) as the eluent to yield **42** as a white foam (4.63 g, 46%).

^{1}H NMR (250 MHz, $CDCl_3$) δ 7.89 (s, 1H, H2 or H8) , 7.86 (s, 1H, H2 or H8), 7.00-7.42 (m, 45H, H^{Trt}), 6.32 (d, *J* = 7.5 Hz, 1H, H1'), 5.16 (dd, *J* = 7.5 Hz, *J* = 4.7 Hz, 1H, H2'), 4,03 (bs, 1H, H4'), 3.26 (dd, *J* = 10.5 Hz, *J* = 3.5 Hz, 1H, H5'b), 3.00 (dd, *J* = 10.5 Hz, *J* = 3.2 Hz, 1H, H5'a), 2.86 (d, *J* = 4.3 Hz, 1H, H3'),

^{13}C NMR (63 MHz, $CDCl_3$) δ 154.1 (C2 or C8), 152.3 (C^{Ad}), 149.3 (C^{Ad}), 145.1 (C^{Trt}), 143.5 (C^{Trt}), 143.2 (C^{Trt}), 139.5 (C2 or C8), 129.0 (C^{Trt}), 128.7 (C^{Trt}), 128.3 (C^{Trt}), 128.1 (C^{Trt}), 127.9 (C^{Trt}), 127.8 (C^{Trt}), 127.6 (C^{Trt}), 127.1 (C^{Trt}), 126.9 (C^{Trt}), 121.3 (C^{Ad}), 87.8 (C^{Trt}), 87.1 (C1'), 86.5 (C^{Trt}), 84.3 (C4'), 76.9 (C2'), 71.4 (C3'), 70.7 (C^{Trt}), 63.9 (C5'),

HRMS: calcd for $C_{67}H_{56}N_5O_4$ [*M+H*]: 994.4332; found: 994.4306.

Iannazzo, L., Laisne, G., Fonvielle, M., Braud, E., Herbeuval, J. P., Arthur, M., & Etheve-Quelquejeu, M. (2015). Synthesis of 3'-Fluoro-tRNA Analogues for Exploring Non-ribosomal Peptide Synthesis in Bacteria. *ChemBioChem*, *16*(3), 477-486.

(43) 9-((2R,3S,4S,5R)-4-fluoro-3-(trityloxy)-5-((trityloxy)methyl)tetrahydrofuran-2-yl)-N-trityl-9H-purin-6-amine

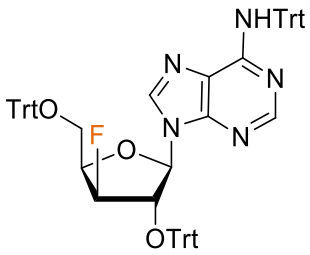

Chemical Formula: $C_{67}H_{54}FN_5O_3$
Molecular Weight: 996,1758

43

Compound **42** (2.00 g, 2.0 mmol) was dissolved in $CHCl_3$ (100 mL) and pyridine (4 mL) was added to the solution. DAST (1.32 mL, 10.0 mmol) was then added and the solution was stirred at room temperature for 24 h. The reaction mixture was quenched with aqueous $NaHCO_3$ and the two layers were separated. The organic layer was then washed with water and the combined aqueous layers were re-extracted with CH_2Cl_2. The combined organic layers were dried over Na_2SO_4, concentrated in vacuo and purified by chromatography using cyclohexane/EtOAc (9/1) as the eluent to afford **43** as a white foam (1.00 g, 50%).

^{1}H NMR (250 MHz, $CDCl_3$): δ 8.10 (s, 1H, H2 or H8), 7.62 (s, 1H, H2 or H8), 7.15-7.35 (m, 45H, H^{Trt}), 6.90 (s, 1H, NH), 6.45 (s, 1H, H1'), 4.38 (d, *J* = 14.5 Hz, 1H, H2'), 4.20 (dt, *J* = 29.7, 6.25 Hz, 1H, H4'), 3.77 (d, *J* = 51.7 Hz, 1H, H3'), 3.43-3.50 (m, 1H, H5'b), 3.24-3.31 (m, 1H, H5'a),

^{19}F NMR (471 MHz, $CDCl_3$): δ = -199.60.

HRMS: calcd for $C_{67}H_{55}FN_5O_3$ [*M+H*]: 996.4278; found: 996.4258.

Iannazzo, L., Laisne, G., Fonvielle, M., Braud, E., Herbeuval, J. P., Arthur, M., & Etheve-Quelquejeu, M. (2015). Synthesis of 3'-Fluoro-tRNA Analogues for Exploring Non-ribosomal Peptide Synthesis in Bacteria. *ChemBioChem*, *16*(3), 477-486.

(44) (2R,3S,4R,5R)-2-(6-amino-9H-purin-9-yl)-4-fluoro-5-(hydroxymethyl)tetrahydrofuran-3-ol

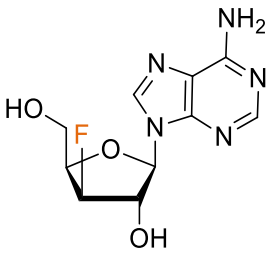

Chemical Formula: $C_{10}H_{12}FN_5O_3$
Molecular Weight: 269,2324

44

Trifluoroacetic acid (645 µL, 8.45 mmol) was added to a solution of **43** (64 mg, 0.65 mmol) in CH_2Cl_2 (6 mL) at 0 °C. The reaction mixture was warmed to rt and further stirred for 1 h. Water and CH_2Cl_2 were then added to the resulting solution. After filtration, the aqueous layer was lyophilized and purified by chromatography using CH_2Cl_2/MeOH (90/10) to afford **44** as a white foam (165 mg, 94%).

^{1}H NMR (500 MHz, CD_3OD): δ 8.22 (s, 1H, H2 or H8), 8.15 (s, 1H, H2 or H8), 6.09 (d, *J* = 2.0 Hz, 1H, H1'), 5.10 (ddd, *J* = 52.0, 3.6, 3.0 Hz, 1H, H3'), 4.71 (dt, *J* = 14.0, 3.5 Hz, 1H, H2'), 4.47 (m, 1H, H4'), 3.99 – 3.90 (m, 2H, H5').

^{13}C NMR (125 MHz, CD_3OD) δ 157.3 (C^{Ad}). 153.8 (C2 or C8), 150.2 (C^{Ad}), 140.3 (C^{Ad}), 140.2 (C2 or C8), 96.7 (d, *J* = 183.2 Hz, C3'), 91.4 (C1'), 83.9 (d, *J* = 19.8 Hz, C4'), 79.7 (d, *J* = 27.1 Hz, C2'), 60.0 (d, *J* =10.7 Hz, C5').

HRMS: calcd for $C_{10}H_{13}FN_5O_3$ [*M+H*]: 270.1002; found: 270.0992.

Iannazzo, L., Laisne, G., Fonvielle, M., Braud, E., Herbeuval, J. P., Arthur, M., & Etheve-Quelquejeu, M. (2015). Synthesis of 3'-Fluoro-tRNA Analogues for Exploring Non-ribosomal Peptide Synthesis in Bacteria. *ChemBioChem*, *16*(3), 477-486.

(45) N-(9-((2R,3S,4R,5R)-4-fluoro-3-hydroxy-5-(hydroxymethyl)tetrahydrofuran-2-yl)-9H-purin-6-yl)benzamide

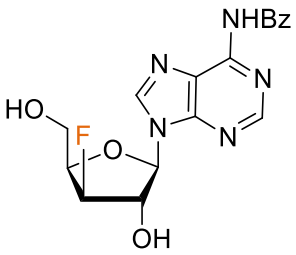

Chemical Formula: $C_{17}H_{16}FN_5O_4$
Molecular Weight: 373,3384

45

To a solution of **44** (199 mg, 0.74 mmol) in pyridine (4.5 mL), trimethylsilyl chloride (610 µL, 4.81 mmol) was added slowly at 0 °C. After stirring 1.5 h at rt, benzoyl chloride (516 µL, 4.44 mmol) was added slowly at 0 °C, and the mixture was stirred at rt overnight. Water (5 mL) was added at 0 °C, and, after stirring 1.5 h at rt, the mixture was concentrated. The residue was dissolved in AcOEt, washed with brine, dried over $MgSO_4$ then concentrated. Flash chromatography (DCM/MeOH 96/4) of the residue yielded compound **45** (266 mg, 88 %) as a yellowish foam.

^{1}H NMR (500 MHz, MeOD) δ 8.72 (s, 1H, H2 or H8), 8.43 (s, 1H, H2 or H8), 8.09 – 8.05 (m, 2H, Bz), 7.67 – 7.62 (m, 1H, Bz), 7.58 – 7.52 (m, 2H, Bz), 6.24 (d, *J* = 1.5 Hz, 1H, H1'), 5.11 (ddd, *J* = 51.4, 3.0, 1.5 Hz, 1H, H3'), 4.78 (dt, *J* = 13.2, 1.5 Hz, 1H, H2'), 4.51 (dtd, *J* = 29.1, 6.0, 3.0 Hz, 1H, H4'), 3.99 (dd, *J* = 11.7, 5.8 Hz, 1H H5'a), 3.95 (ddd, *J* = 11.8, 6.2, 1.4 Hz, 1H, H5'b).

^{13}C NMR (126 MHz, MeOD) δ 168.14 (s, C=O), 153.36 (s, C2 or C8), 153.12 (s, Cq), 151.10 (s, Cq), 143.37 (d, *J* = 6.8 Hz, H2 or H8), 134.96 (s, Cq), 133.91 (s, *p*-CH^{Bz}), 129.76 (s, 2C, Bz), 129.43 (s, 2C, Bz), 125.06 (s, Cq), 96.73 (d, *J* = 191.5 Hz, C3'), 91.72 (s, C1'), 84.40 (d, *J* = 19.4 Hz, C4'), 79.72 (d, *J* = 26.4 Hz, C2'), 59.96 (d, *J* = 10.5 Hz).

^{19}F NMR (471 MHz, MeOD) δ -203.12 (s).

HRMS: calcd for $C_{17}H_{17}FN_5O_4$ [*M+H*]: 374.1265; found: 374.1257.

---

(46) N-(9-((2R,3S,4R,5R)-5-((bis(4-methoxyphenyl)(phenyl)methoxy)methyl)-4-fluoro-3-hydroxytetrahydrofuran-2-yl)-9H-purin-6-yl)benzamide

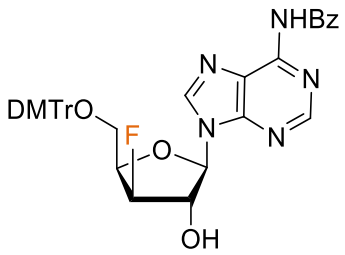

Chemical Formula: $C_{38}H_{34}FN_5O_6$
Molecular Weight: 675,7049

46

Compound **45** (232 mg, 0.622 mmol) and DMAP (76 mg, 0.622 mmol) were dissolved in pyiridine (4.5 mL), then dimethoxytrityl chloride (316 mg, 0.933 mmol) was added. After stirring the mixture for 1.5 h, another equivalent of DMTrCl (316 mg, 0.933 mmol) was added. The reaction mixture was stirred for 2 h. Methanol (5 mL) was added, and the mixture was then concentrated. The residue was dissolved in DCM, washed with brine, dried of $MgSO_4$, and concentrated. Flash chromatography (Cyclohexane/AcOEt 5/5 to 0/10) of the residue yielded **46** (387 mg, 92 %) as a white amorphous solid.

^{1}H NMR (500 MHz, $CDCl_3$) δ 9.04 (s, 1H, NH), 8.72 (s, 1H, H2 or H8), 8.08 (s, 1H, H2 or H8), 7.99 (d, *J* = 7.4 Hz, 2H), 7.62 – 7.56 (m, 1H), 7.51 (m, 2H), 7.46 (m, 2H), 7.37 – 7.32 (m, 4H), 7.28 (m, 2H), 7.21 (m, 1H), 6.86 – 6.80 (m, 4H), 6.20 (d, *J* = 1.6 Hz, 1H, H1'), 5.14 (ddd, *J* = 51.5, 2.8, 1.3 Hz, 1H, H3'), 5.09 – 5.05 (bs, 1H, OH), 4.75 (d, *J* = 14.9 Hz, 1H, H2'), 4.65 (dtd, *J* = 28.8, 5.9, 3.0 Hz, 1H, H4'), 3.78 (s, 6H, OMe), 3.64 – 3.58 (m, 1H, H5'a), 3.48 (dd, *J* = 9.9, 5.4 Hz, 1H, H5'b).

^{13}C NMR (126 MHz, $CDCl_3$) δ 164.73 (C=O), 158.78 (Cq), 158.75 (Cq), 152.66 (C2 or C8), 151.12 (Cq), 149.54 (Cq) 144.64 (Cq), 141.02 (d, *J* = 5.2 Hz, C2 or C8), 135.88 (Cq), 135.68 (Cq), 133.65 (*p*-CH^{Bz}), 133.07 (Cq), 130.27 (2C, *o*-CH^{DMTr}), 130.17 (2C, *o*-CH^{DMTr}), 129.07 (2C, *m*-CH^{Bz}), 128.26 (2C, *o*-CH^{DMTr}), 128.03 (2C, *m*-CH^{DMTr}), 127.95 (2C, *o*-CH^{Bz}), 127.09 (*p*-CH^{DMTr}), 123.13 (Cq), 113.36 (2C, *m*-CH^{DMTr}), 113.34 (2C, *m*-CH^{DMTr}), 95.33 (d, *J* = 185.2 Hz, C3'), 91.18 (C1'), 86.83 (Cq), 82.14 (d, *J* = 19.4 Hz, C4'), 79.61 (d, *J* = 27.6 Hz, C2'), 60.72 (d, *J* = 8.9 Hz, C5'), 55.38 (2C, OMe).

^{19}F NMR (471 MHz, $CDCl_3$) δ -200.70 (s).

HRMS: calcd for $C_{38}H_{35}FN_5O_6$ [*M+H*]: 676.2571; found: 676.2567.

---

(47) N-(9-((2R,4S,5R)-5-((bis(4-methoxyphenyl)(phenyl)methoxy)methyl)-4-fluoro-3-oxotetrahydrofuran-2-yl)-9H-purin-6-yl)benzamide

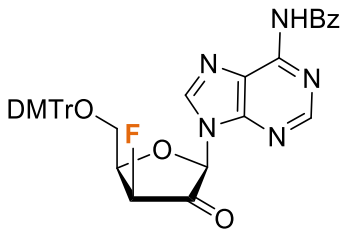

Chemical Formula: $C_{38}H_{32}FN_5O_6$
Molecular Weight: 673,6890

47

To a solution of compound **46** (376 mg, 0.556 mmol) in DCM (9 mL), at 0 °C, was added a solution of Dess-Martin Periodinane (708 mg, 1.67 mmol) in DCM (9 mL). The reaction mixture was stirred at 0 °C for 3 h, then was poured into a saturated aqueous solution of $NaHCO_3$ and $Na_2S_2O_3$. After separation of the phases, the aqueous layer was extracted twice with DCM. The organic layers were combined, dried over $MgSO_4$, concentrated and the residue was purified by flash chromatography (Cyclohexane/AcOEt 4/6 to 0/10) to yield compound **47** (265 mg, 71 %) as a white amorphous solid.

^{1}H NMR (500 MHz, $CDCl_3$) δ 9.08 (s, 1H, NH), 8.40 (s, 1H, H8), 8.05 (s, 1H, H2), 7.93 (d, *J* = 7.4 Hz, 2H, *o*-CH^{Bz}), 7.54 – 7.50 (m, 1H, *p*-CH^{Bz}), 7.47-7.41 (m, 4H, *m*-CH^{Bz} and *o*-CH^{DMTr}), 7.33 (d, *J* = 8.8 Hz, 4H, *o'*-CH^{DMTr}), 7.28 (dd, *J* = 5.2, 4.3 Hz, 2H, *m*-CH^{DMTr}), 7.19-7.16 (m, 1H, *p*-CH^{DMTr}), δ 6.80 (dd, *J* = 9.0, 3.6 Hz, 4H, *m'*-CH^{DMTr}), 6.27 (s, 1H, H1'), 4.94 (d, *J* = 54.1 Hz, 1H, H3'), 4.59 (d, *J* = 29.2 Hz, 1H, H4'), 3.75 (s, 3H, -OMe^{DMTr}), 3.75 (s, 3H, -OMe^{DMTr}), 3.54 – 3.46 (m, 2H, H5').

^{13}C NMR (126 MHz, $CDCl_3$) δ 165.52, 158.82, 158.73 (2C), 152.34, 152.07, 148.20, 144.69, 143.21 (d, *J* = 9.5 Hz), 135.87, 135.80, 133.31, 133.16, 130.22 (2C), 130.19 (2C), 129.03 (2C), 128.27 (2C), 128.06 (2C), 128.03 (2C), 127.94, 127.06, 113.36 (2C), 113.34 (2C), 93.88 (d, *J* = 190.4 Hz, C3'), 88.65 (C1'), 86.74, 80.00 (d, *J* = 18.0 Hz, C4'), 60.81 (d, *J* = 9.0 Hz, C5'), 55.36 (2C).

^{19}F NMR (471 MHz, $CDCl_3$) δ -205.44 (s).

---

(48) N-(9-((2R,3R,4R,5R)-5-((bis(4-methoxyphenyl)(phenyl)methoxy)methyl)-4-fluoro-3-hydroxytetrahydrofuran-2-yl)-9H-purin-6-yl)benzamide

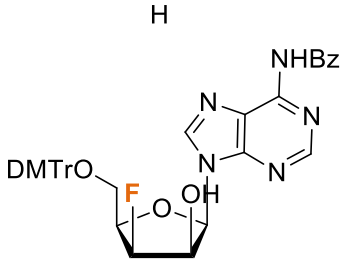

Chemical Formula: $C_{38}H_{34}FN_5O_6$
Molecular Weight: 675,7049

48

To a solution of compound **47** (180 mg, 0.267 mmol) in a 15 to 1 mixture of EtOH and water (1.7 mL), $NaBH_4$ (14 mg, 0.37 mmol) was added at 0 °C. The reaction mixture was stirred for 2 h at rt, before being diluted in AcOEt, then washed with brine. The organic layer was dried over MgSO4, concentrated, and the residue was purified by flash chromatography (Cyclohexane/AcOEt 4/6 to 1/9) to yield compound **48** (46 mg, 26 %) as a yellowish foam.

^{1}H NMR (500 MHz, $CDCl_3$) δ 9.19 (s, 1H, NH), 8.59 (s, 1H, H8), 8.06 (d, *J* = 7.4 Hz, 2H, *o*-CH^{Bz}), 7.86 (s, 1H, H2), 7.59 (t, *J* = 7.4 Hz, 1H, *p*-CH^{Bz}), 7.52 (t, *J* = 7.6 Hz, 2H, *m*-CH^{Bz}), 7.48 – 7.45 (m, 2H, *o*-CH^{DMTr}), 7.36 (d, *J* = 1.4 Hz, 2H, *o'*-CH^{DMTr}), 7.34 (d, *J* = 1.4 Hz, 2H, *o'*-CH^{DMTr}), 7.27 (t, *J* = 7.6 Hz, 2H, *m*-CH^{DMTr}), 7.20 (t, *J* = 7.3 Hz, 1H, *p*-CHD^{MTr}), 6.81 (d, *J* = 3.8 Hz, 2H, *m'*-CH^{DMTr}), 6.79 (d, *J* = 3.8 Hz, 2H, *m'*-CH^{DMTr}), 6.52 (d, *J* = 6.9 Hz, 1H, H1'), 5.24 (dt, *J* = 54.6, 2.7 Hz, 1H, H3'), 4.86 (d, *J* = 29.2 Hz, 1H, H2'), 4.32 (dtd, *J* = 30.5, 6.1, 1.9 Hz, 1H, H4'), 3.75 (s, 3H, OMe^{DMTr}), 3.75 (s, 3H, OMe^{DMTr}), 3.60 (d, *J* = 6.1 Hz, 2H, H5').
^{13}C NMR (126 MHz, $CDCl_3$) δ 164.84 (C=O^{Bz}), 158.78 (*p'*-Cq^{DMTr}), 158.77 (*p'*-Cq^{DMTr}), 152.99 (C8), 151.55 (C4), 148.36 (C5), 144.57 ($C1^{DMTr}$), 142.44 (d, *J* = 12.6 Hz, C2), 135.75 ($C1'^{DMTr}$), 135.64 ($C1'^{DMTr}$), 134.06 ($C1^{Bz}$), 132.67 (*p*-CH^{Bz}), 130.18 (2C, *o'*-CH^{DMTr}), 130.12 (2C, *o'*-CH^{DMTr}), 128.77 (2C, *m*-CH^{Bz}), 128.20 (2C, *o*-CH^{Bz}), 128.20 (2C, *o*-CH^{DMTr}), 128.05 (2C, *m*-CH^{DMTr}), 127.09 (*p*-CH^{DMTr}), 120.91 (C6), 113.37 (4C, *m'*-CH^{DMTr}), 91.80 (d, *J* = 187.7 Hz, C3'), 86.89 (-CAr_3^{DMTr}), 83.12 (C1'), 79.47 (d, *J* = 17.6 Hz, C4'), 74.01 (d, *J* = 16.4 Hz, C2'), 61.04 (d, *J* = 7.6 Hz, C5'), 55.33 (2C, -OMe^{DMTr}).
^{19}F NMR (471 MHz, $CDCl_3$) δ -213.34 (s).

HRMS: calcd for $C_{38}H_{35}FN_5O_6$ [*M+H*]: 676.2571; found: 676.2562.

---

(49) (2R,3R,4S,5R)-2-(6-benzamido-9H-purin-9-yl)-5-((bis(4-methoxyphenyl)(phenyl)methoxy)methyl)-4-fluorotetrahydrofuran-3-yl trifluoromethanesulfonate

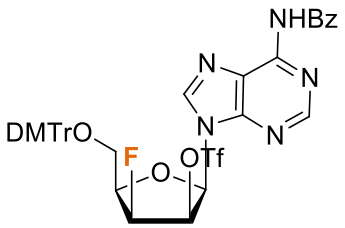

Chemical Formula: $C_{39}H_{33}F_4N_5O_8S$
Molecular Weight: 807,7666

49

To a solution of **48** (46 mg, 0.068 mmol) in DCM (645 µL), triflyl chloride (14 µL, 0.14 mmol) and DMAP (25 mg, 0.20 mmol) were added at 0 °C. The reaction mixture was stirred at rt for 1 h, until the starting SM was entirely consumed on TLC. The reaction mixture was then partitioned between DCM and brine. The phases were separated, and the aqueous layer was extracted twice with DCM. The combined organic layers were dried over sodium sulfate and concentrated product. Crude **49** (90 mg) was directly used for subsequent azidation (*cf* compound **40**).

---

(50) 9-((2R,3S,4R,5R)-3-azido-5-((bis(4-methoxyphenyl)(phenyl)methoxy)methyl)-4-fluorotetrahydrofuran-2-yl)-9H-purin-6-amine

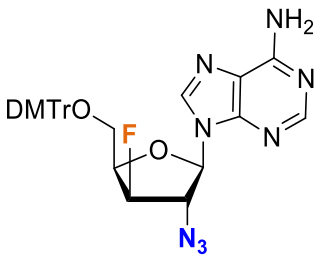

Chemical Formula: $C_{31}H_{29}FN_8O_4$
Molecular Weight: 596,6116

50

On Compound **40** (30 mg, 0.043 mmol) was dissolved in a 3/1 EtOH/NH4OH mixture, and then heated up to 55 °C for 1.5 h. The mixture was then concentrated, and the residue was purified by flash chromatography (Cyclohexane/AcOEt 3/7) to yield compound **50** (13 mg, 51 %) as a white amorphous solid.

^{1}H NMR (500 MHz, $CDCl_3$) δ 8.36 (s, 1H, H2), 7.84 (s, 1H, H8), 7.48 – 7.45 (m, 2H, *o*-CH^{DMTr}), 7.38 – 7.34 (m, 4H, *o'*-CH^{DMTr}), 7.30 (t, *J* = 7.6 Hz, 2H, *m*-CH^{DMTr}), 7.23 (t, *J* = 7.3 Hz, 1H, *p*-CH^{DMTr}), 6.85 (d, *J* = 8.7 Hz, 4H, *m'*-CH^{DMTr}), 6.20 (d, *J* = 1.6 Hz, 1H, H1'), 5.80 (s, 2H, NH_2), 5.09 (dd, *J* = 50.6, 1.8 Hz, 1H, H3'), 4.67 (d, *J* = 15.1 Hz, 1H, H2'), 4.46 (dtd, *J* = 29.7, 6.1, 2.6 Hz, 1H, H4'), 3.80 (s, 3H, OMe^{DMTr}), 3.80 (s, 3H, OMe^{DMTr}), 3.63 (ddd, *J* = 10.9, 6.7, 2.9 Hz, 1H, H5'a), 3.50 (dd, *J* = 9.9, 5.8 Hz, 1H, H5'b).

^{13}C NMR (126 MHz, $CDCl_3$) δ 158.85 (*p'*-C^{DMTr}), 158.83 (*p'*-C^{DMTr}), 155.54 (C6), 153.51 (C2), 149.57 (C4), 144.56 (*Ci*^{DMTr}), 138.00 (d, *J* = 5.1 Hz, C8), 135.75 (*Ci'*^{DMTr}), 135.60 (*Ci'*^{DMTr}), 130.23 (2C, *o'*-CH^{DMTr}), 130.17 (2C, *o'*-CH^{DMTr}), 128.24 (2C, *o*-CH^{DMTr}), 128.08 (2C, *m*-CH^{DMTr}), 127.17 (*p*-CH^{DMTr}), 119.96 (C5), 113.41 (2C, *m'*-CH^{DMTr}), 113.40 (2C, *m'*-CH^{DMTr}), 93.88 (d, *J* = 189.0 Hz, C3'), 88.44 (C1'), 86.92 (Cq^{DMTr}), 82.06 (d, *J* = 19.2 Hz, C4'), 69.49 (d, *J* = 27.6 Hz, C2'), 60.50 (d, *J* = 9.0 Hz, C5'), 55.39 (s, -OMe^{DMTr}).

^{19}F NMR (471 MHz, $CDCl_3$) δ -197.03 (s).

HRMS: Calcd. for $C_{31}H_{30}FN_8O_4$ [*M+H*]: 597.2374; Found: 597.2363

---

(51) (52) (53) (54) (55) (56) (57) (58)

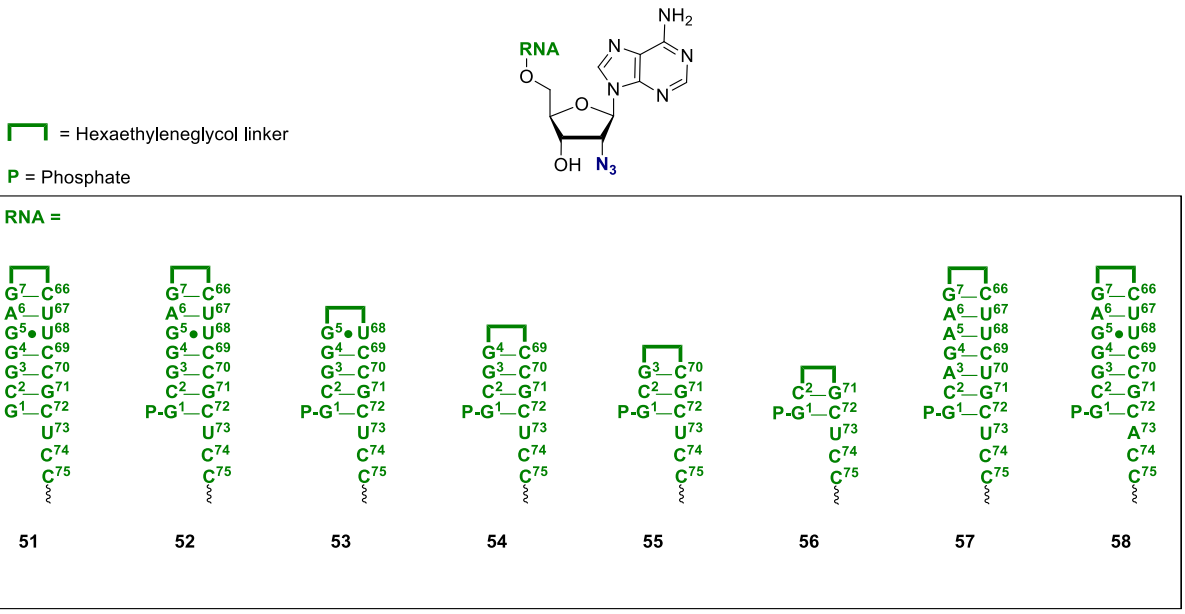

Oligos **51** to **58** were synthesized according to the general procedure for solid-phase synthesis of oligoribonucleotides.

Purification was done by reversed-phase HPLC on a C18 semi-preparative column.

MS:

Compound **51;** (*m/z*): calculated [*M-H*] 6168; found 6168

Compound **52;** (*m/z*): calculated [*M-H*] 6090; found 6089

Compound **53;** (*m/z*): calculated [*M-H*] 4883; found 4883

Compound **54;** (*m/z*): calculated [*M*] 4232; found 4232

Compound **55;** (*m/z*): calculated [*M*] 3582; found 3582

Compound 5**6;** (*m/z*): calculated [*M-H*] 2931; found 2931

Compound **57;** (*m/z*): calculated [*M-H*] 6137; found 6137

Compound **58;** (*m/z*): calculated [*M-H*] 6191; found 6191

(59)

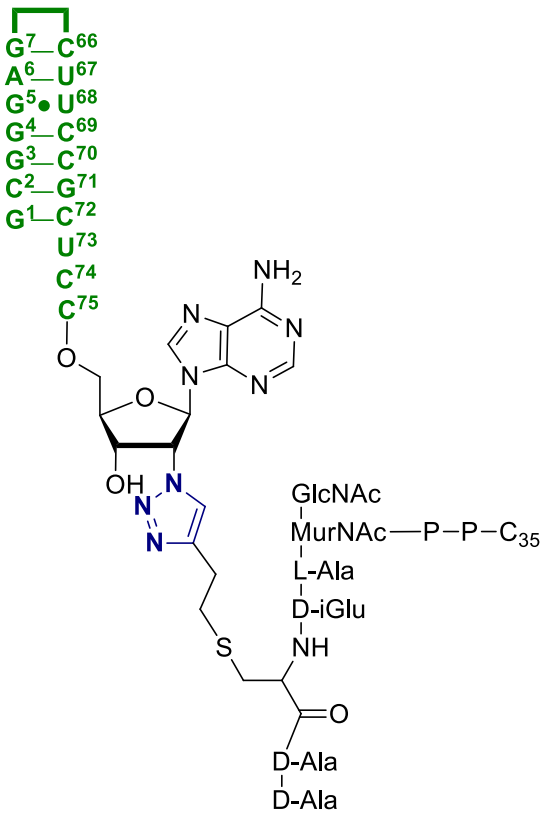

59

Oligo **52** (0.3 nmol, final concentration 0.06 mM) reacted with the alkyne-bearing analog of lipid II (final concentration 0.11 mM) in the presence of THPTA (3.5 mM), $CuSO_4$ (0.5 mM), sodium ascorbate (5 mM), a phosphate buffer pH8 (100 mM) in a DMF/Water mixture (16 % DMF, total volume 5 µL). **59** was purified by gel (acrylamide/urea 7M/12 %). The retarded band was excised and 59 was recovered through electroelution and dialyse again RNAse-free water. UV-dosage allowed to estimate the yield at 18 %.

MS: average mass calcd. for $C_{257}H_{359}N_{77}O_{159}P_{20}S$: 7722.6; found: 7723.0.

---

(61) N-(9-((2R,3R,4S,5R)-3-azido-4-((tert-butyldimethylsilyl)oxy)-5-(hydroxymethyl)tetrahydrofuran-2-yl)-9H-purin-6-yl)benzamide

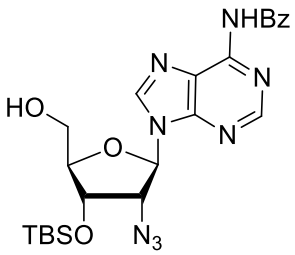

Chemical Formula: $C_{23}H_{30}N_8O_4Si$
Molecular Weight: 510,6210

61

To a solution of **7** (250 mg, 0,400 mmol) in THF (2,7 mL), a 1/1 H_2O/TFA (3 mL) was added at 0 °C. After being stirred at rt for 1 h, the reaction mixture is diluted by AcOEt and poured on a sodium hydrogenocarbonate aqueous solution at 0 °C. The phases were separated and the aqeous phase was extracted twice with AcOEt. The combined organic layers were dried over sodium sulfate and concentrated. Flash chromatography of the residue (Cyclohexane/AcOEt 4/6) yielded **8** (199 mg, quant.) as a white amorphous solid.

^{1}H NMR (250 MHz, $CDCl_3$) δ 8.73 (s, 1H, H2 or H8), 8.28 (s, 1H, H2 or H8), 8.24 (bs, 1H, NH^{Bz}), 8.05-7.86 (m, 2H, H^{Bz}), 7.61-7.52 (m, 1H, H^{Bz}), 7.49-7.38 (m, 2H, H^{Bz}), 6.06 (d, *J* = 8.1 Hz, 1H, H1'), 4.69-4.54 (m, 2H, H2'/H3'), 4.23-4.17 (m, 1H, H4'), 3.95 (dd, *J* = 1.9, 12.9 Hz, 1H, H5'a), 3.77-3.66 (m, 1H, H5'b), 0.95 (s, 9H, *t*Bu^{TBS}), 0.18 (s, 3H, Me^{TBS}), 0.14 (s, 3H, Me^{TBS}).

^{13}C NMR (63 MHz, $CDCl_3$) δ 165.5 ($C{=}O^{Bz}$), 152.2 (C2 or C8), 150.9, 150.1 (2 x Cq^{Ad}), 143.3 (C2 or C8), 133.3 (CH^{Bz}), 132.9 (Cq^{Bz}), 129.0, 128.2 (4 x CH^{Bz}), 124.1 (Cq^{Ad}), 89.5 (C4'), 88.5 C1'), 74.1 (C3'), 64.6 (C2'), 62.5 (C5'), 25.8 (*t*Bu^{TBS}), 18.2 (Cq^{TBS}), -4.7, -4.8 (2 x Me^{TBS}).

Fonvielle, M., Mellal, D., Patin, D., Lecerf, M., Blanot, D., Bouhss, A., ... & Ethève-Quelquejeu, M. (2013). Efficient Access to Peptidyl-RNA Conjugates for Picomolar Inhibition of Non-ribosomal $FemX_{Wv}$ Aminoacyl Transferase.*Chemistry–A European Journal*, *19*(4), 1357-1363.

(62) (2R,3S,5R)-5-(4-acetamido-2-oxopyrimidin-1(2H)-yl)-2-(hydroxymethyl)tetrahydrofuran-3-yl (((2R,3S,4R,5R)-4-azido-5-(6-benzamido-9H-purin-9-yl)-3-((tert-butyldimethylsilyl)oxy)tetrahydrofuran-2-yl)methyl) hydrogen phosphate

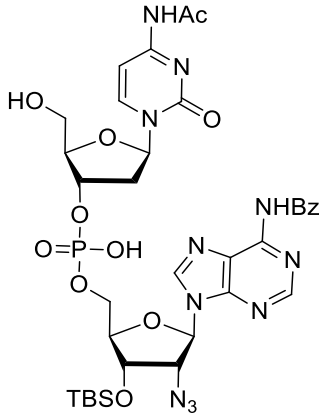

62

Chemical Formula: $C_{34}H_{44}N_{11}O_{11}PSi$
Molecular Weight: 841,8395

To a solution of the adenosine derivative **61** (66 mg, 0.130 mmol) in DCM (700 µL) at rt under argon atmosphere, tetrazole in a 0.45 solution in MeCN (2.9 mL, 1.29 mmol) and Ac-dC-PCNE (250 mg, 0.324 mmol) were added. After stirring for 1 h at rt, 0.1 M iodine in THF-H_2O-pyridine (75:2:20, 3.3 mL, 0.325 mmol) was added. After 30 min, the reaction mixture was diluted with EtOAc (10 mL), washed with, aqueous saturated $Na_2S_2O_3$ solution. The phases were separated, and the aqueous layer was extracted twice with AcOEt. The combined organic layers were dried over sodium sulfate and concentrated. On the residue was added TCA in a 0.18 M solution in DCM (7.2 mL, 1.3 mmol) and the mixture was stirred at rt for 30 min. The reaction mixture was partitioned between DCM and a sodium hydrogenocarbonate aqeous solution. The phases were separated. The aqeous layer was extracted twice with DCM. The combined organic layers were dried over sodium sulfate and concentrated. Flash chromatography yielded **62** (95 mg, 82 %) as a white amorphous solid.

^{1}H NMR (250 MHz, $CDCl_3$) δ 9.44 (bs, 1H, NH^{Ac}), 8.75 (s, 1H, $H2^{Ad}$ or $H8^{Ad}$), 8.31 (s, 1H, $H2^{Ad}$ or $H8^{Ad}$), 8.16 (d, *J* = 1.9 Hz, 1H, $H6^{Cyt}$), 8.05-8.02 (m, 2H, H^{Bz}), 7.60-7.57 (m, 1H, H^{Bz}), 7.51-7.48 (m, 2H, H^{Bz}), 7.31 (d, *J* = 2.8 Hz, 1H, $H5^{Cyt}$), 6.16-6.09 (m, 2H, $H1'^{Ad}$, $H1'^{Cyt}$), 5.14-5.07 (m, 1H, $H3'^{Cyt}$), 4.97-4.93 (m, 1H, $H3'^{Ad}$), 4.80-4.75 (m, 1H, $H2'^{Ad}$), 4.27-4.15 (m, 5H, OCH_2, $H4'^{Ad}$, $H5'^{Cyt}$), 3.77-3.73 (m, 2H, $H5'^{Ad}$), 2.76-2.74 (m, 2H, CH_2^{CN}), 2.68-2.63 (m, 1H, $H2'a^{Cyt}$), 2.37-2.28 (m, 1H, $H2'b^{Cyt}$), 2.18 (s, 3H, Me^{Ac}), 0.97 (s, 9H, *t*Bu^{TBS}), 0.21 (s, 3H, Me^{TBS}), 0.20 (s, 3H, Me^{TBS}).

^{13}C NMR (63 MHz, $CDCl_3$) δ 170.7 ($C=O^{Ac}$), 162.6 ($C=O^{Bz}$), 155.5 ($C2^{Ad}$ or $C8^{Ad}$), 152.7 ($C=O^{Cyt}$) 145.3 ($C6^{Cyt}$), 142.5, ($C2^{Ad}$ or $C8^{Ad}$), 133.0, 128.9, 128.3 (5 x CH^{Bz}), 116.5 (CN) , 96.8 ($C5^{Cyt}$), 87.8 ($C1'^{Ad}$), 87.3 ($C1'^{Cyt}$), 77.5 ($C3'^{Cyt}$), 71.9 ($C3'^{Ad}$), 62.7 ($C2'^{Ad}$), 62.7 (OCH_2) 61.5 ($C5'^{Cyt}$), 61.3 ($C5'^{Ad}$), 39.7 ($C2'^{Cyt}$), 25.8 (*t*Bu^{TBS}), 25.0 ($CH_3{}^{Ac}$), 18.5 (CH_2^{CN}), 18.1 (Cq^{TBS}), -4.5, -4.8 (2 x Me^{TBS}).

Fonvielle, M. *et al.*. (2013). Efficient Access to Peptidyl-RNA Conjugates for Picomolar Inhibition of Non-ribosomal FemXWv Aminoacyl Transferase.*Chemistry–A European Journal*, *19*(4), 1357-1363.

(63) ((2R,3S,5R)-5-(4-amino-2-oxopyrimidin-1(2H)-yl)-3-(((((2R,3S,4R,5R)-5-(6-amino-9H-purin-9-yl)-4-azido-3-((tert-butyldimethylsilyl)oxy)tetrahydrofuran-2-yl)methoxy)(hydroxy)phosphoryl)oxy)tetrahydrofuran-2-yl)methyl dihydrogen phosphate

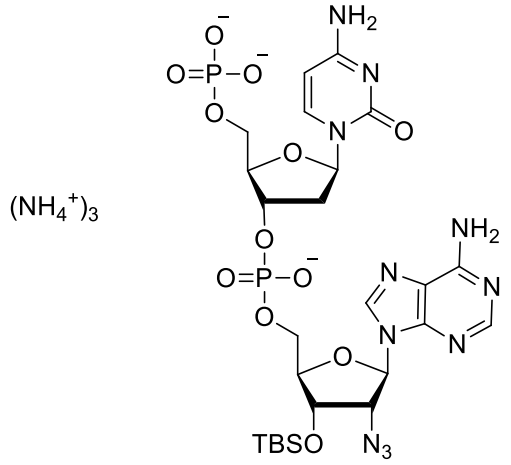

$(NH_4^+)_3$

Chemical Formula: $C_{25}H_{48}N_{14}O_{12}P_2Si$
Molecular Weight: 826,7682

63

To a solution of **62** (115 mg, 130 µmol) in acetonitrile (400 µL), Bis(2-cyanoethyl)diisopropylphosphoramidite (88 mg, 320 µmol) was added. Tetrazole in a 0.45 M solution in MeCN (2.8 mL, 1.3 mmol) was then added. The reaction mixture was stirred at rt for 3 h. Iodine in a 0.1 M solution in a 75/2/20 THF/water/pyridine mixture (3.2 mL, 320 µmol) was added. The reaction mixture was stirred at rt for 1 h and partitioned between AcOEt and an aqueous solution of hydrogenocarbonate. The phases were separated, and the aqueous layer was extracted twice with AcOEt. The combined organic layers were dried over sodium sulfate and concentrated. Aqueous 5 M $MeNH_2$ (15 mL) was added on the residue. The reaction mixture was stirred at rt overnight and concentrated. **63 w**as purified by HPLC, lyophilized, and recovered as a white solid (35 mg, 33 %).

^{1}H NMR (500 MHz, D_2O) δ 8.47 (s, 1H, $H2^{Ad}$ or $H8^{Ad}$), 8.30 (s, 1H, $H2^{Ad}$ or $H8^{Ad}$), 7.86 (d, *J* = 7.7 Hz, 1H, $H6^{Cyt}$), 6.19 (d, *J* = 4.8 Hz, 1H, $H5^{Cyt}$), 6.13-6.06 (m, 2H, $H1'^{Ad}$, $H1'^{Cyt}$), 4.97 (t, *J* = 5.5 Hz, 1H, $H3'^{Ad}$), 4.89-4.84 (m, 1H, $H3'^{Cyt}$), 4.34-4.28 (m, 2H, H4'Ad, $H4'^{Cyt}$), 4.24-4.10 (m, 2H, $H5'^{Ad}$), 4.05-4.01 (m, 2H, $H5'^{Cyt}$), 2.42 (ddd, *J* = 2.7, 5.4, 7.9 Hz, 1H, $H2'^{Cyt}$), 1.93-1.85 (m, 1H, $H2'^{Cyt}$), 1.00 (s, 9H, $t\text{Bu}^{TBS}$), 0.28 (s, 3H, Me^{TBS}), 0.27 (s, 3H, Me^{TBS}).

^{13}C NMR (101 MHz, D_2O) δ 155.4 ($C{=}O^{Cyt}$), 155.0 ($C2^{Ad}$ or $C8^{Ad}$), 152.5 ($C2^{Ad}$ or $C8^{Ad}$), 141.8 ($C6^{Cyt}$), 139.7 (Cq), 96.0 ($C1'^{Cyt}$), 85.7 ($C1'^{Ad}$), 85.5 ($C5^{Cyt}$), 84.7 ($C4'^{Cyt}$), 84.6 ($C4'^{Ad}$), 83.5 ($C3'^{Ad}$), 70.4 ($C2'^{Ad}$), 64.9 ($C3'^{Cyt}$), 64.5 ($C5'^{Cyt}$), 64.2 ($C5'^{Ad}$), 38.1 ($C2'^{Cyt}$).

Fonvielle, M. *et al.*. (2013). Efficient Access to Peptidyl-RNA Conjugates for Picomolar Inhibition of Non-ribosomal FemXWv Aminoacyl Transferase.*Chemistry–A European Journal*, *19*(4), 1357-1363.

(64) ((2R,3S,5R)-5-(4-amino-2-oxopyrimidin-1(2H)-yl)-3-(((((2R,3S,4R,5R)-5-(6-amino-9H-purin-9-yl)-4-azido-3-hydroxytetrahydrofuran-2-yl)methoxy)(hydroxy)phosphoryl)oxy)tetrahydrofuran-2-yl)methyl dihydrogen phosphate

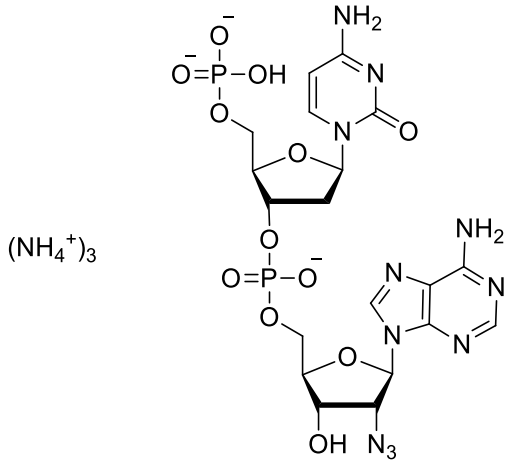

$(NH_4^+)_3$

Chemical Formula: $C_{19}H_{35}N_{14}O_{12}P_2$
Molecular Weight: 713,5153

64

A 1/2/1mixture of a 6 M aqueous HCl solution/THF/MeOH was added on **63** (34 mg, 44 µmol). The reaction mixture was stirred at rt overnight and concentrated. 64 was purified by HPLC, lyophilized and recovered as a white solid (14 mg, 44 %).

^{1}H NMR (400 MHz, D_2O) δ 8.49 (s, 1H, $H2^{Ad}$ or $H8^{Ad}$), 8.25 (s, 1H, $H2^{Ad}$ or $H8^{Ad}$), 7.81 (d, *J* = 7.7 Hz, 1H, $H6^{Ad}$), 6.13-6.10 (m, 2H, $H5^{Cyt}$, $H1'^{Ad}$), 6.08 (d, *J* = 8.0 Hz, 1H, $H1'^{Cyt}$), 4.87-4.84 (m, 2H, $H2'^{Ad}$, $H3'^{Cyt}$), 4.76-4.74 (m, 1H, $H4'^{Cyt}$), 4.38-4.34 (m, 1H, $H3'^{Ad}$), 4.31-4.27 (m, 1H, $H4'^{Ad}$), 4.22-4.12 (m, 2H, $H5'^{Ad}$), 4.02 (dd, *J* = 2.6, 4.6 Hz, 2H, $H5'^{Cyt}$), 2.40 (ddd, *J* = 1.9, 5.7, 7.7 Hz, 1H, $H2'a^{Cyt}$), 1.92-1.85 (m, 1H, $H2'b^{Cyt}$).

^{13}C NMR (101 MHz, D_2O) δ 155.4 ($C=O^{Cyt}$), 155.0 ($C2^{Ad}$or $C8^{Ad}$), 152.5 ($C2^{Ad}$or $C8^{Ad}$), 141.8 ($C6^{Cyt}$), 139.7(Cq), 96.0 ($C1'^{Cyt}$), 85.7 ($C1'^{Ad}$), 85.5 ($C5^{Cyt}$), 84.7 ($C4'^{Cyt}$), 84.6 ($C4'^{Ad}$), 83.5 ($C3'^{Ad}$), 70.4 ($C2'^{Ad}$), 64.9 ($C3'^{Cyt}$), 64.5 ($C5'^{Cyt}$), 64.2 ($C5'^{Ad}$), 38.1 ($C2'^{Cyt}$).

^{31}P NMR (^{1}H decoupled, 162 MHz, D_2O) δ 0.19, -1.12 (2s).

Fonvielle, M. *et al.*. (2013). Efficient Access to Peptidyl-RNA Conjugates for Picomolar Inhibition of Non-ribosomal FemXWv Aminoacyl Transferase.*Chemistry–A European Journal*, *19*(4), 1357-1363.

(65) ((2R,3S,5R)-5-(4-amino-2-oxopyrimidin-1(2H)-yl)-3-(((((2R,3S,4R,5R)-5-(6-amino-9H-purin-9-yl)-4-(4-(hept-6-yn-1-yl)-1H-1,2,3-triazol-1-yl)-3-hydroxytetrahydrofuran-2-yl)methoxy)(hydroxy)phosphoryl)oxy)tetrahydrofuran-2-yl)methyl dihydrogen phosphate

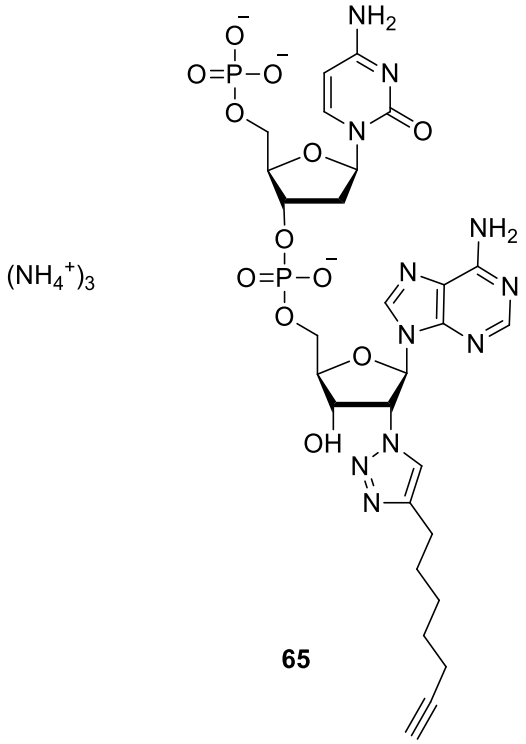

$(NH_4^+)_3$

65

Chemical Formula: $C_{28}H_{46}N_{14}O_{12}P_2$
Molecular Weight: 832,6990

To a solution of **64** (5 mg, 7.6 µmol) in a 1/1 DMF/, copper(II) sulfate pentahydrate (0.94 mg, 3.8 µmol), sodium ascorbate (7.5 mg, 38 µmol) and THPTA (12 mg, 26 µmol) were added. Nonadiyne (0.9 mg, 7.5 µmol) was added, the reaction mixture was stirred at 30 °C for one day and was then concentrated. HPLC purification of the residue yielded **65** (1.7 mg, 29 %) as a white solid.

^{1}H NMR (600 MHz, D_2O) δ 8.55 (s, 1H, $H2^{Ad}$or $H8^{Ad}$), 8.17 (s, 1H, $H2^{Ad}$ or $H8^{Ad}$), 7.96 (s, 1H, $H^{triazole}$), 7.92 (d, J = 7.7 Hz, 1H, $H6^{Cyt}$), 6.86 (d, J = 6.7 Hz, 1H, $H1'^{Ad}$), 6.17-6.08 (m, 2H, $H1'^{Cyt}$, $H5^{Cyt}$), 5.95-5.90 (m, 1H, $H2'^{Ad}$), 5.00-4.86 (m, 2H, $H3'^{Ad}$, $H3'^{Cyt}$), 4.59-4.51 (m, 1H, $H4'^{Ad}$), 4.37-4.31 (m, 1H, $H4'^{Cyt}$), 4.29-4,.19 (m, 1H, $H5'a^{Ad}$), 4.15-4.08 (m, 1H, $H5'b^{Ad}$), 4.07-3.99 (m, 2H, $H5'^{Cyt}$), 3.23-3.15 (m, 1H, H^{alkyne}), 2.67-2.57 (m, 2H, CH2), 2.55-2.48 (m, 1H, $H2'a^{Cyt}$), 2.19-2.12 (m, 1H, $H3'^{Cyt}$), 2.09-2.06 (m, 2H, CH2), 2.04-1.97 (m, 1H, $H2'b^{Cyt}$), 1.56-1.49 (m, 2H, CH_2), 1.36-1.29 (m, 2H, CH_2), 1.26-1.15 (m, 2H, CH_2).

^{13}C NMR (151 MHz, D_2O) δ 179.8 ($C=O^{Cyt}$), 161.6 (Cq^{Ad}), 159.7 (Cq^{Cyt}), 154.5 ($C2^{Ad}$or $C8^{Ad}$), 151.7 (Cq^{Ad}), 148.8 ($Cq^{triazole}$), 142.9 ($C6^{Cyt}$), 124.0 ($C^{triazole}$), 95.7 ($C5^{Cyt}$), 86.1 ($C1'^{Cyt}$), 84.7 ($C1'^{Ad}$), 84.2 (Cq^{alkyne}), 82.9 ($C4'^{Cyt}$), 81.7 ($C4'^{Ad}$), 76.2 ($C3'^{Cyt}$), 69.8 ($C3'^{Ad}$), 68.9 ($C2'^{Ad}$), 65.2 ($C5'^{Cyt}$), 64.6 ($C5'^{Ad}$), 38.4 ($C2'^{Cyt}$), 27.7, 27.1, 26.9, 24.2, 17.3 (5 x CH_2).

HRMS: (ESI-) m/z calcd for $C_{28}H_{36}N_{11}O_{12}P_2$[*M - H*]: 780.2026; found: 780.1884.

Bibliography

List of references

(1) Fleming, A. On the antibacterial action of cultures of a penicillium, with special reference to their use in the isolation of B. influenzae. *Br. J. Exp. Pathol.* **1929**, *10* (3), 226.

(2) Brown, E. D.; Wright, G. D. Antibacterial drug discovery in the resistance era. *Nature* **2016**, *529* (7586), 336–343 DOI: 10.1038/nature17042.

(3) D'Costa, V. M.; King, C. E.; Kalan, L.; Morar, M.; Sung, W. W. L.; Schwarz, C.; Froese, D.; Zazula, G.; Calmels, F.; Debruyne, R.; et al. Antibiotic resistance is ancient. *Nature* **2011**, *477* (7365), 457–461 DOI: 10.1038/nature10388.

(4) Macarron, R.; Banks, M. N.; Bojanic, D.; Burns, D. J.; Cirovic, D. A.; Garyantes, T.; Green, D. V.; Hertzberg, R. P.; Janzen, W. P.; Paslay, J. W.; et al. Impact of high-throughput screening in biomedical research. *Nat. Rev. Drug Discov.* **2011**, *10* (3), 188–195.

(5) WHO | Antibiotic resistance http://www.who.int/mediacentre/factsheets/antibiotic-resistance/en/ (accessed May 4, 2016).

(6) Vollmer, W. Structural variation in the glycan strands of bacterial peptidoglycan. *FEMS Microbiol. Rev.* **2008**, *32* (2), 287–306 DOI: 10.1111/j.1574-6976.2007.00088.x.

(7) Silver, L. L. Challenges of Antibacterial Discovery. *Clin. Microbiol. Rev.* **2011**, *24* (1), 71–109 DOI: 10.1128/CMR.00030-10.

(8) Nikolaidis, I.; Favini-Stabile, S.; Dessen, A. Resistance to antibiotics targeted to the bacterial cell wall: The Bacterial Cell Wall as a Target for Antibiotics. *Protein Sci.* **2014**, *23* (3), 243–259 DOI: 10.1002/pro.2414.

(9) Caminero, J. A.; Sotgiu, G.; Zumla, A.; Migliori, G. B. Best drug treatment for multidrug-resistant and extensively drug-resistant tuberculosis. *Lancet Infect. Dis.* **2010**, *10* (9), 621–629.

(10) Chung, B. C.; Zhao, J.; Gillespie, R. A.; Kwon, D.-Y.; Guan, Z.; Hong, J.; Zhou, P.; Lee, S.-Y. Crystal Structure of MraY, an Essential Membrane Enzyme for Bacterial Cell Wall Synthesis. *Science* **2013**, *341* (6149), 1012–1016 DOI: 10.1126/science.1236501.

(11) Bugg, T.; Lloyd, A.; Roper, D. Phospho-MurNAc-Pentapeptide Translocase (MraY) as a Target for Antibacterial Agents and Antibacterial Proteins. *Infect. Disord. - Drug Targets* **2006**, *6* (2), 85–106 DOI: 10.2174/187152606784112128.

(12) Ha, S.; Walker, D.; Shi, Y.; Walker, S. The 1.9 \AA crystal structure of Escherichia coli MurG, a membrane-associated glycosyltransferase involved in peptidoglycan biosynthesis. *Protein Sci.* **2000**, *9* (6), 1045–1052.

(13) Hu, Y.; Chen, L.; Ha, S.; Gross, B.; Falcone, B.; Walker, D.; Mokhtarzadeh, M.; Walker, S. Crystal structure of the MurG: UDP-GlcNAc complex reveals common structural principles of a superfamily of glycosyltransferases. *Proc. Natl. Acad. Sci.* **2003**, *100* (3), 845–849.

(14) Helm, J. S.; Hu, Y.; Chen, L.; Gross, B.; Walker, S. Identification of Active-Site Inhibitors of MurG Using a Generalizable, High-Throughput Glycosyltransferase Screen. *J. Am. Chem. Soc.* **2003**, *125* (37), 11168–11169 DOI: 10.1021/ja036494s.

(15) Hu, Y.; Helm, J. S.; Chen, L.; Ginsberg, C.; Gross, B.; Kraybill, B.; Tiyanont, K.; Fang, X.; Wu, T.; Walker, S. Identification of selective inhibitors for the glycosyltransferase MurG via high-throughput screening. *Chem. Biol.* **2004**, *11* (5), 703–711.

(16) Mohammadi, T.; van Dam, V.; Sijbrandi, R.; Vernet, T.; Zapun, A.; Bouhss, A.; Diepeveen-de Bruin, M.; Nguyen-Distèche, M.; de Kruijff, B.; Breukink, E. Identification of FtsW as a transporter of lipid-linked cell wall precursors across the membrane. *EMBO J.* **2011**, *30* (8), 1425–1432.

(17) Berger-Bächi, B. Insertional inactivation of staphylococcal methicillin resistance by Tn551. *J. Bacteriol.* **1983**, *154* (1), 479–487.

(18) BÄCHI-BERGER, B. Genetics of methicillin resistance in Staphylococeus aureus. *J. Antimicrob. Chemother.* **1989**, *23* (5), 671–672.

(19) Berger-Bächi, B.; Strässle, A.; Gustafson, J. E.; Kayser, F. H. Mapping and characterization of multiple chromosomal factors involved in methicillin resistance in Staphylococcus aureus. *Antimicrob. Agents Chemother.* **1992**, *36* (7), 1367–1373.

(20) Ling, B.; Berger-Bächi, B. Increased Overall Antibiotic Susceptibility in Staphylococcus aureus femAB Null Mutants. *Antimicrob. Agents Chemother.* **1998**, *42* (4), 936–938.

(21) Hegde, S. S.; Shrader, T. E. FemABX Family Members Are Novel Nonribosomal Peptidyltransferases and Important Pathogen-specific Drug Targets. *J. Biol. Chem.* **2001**, *276* (10), 6998–7003 DOI: 10.1074/jbc.M008591200.

(22) Rohrer, S.; Berger-Bachi, B. FemABX Peptidyl Transferases: a Link between Branched-Chain Cell Wall Peptide Formation and -Lactam Resistance in Gram-Positive Cocci. *Antimicrob. Agents Chemother.* **2003**, *47* (3), 837–846 DOI: 10.1128/AAC.47.3.837-846.2003.

(23) Giannouli, S.; Kyritsis, A.; Malissovas, N.; Becker, H. D.; Stathopoulos, C. On the role of an unusual tRNAGly isoacceptor in Staphylococcus aureus. *Biochimie* **2009**, *91* (3), 344–351 DOI: 10.1016/j.biochi.2008.10.009.

(24) Biarrotte-Sorin, S.; Maillard, A. P.; Delettré, J.; Sougakoff, W.; Arthur, M.; Mayer, C. Crystal Structures of Weissella viridescens FemX and Its Complex with UDP-MurNAc-Pentapeptide: Insights into FemABX Family Substrates Recognition. *Structure* **2004**, *12* (2), 257–267 DOI: 10.1016/j.str.2004.01.006.

(25) Benson, T. E.; Prince, D. B.; Mutchler, V. T.; Curry, K. A.; Ho, A. M.; Sarver, R. W.; Hagadorn, J. C.; Choi, G. H.; Garlick, R. L. X-ray crystal structure of Staphylococcus aureus FemA. *Structure* **2002**, *10* (8), 1107–1115.

(26) Villet, R.; Fonvielle, M.; Busca, P.; Chemama, M.; Maillard, A. P.; Hugonnet, J.-E.; Dubost, L.; Marie, A.; Josseaume, N.; Mesnage, S.; et al. Idiosyncratic features in tRNAs participating in bacterial cell wall synthesis. *Nucleic Acids Res.* **2007**, *35* (20), 6870–6883 DOI: 10.1093/nar/gkm778.

(27) Fonvielle, M.; Chemama, M.; Villet, R.; Lecerf, M.; Bouhss, A.; Valéry, J.-M.; Ethève-Quelquejeu, M.; Arthur, M. Aminoacyl-tRNA recognition by the FemXWv transferase for bacterial cell wall synthesis. *Nucleic Acids Res.* **2009**, *37* (5), 1589–1601 DOI: 10.1093/nar/gkn1039.

(28) Schmeing, T. M.; Voorhees, R. M.; Kelley, A. C.; Gao, Y.-G.; Murphy, F. V.; Weir, J. R.; Ramakrishnan, V. The Crystal Structure of the Ribosome Bound to EF-Tu and Aminoacyl-tRNA. *Science* **2009**, *326* (5953), 688–694 DOI: 10.1126/science.1179700.

(29) Fonvielle, M.; Chemama, M.; Lecerf, M.; Villet, R.; Busca, P.; Bouhss, A.; Ethève-Quelquejeu, M.; Arthur, M. Decoding the Logic of the tRNA Regiospecificity of Nonribosomal FemXWv Aminoacyl Transferase. *Angew. Chem. Int. Ed.* **2010**, *49* (30), 5115–5119 DOI: 10.1002/anie.201001473.

(30) Fonvielle, M.; Li de La Sierra-Gallay, I.; El-Sagheer, A. H.; Lecerf, M.; Patin, D.; Mellal, D.; Mayer, C.; Blanot, D.; Gale, N.; Brown, T.; et al. The Structure of FemXWv in Complex with a Peptidyl-RNA Conjugate: Mechanism of Aminoacyl Transfer from Ala-tRNAAla to Peptidoglycan Precursors. *Angew. Chem. Int. Ed.* **2013**, *52* (28), 7278–7281 DOI: 10.1002/anie.201301411.

(31) Berger-Bächi, B.; Tschierske, M. Role of fem factors in methicillin resistance. *Drug Resist. Updat.* **1998**, *1* (5), 325–335 DOI: 10.1016/S1368-7646(98)80048-4.

(32) Stranden, A. M.; Ehlert, K.; Labischinski, H.; Berger-Bächi, B. Cell wall monoglycine cross-bridges and methicillin hypersusceptibility in a femAB null mutant of methicillin-resistant Staphylococcus aureus. *J. Bacteriol.* **1997**, *179* (1), 9–16.

(33) Stapleton, P. D.; Taylor, P. W. Methicillin resistance in Staphylococcus aureus: mechanisms and modulation. *Sci. Prog.* **2002**, *85* (1), 57–72.

(34) Ton-That, H.; Faull, K. F.; Schneewind, O. Anchor Structure of Staphylococcal Surface Proteins A BRANCHED PEPTIDE THAT LINKS THE CARBOXYL TERMINUS OF PROTEINS TO THE CELL WALL. *J. Biol. Chem.* **1997**, *272* (35), 22285–22292.

(35) Meister, G. *RNA Biology*.

(36) Machnicka, M. A.; Milanowska, K.; Osman Oglou, O.; Purta, E.; Kurkowska, M.; Olchowik, A.; Januszewski, W.; Kalinowski, S.; Dunin-Horkawicz, S.; Rother, K. M.; et al. MODOMICS: a database of RNA modification pathways--2013 update. *Nucleic Acids Res.* **2013**, *41* (D1), D262–D267 DOI: 10.1093/nar/gks1007.

(37) El Yacoubi, B.; Bailly, M.; de Crécy-Lagard, V. Biosynthesis and Function of Posttranscriptional Modifications of Transfer RNAs. *Annu. Rev. Genet.* **2012**, *46* (1), 69–95 DOI: 10.1146/annurev-genet-110711-155641.

(38) Gustilo, E. M.; Vendeix, F. A.; Agris, P. F. tRNA's modifications bring order to gene expression. *Curr. Opin. Microbiol.* **2008**, *11* (2), 134–140 DOI: 10.1016/j.mib.2008.02.003.

(39) Durdevic, Z.; Schaefer, M. tRNA modifications: Necessary for correct tRNA-derived fragments during the recovery from stress? *BioEssays* **2013**, *35* (4), 323–327 DOI: 10.1002/bies.201200158.

(40) Kirchner, S.; Ignatova, Z. Emerging roles of tRNA in adaptive translation, signalling dynamics and disease. *Nat. Rev. Genet.* **2014**, *16* (2), 98–112 DOI: 10.1038/nrg3861.

(41) Haeusler, R. A.; Engelke, D. R. Spatial organization of transcription by RNA polymerase III. *Nucleic Acids Res.* **2006**, *34* (17), 4826–4836 DOI: 10.1093/nar/gkl656.

(42) Thompson, M.; Haeusler, R. A.; Good, P. D.; Engelke, D. R. Nucleolar clustering of dispersed tRNA genes. *Science* **2003**, *302* (5649), 1399–1401.

(43) Marquez, S. M.; Chen, J. L.; Evans, D.; Pace, N. R. Structure and Function of Eukaryotic Ribonuclease P RNA. *Mol. Cell* **2006**, *24* (3), 445–456 DOI: 10.1016/j.molcel.2006.09.011.

(44) Torres-Larios, A.; Swinger, K. K.; Krasilnikov, A. S.; Pan, T.; Mondragón, A. Crystal structure of the RNA component of bacterial ribonuclease P. *Coord. Struct. Factors Have Been Deposited Protein Data Bank Access. Code 2A2ENature* **2005**, *437* (7058), 584–587 DOI: 10.1038/nature04074.

(45) Xiong, Y.; Steitz, T. A story with a good ending: tRNA 3'-end maturation by CCA-adding enzymes. *Curr. Opin. Struct. Biol.* **2006**, *16* (1), 12–17 DOI: 10.1016/j.sbi.2005.12.001.

(46) Vogel, A.; Schilling, O.; Späth, B.; Marchfelder, A. The tRNase Z family of proteins: physiological functions, substrate specificity and structural properties. *Biol. Chem.* **2005**, *386* (12) DOI: 10.1515/BC.2005.142.

(47) Köhler, A.; Hurt, E. Exporting RNA from the nucleus to the cytoplasm. *Nat. Rev. Mol. Cell Biol.* **2007**, *8* (10), 761–773 DOI: 10.1038/nrm2255.

(48) Chernyakov, I.; Whipple, J. M.; Kotelawala, L.; Grayhack, E. J.; Phizicky, E. M. Degradation of several hypomodified mature tRNA species in Saccharomyces cerevisiae is mediated by Met22 and the 5'-3' exonucleases Rat1 and Xrn1. *Genes Dev.* **2008**, *22* (10), 1369–1380 DOI: 10.1101/gad.1654308.

(49) Thompson, D. M.; Parker, R. Stressing Out over tRNA Cleavage. *Cell* **2009**, *138* (2), 215–219 DOI: 10.1016/j.cell.2009.07.001.

(50) Whitney, M. L.; Hurto, R. L.; Shaheen, H. H.; Hopper, A. K. Rapid and reversible nuclear accumulation of cytoplasmic tRNA in response to nutrient availability. *Mol. Biol. Cell* **2007**, *18* (7), 2678–2686.

(51) Murguía, J. R.; Serrano, R. New functions of protein kinase Gcn2 in yeast and mammals. *IUBMB Life* **2012**, *64* (12), 971–974 DOI: 10.1002/iub.1090.

(52) Qiu, H.; Hu, C.; Anderson, J.; Björk, G. R.; Sarkar, S.; Hopper, A. K.; Hinnebusch, A. G. Defects in tRNA Processing and Nuclear Export InduceGCN4 Translation Independently of Phosphorylation of the α Subunit of Eukaryotic Translation Initiation Factor 2. *Mol. Cell. Biol.* **2000**, *20* (7), 2505–2516.

(53) Sheppard, K.; Yuan, J.; Hohn, M. J.; Jester, B.; Devine, K. M.; Soll, D. From one amino acid to another: tRNA-dependent amino acid biosynthesis. *Nucleic Acids Res.* **2008**, *36* (6), 1813–1825 DOI: 10.1093/nar/gkn015.

(54) Yuan, J.; Hohn, M. J.; Sherrer, R. L.; Palioura, S.; Su, D.; Söll, D. A tRNA-dependent cysteine biosynthesis enzyme recognizes the selenocysteine-specific tRNA in *Escherichia coli*. *FEBS Lett.* **2010**, *584* (13), 2857–2861 DOI: 10.1016/j.febslet.2010.05.028.

(55) Giegé, R.; Florentz, C.; Kern, D.; Gangloff, J.; Eriani, G.; Moras, D. Aspartate identity of transfer RNAs. *Biochimie* **1996**, *78* (7), 605–623 DOI: 10.1016/S0300-9084(96)80007-1.

(56) Giegé, R.; Sissler, M.; Florentz, C. Universal rules and idiosyncratic features in tRNA identity. *Nucleic Acids Res.* **1998**, *26* (22), 5017–5035 DOI: 10.1093/nar/26.22.5017.

(57) McClain, W. H. Rules that Govern tRNA Identity in Protein Synthesis. *J. Mol. Biol.* **1993**, *234* (2), 257–280 DOI: 10.1006/jmbi.1993.1582.

(58) Giegé, R.; Frugier, M.; Rudinger, J. tRNA mimics. *Curr. Opin. Struct. Biol.* **1998**, *8* (3), 286–293 DOI: 10.1016/S0959-440X(98)80060-2.

(59) Francklyn, C.; Schimmel, P. Aminoacylation of RNA minihelices with alanine. *Nature* **1989**, *337* (6206), 478–481 DOI: 10.1038/337478a0.

(60) Francklyn, C.; Schimmel, P. Enzymatic aminoacylation of an eight-base-pair microhelix with histidine. *Proc. Natl. Acad. Sci.* **1990**, *87* (21), 8655–8659 DOI: 10.1073/pnas.87.21.8655.

(61) Francklyn, C.; Shi, J. P.; Schimmel, P. Overlapping nucleotide determinants for specific aminoacylation of RNA microhelices. *Science* **1992**, *255* (5048), 1121–1125.

(62) Sampson, J. R.; Saks, M. E. Contributions of discrete tRNASer domains to aminoacylation by E.coli seryl-tRNA synthetase: a kinetic analysis using model RNA substrates. *Nucleic Acids Res.* **1993**, *21* (19), 4467–4475 DOI: 10.1093/nar/21.19.4467.

(63) Frugier, M.; Florentz, C.; Giegé, R. Efficient aminoacylation of resected RNA helices by class II aspartyl-tRNA synthetase dependent on a single nucleotide. *EMBO J.* **1994**, *13* (9), 2218–2226.

(64) Martinis, S. A.; Schimmel, P. Enzymatic aminoacylation of sequence-specific RNA minihelices and hybrid duplexes with methionine. *Proc. Natl. Acad. Sci.* **1992**, *89* (1), 65–69.

(65) Nureki, O.; Niimi, T.; Muramatsu, T.; Kanno, H.; Kohno, T.; Florentz, C.; Giegé, R.; Yokoyama, S. Molecular Recognition of the Identity-determinant Set of Isoleucine Transfer RNA from Escherichia coli. *J. Mol. Biol.* **1994**, *236* (3), 710–724 DOI: 10.1006/jmbi.1994.1184.

(66) Wright, D. J.; Martinis, S. A.; Jahn, M.; Söll, D.; Schimmel, P. Acceptor stem and anticodon RNA hairpin helix interactions with glutamine tRNA synthetase. *Biochimie* **1993**, *75* (12), 1041–1049 DOI: 10.1016/0300-9084(93)90003-B.

(67) Frugier, M.; Florentz, C.; Giegé, R. Anticodon-independent aminoacylation of an RNA minihelix with valine. *Proc. Natl. Acad. Sci.* **1992**, *89* (9), 3990–3994 DOI: 10.1073/pnas.89.9.3990.

(68) Sherlin, L. D.; Bullock, T. L.; Newberry, K. J.; Lipman, R. S. A.; Hou, Y.-M.; Beijer, B.; Sproat, B. S.; Perona, J. J. Influence of transfer RNA tertiary structure on aminoacylation efficiency by glutaminyl and cysteinyl-tRNA synthetases1. *J. Mol. Biol.* **2000**, *299* (2), 431–446 DOI: 10.1006/jmbi.2000.3749.

(69) McClain, W. H.; Foss, K. Changing the acceptor identity of a transfer RNA by altering nucleotides in a “variable pocket.” *Science* **1988**, *241* (4874), 1804–1807 DOI: 10.1126/science.2459773.

(70) Beuning, P. J.; Musier-Forsyth, K. Transfer RNA recognition by aminoacyl-tRNA synthetases. *Biopolymers* **1999**, *52* (1), 1–28 DOI: 10.1002/(SICI)1097-0282(1999)52:1<1::AID-BIP1>3.0.CO;2-W.

(71) Shepherd, J.; Ibba, M. Direction of aminoacylated transfer RNAs into antibiotic synthesis and peptidoglycan-mediated antibiotic resistance. *FEBS Lett.* **2013**, *587* (18), 2895–2904 DOI: 10.1016/j.febslet.2013.07.036.

(72) Jahn, D.; Verkamp, E.; So¨ll, D. Glutamyl-transfer RNA: a precursor of heme and chlorophyll biosynthesis. *Trends Biochem. Sci.* **1992**, *17* (6), 215–218 DOI: 10.1016/0968-0004(92)90380-R.

(73) Roy, H.; Ibba, M. RNA-dependent lipid remodeling by bacterial multiple peptide resistance factors. *Proc. Natl. Acad. Sci.* **2008**, *105* (12), 4667–4672 DOI: 10.1073/pnas.0800006105.

(74) Gondry, M.; Sauguet, L.; Belin, P.; Thai, R.; Amouroux, R.; Tellier, C.; Tuphile, K.; Jacquet, M.; Braud, S.; Courçon, M.; et al. Cyclodipeptide synthases are a family of tRNA-dependent peptide bond–forming enzymes. *Nat. Chem. Biol.* **2009**, *5* (6), 414–420 DOI: 10.1038/nchembio.175.

(75) Vetting, M. W.; Hegde, S. S.; Blanchard, J. S. The structure and mechanism of the Mycobacterium tuberculosis cyclodityrosine synthetase. *Nat. Chem. Biol.* **2010**, *6* (11), 797–799 DOI: 10.1038/nchembio.440.

(76) Bonnefond, L.; Arai, T.; Sakaguchi, Y.; Suzuki, T.; Ishitani, R.; Nureki, O. Structural basis for nonribosomal peptide synthesis by an aminoacyl-tRNA synthetase paralog. *Proc. Natl. Acad. Sci.* **2011**, *108* (10), 3912–3917 DOI: 10.1073/pnas.1019480108.

(77) Zhang, W.; Ntai, I.; Kelleher, N. L.; Walsh, C. T. tRNA-dependent peptide bond formation by the transferase PacB in biosynthesis of the pacidamycin group of pentapeptidyl nucleoside antibiotics. *Proc. Natl. Acad. Sci.* **2011**, *108* (30), 12249–12253 DOI: 10.1073/pnas.1109539108.

(78) Leibowitz, M. J.; Soffer, R. L. Enzymatic Modification of Proteins III. PURIFICATION AND PROPERTIES OF A LEUCYL, PHENYLALANYL TRANSFER RIBONUCLEIC ACID-PROTEIN TRANSFERASE FROM ESCHERICHIA COLI. *J. Biol. Chem.* **1970**, *245* (8), 2066–2073.

(79) Watanabe, K.; Toh, Y.; Suto, K.; Shimizu, Y.; Oka, N.; Wada, T.; Tomita, K. Protein-based peptide-bond formation by aminoacyl-tRNA protein transferase. *Nature* **2007**, *449* (7164), 867–871 DOI: 10.1038/nature06167.

(80) Varshavsky, A. The N-end rule: functions, mysteries, uses. *Proc. Natl. Acad. Sci.* **1996**, *93* (22), 12142–12149.

(81) Khorana, H. G. Nucleic acid synthesis. *Pure Appl. Chem.* **1968**, *17* (3–4) DOI: 10.1351/pac196817030349.

(82) Khorana, H. G. Synthesis in the study of nucleic acids. The Fourth Jubilee Lecture. *Biochem. J.* **1968**, *109* (5), 709–725 DOI: 10.1042/bj1090709c.

(83) Michelson, A. M.; Todd, A. R. Nucleotides part XXXII. Synthesis of a dithymidine dinucleotide containing a 3': 5'-internucleotidic linkage. *J. Chem. Soc. Resumed* **1955**, No. 0, 2632–2638 DOI: 10.1039/JR9550002632.

(84) Agarwal, K. L.; Yamazaki, A.; Cashion, P. J.; Khorana, H. G. Chemical Synthesis of Polynucleotides. *Angew. Chem. Int. Ed. Engl.* **1972**, *11* (6), 451–459 DOI: 10.1002/anie.197204511.

(85) Letsinger, R. L.; Mahadevan, V. Stepwise Synthesis of Oligodeoxyribonucleotides on an Insoluble Polymer Support1, 2. *J. Am. Chem. Soc.* **1966**, *88* (22), 5319–5324.

(86) Amarnath, V.; Broom, A. D. Chemical synthesis of oligonucleotides. *Chem. Rev.* **1977**, *77* (2), 183–217 DOI: 10.1021/cr60306a002.

(87) Sonveaux, E. The organic chemistry underlying DNA synthesis. *Bioorganic Chem.* **1986**, *14* (3), 274–325 DOI: 10.1016/0045-2068(86)90038-6.

(88) Narang, S. A. DNA synthesis. *Tetrahedron* **1983**, *39* (1), 3–22 DOI: 10.1016/S0040-4020(01)97623-9.

(89) Letsinger, R. L.; Finnan, J. L.; Heavner, G. A.; Lunsford, W. B. Nucleotide chemistry. XX. Phosphite coupling procedure for generating internucleotide links. *J. Am. Chem. Soc.* **1975**, *97* (11), 3278–3279.

(90) Letsinger, R. L.; Lunsford, W. B. Synthesis of thymidine oligonucleotides by phosphite triester intermediates. *J. Am. Chem. Soc.* **1976**, *98* (12), 3655–3661.

(91) Efcavitch, J. W.; Heiner, C. Depurination As a Yield Decreasing Mechanism in Oligodeoxynucleotide Synthesis. *Nucleosides Nucleotides* **1985**, *4* (1–2), 267–267 DOI: 10.1080/07328318508077883.

(92) Matteucci, M. D.; Caruthers, M. H. Synthesis of deoxyoligonucleotides on a polymer support. *J. Am. Chem. Soc.* **1981**, *103* (11), 3185–3191 DOI: 10.1021/ja00401a041.

(93) Adams, S. P.; Kavka, K. S.; Wykes, E. J.; Holder, S. B.; Galluppi, G. R. Hindered dialkylamino nucleoside phosphite reagents in the synthesis of two DNA 51-mers. *J. Am. Chem. Soc.* **1983**, *105* (3), 661–663.

(94) Beaucage, S. L.; Caruthers, M. H. Deoxynucleoside phosphoramidites—A new class of key intermediates for deoxypolynucleotide synthesis. *Tetrahedron Lett.* **1981**, *22* (20), 1859–1862 DOI: 10.1016/S0040-4039(01)90461-7.

(95) McBride, L. J.; Caruthers, M. H. An investigation of several deoxynucleoside phosphoramidites useful for synthesizing deoxyoligonucleotides. *Tetrahedron Lett.* **1983**, *24* (3), 245–248 DOI: 10.1016/S0040-4039(00)81376-3.

(96) Caruthers, M. H. Gene synthesis machines: DNA chemistry and its uses. *Science* **1985**, *230* (4723), 281–285 DOI: 10.1126/science.3863253.

(97) Caruthers, M. H. Chemical synthesis of DNA. *J. Chem. Educ.* **1989**, *66* (7), 577 DOI: 10.1021/ed066p577.

(98) Reese, C. B. The Chemical Synthesis of Oligo- and Poly-ribonucleotides. In *Nucleic Acids and Molecular Biology*; Eckstein, P. D. F., Lilley, D. D. M. J., Eds.; Nucleic Acids and Molecular Biology; Springer Berlin Heidelberg, 1989; pp 164–181.

(99) *Chemistry of organo-hybrids: synthesis and characterization of functional nano-objects*; Charleux, B., Copéret, C., Lacóte, E., Eds.; Wiley: Hoboken, New Jersey, 2015.

(100) Malakhov, A. D.; Malakhova, E. V.; Kuznitsova, S. V.; Grechishnikova, I. V.; Prokhorenko, I. A.; Skorobogatyi, M. V.; Korshun, V. A.; Berlin, Y. A. Synthesis and fluorescent properties of 5-(1-pyrenylethynyl)-2'-deoxyuridine-containing oligodeoxynucleotides. *Russ. J. Bioorganic Chem.* **2000**, *26* (1), 34–44.

(101) Ban, N.; Nissen, P.; Hansen, J.; Moore, P. B.; Steitz, T. A. The Complete Atomic Structure of the Large Ribosomal Subunit at 2.4 Å Resolution. *Science* **2000**, *289* (5481), 905–920 DOI: 10.1126/science.289.5481.905.

(102) Zhang, B.; Zhang, L.; Sun, L.; Cui, Z. Synthesis of pCpCpA-3'- *NH* -Phenylalanine as a Ribosomal Substrate. *Org. Lett.* **2002**, *4* (21), 3615–3618 DOI: 10.1021/ol026560f.

(103) Zhong, M.; Strobel, S. A. Synthesis of the Ribosomal P-Site Substrate CCA-pcb. *Org. Lett.* **2006**, *8* (1), 55–58 DOI: 10.1021/ol052484f.

(104) Huang, K. S.; Carrasco, N.; Pfund, E.; Strobel, S. A. Transition State Chirality and Role of the Vicinal Hydroxyl in the Ribosomal Peptidyl Transferase Reaction †. *Biochemistry (Mosc.)* **2008**, *47* (34), 8822–8827 DOI: 10.1021/bi800299u.

(105) Schmeing, T. M.; Huang, K. S.; Kitchen, D. E.; Strobel, S. A.; Steitz, T. A. Structural Insights into the Roles of Water and the 2' Hydroxyl of the P Site tRNA in the Peptidyl Transferase Reaction. *Mol. Cell* **2005**, *20* (3), 437–448 DOI: 10.1016/j.molcel.2005.09.006.

(106) Huang, K. S.; Weinger, J. S.; Butler, E. B.; Strobel, S. A. Regiospecificity of the Peptidyl tRNA Ester within the Ribosomal P Site. *J. Am. Chem. Soc.* **2006**, *128* (10), 3108–3109 DOI: 10.1021/ja0554099.

(107) Chapuis, H.; Strazewski, P. Shorter puromycin analog synthesis by means of an efficient Staudinger–Vilarrasa coupling. *Tetrahedron* **2006**, *62* (51), 12108–12115 DOI: 10.1016/j.tet.2006.09.045.

(108) Charafeddine, A.; Dayoub, W.; Chapuis, H.; Strazewski, P. First Synthesis of 2'-Deoxyfluoropuromycin Analogues: Experimental Insight into the Mechanism of the Staudinger Reaction. *Chem. - Eur. J.* **2007**, *13* (19), 5566–5584 DOI: 10.1002/chem.200700058.

(109) Michel, B. Y.; Strazewski, P. Total Syntheses of a Conformationally Locked *North* -Type Methanocarba Puromycin Analogue and a Dinucleotide Derivative. *Chem. - Eur. J.* **2009**, *15* (25), 6244–6257 DOI: 10.1002/chem.200802629.

(110) Roesser, J. R.; Xu, C.; Payne, R. C.; Surratt, C. K.; Hecht, S. M. Preparation of misacylated aminoacyl-tRNAPhe's useful as probes of the ribosomal acceptor site. *Biochemistry (Mosc.)* **1989**, *28* (12), 5185–5195.

(111) Heckler, T. G.; Chang, L. H.; Zama, Y.; Naka, T.; Chorghade, M. S.; Hecht, S. M. T4 RNA ligase mediated preparation of novel" chemically misacylated" tRNAPheS. *Biochemistry (Mosc.)* **1984**, *23* (7), 1468–1473.

(112) Heckler, T. G.; Chang, L. H.; Zama, Y.; Naka, T.; Hecht, S. M. Preparation of "2,("3)-O-Acyl-pCpA derivatives as substrates for T4 RNA ligase-mediated "chemical aminoacylation." *Tetrahedron* **1984**, *40* (1), 87–94 DOI: 10.1016/0040-4020(84)85106-6.

(113) Steger, J.; Graber, D.; Moroder, H.; Geiermann, A.-S.; Aigner, M.; Micura, R. Efficient Access to Nonhydrolyzable Initiator tRNA Based on the Synthesis of 3′-Azido-3′-Deoxyadenosine RNA. *Angew. Chem. Int. Ed.* **2010**, *49* (41), 7470–7472 DOI: 10.1002/anie.201003424.

(114) Steger, J.; Micura, R. Functionalized polystyrene supports for solid-phase synthesis of glycyl-, alanyl-, and isoleucyl-RNA conjugates as hydrolysis-resistant mimics of peptidyl-tRNAs. *Bioorg. Med. Chem.* **2011**, *19* (17), 5167–5174 DOI: 10.1016/j.bmc.2011.07.018.

(115) Neuner, S.; Micura, R. Synthesis of aminoacylated N6,N6-dimethyladenosine solid support for efficient access to hydrolysis-resistant 3′-charged tRNA mimics. *Bioorg. Med. Chem.* **2014**, *22* (24), 6989–6995 DOI: 10.1016/j.bmc.2014.09.054.

(116) Geiermann, A.-S.; Polacek, N.; Micura, R. Native Chemical Ligation of Hydrolysis-Resistant 3′-Peptidyl–tRNA Mimics. *J. Am. Chem. Soc.* **2011**, *133* (47), 19068–19071 DOI: 10.1021/ja209053b.

(117) Geiermann, A.-S.; Micura, R. Selective Desulfurization Significantly Expands Sequence Variety of 3′-Peptidyl–tRNA Mimics Obtained by Native Chemical Ligation. *ChemBioChem* **2012**, *13* (12), 1742–1745 DOI: 10.1002/cbic.201200368.

(118) Graber, D.; Moroder, H.; Steger, J.; Trappl, K.; Polacek, N.; Micura, R. Reliable semi-synthesis of hydrolysis-resistant 3′-peptidyl-tRNA conjugates containing genuine tRNA modifications. *Nucleic Acids Res.* **2010**, *38* (19), 6796–6802 DOI: 10.1093/nar/gkq508.

(119) Rigger, L.; Schmidt, R. L.; Holman, K. M.; Simonović, M.; Micura, R. The Synthesis of Methylated, Phosphorylated, and Phosphonated 3′-Aminoacyl-tRNA ^{Sec} Mimics. *Chem. - Eur. J.* **2013**, *19* (47), 15872–15878 DOI: 10.1002/chem.201302188.

(120) Cressina, E.; Lloyd, A. J.; De Pascale, G.; Roper, D. I.; Dowson, C. G.; Bugg, T. D. H. Adenosine phosphonate inhibitors of lipid II: Alanyl tRNA ligase MurM from Streptococcus pneumoniae. *Bioorg. Med. Chem. Lett.* **2007**, *17* (16), 4654–4656 DOI: 10.1016/j.bmcl.2007.05.071.

(121) Chemama, M.; Fonvielle, M.; Arthur, M.; Valéry, J.-M.; Etheve-Quelquejeu, M. Synthesis of Stable Aminoacyl-tRNA Analogues Containing Triazole as a Bioisoster of Esters. *Chem. – Eur. J.* **2009**, *15* (8), 1929–1938 DOI: 10.1002/chem.200801563.

(122) Chemama, M.; Fonvielle, M.; Villet, R.; Arthur, M.; Valéry, J.-M.; Etheve-Quelquejeu, M. Stable Analogues of Aminoacyl-tRNA for Inhibition of an Essential Step of Bacterial Cell-Wall Synthesis. *J. Am. Chem. Soc.* **2007**, *129* (42), 12642–12643 DOI: 10.1021/ja0749946.

(123) Fonvielle, M.; Mellal, D.; Patin, D.; Lecerf, M.; Blanot, D.; Bouhss, A.; Santarem, M.; Mengin-Lecreulx, D.; Sollogoub, M.; Arthur, M.; et al. Efficient Access to Peptidyl-RNA Conjugates for Picomolar Inhibition of Non-ribosomal FemXWv Aminoacyl Transferase. *Chem. – Eur. J.* **2013**, *19* (4), 1357–1363 DOI: 10.1002/chem.201201999.

(124) Friedmann, E.; Marrian, D. H.; Simon-Reuss, I. Antimitotic Action of Maleimide and Related Substances. *Br. J. Pharmacol. Chemother.* **1949**, *4* (1), 105–108 DOI: 10.1111/j.1476-5381.1949.tb00521.x.

(125) Friedmann, E.; Marrian, D. H.; Simon-Reuss, I. Mitosis of chick fibroblasts in the presence of unsaturated imides and sulphydryl compounds. *Biochim. Biophys. Acta* **1952**, *9*, 61–64 DOI: 10.1016/0006-3002(52)90120-0.

(126) Kajfež, T.; Kamenar, B.; Piližota, V.; Fleš, D. Crystal and Molecular Structures of *N*-Phenylmaleimide and *N*-Phenyl-2,3-dimethylmaleimide. *Croat. Chem. Acta* **2003**, *76* (4), 343–346.

(127) Bodige, S. G.; Méndez-Rojas, M. A.; Watson, W. H. Structure and properties of N-phenylmaleimide derivatives. *J. Chem. Crystallogr. 29* (1), 57–66 DOI: 10.1023/A:1009571214760.

(128) Ishii, Y.; Lehrer, S. S. Effects of the state of the succinimido-ring on the fluorescence and structural properties of pyrene maleimide-labeled alpha alpha-tropomyosin. *Biophys. J.* **1986**, *50* (1), 75–80.

(129) Wu, C.-W.; Yarbrough, L. R.; Wu, F. Y. H. N-(1-Pyrene)maleimide: a fluorescent crosslinking reagent. *Biochemistry (Mosc.)* **1976**, *15* (13), 2863–2868 DOI: 10.1021/bi00658a025.

(130) Smyth, D. G.; Blumenfeld, O. O.; Konigsberg, W. Reactions of N-ethylmaleimide with peptides and amino acids. *Biochem. J.* **1964**, *91* (3), 589–595.

(131) Brown, R. D.; Matthews, K. S. Chemical modification of lactose repressor protein using N-substituted maleimides. *J. Biol. Chem.* **1979**, *254* (12), 5128–5134.

(132) Westheimer, F. H.; Schmidt Jr, D. E. pK of the lysine amino group at the active site of acetoacetate decarboxylase. *Biochemistry (Mosc.)* **1971**, *10* (7), 1249–1253.

(133) Anderson, G. W.; Zimmerman, J. E.; Callahan, F. M. The use of esters of N-hydroxysuccinimide in peptide synthesis. *J. Am. Chem. Soc.* **1964**, *86* (9), 1839–1842.

(134) Lowe, A. The chemistry of isocyanates. *Proc. R. Soc. Med.* **1970**, *63* (4), 367–368.

(135) Koniev, O.; Wagner, A. Developments and recent advancements in the field of endogenous amino acid selective bond forming reactions for bioconjugation. *Chem Soc Rev* **2015**, *44* (15), 5495–5551 DOI: 10.1039/C5CS00048C.

(136) Tuls, J.; Geren, L.; Millett, F. Fluorescein isothiocyanate specifically modifies lysine 338 of cytochrome P-450scc and inhibits adrenodoxin binding. *J. Biol. Chem.* **1989**, *264* (28), 16421–16425.

(137) Burtnick, L. D. Modification of actin with fluorescein isothiocyanate. *Biochim. Biophys. Acta BBA - Protein Struct. Mol. Enzymol.* **1984**, *791* (1), 57–62 DOI: 10.1016/0167-4838(84)90281-4.

(138) MIKI, M. The recovery of the polymerizability of Lys-61-labelled actin by the addition of phalloidin. *Eur. J. Biochem.* **1987**, *164* (1), 229–235.

(139) Miki, M. Interaction of Lys-61 Labeled Actin with Myosin Subfragment-1 and the Regulatory Proteins. *J. Biochem. (Tokyo)* **1989**, *106* (4), 651–655.

(140) Smith, G. P. Kinetics of Amine Modification of Proteins. *Bioconjug. Chem.* **2006**, *17* (2), 501–506 DOI: 10.1021/bc0503061.

(141) Mädler, S.; Bich, C.; Touboul, D.; Zenobi, R. Chemical cross-linking with NHS esters: a systematic study on amino acid reactivities. *J. Mass Spectrom.* **2009**, *44* (5), 694–706 DOI: 10.1002/jms.1544.

(142) Cuatrecasas, P.; Parikh, I. Adsorbents for affinity chromatography. Use of N-hydroxysuccinimide esters of agarose. *Biochemistry (Mosc.)* **1972**, *11* (12), 2291–2299.

(143) Yang, W.-C.; Mirzaei, H.; Liu, X.; Regnier, F. E. Enhancement of Amino Acid Detection and Quantification by Electrospray Ionization Mass Spectrometry. *Anal. Chem.* **2006**, *78* (13), 4702–4708 DOI: 10.1021/ac0600510.

(144) Huang, Y.-L.; Wu, C.-Y. Carbohydrate-based vaccines: challenges and opportunities. *Expert Rev. Vaccines* **2010**, *9* (11), 1257–1274 DOI: 10.1586/erv.10.120.

(145) Lee, R. T.; Lee, Y. C. Preparation and some biochemical properties of neoglycoproteins produced by reductive amination of thioglycosides containing an. omega.-aldehydoaglycon. *Biochemistry (Mosc.)* **1980**, *19* (1), 156–163.

(146) Gray, G. R. The direct coupling of oligosaccharides to proteins and derivatized gels. *Arch. Biochem. Biophys.* **1974**, *163* (1), 426–428.

(147) Bozler, H.; Jany, K. D.; Pfleiderer, G. Synthesis and application of a fluorescent imido ester for specific labelling of amino groups in proteins. *Biochim. Biophys. Acta BBA-Protein Struct. Mol. Enzymol.* **1983**, *749* (3), 238–243.

(148) Dworschack, R.; Tarr, G.; Plapp, B. V. Identification of the lysine residue modified during the activation by acetimidylation of horse liver alcohol dehydrogenase. *Biochemistry (Mosc.)* **1975**, *14* (2), 200–203.

(149) Gavrilyuk, J. I.; Wuellner, U.; Barbas, C. F. β-Lactam-based approach for the chemical programming of aldolase antibody 38C2. *Bioorg. Med. Chem. Lett.* **2009**, *19* (5), 1421–1424 DOI: 10.1016/j.bmcl.2009.01.028.

(150) Gavrilyuk, J. I.; Wuellner, U.; Salahuddin, S.; Goswami, R. K.; Sinha, S. C.; Barbas, C. F. An efficient chemical approach to bispecific antibodies and antibodies of high valency. *Bioorg. Med. Chem. Lett.* **2009**, *19* (14), 3716–3720 DOI: 10.1016/j.bmcl.2009.05.047.

(151) Dadová, J.; Orság, P.; Pohl, R.; Brázdová, M.; Fojta, M.; Hocek, M. Vinylsulfonamide and Acrylamide Modification of DNA for Cross-linking with Proteins. *Angew. Chem. Int. Ed.* **2013**, *52* (40), 10515–10518 DOI: 10.1002/anie.201303577.

(152) Morales-Sanfrutos, J.; Lopez-Jaramillo, J.; Ortega-Muñoz, M.; Megia-Fernandez, A.; Perez-Balderas, F.; Hernandez-Mateo, F.; Santoyo-Gonzalez, F. Vinyl sulfone: a versatile function for simple bioconjugation and immobilization. *Org Biomol Chem* **2010**, *8* (3), 667–675 DOI: 10.1039/B920576D.

(153) Valero, E.; Tambalo, S.; Marzola, P.; Ortega-Muñoz, M.; López-Jaramillo, F. J.; Santoyo-González, F.; de Dios López, J.; Delgado, J. J.; Calvino, J. J.; Cuesta, R.; et al. Magnetic Nanoparticles-Templated Assembly of Protein Subunits: A New Platform for Carbohydrate-Based MRI Nanoprobes. *J. Am. Chem. Soc.* **2011**, *133* (13), 4889–4895 DOI: 10.1021/ja110014p.

(154) Megia-Fernandez, A.; Hernandez-Mateo, F.; Santoyo-Gonzalez, F. Vinyl sulfone-based ferrocenylation reagents: applications in conjugation and bioconjugation. *Org. Biomol. Chem.* **2013**, *11* (16), 2586 DOI: 10.1039/c3ob27209e.

(155) Tietze, L. F.; Arlt, M.; Beller, M.; Jähde, E.; Rajewsky, M. F.; others. Anticancer agents, 15. Squaric acid diethyl ester: a new coupling reagent for the formation of drug biopolymer conjugates. Synthesis of squaric acid ester amides and diamides. *Chem. Ber.* **1991**, *124* (5), 1215–1221.

(156) Tietze, L. F.; Schroeter, C.; Gabius, S.; Brinck, U.; Goerlach-Graw, A.; Gabius, H. J. Conjugation of p-aminophenyl glycosides with squaric acid diester to a carrier protein and the use of the neoglycoprotein in the histochemical detection of lectins. *Bioconjug. Chem.* **1991**, *2* (3), 148–153.

(157) Wurm, F. R.; Klok, H.-A. Be squared: expanding the horizon of squaric acid-mediated conjugations. *Chem. Soc. Rev.* **2013**, *42* (21), 8220–8236 DOI: 10.1039/C3CS60153F.

(158) Dingels, C.; Wurm, F.; Wagner, M.; Klok, H.-A.; Frey, H. Squaric Acid Mediated Chemoselective PEGylation of Proteins: Reactivity of Single-Step-Activated α-Amino Poly(ethylene glycol)s. *Chem. - Eur. J.* **2012**, *18* (52), 16828–16835 DOI: 10.1002/chem.201200182.

(159) Wurm, F.; Dingels, C.; Frey, H.; Klok, H.-A. Squaric Acid Mediated Synthesis and Biological Activity of a Library of Linear and Hyperbranched Poly(Glycerol)–Protein Conjugates. *Biomacromolecules* **2012**, *13* (4), 1161–1171 DOI: 10.1021/bm300103u.

(160) Dingels, C.; Müller, S. S.; Steinbach, T.; Tonhauser, C.; Frey, H. Universal Concept for the Implementation of a Single Cleavable Unit at Tunable Position in Functional Poly(ethylene glycol)s. *Biomacromolecules* **2013**, *14* (2), 448–459 DOI: 10.1021/bm3016797.

(161) Whitfield, R. E.; Friedman, M. Chemical Modification of Wool with Dicarbonyl Compounds in Dimethyl Sulfoxide. *Text. Res. J.* **1972**, *42* (6), 344–346 DOI: 10.1177/004051757204200608.

(162) Kaiser, A.; Gaidzik, N.; Westerlind, U.; Kowalczyk, D.; Hobel, A.; Schmitt, E.; Kunz, H. A Synthetic Vaccine Consisting of a Tumor-Associated Sialyl-T_N-MUC1 Tandem-Repeat Glycopeptide and Tetanus Toxoid: Induction of a Strong and Highly Selective Immune Response. *Angew. Chem. Int. Ed.* **2009**, *48* (41), 7551–7555 DOI: 10.1002/anie.200902564.

(163) Ohara, K.; Takeda, Y.; Daikoku, S.; Hachisu, M.; Seko, A.; Ito, Y. Profiling Aglycon-Recognizing Sites of UDP-glucose:glycoprotein Glucosyltransferase by Means of Squarate-Mediated Labeling. *Biochemistry (Mosc.)* **2015**, *54* (31), 4909–4917 DOI: 10.1021/acs.biochem.5b00785.

(164) Yan, H.; Aguilar, A. L.; Zhao, Y. Preparation of carbohydrate–oligonucleotide conjugates using the squarate spacer. *Bioorg. Med. Chem. Lett.* **2007**, *17* (23), 6535–6538 DOI: 10.1016/j.bmcl.2007.09.078.

(165) Zhao, Y.; Tram, K.; Yan, H. Synthesis and characterization of mannosylated oligoribonucleotides. *Carbohydr. Res.* **2009**, *344* (16), 2137–2143 DOI: 10.1016/j.carres.2009.08.033.

(166) Mellal, D.; Fonvielle, M.; Santarem, M.; Chemama, M.; Schneider, Y.; Iannazzo, L.; Braud, E.; Arthur, M.; Etheve-Quelquejeu, M. Synthesis and biological evaluation of non-isomerizable analogues of Ala-tRNAAla. *Org. Biomol. Chem.* **2013**, *11* (36), 6161 DOI: 10.1039/c3ob41206g.

(167) Sato, K.; Seio, K.; Sekine, M. Squaryl Group as a New Mimic of Phosphate Group in Modified Oligodeoxynucleotides: Synthesis and Properties of New Oligodeoxynucleotide Analogues Containing an Internucleotidic Squaryldiamide Linkage. *J. Am. Chem. Soc.* **2002**, *124* (43), 12715–12724 DOI: 10.1021/ja027131f.

(168) Nuzzi, A.; Massi, A.; Dondoni, A. Model Studies Toward the Synthesis of Thymidine Oligonucleotides with Triazole Internucleosidic LinkagesVia Iterative Cu(I)-Promoted Azide–Alkyne Ligation Chemistry. *QSAR Comb. Sci.* **2007**, *26* (11–12), 1191–1199 DOI: 10.1002/qsar.200740079.

(169) El-Sagheer, A. H.; Brown, T. Click chemistry with DNA. *Chem. Soc. Rev.* **2010**, *39* (4), 1388 DOI: 10.1039/b901971p.

(170) Kolb, H. C.; Finn, M. G.; Sharpless, K. B. Click Chemistry: Diverse Chemical Function from a Few Good Reactions. *Angew. Chem. Int. Ed.* **2001**, *40* (11), 2004–2021 DOI: 10.1002/1521-3773(20010601)40:11<2004::AID-ANIE2004>3.0.CO;2-5.

(171) Rostovtsev, V. V.; Green, L. G.; Fokin, V. V.; Sharpless, K. B. A Stepwise Huisgen Cycloaddition Process: Copper(I)-Catalyzed Regioselective “Ligation” of Azides and Terminal Alkynes. *Angew. Chem.* **2002**, *114* (14), 2708–2711 DOI: 10.1002/1521-3757(20020715)114:14<2708::AID-ANGE2708>3.0.CO;2-0.

(172) Tornøe, C. W.; Christensen, C.; Meldal, M. Peptidotriazoles on Solid Phase: [1,2,3]-Triazoles by Regiospecific Copper(I)-Catalyzed 1,3-Dipolar Cycloadditions of Terminal Alkynes to Azides. *J. Org. Chem.* **2002**, *67* (9), 3057–3064 DOI: 10.1021/jo011148j.

(173) Bock, V. D.; Hiemstra, H.; van Maarseveen, J. H. CuI-Catalyzed Alkyne-Azide "Click" Cycloadditions from a Mechanistic and Synthetic Perspective. *Eur. J. Org. Chem.* **2006**, *2006* (1), 51–68 DOI: 10.1002/ejoc.200500483.

(174) Zhan, W.; Barnhill, H. N.; Sivakumar, K.; Tian, H.; Wang, Q. Synthesis of hemicyanine dyes for "click" bioconjugation. *Tetrahedron Lett.* **2005**, *46* (10), 1691–1695 DOI: 10.1016/j.tetlet.2005.01.066.

(175) Kalvet, I.; Tammiku-Taul, J.; Mäeorg, U.; Tämm, K.; Burk, P.; Sikk, L. NMR and DFT Study of the Copper(I)-Catalyzed Cycloaddition Reaction: H/D Scrambling of Alkynes and Variable Reaction Order of the Catalyst. *ChemCatChem* **2016**, *8* (10), 1804–1808 DOI: 10.1002/cctc.201600176.

(176) Makarem, A.; Berg, R.; Rominger, F.; Straub, B. F. A Fluxional Copper Acetylide Cluster in CuAAC Catalysis. *Angew. Chem. Int. Ed.* **2015**, *54* (25), 7431–7435 DOI: 10.1002/anie.201502368.

(177) Gierlich, J.; Gutsmiedl, K.; Gramlich, P. M. E.; Schmidt, A.; Burley, G. A.; Carell, T. Synthesis of Highly Modified DNA by a Combination of PCR with Alkyne-Bearing Triphosphates and Click Chemistry. *Chem. - Eur. J.* **2007**, *13* (34), 9486–9494 DOI: 10.1002/chem.200700502.

(178) Gramlich, P. M. E.; Wirges, C. T.; Gierlich, J.; Carell, T. Synthesis of Modified DNA by PCR with Alkyne-Bearing Purines Followed by a Click Reaction. *Org. Lett.* **2008**, *10* (2), 249–251 DOI: 10.1021/ol7026015.

(179) Seela, F.; Sirivolu, V. R. DNA Containing Side Chains with Terminal Triple Bonds: Base-Pair Stability and Functionalization of Alkynylated Pyrimidines and 7-Deazapurines. *Chem. Biodivers.* **2006**, *3* (5), 509–514.

(180) Kanan, M. W.; Rozenman, M. M.; Sakurai, K.; Snyder, T. M.; Liu, D. R. Reaction discovery enabled by DNA-templated synthesis and in vitro selection. *Nature* **2004**, *431* (7008), 545–549.

(181) Chan, T. R.; Hilgraf, R.; Sharpless, K. B.; Fokin, V. V. Polytriazoles as Copper(I)-Stabilizing Ligands in Catalysis. *Org. Lett.* **2004**, *6* (17), 2853–2855 DOI: 10.1021/ol0493094.

(182) Sejwal, P.; Han, Y.; Shah, A.; Luk, Y.-Y. Water-Driven Chemoselective Reaction of Squarate Derivatives with Amino Acids and Peptides. *Org. Lett.* **2007**, *9* (23), 4897–4900 DOI: 10.1021/ol702275q.

(183) Saxon, E.; Armstrong, J. I.; Bertozzi, C. R. A "Traceless" Staudinger Ligation for the Chemoselective Synthesis of Amide Bonds. *Org. Lett.* **2000**, *2* (14), 2141–2143 DOI: 10.1021/ol006054v.

(184) Nilsson, B. L.; Kiessling, L. L.; Raines, R. T. Staudinger Ligation: A Peptide from a Thioester and Azide. *Org. Lett.* **2000**, *2* (13), 1939–1941 DOI: 10.1021/ol0060174.

(185) Soellner, M. B.; Nilsson, B. L.; Raines, R. T. Reaction Mechanism and Kinetics of the Traceless Staudinger Ligation. *J. Am. Chem. Soc.* **2006**, *128* (27), 8820–8828 DOI: 10.1021/ja060484k.

(186) van Berkel, S. S.; van Eldijk, M. B.; van Hest, J. C. M. Staudinger Ligation as a Method for Bioconjugation. *Angew. Chem. Int. Ed.* **2011**, *50* (38), 8806–8827 DOI: 10.1002/anie.201008102.

(187) Schilling, C. I.; Jung, N.; Biskup, M.; Schepers, U.; Bräse, S. Bioconjugation via azide–Staudinger ligation: an overview. *Chem. Soc. Rev.* **2011**, *40* (9), 4840 DOI: 10.1039/c0cs00123f.

(188) Grandjean, C.; Boutonnier, A.; Guerreiro, C.; Fournier, J.-M.; Mulard, L. A. On the Preparation of Carbohydrate−Protein Conjugates Using the Traceless Staudinger Ligation. *J. Org. Chem.* **2005**, *70* (18), 7123–7132 DOI: 10.1021/jo0505472.

(189) Nisic, F.; Speciale, G.; Bernardi, A. Stereoselective Synthesis of α- and β-Glycofuranosyl Amides by Traceless Ligation of Glycofuranosyl Azides. *Chem. - Eur. J.* **2012**, *18* (22), 6895–6906 DOI: 10.1002/chem.201200309.

(190) Nisic, F.; Bernardi, A. Stereoselective synthesis of N-galactofuranosyl amides. *Carbohydr. Res.* **2011**, *346* (4), 465–471 DOI: 10.1016/j.carres.2010.12.020.

(191) Bianchi, A.; Bernardi, A. Traceless Staudinger Ligation of Glycosyl Azides with Triaryl Phosphines: Stereoselective Synthesis of Glycosyl Amides †. *J. Org. Chem.* **2006**, *71* (12), 4565–4577 DOI: 10.1021/jo060409s.

(192) Mamat, C.; Franke, M.; Peppel, T.; Köckerling, M.; Steinbach, J. Synthesis, structure determination, and (radio-)fluorination of novel functionalized phosphanes suitable for the traceless Staudinger ligation. *Tetrahedron* **2011**, *67* (25), 4521–4529 DOI: 10.1016/j.tet.2011.04.091.

(193) Gimisis, T.; Ialongo, G.; Chatgilialoglu, C. Generation of C-1′ radicals through a β-(acyloxy) alkyl rearrangement in modified purine and pyrimidine nucleosides. *Tetrahedron* **1998**, *54* (3), 573–592.

(194) Chalker, J. M.; Lercher, L.; Rose, N. R.; Schofield, C. J.; Davis, B. G. Conversion of Cysteine into Dehydroalanine Enables Access to Synthetic Histones Bearing Diverse Post-Translational Modifications. *Angew. Chem. Int. Ed.* **2012**, *51* (8), 1835–1839 DOI: 10.1002/anie.201106432.

(195) Sundaralingam, M. Stereochemistry of nucleic acids and their constituents. IV. Allowed and preferred conformations of nucleosides, nucleoside mono-, di-, tri-, tetraphosphates, nucleic acids and polynucleotides. *Biopolymers* **1969**, *7* (6), 821–860.

(196) Altona, C. t; Sundaralingam, M. Conformational analysis of the sugar ring in nucleosides and nucleotides. New description using the concept of pseudorotation. *J. Am. Chem. Soc.* **1972**, *94* (23), 8205–8212.

(197) Marquez, V. E.; Siddiqui, M. A.; Ezzitouni, A.; Russ, P.; Wang, J.; Wagner, R. W.; Matteucci, M. D. Nucleosides with a twist. Can fixed forms of sugar ring pucker influence biological activity in nucleosides and oligonucleotides? *J. Med. Chem.* **1996**, *39* (19), 3739–3747.

(198) Marquez, V. E.; Ezzitouni, A.; Russ, P.; Siddiqui, M. A.; Ford, H.; Feldman, R. J.; Mitsuya, H.; George, C.; Barchi, J. J. HIV-1 reverse transcriptase can discriminate between two conformationally locked carbocyclic AZT triphosphate analogues. *J. Am. Chem. Soc.* **1998**, *120* (12), 2780–2789.

(199) Yamada, K.; Wahba, A. S.; Bernatchez, J. A.; Ilina, T.; Martínez-Montero, S.; Habibian, M.; Deleavey, G. F.; Götte, M.; Parniak, M. A.; Damha, M. J. Nucleotide Sugar Pucker Preference Mitigates Excision by HIV-1 RT. *ACS Chem. Biol.* **2015**, *10* (9), 2024–2033 DOI: 10.1021/acschembio.5b00263.

(200) Marquez, V. E.; Ben-Kasus, T.; Barchi, J. J.; Green, K. M.; Nicklaus, M. C.; Agbaria, R. Experimental and Structural Evidence that Herpes 1 Kinase and Cellular DNA Polymerase(s) Discriminate on the Basis of Sugar Pucker. *J. Am. Chem. Soc.* **2004**, *126* (2), 543–549 DOI: 10.1021/ja037929e.

(201) Jepsen, J. S.; Sørensen, M. D.; Wengel, J. Locked nucleic acid: a potent nucleic acid analog in therapeutics and biotechnology. *Oligonucleotides* **2004**, *14* (2), 130–146.

(202) Imanishi, T.; Obika, S. BNAs: novel nucleic acid analogs with a bridged sugar moiety. *Chem. Commun.* **2002**, No. 16, 1653–1659 DOI: 10.1039/b201557a.

(203) Mathé, C.; Périgaud, C. Recent Approaches in the Synthesis of Conformationally Restricted Nucleoside Analogues. *Eur. J. Org. Chem.* **2008**, *2008* (9), 1489–1505 DOI: 10.1002/ejoc.200700946.

(204) Weinger, J. S.; Parnell, K. M.; Dorner, S.; Green, R.; Strobel, S. A. Substrate-assisted catalysis of peptide bond formation by the ribosome. *Nat. Struct. Mol. Biol.* **2004**, *11* (11), 1101–1106 DOI: 10.1038/nsmb841.

(205) Erande, N.; Gunjal, A. D.; Fernandes, M.; Kumar, V. A. Probing the furanose conformation in the 2'–5'strand of isoDNA : RNA duplexes by freezing the nucleoside conformations. *Chem. Commun.* **2011**, *47* (13), 4007 DOI: 10.1039/c0cc05402j.

(206) Erande, N.; Gunjal, A. D.; Fernandes, M.; Gonnade, R.; Kumar, V. A. Synthesis and structural studies of S-type/N-type-locked/frozen nucleoside analogues and their incorporation in RNA-selective, nuclease resistant 2'–5' linked oligonucleotides. *Org Biomol Chem* **2013**, *11* (5), 746–757 DOI: 10.1039/C2OB26762D.

(207) Dawadi, S.; Viswanathan, K.; Boshoff, H. I.; Barry, C. E.; Aldrich, C. C. Investigation and Conformational Analysis of Fluorinated Nucleoside Antibiotics Targeting Siderophore Biosynthesis. *J. Org. Chem.* **2015**, *80* (10), 4835–4850 DOI: 10.1021/acs.joc.5b00550.

(208) Martínez-Montero, S.; Deleavey, G. F.; Kulkarni, A.; Martín-Pintado, N.; Lindovska, P.; Thomson, M.; González, C.; Götte, M.; Damha, M. J. Rigid 2′,4′-Difluororibonucleosides: Synthesis, Conformational Analysis, and Incorporation into Nascent RNA by HCV Polymerase. *J. Org. Chem.* **2014**, *79* (12), 5627–5635 DOI: 10.1021/jo500794v.

(209) Martínez-Montero, S.; Deleavey, G. F.; Martín-Pintado, N.; Fakhoury, J. F.; González, C.; Damha, M. J. Locked 2′-Deoxy-2′,4′-Difluororibo Modified Nucleic Acids: Thermal Stability, Structural Studies, and siRNA Activity. *ACS Chem. Biol.* **2015**, *10* (9), 2016–2023 DOI: 10.1021/acschembio.5b00218.

(210) Martínez-Montero, S.; Deleavey, G. F.; Dierker-Viik, A.; Lindovska, P.; Ilina, T.; Portella, G.; Orozco, M.; Parniak, M. A.; González, C.; Damha, M. J. Synthesis and Properties of 2′-Deoxy-2′,4′-difluoroarabinose-Modified Nucleic Acids. *J. Org. Chem.* **2015**, *80* (6), 3083–3091 DOI: 10.1021/jo502948t.

(211) Nissen, P.; Thirup, S.; Kjeldgaard, M.; Nyborg, J. The crystal structure of Cys-tRNA Cys–EF-Tu–GDPNP reveals general and specific features in the ternary complex and in tRNA. *Structure* **1999**, *7* (2), 143–156.

(212) Nissen, P.; Kjeldgaard, M.; Thirup, S.; Polekhina, G.; Reshetnikova, L.; Clark, B. F.; Nyborg, J. Crystal Structure of the Ternary EF-Tu, Complex of Phe-tRNA, and a GTP Analog.

(213) LEEUW, H. P.; JAGER, J. R.; KOENERS, H. J.; BOOM, J. H.; ALTONA, C. Puromycin and some of its analogues: Conformational properties in solution. *Eur. J. Biochem.* **1977**, *76* (1), 209–217.

(214) Nissen, P.; Hansen, J.; Ban, N.; Moore, P. B.; Steitz, T. A. The Structural Basis of Ribosome Activity in Peptide Bond Synthesis. *Science* **2000**, *289* (5481), 920–930 DOI: 10.1126/science.289.5481.920.

(215) Iannazzo, L.; Laisné, G.; Fonvielle, M.; Braud, E.; Herbeuval, J.-P.; Arthur, M.; Etheve-Quelquejeu, M. Synthesis of 3′-Fluoro-tRNA Analogues for Exploring Non-ribosomal Peptide Synthesis in Bacteria. *ChemBioChem* **2015**, *16* (3), 477–486 DOI: 10.1002/cbic.201402523.

(216) Altona, C.; Sundaralingam, M. Conformational analysis of the sugar ring in nucleosides and nucleotides. Improved method for the interpretation of proton magnetic resonance coupling constants. *J. Am. Chem. Soc.* **1973**, *95* (7), 2333–2344.

(217) Gadikota, R. R.; Callam, C. S.; Wagner, T.; Del Fraino, B.; Lowary, T. L. 2,3-Anhydro Sugars in Glycoside Bond Synthesis. Highly Stereoselective Syntheses of Oligosaccharides Containing α- and β-Arabinofuranosyl Linkages. *J. Am. Chem. Soc.* **2003**, *125* (14), 4155–4165 DOI: 10.1021/ja029302m.

(218) Srivastav, N. C.; Shakya, N.; Mak, M.; Agrawal, B.; Tyrrell, D. L.; Kumar, R. Antiviral Activity of Various 1-(2′-Deoxy-β- D -lyxofuranosyl), 1-(2′-Fluoro-β- D -xylofuranosyl), 1-(3′-Fluoro-β- D -arabinofuranosyl), and 2′-Fluoro-2′,3′-didehydro-2′,3′-dideoxyribose Pyrimidine Nucleoside Analogues against Duck Hepatitis B Virus (DHBV) and Human Hepatitis B Virus (HBV) Replication. *J. Med. Chem.* **2010**, *53* (19), 7156–7166 DOI: 10.1021/jm100803c.

(219) Miyai, K.; Robins, R. K.; Tolman, R. L. Synthesis of 9-(3-deoxy-3-fluoro-. beta.-D-arabinofuranosyl) adenine. *J. Med. Chem.* **1972**, *15* (10), 1092–1093.

(220) Cook, P. D. Oligonucleotides having chiral phosphorus linkages, May 2001.

(221) Peuchmaur, M.; Wong, Y.-S. Diastereodivergent Strategies for the Synthesis of Homochiral Aculeatins. *J. Org. Chem.* **2007**, *72* (14), 5374–5379 DOI: 10.1021/jo0707986.

(222) Matteucci, M. D.; Caruthers, M. H. The use of zinc bromide for removal of dimethoxytrityl ethers from deoxynucleosides. *Tetrahedron Lett.* **1980**, *21* (34), 3243–3246 DOI: 10.1016/S0040-4039(00)78657-6.

(223) Staphylococci http://www.pasteur.fr/en/institut-pasteur/press/fact-sheets/staphylococci (accessed Sep 21, 2016).

(224) Chambers, H. F.; DeLeo, F. R. Waves of resistance: Staphylococcus aureus in the antibiotic era. *Nat. Rev. Microbiol.* **2009**, *7* (9), 629–641 DOI: 10.1038/nrmicro2200.

(225) Rohrer, S.; Ehlert, K.; Tschierske, M.; Labischinski, H.; Berger-Bächi, B. The essential Staphylococcus aureus gene fmhB is involved in the first step of peptidoglycan pentaglycine interpeptide formation. *Proc. Natl. Acad. Sci.* **1999**, *96* (16), 9351–9356.

(226) Berger-Bächi, B.; Rohrer, S. Factors influencing methicillin resistance in staphylococci. *Arch. Microbiol. 178* (3), 165–171 DOI: 10.1007/s00203-002-0436-0.

(227) Ruzin, A.; Severin, A.; Ritacco, F.; Tabei, K.; Singh, G.; Bradford, P. A.; Siegel, M. M.; Projan, S. J.; Shlaes, D. M. Further Evidence that a Cell Wall Precursor [C55-MurNAc-(Peptide)-GlcNAc] Serves as an Acceptor in a Sorting Reaction. *J. Bacteriol.* **2002**, *184* (8), 2141–2147 DOI: 10.1128/JB.184.8.2141-2147.2002.

(228) Navarre, W. W.; Schneewind, O. Surface Proteins of Gram-Positive Bacteria and Mechanisms of Their Targeting to the Cell Wall Envelope. *Microbiol. Mol. Biol. Rev.* **1999**, *63* (1), 174–229.

(229) Schneider, T.; Senn, M. M.; Berger-Bächi, B.; Tossi, A.; Sahl, H.-G.; Wiedemann, I. In vitro assembly of a complete, pentaglycine interpeptide bridge containing cell wall precursor (lipid II-Gly5) of Staphylococcus aureus. *Mol. Microbiol.* **2004**, *53* (2), 675–685 DOI: 10.1111/j.1365-2958.2004.04149.x.

(230) Green, C. J.; Vold, B. S. Staphylococcus aureus has clustered tRNA genes. *J. Bacteriol.* **1993**, *175* (16), 5091–5096.

(231) Chang, A. T.; Nikonowicz, E. P. Solution Nuclear Magnetic Resonance Analyses of the Anticodon Arms of Proteinogenic and Nonproteinogenic tRNAGly. *Biochemistry (Mosc.)* **2012**, *51* (17), 3662–3674 DOI: 10.1021/bi201900j.

(232) Arbeloa, A.; Hugonnet, J.-E.; Sentilhes, A.-C.; Josseaume, N.; Dubost, L.; Monsempes, C.; Blanot, D.; Brouard, J.-P.; Arthur, M. Synthesis of Mosaic Peptidoglycan Cross-bridges by Hybrid Peptidoglycan Assembly Pathways in Gram-positive Bacteria. *J. Biol. Chem.* **2004**, *279* (40), 41546–41556 DOI: 10.1074/jbc.M407149200.

(233) Barthes, N. P. F.; Gavvala, K.; Dziuba, D.; Bonhomme, D.; Karpenko, I. A.; Dabert-Gay, A. S.; Debayle, D.; Demchenko, A. P.; Benhida, R.; Michel, B. Y.; et al. Dual emissive analogue of deoxyuridine as a sensitive hydration-reporting probe for discriminating mismatched from matched DNA and DNA/DNA from DNA/RNA duplexes. *J Mater Chem C* **2016**, *4* (14), 3010–3017 DOI: 10.1039/C5TC03427B.

(234) Gavvala, K.; Barthes, N. P. F.; Bonhomme, D.; Dabert-Gay, A. S.; Debayle, D.; Michel, B. Y.; Burger, A.; Mély, Y. A turn-on dual emissive nucleobase sensitive to mismatches and duplex conformational changes. *RSC Adv* **2016**, *6* (90), 87142–87146 DOI: 10.1039/C6RA19061H.

(235) Ström, K.; Sjögren, J.; Broberg, A.; Schnürer, J. Lactobacillus plantarum MiLAB 393 produces the antifungal cyclic dipeptides cyclo(L-Phe-L-Pro) and cyclo(L-Phe-trans-4-OH-L-Pro) and 3-phenyllactic acid. *Appl. Environ. Microbiol.* **2002**, *68* (9), 4322–4327.

(236) Kohn, H.; Widger, W. The Molecular Basis for the Mode of Action of Bicyclomycin. *Curr. Drug Targets - Infect. Disord.* **2005**, *5* (3), 273–295.

(237) Waring, P.; Beaver, J. Gliotoxin and related epipolythiodioxopiperazines. *Gen. Pharmacol. Vasc. Syst.* **1996**, *27* (8), 1311–1316 DOI: 10.1016/S0306-3623(96)00083-3.

(238) Lautru, S.; Gondry, M.; Genet, R.; Pernodet, J.-L. The Albonoursin Gene Cluster of S. noursei: Biosynthesis of Diketopiperazine Metabolites Independent of Nonribosomal Peptide Synthetases. *Chem. Biol.* **2002**, *9* (12), 1355–1364 DOI: 10.1016/S1074-5521(02)00285-5.

(239) Sauguet, L.; Moutiez, M.; Li, Y.; Belin, P.; Seguin, J.; Du, M.-H. L.; Thai, R.; Masson, C.; Fonvielle, M.; Pernodet, J.-L.; et al. Cyclodipeptide synthases, a family of class-I aminoacyl-tRNA synthetase-like enzymes involved in non-ribosomal peptide synthesis. *Nucleic Acids Res.* **2011**, *39* (10), 4475–4489 DOI: 10.1093/nar/gkr027.

(240) Santarem, M.; Fonvielle, M.; Sakkas, N.; Laisné, G.; Chemama, M.; Herbeuval, J.-P.; Braud, E.; Arthur, M.; Etheve-Quelquejeu, M. Synthesis of 3'-triazoyl-dinucleotides as precursors of stable Phe-tRNAPhe and Leu-tRNALeu analogues. *Bioorg. Med. Chem. Lett.* **2014**, *24* (15), 3231–3233 DOI: 10.1016/j.bmcl.2014.06.027.

Publications

Bioorganic & Medicinal Chemistry Letters 24 (2014) 3231–3233

Contents lists available at ScienceDirect

Bioorganic & Medicinal Chemistry Letters

journal homepage: www.elsevier.com/locate/bmcl

Synthesis of 3′-triazoyl-dinucleotides as precursors of stable Phe-tRNA^{Phe} and Leu-tRNA^{Leu} analogues

Marco Santarem [a], Matthieu Fonvielle [b], Nicolas Sakkas [c], Guillaume Laisné [c], Maryline Chemama [a], Jean-Philippe Herbeuval [c], Emmanuelle Braud [c], Michel Arthur [b], Mélanie Etheve-Quelquejeu [c,*]

[a] Institut Parisien de Chimie Moléculaire, CNRS UMR 7201, Université Pierre et Marie Curie Paris 6, 4, place Jussieu, 75005 Paris, France
[b] Centre de Recherche des Cordeliers, LRMA, Equipe 12, INSERM UMR S 1138, Université Pierre et Marie Curie–Paris 6, UMR S 1138, Paris F-75006, France; Université Paris Descartes, Sorbonne Paris Cité, UMR S 1138, Paris F-75006 France
[c] Chemistry & Biology Nucleo(s)tides & Immunology for Therapy (CBNIT), CNRS UMR8601, Université Paris Descartes, PRES Sorbonne Paris Cité, 45 rue des Saints-Pères, 75270 Paris Cedex 06, France

ARTICLE INFO

Article history:
Received 28 May 2014
Revised 9 June 2014
Accepted 10 June 2014
Available online 19 June 2014

Keywords:
Aminoacyl-tRNA
Click chemistry
Cyclodipeptides synthases
Dinucleotides
Cycloaddition

ABSTRACT

We report here the synthesis of stable Phe-tRNA^{Phe} and Leu-tRNA^{Leu} analogues containing a 1,2,3-triazole ring instead of the ribose-amino acid ester bond. The 1,2,3-triazole ring is generated by dipolar cycloaddition of alkyne Phe and Leu analogues to 3′-azido-3′-deoxyadenosine via the Cu^{I}-catalysed Huisgen, Meldal, Sharpless 1,3-cycloaddition. The corresponding triazoyl pdCpA dinucleotides, obtained by classical phosphoramidite chemistry, were enzymatically ligated to 22-nt or 74-nt RNA generating stable Phe-tRNA^{Phe} analogues containing the acceptor stem or full tRNA moieties, respectively. These molecules represent useful tools to study the contribution of the RNA and amino acid moieties in stabilization of aminoacyl-tRNA/protein complexes.

Aminoacyl-tRNAs have important roles in a variety of biological processes in addition to protein synthesis by ribosomes.[1] Recently, cyclodipeptide synthases (CDPSs) were shown to use aminoacyl-tRNAs as substrates to catalyze the formation of the two peptide bonds of various cyclodipeptides[2] (Fig. 1). The cyclodipeptides form the diketopiperazine (DKP) scaffold of a variety of natural products with interesting biological properties, including antibacterial,[3] antiviral,[4] antitumoral,[5] immunosuppressive[6] and anti-inflammatory[7] activities. The first member of the CDPS family to be identified was AlbC from *Streptomyces noursei*, which has been showed to use mainly Phe-tRNA^{Phe} and Leu-tRNA^{Leu} as substrates to preferentially synthesize cyclo(L-Phe-L-Leu)[2]. The crystal structures of AlbC, YvmC-Blic, and Rv2275 CDPSs revealed a compact α/β structure containing a Rossman-fold domain[8] and similarities with aminoacyl-tRNA synthases (aaRS). These findings suggest that all CDPSs share a common aaRS-like architecture and catalytic mechanism. Moreover, biochemical data indicated that YvmC-Blic binds tRNA and generates cyclo(L-Leu-L-Leu) via formation of an aminoacyl-enzyme intermediate.[8c] However, recognition mode of

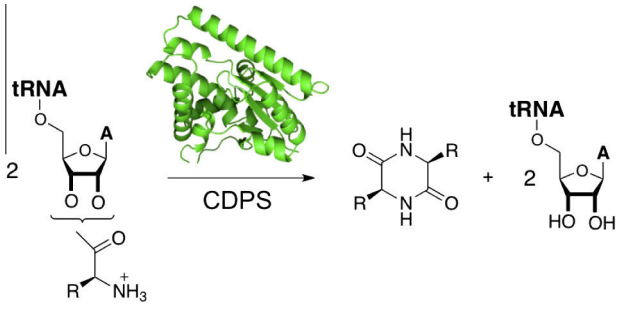

Figure 1. Synthesis of cyclodipeptides by CDPS. R = Phe and Leu for AlbC from *Streptomyces noursei*; A = Adénosine.

the RNA moiety of the substrates remains elusive since no crystal structures of CDPS in complexes with aminoacyl-tRNAs have been resolved. In such substrates, the ester bond connecting the amino acid residue to the 2′ or 3′ position of the terminal nucleotide is labile with half-lives from 10 min to 1 h at neutral pH.[9] *Trans*-esterification between the 2′ and 3′ positions occurs in the absence of enzyme with a rate and thermodynamic equilibrium constant of 5 s^{-1} and 1, respectively.[10] We have shown that triazole rings act

* Corresponding author. Tel.: +33 0142864026.
E-mail address: melanie.etheve-quelquejeu@parisdescartes.fr (M. Etheve-Quelquejeu).

http://dx.doi.org/10.1016/j.bmcl.2014.06.027
0960-894X/

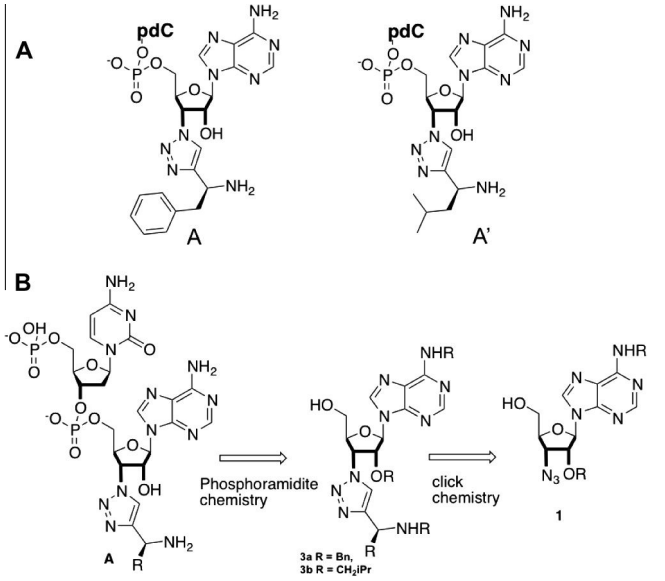

Figure 2. Structure of stable Phe-tRNA^{Phe} and Leu-tRNA^{Leu} analogues (A) and retrosynthesis (B).

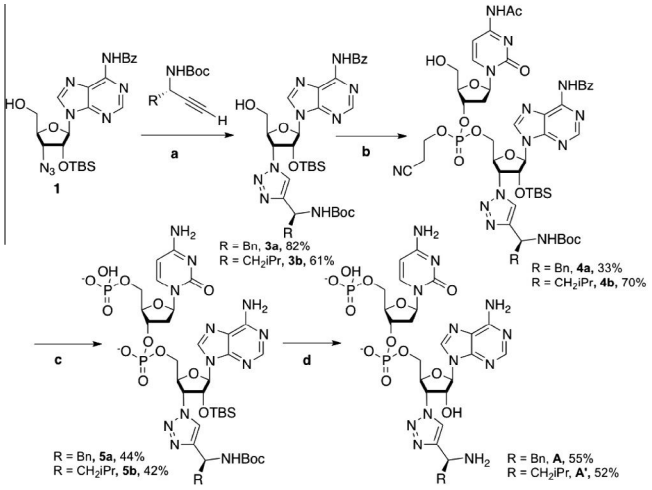

Scheme 2. Synthesis of 3′-triazoyl-dinucleotides **A** and **A′**. (a) $CuSO_4$, sodium ascorbate, THF/H_2O, rt, 24 h; (b) (i) Ac-dC-PCNE, tetrazole, rt, 1 h, CH_3CN, (ii) I_2, H_2O/pyr/THF, rt, 30 min, (iii) TCA, CH_2Cl_2, rt, 30 min; (c) (i) $iPr_2NP(OCH_2CH_2CN)_2$, tetrazole, CH_3CN, rt, 1 h, (ii) I_2, H_2O/pyr/THF, rt, 30 min, (iii) $MeNH_2$, rt, 24 h; (d) HCl/THF/MeOH (1:2:1), rt, 24 h.

as surrogates of the ester bond and provide non-hydrolysable and non-isomerisable analogues of Ala-tRNA^{Ala}.[11] These analogues are good candidates for crystallization of enzyme/aminoacyl-tRNA complexes and for the investigation of catalytic mechanisms, as recently shown for the Fem transferases involved in bacterial cell wall synthesis.[12]

We describe here the synthesis of triazoyl-dinucleotides **A** and **A′**, mimicking the terminal sequence pCpA of Phe-tRNA^{Phe} and Leu-tRNA^{Leu} (Fig. 2A). The general strategy for the preparation of the target compounds **A** and **A′** is outlined in Figure 2B. We planned to synthesize dinucleotides by coupling monomers **3a** and **3b** with Ac-dC-CE phosphoramidite. The key step to obtain monomers **3a** and **3b** was the cycloaddition of alkyne amino acids with azido-adenosine **1**. Knowing that AlbC catalyzes essentially the synthesis of cyclodipeptide Phe-Phe and Phe-Leu, we focused our attention on the synthesis of alkynes **2a** and **2b** (Scheme 1) providing mimics of Phe and Leu. Conversion of N-Boc-aminomethylesters into the corresponding alkynes **2** was achieved by a Seyferth–Gilbert homologation of the α-amino aldehydes using the Bestmann-Ohira reagent.[13] Alkynes **2a**[14] and **2b**[14b] were obtained in 73% and 45% yields, respectively, (Scheme 1).

Cycloaddition of organic azides and alkynes is the most direct route to 1,2,3-triazoles.[15] The use of Cu^{I} as a catalyst has the advantage of providing exclusively the 1,4-disubstitued 1,2,3-triazole regioisomers. Alkynes **2a** and **2b** reacted with the known 3′-azido-2′-O-(*tert*-butyldimethylsilyl)-3′-deoxyadenosine **1**[11a] in presence of copper(II) sulfate and sodium ascorbate. The 3′-triazoyl deoxyadenosine **3a** and **3b** were obtained in 82% and 61% yields, respectively, (Scheme 2). From nucleosides **3a** and **3b**, the phosphoramidite approach was used to obtain the corresponding dinucleotides **A** and **A′** (Scheme 2). For the latter transformation, commercially available deoxycytidine phosphoramidite is mixed with nucleosides **3a** or **3b** and tetrazole in acetonitrile to form the corresponding phosphite triester intermediates. The crude products were oxidized with a solution of iodine and treated with trichloroacetic acid to afford compounds **4a** and **4b** in 33% and 70% yields, respectively. A phosphorylation step in 5′-position of **4a** and **4b** was necessary because T4 RNA ligase catalyzes the ligation of a 5′-phosphate-dinucleotide to the 3′-OH extremity of an incomplete tRNA (see below). In order to obtain the two protected dinucleotides, compounds **4a** and **4b** were mixed with the phosphitylation reagent bis(2-cyanoethyl) diisopropylphosphoramidite in the presence of tetrazole. Removal of acetyl, cyanoethyl and benzoyl groups with a solution of methylamine afforded the desired compounds **5a** and **5b** in 44% and 42% yields, respectively. Eventually, the TBS and *N*-Boc protecting groups were removed by stirring with a solution of HCl during 24 h, producing the deprotected dinucleotides **A** and **A′** in 55% and 52% yields, respectively.

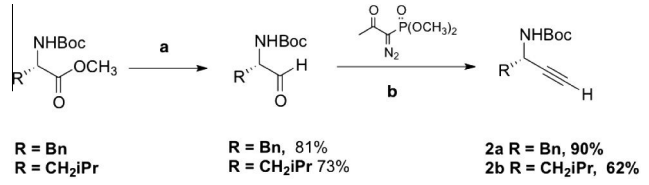

Scheme 1. Synthesis of alkynes **2a** and **2b**. (a) DIBAL-H, CH_2Cl_2, −78 °C, 1 h; (b) K_2CO_3, MeOH, 0 °C 1 h, then rt, 24 h.

The Phe-tRNA^{Phe} analogues were obtained by enzymatic ligation of dinucleotides **A** with 74- and 22-nt RNA molecules (Fig. 3). Addition of pdCpA to these RNAs generate the sequence of the full tRNA^{Phe} or its acceptor arm, respectively. The ligation reaction is catalyzed by T4 RNA ligase, which tolerates a wide range of modifications of the adenosine, including a triazole ring in 2′ or 3′ position.[11a] The ligation was performed in HEPES buffer containing the 74- and 22-nt RNAs, compound **A**, T4 RNA ligase, ATP and $MgCl_2$. After two hours, the Phe-tRNA^{Phe} analogues were purified by anion-exchange chromatography and analyzed by denaturating polyacrylamide gel electrophoresis (Fig. 3).

In summary, we synthesised two dinucleotides pdCpA, containing a 3′-terminal triazoyl-deoxyadenosine mimicking the 3′-terminal sequence of Phe-tRNA^{Phe} and Leu-tRNA^{Leu}. These molecules are stable analogues of aminoacyl-tRNAs because the triazole rings act as bio-isoster of the ester bond and provide non-hydrolysable and non-isomerisable analogues of Phe-tRNA^{Phe} and Leu-tRNA^{Leu}. Dinucleotide **A** underwent enzymatic ligation to a 22nt-microhelix and to a 74nt-RNA to afford two Phe-tRNA^{Phe} analogues. These compounds are currently investigated as ligands for co-crystallization with cyclodipeptide synthetase AlbC.

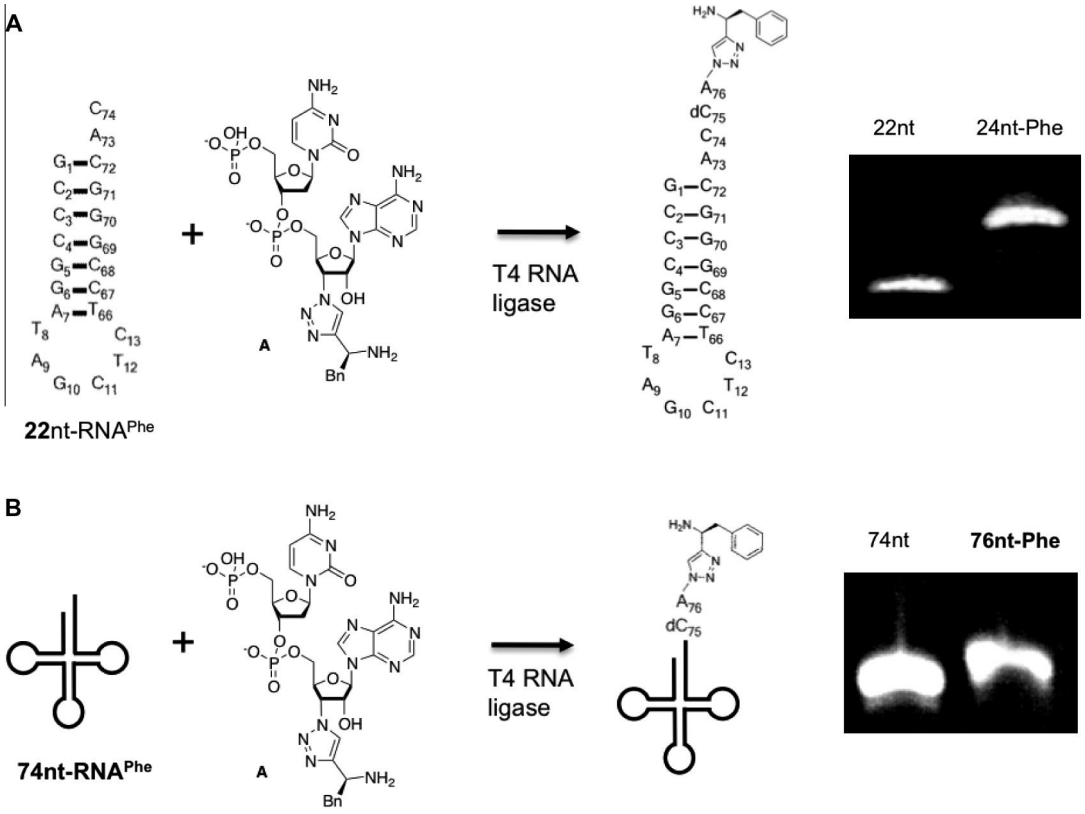

Figure 3. Ligation of **A** to 22-nt by T4 RNA ligase (A); Ligation of **A** to 74-nt by T4 RNA ligase (B).

Acknowledgments

The ANR CyDiPepS and MimictRNA supported this work.

Supplementary data

Supplementary data (experimental details for the preparation of nucleosides and nucleotides) associated with this article can be found, in the online version, at http://dx.doi.org/10.1016/j.bmcl.2014.06.027.

References and notes

1. (a) von Dohren, H. *Nat. Chem. Biol.* **2009**, *5*, 374; (b) Shepherd, J.; Ibba, M. *FEBS Lett.* **2013**, *587*, 2895.
2. Gondry, M.; Sauguet, L.; Belin, P.; Thai, R.; Amouroux, R.; Tellier, C.; Tuphile, K.; Jacquet, M.; Braud, S.; Courcon, M.; Masson, C.; Dubois, S.; Lautru, S.; Lecoq, A.; Hashimoto, S.; Genet, R.; Pernodet, J. L. *Nat. Chem. Biol.* **2009**, *5*, 414.
3. Cain, C. C.; Lee, D. H.; Waldo, R. H.; Henry, A. T.; Casida, E. J.; Wani, M. C.; Wall, M. E.; Oberlies, N. H.; Falkinham, J. O. *Antimicrob. Agents Chemother.* **2003**, *47*, 2113.
4. Rodriguez, P. L.; Carrasco, L. *J. Virol.* **1992**, *66*, 1971.
5. Jia, J. M.; Ma, X. C.; Wu, C. F.; Wu, L. J.; Hu, G. S. *Chem. Pharm. Bull. (Tokyo)* **2005**, *53*, 582.
6. Waring, P.; Beaver, J. *Gen. Pharmacol.* **1996**, *27*, 1311.
7. Minelli, A.; Grottelli, S.; Mierla, A.; Pinnen, F.; Cacciatore, I.; Bellezza, I. *Int. J. Biochem. Cell. B* **2012**, *44*, 525.
8. (a) Sauguet, L.; Moutiez, M.; Li, Y.; Belin, P.; Seguin, J.; Le Du, M. H.; Thai, R.; Masson, C.; Fonvielle, M.; Pernodet, J. L.; Charbonnier, J. B.; Gondry, M. *Nucleic Acids Res.* **2011**, *39*, 4475; (b) Vetting, M. W.; Hegde, S. S.; Blanchard, J. S. *Nat. Chem. Biol.* **2010**, *6*, 797; (c) Bonnefond, L.; Arai, T.; Sakaguchi, Y.; Suzuki, T.; Ishitani, R.; Nureki, O. *Proc. Natl. Acad. Sci. U.S.A.* **2011**, *108*, 3912.
9. Hentzen, D.; Mandel, P.; Garel, J. P. *Biochim. Biophys. Acta* **1972**, *281*, 228.
10. Taiji, M.; Yokoyama, S.; Miyazawa, T. *Biochemistry* **1983**, *22*, 3220.
11. (a) Chemama, M.; Fonvielle, M.; Arthur, M.; Valery, J. M.; Etheve-Quelquejeu, M. *Chem.-Eur. J.* **2009**, *15*, 1929; (b) Fonvielle, M.; Chemama, M.; Lecerf, M.; Villet, R.; Busca, P.; Bouhss, A.; Etheve-Quelquejeu, M.; Arthur, M. *Angew. Chem., Int. Ed.* **2010**, *49*, 5115.
12. (a) Fonvielle, M.; de La Sierra-Gallay, I. L.; El-Sagheer, A. H.; Lecerf, M.; Patin, D.; Mellal, D.; Mayer, C.; Blanot, D.; Gale, N.; Brown, T.; van Tilbeurgh, H.; Etheve-Quelquejeu, M.; Arthur, M. *Angew. Chem., Int. Ed.* **2013**, *52*, 7278; (b) Fonvielle, M.; Mellal, D.; Patin, D.; Lecerf, M.; Blanot, D.; Bouhss, A.; Santarem, M.; Mengin-Lecreulx, D.; Sollogoub, M.; Arthur, M.; Etheve-Quelquejeu, M. *Chem.-Eur. J.* **2013**, *19*, 1357.
13. (a) Ohira, S. *Synth. Commun.* **1989**, *19*, 561; (b) Roth, G. J.; Liepold, B.; Muller, S. G.; Bestmann, H. J. *Synthesis-Stuttgart* **2004**, 59.
14. (a) Proteau-Gagne, A.; Rochon, K.; Roy, M.; Albert, P. J.; Guerin, B.; Gendron, L.; Dory, Y. L. *Bioorg. Med. Chem. Lett.* **2013**, *23*, 5267; (b) Detz, R. J.; Abiri, Z.; le Griel, R.; Hiemstra, H.; van Maarseveen, J. H. *Chem.-Eur. J.* **2011**, *17*, 5921.
15. (a) Rostovtsev, V. V.; Green, L. G.; Fokin, V. V.; Sharpless, K. B. *Angew. Chem., Int. Ed.* **2002**, *41*, 2596; (b) Tornoe, C. W.; Christensen, C.; Meldal, M. *J. Org. Chem.* **2002**, *67*, 3057.

RNA Modifications

International Edition: DOI: 10.1002/anie.201606843
German Edition: DOI: 10.1002/ange.201606843

Electrophilic RNA for Peptidyl-RNA Synthesis and Site-Specific Cross-Linking with tRNA-Binding Enzymes

Matthieu Fonvielle[+], Nicolas Sakkas[+], Laura Iannazzo, Chloé Le Fournis, Delphine Patin, Dominique Mengin-Lecreulx, Afaf El-Sagheer, Emmanuelle Braud, Sébastien Cardon, Tom Brown, Michel Arthur[+], and Mélanie Etheve-Quelquejeu[+]**

Abstract: *RNA functionalization is challenging due to the instability of RNA and the limited range of available enzymatic reactions. We developed a strategy based on solid phase synthesis and post-functionalization to introduce an electrophilic site at the 3′ end of tRNA analogues. The squarate diester used as an electrophile enabled sequential amidation and provided asymmetric squaramides with high selectivity. The squaramate-RNAs specifically reacted with the lysine of UDP-MurNAc-pentapeptide, a peptidoglycan precursor used by the aminoacyl-transferase $FemX_{Wv}$ for synthesis of the bacterial cell wall. The peptidyl-RNA obtained with squaramate-RNA and unprotected UDP-MurNAc-pentapeptide efficiently inhibited $FemX_{Wv}$. The squaramate unit also promoted specific cross-linking of RNA to the catalytic Lys of $FemX_{Wv}$ but not to related transferases recognizing different aminoacyl-tRNAs. Thus, squaramate-RNAs provide specificity for cross-linking with defined groups in complex biomolecules due to its unique reactivity.*

Chemical modification of RNA for conjugation with peptides, proteins, and other biomolecules is notoriously underdeveloped in spite of increasing interest in the field of chemical biology.[1] The most common methods are based on solid-phase synthesis (SPS) of RNA enabling the site-specific incorporation of reactive nucleotide analogues for post-functionalization.[2] Alternatively, modified nucleotides can be enzymatically incorporated into RNA but this strategy is limited by the specificity of RNA polymerases. Several approaches have successfully overcome this problem, including priming of in vitro transcription with modified nucleotides and dinucleotides,[3] 3′ extension with poly(A) polymerase,[4] post-transcriptional modifications by S-adenosylmethionine-dependent methyltransferases,[5] and expansion of the genetic code using unnatural bases both in the DNA template and RNA transcript.[6] Reaction of benzyl-guanine-RNA with the deaminase domain of the enzyme ADAR fused to the protein of interest provides RNA–protein adducts.[7] T4 RNA ligase offers flexibility, but this approach is restricted to modification of the 3′ extremity.

An initial challenge for RNA conjugation is the design of chemical groups that are compatible with SPS and RNA stability. A second challenge is the choice of a chemoselective reaction for the post-functionalization step. In the literature, nucleotide precursors were designed to incorporate azido or alkyne groups for Huisgen–Sharpless cycloaddition in RNA[3d,8] and DNA.[9] Aldehyde groups have also been incorporated for hydrazone formation.[10] Other reactions, such as Staudinger ligation,[11] or Michael addition,[12] have only been applied to DNA. Incorporation of amino or thiol nucleophiles is widely used because they are unreactive with the RNA core and their synthesis is based on commercially available phosphoramidites. However, this approach requires introduction of an electrophilic site or a thiol group into the biomolecule partner. For proteins, this can be achieved by site-directed mutagenesis to introduce a cysteine residue at the desired position. The incorporation of electrophilic groups has been based on modifications of natural amino acids, such as lysine residues, for introduction of a maleimide group,[13] or cysteine residues for conversion to dehydroalanine.[14] In contrast, the reverse approach based on electrophilic RNAs potentially provides access to cross-linking with unmodified peptides and proteins, which naturally contain

[*] Dr. M. Fonvielle,[+] C. Le Fournis, S. Cardon, Dr. M. Arthur[+]
Laboratoire de Recherche Moléculaire sur les Antibiotiques Centre de Recherche des Cordeliers
Equipe 12, UMR S 1138; INSERM
Université Pierre et Marie Curie-Paris 6
Université Paris Descartes
15 rue de L'Ecole de Médecine, Paris, F-75006 (France)
E-mail: michel.arthur@crc.jussieu.fr

N. Sakkas,[+] Dr. L. Iannazzo, Dr. E. Braud, Dr. M. Etheve-Quelquejeu[+]
Laboratoire de Chimie et de Biochimie Pharmacologiques et Toxicologiques
Université Paris Descartes, UMR 8601
Paris, F-75006 (France)
and
CNRS UMR 8601
Paris, F-75006 (France)
E-mail: melanie.etheve-quelquejeu@parisdescartes.fr

D. Patin, Dr. D. Mengin-Lecreulx
Institute for Integrative Biology of the Cell (I2BC), CEA, CNRS
Univ Paris-Sud, Université Paris-Saclay
91198, Gif-sur-Yvette cedex (France)

Dr. A. El-Sagheer, Dr. T. Brown
Department of Chemistry
University of Oxford, Chemistry Research Laboratory
12 Mansfield Road, Oxford, OX1 3TA (UK)

Dr. A. El-Sagheer
Chemistry Branch, Dept. of Science and Mathematics
Faculty of Petroleum and Mining Engineering
Suez Canal University
Suez, 43721 (Egypt)

[+] These authors contributed equally to this work.

Supporting information and the ORCID identification number(s) for the author(s) of this article can be found under http://dx.doi.org/10.1002/anie.201606843.

nucleophilic sites. In that case, the main limitation is the lack of specificity for a defined residue in peptides and proteins. Herein, we report a new electrophilic RNA derivative based on a squarate group, which specifically reacts with amino groups (Figure 1). We report the synthesis of a peptidyl–RNA

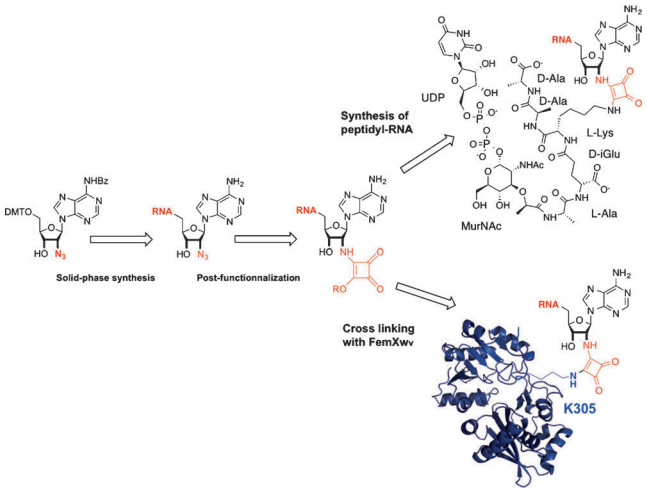

Figure 1. Synthesis of squaramate-RNA for peptidyl-RNA synthesis and cross-linking with active site K^{305} of the aminoacyl-transferase $FemX_{Wv}$. MurNAc, *N*-acetyl muramic acid; UDP, uridine-diphosphate.

conjugate and its biological evaluation as an inhibitor of the $FemX_{Wv}$ aminoacyl-transferase involved in bacterial cell wall synthesis.[15] We also show that the reactivity of the squaramate-RNA with surface-exposed non-catalytic lysine residues is limited. This enables specific formation of a covalent adduct between the squaramate-RNA and a catalytic lysine of the $FemX_{Wv}$ transferase. The unprecedented advantage of our methodology is that it does not require any modification of the protein or peptide partner used for the post-functionalization step.

Our strategy to access squaramate-RNA is based on incorporation of 2′-azido-2′-deoxyadenosine[16] at the 3′ extremity of RNA by SPS, reduction of the azido group, and addition of a squarate diester for subsequent ligation with amine containing partners (Figure 1). The relevant feature of the squarate diester group is the reduced reactivity of the mono-squaramide (also called squaramate) resulting from the first amidation step of the diester. This enables sequential amidation leading to asymmetric squaramides with high selectivity and in high yields. Diester-squarate-mediated coupling has been applied to synthesis of carbohydrate conjugates,[17] peptide-protein conjugates,[18] and oligodeoxyribonucleotide[19] or poly U-carbohydrate[20] conjugates. To investigate the relevance of this strategy for the synthesis of RNA–peptide conjugates, we first tested the two-step reaction using nucleoside and lysine as surrogates of RNA and peptide, respectively (Scheme 1).

The synthesis started by addition of commercially available diethylsquarate to the 2′-deoxy-2′-amino-adenosine **1**[21] in basic conditions. The reaction provided 2′-squaramate adenosine **2** in 80% yield. As expected,[22] no symmetric bis-

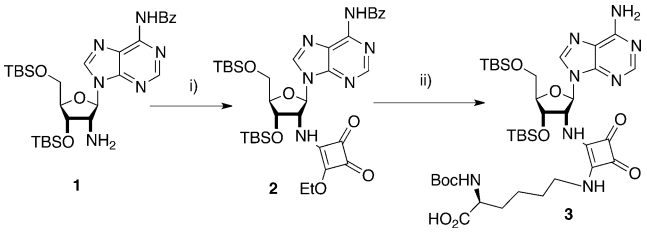

Scheme 1. Synthesis of 2′-squaramate-adenosine **2** and bis-squaramide **3**. Conditions: i) Diethylsquarate, DIPEA, EtOH, RT, 1 h, 80%. ii) Boc-Lys-OH, DIPEA, EtOH, 40 °C, 24 h, 73%.

squaramide formation was observed. Reaction of **2** with Boc-Lys in harsher conditions yielded the asymmetric bis-squaramide **3** in 73% yield. In those conditions, loss of the benzoyl protecting group of the nucleobase occurred but did not interfere with the reaction.

We then investigated squarate-mediated ligation for the synthesis of peptidyl–RNA conjugates. The RNA partners were oligonucleotides mimicking various portions of the tRNA acceptor arm (Scheme 2, inset). The peptidyl partner

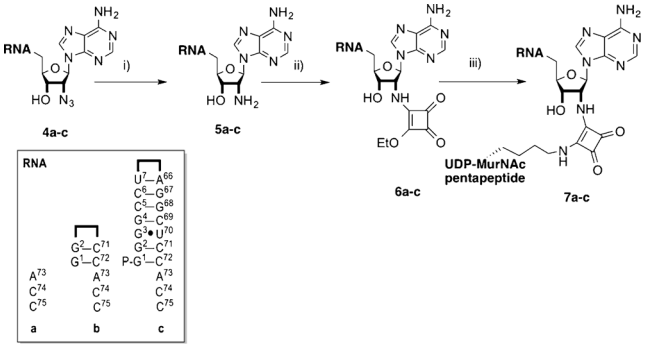

Scheme 2. Synthesis of squaramate-RNAs and peptidyl-RNAs. Conditions: i) TCEP, Tris-HCl pH 8.0, H_2O, −20 °C, 12 h, **5a** 51%, **5b** 44%, **5c** 47%; ii) Diethylsquarate (100 equiv.), HEPES pH 7.5, 20% DMF in H_2O, RT, 3 h, **6a** 79%, **6b** 75%, **6c** 75%; iii) UDP-MurNAc-pentapeptide, borate buffer pH 9.2, 10% DMF in H_2O, 37 °C, 72 h, **7a** 23%, **7b** 40%, **7c** 45%. The inset shows the sequence of the oligonucleotides linked to the 5′ position of **4**, **5**, **6**, and **7**. Base-pairing in **b** and **c** is stabilized by a phosphoethylene glycol linker introduced by SPS.[25]

was UDP-MurNAc-pentapeptide, the native cytoplasmic precursor for synthesis of bacterial cell wall peptidoglycan[23] (Scheme 2). For optimization, we first tested the 2′-azido-ACCA tetranucleotide **4a**, which was obtained by SPS (Supporting Information). The ACCA sequence of **4a** corresponds to the single-strand 3′ extremity of most tRNAs. TCEP-mediated chemical reduction of the azido group[24] of **4a** afforded the 2′-amino-tetranucleotide **5a** in 51% yield. The addition of diethylsquarate onto **5a** led to squaramate **6a** in 79% yield. We then investigated the reaction of the squaramate **6a** with UDP-MurNAc-pentapeptide, which contains a single amino group (Figure 1). The RNA-UDP-MurNAc-pentapeptide **7a** was obtained in 23% yield in borate buffer (500 mM; pH 9.2) with an excess of UDP-MurNAc-pentapeptide (10 equivalents). The same

approach was used to obtain RNA-UDP-MurNAc-pentapeptide conjugates **7b** and **7c** containing larger portions of the tRNA acceptor arm. The conjugates **7b** and **7c** contained 2 and 7 base pairs of the acceptor arm, respectively, in addition to the ACCA extremity present in **7a**. Increasing the size of the RNA moiety did not reduce the yield of the reactions (Scheme 2). These results show that the squarate-mediated ligation provides a versatile route to peptidyl–RNA adducts. It is fully compatible with unprotected UDP-MuNAc-pentapeptide, which contains phosphate groups, carbohydrate hydroxyls, and carboxyl groups (Figure 1).

The RNA-UDP-MurNAc-pentapeptide conjugate **7c** was biologically evaluated as an inhibitor of the aminoacyl transferase $FemX_{Wv}$ from *Weissella viridescens*, which catalyzes the transfer of L-Ala from Ala-tRNA^{Ala} to the peptidoglycan precursor UDP-MurNAc-pentapeptide[15] (Figure 2A). The conjugate **7c** was expected to inhibit $FemX_{Wv}$

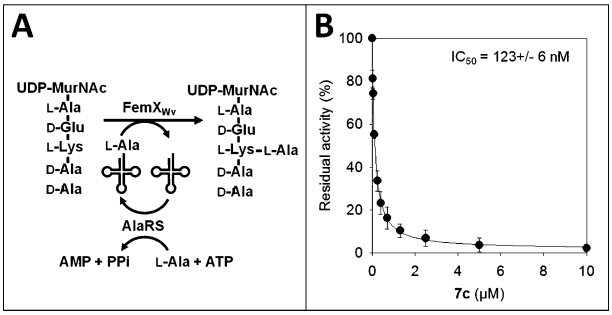

Figure 2. Inhibition of $FemX_{Wv}$ by the peptidyl-RNA **7c.** A) Amino-acyl transfer reaction catalyzed by $FemX_{Wv}$. AlaRS, alanyl-tRNA synthetase. B) Residual activity of $FemX_{Wv}$ in the presence of increasing concentrations of **7c**.

because it combines the two substrates of the aminoacyl-transfer reaction linked by a stable squaramide, as previously shown for similar bi-substrate inhibitors generated by Huisgen-Sharpless cycloaddition.[26] $FemX_{Wv}$ was inhibited by the conjugate **7c** with an IC_{50} of 123 ± 6 nM (Figure 2B). This value is three orders of magnitude higher than the IC_{50} of 0.15 ± 0.01 nM previously reported for the bi-substrate containing the same RNA and UDP-MurNAc-pentapeptide moieties linked by a triazole ring.[26a] Together, these results indicate that the squarate-mediated ligation generated a potent inhibitor, although the triazole linker is clearly favored within the $FemX_{Wv}$ active site. Nonetheless, the squaramide expands the repertoire of linkers available to generate bi-substrate inhibitors.

Our next objective was to test the cross-linking of squaramate-RNAs with $FemX_{Wv}$. Ala-tRNA^{Ala} recognition by $FemX_{Wv}$ was previously shown to mainly involve interactions with the tRNA^{Ala} acceptor arm.[26b,27] The $FemX_{Wv}$ protein partner of the ligation reaction contains 18 lysine residues in addition to the catalytic residue K^{305}, which is thought to stabilize the tetrahedral intermediate generated by nucleophilic attack of the carbonyl of Ala-tRNA^{Ala} by the amine of UDP-MurNAc-pentapeptide.[26b] Incubation of $FemX_{Wv}$ with squaramate-RNA **6c** (Scheme 2) led to marginal cross-linking (data not shown). In contrast, squaramate-RNA **6d**, containing a methyl-ester-squarate instead of an ethyl-ester-squarate (Scheme 3), was efficiently ligated to $FemX_{Wv}$ (Figure 3A). The reaction was carried out in the conditions previously used for the formation of the RNA-UDP-MurNAc-pentapeptide adduct (500 mM borate buffer, pH 9.2, 5 h, 20°C) using $FemX_{Wv}$ (50 μM) and **6d** (25 μM) in a 2:1 molar ratio. PAGE under denaturing conditions was used to monitor covalent cross-linking (Figure 3A). RNA–protein adducts were detected both by Coomassie blue staining and immuno-detection of $FemX_{Wv}$. Cross-linking of $FemX_{Wv}$ $K^{305}A$ mutant was not observed, indicating that none of the 18 other lysine residues of the protein reacted with squaramate-RNA **6d** (Figure 3A). Thus, the observed specificity for K^{305} likely results from binding of squaramate-RNA **6d** into the $FemX_{Wv}$ active site.

A fluorescein was introduced onto uracil of the U^7–A^{66} base pair in order to generate fluorescent probe **6e** (Scheme 3) for direct detection of the RNA moiety in RNA–protein adducts. The same RNA–protein adduct was observed by Coomassie blue staining, fluorescence, and

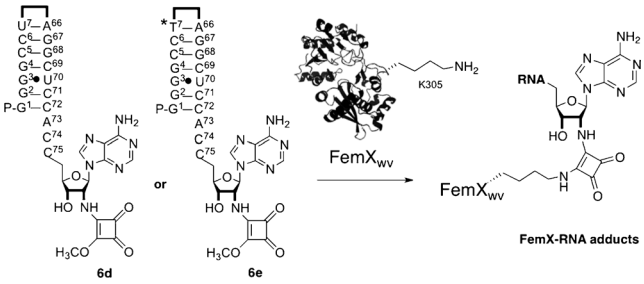

Scheme 3. Covalent cross-linking of squaramate-RNAs **6d** or **6e** with aminoacyl-transferase $FemX_{Wv}$. Conditions: 500 mM borate buffer, pH 9.2, 5 h, 20°C, $FemX_{Wv}$ (50 μM), **6d** or **6e** (25 μM). (See the *T structural formula in the Supporting Information).

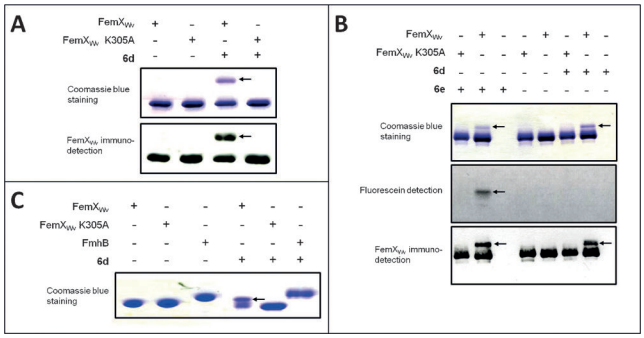

Figure 3. Analyses of the cross-linking of Fem transferases and squaramate-RNAs. A) Proteins and cross-linking adducts were separated by SDS-PAGE and detected by Coomassie blue staining and immuno-detection of $FemX_{Wv}$. B) Detection of cross-linking products obtained with squaramate **6d** and fluorescent squaramate **6e** by Coomassie blue staining, fluorescence, and Western blot. Immunodetection was performed with rabbit anti-$FemX_{Wv}$ primary antibodies and goat anti-rabbit secondary antibodies conjugated to horse radish peroxidase. C) Cross-linking of $FemX_{Wv}$, $FemX_{Wv}$ $K^{305}A$, and FmhB with squaramate **6d**. The arrows indicate the position of the $FemX_{Wv}$-squaramide adducts.

immuno-detection of $FemX_{Wv}$ (Figure 3B). This observation confirmed the presence of the $FemX_{Wv}$ and RNA moieties in the protein band detected by Coomassie blue staining. These results indicate that functionalization of RNA with fluorescein was fully compatible with the synthetic route of the squaramate-containing electrophilic RNA.

The role of RNA-binding in the cross-linking reaction involving K^{305} of $FemX_{WV}$ and the squaramate-RNA was further investigated by testing another member of the Fem aminoacyl-transferase family that does not recognize Ala-$tRNA^{Ala}$. We chose FmhB from *Staphylococcus aureus*, which specifically transfers a glycyl residue from Gly-$tRNA^{Gly}$ to peptidoglycan precursors and efficiently discriminate between Gly-$tRNA^{Gly}$ and Ala-$tRNA^{Ala}$.[28] In spite of the presence of the conserved K^{305} residue in the FmhB active site and of 49 additional lysine residues, no cross-linking of squaramate-RNA **6d** with FmhB was observed (Figure 3C). These observations confirm that binding of **6d** to the $FemX_{Wv}$ active site is required for cross-linking.

In conclusion, we have developed a versatile route for the synthesis of electrophilic RNAs based on post-functionalization of an azido group incorporated by SPS. The post-functionalization step involved the addition of a squarate diester following reduction of the azido group. This strategy was fully compatible with the introduction of other functionalities in the RNA moiety, including a fluorescent probe for the detection of RNA–enzyme adducts and a hairpin loop linker for stabilization of RNA base-pairing. The squaramate-RNAs specifically reacted with the primary amine of unprotected UDP-MurNAc-pentapeptide in spite of the presence of phosphate, hydroxyl, and carboxylic acid groups in this biomolecule. The first application of this methodology for peptidyl-RNA synthesis provided a potent inhibitor of $FemX_{Wv}$. A squaramate-RNA containing the acceptor arm of $tRNA^{Ala}$ was also found to specifically react with the catalytic Lys residue of $FemX_{Wv}$ (K^{305}), despite the presence of several additional lysines, including surface exposed residues. RNA binding into the $FemX_{Wv}$ catalytic cavity was essential for cross-linking because adducts were not observed with FmhB, which recognizes Gly-$tRNA^{Gly}$ instead of Ala-$tRNA^{Ala}$.

The unique cross-linking features of the squarate moiety provide a powerful and versatile tool for synthesis of peptidyl-RNAs. The only prerequisite is that the RNA carries an aliphatic primary amino group, which was generated from an azido group in the current study, but could also be incorporated using commercially available protected 2′-amino or 2′-aminoalkyl nucleoside building blocks, thereby providing access to bioconjugation at internal RNA positions. In contrast to others methods, natural peptides and proteins can be used for cross-linking without any modification. The assay conditions can be designed to provide specificity for lysine residues within enzyme active sites, as documented for $FemX_{Wv}$. The squaramate RNAs could therefore potentially be used to probe the reactivity of lysine residues in tRNA-dependent enzymes, generate stable RNA–protein adducts for X-ray diffraction analyses, and identify unknown tRNA-interacting proteins.

Acknowledgements

This project was funded by ANR (MimictRNA project). N. Sakkas was funded by a DGA-MRIS scholarship.

Keywords: crosslinking · Fem transferases · post-functionalization · RNA modifications · squarates

[1] a) K. Fauster, M. Hartl, T. Santner, M. Aigner, C. Kreutz, K. Bister, E. Ennifar, R. Micura, *ACS Chem. Biol.* **2012**, *7*, 581 – 589; b) A. Latorre, A. Somoza, *Angew. Chem. Int. Ed.* **2016**, *55*, 3548 – 3550; *Angew. Chem.* **2016**, *128*, 3608 – 3610; c) S. Flur, R. Micura, *Methods* **2016**, *107*, 79 – 88; d) M. Tomás-Gamasa, S. Serdjukow, M. Su, M. Muller, T. Carell, *Angew. Chem. Int. Ed.* **2015**, *54*, 796 – 800; *Angew. Chem.* **2015**, *127*, 809 – 813.

[2] a) B. Charleux, C. Copéret, E. Lacóte in *Chemistry of Organo-Hybrids: Synthesis and Characterization of Functional Nano-Objects*, Eds.: M. Arthur, M. Etheve-Quelquejeu, Wiley-VCH, Weinheim, **2015**, Chapter 8; b) C. Paris, O. Brun, E. Pedroso, A. Grandas, *Molecules* **2015**, *20*, 6389 – 6408; c) A. Biscans, S. Rouanet, J. J. Vasseur, C. Dupouy, F. Debart, *Org. Biomol. Chem.* **2016**, *14*, 7010; d) E. Paredes, M. Evans, S. R. Das, *Methods* **2011**, *54*, 251 – 259.

[3] a) A. Samanta, A. Krause, A. Jaschke, *Chem. Commun.* **2014**, *50*, 1313 – 1316; b) R. Fiammengo, K. Musilek, A. Jaschke, *J. Am. Chem. Soc.* **2005**, *127*, 9271 – 9276; c) D. Williamson, M. J. Cann, D. R. Hodgson, *Chem. Commun.* **2007**, 5096 – 5098; d) E. Paredes, S. R. Das, *ChemBioChem* **2011**, *12*, 125 – 131.

[4] M. L. Winz, A. Samanta, D. Benzinger, A. Jaschke, *Nucleic Acids Res.* **2012**, *40*, e78.

[5] a) Y. Motorin, J. Burhenne, R. Teimer, K. Koynov, S. Willnow, E. Weinhold, M. Helm, *Nucl. Acids Res.* **2011**, *39*, 1943 – 1952; b) M. Tomkuviene, B. Clouet-O'Orval, I. Cerniauskas, E. Weinhold, S. Klimasauskas, *Nucleic Acids Res.* **2012**, *40*, 6765 – 6773; c) J. Zhang, Y. G. Zheng, *ACS Chem. Biol.* **2016**, *11*, 583 – 597.

[6] a) C. Domnick, F. Eggert, S. Kath-Schorr, *Chem. Commun.* **2015**, *51*, 8253 – 8256; b) F. Eggert, S. Kath-Schorr, *Chem. Commun.* **2016**, *52*, 7284 – 7287.

[7] a) T. Stafforst, M. F. Schneider, *Angew. Chem. Int. Ed.* **2012**, *51*, 11166 – 11169; *Angew. Chem.* **2012**, *124*, 11329 – 11332; b) P. Vogel, T. Stafforst, *ChemMedChem* **2014**, *9*, 2021 – 2025; c) J. Xu, T. J. Carrocci, A. A. Hoskins, *Chem. Commun.* **2016**, *52*, 549 – 552.

[8] a) K. Onizuka, A. Shibata, Y. Taniguchi, S. Sasaki, *Chem. Commun.* **2011**, *47*, 5004 – 5006; b) J. Willibald, J. Harder, K. Sparrer, K. K. Conzelmann, T. Carell, *J. Am. Chem. Soc.* **2012**, *134*, 12330 – 12333; c) F. Li, J. Dong, X. Hu, W. Gong, J. Li, J. Shen, H. Tian, J. Wang, *Angew. Chem. Int. Ed.* **2015**, *54*, 4597 – 4602; *Angew. Chem.* **2015**, *127*, 4680 – 4685.

[9] a) P. M. Gramlich, S. Warncke, J. Gierlich, T. Carell, *Angew. Chem. Int. Ed.* **2008**, *47*, 3442 – 3444; *Angew. Chem.* **2008**, *120*, 3491 – 3493; b) P. M. Gramlich, C. T. Wirges, A. Manetto, T. Carell, *Angew. Chem. Int. Ed.* **2008**, *47*, 8350 – 8358; *Angew. Chem.* **2008**, *120*, 8478 – 8487; c) F. Seela, V. R. Sirivolu, P. Chittepu, *Bioconjugate Chem.* **2008**, *19*, 211 – 224.

[10] a) V. Raindlová, R. Pohl, M. Sanda, M. Hocek, *Angew. Chem. Int. Ed.* **2010**, *49*, 1064 – 1066; *Angew. Chem.* **2010**, *122*, 1082 – 1084; b) S. Pfander, R. Fiammengo, S. I. Kirin, N. Metzler-Nolte, A. Jaschke, *Nucleic Acids Res.* **2007**, *35*, e25.

[11] S. H. Weisbrod, A. Baccaro, A. Marx, *Methods Mol. Biol.* **2011**, *751*, 195 – 207.

[12] a) J. Dadová, P. Orsag, R. Pohl, M. Brazdova, M. Fojta, M. Hocek, *Angew. Chem. Int. Ed.* **2013**, *52*, 10515 – 10518; *Angew.*

Chem. **2013**, *125*, 10709 – 10712; b) S. Kusano, S. Ishiyama, S. L. Lam, T. Mashima, M. Katahira, K. Miyamoto, M. Aida, F. Nagatsugi, *Nucleic Acids Res.* **2015**, *43*, 7717 – 7730.
[13] N. Krall, F. P. da Cruz, O. Boutureira, G. J. Bernardes, *Nat. Chem.* **2016**, *8*, 103 – 113.
[14] J. M. Chalker, L. Lercher, N. R. Rose, C. J. Schofield, B. G. Davis, *Angew. Chem. Int. Ed.* **2012**, *51*, 1835 – 1839; *Angew. Chem.* **2012**, *124*, 1871 – 1875.
[15] J. L. Mainardi, R. Villet, T. D. Bugg, C. Mayer, M. Arthur, *FEMS Microbiol. Rev.* **2008**, *32*, 386 – 408.
[16] M. Fonvielle, M. Chemama, M. Lecerf, R. Villet, P. Busca, A. Bouhss, M. Etheve-Quelquejeu, M. Arthur, *Angew. Chem. Int. Ed.* **2010**, *49*, 5115 – 5119; *Angew. Chem.* **2010**, *122*, 5241 – 5245.
[17] a) E. V. Shmendel', M. A. Maslov, N. G. Morozova, G. A. Serebrennikova, *Russ. Chem. B+* **2010**, *59*, 2281 – 2289; b) D. J. Lefeber, J. P. Kamerling, J. F. Vliegenthart, *Chem. Eur. J.* **2001**, *7*, 4411 – 4421.
[18] a) F. R. Wurm, H. A. Klok, *Chem. Soc. Rev.* **2013**, *42*, 8220 – 8236; b) F. Wurm, T. Steinbach, H. A. Klok, *Chem. Commun.* **2013**, *49*, 7815 – 7817; c) K. Ohara, Y. Takeda, S. Daikoku, M. Hachisu, A. Seko, Y. Ito, *Biochemistry* **2015**, *54*, 4909 – 4917; d) L. Martínez, G. Martorell, A. Sampedro, P. Ballester, A. Costa, C. Rotger, *Org. Lett.* **2015**, *17*, 2980 – 2983.
[19] K. Sato, K. Seio, M. Sekine, *Nucleic Acids Res.* **2001**, *1*, 121 – 122.
[20] Y. Zhao, K. Tram, H. Yan, *Carbohydr. Res.* **2009**, *344*, 2137 – 2143.
[21] D. Mellal, M. Fonvielle, M. Santarem, M. Chemama, Y. Schneider, L. Iannazzo, E. Braud, M. Arthur, M. Etheve-Quelquejeu, *Org. Biomol. Chem.* **2013**, *11*, 6161 – 6169.
[22] R. I. Storer, C. Aciro, L. H. Jones, *Chem. Soc. Rev.* **2011**, *40*, 2330 – 2346.
[23] a) A. Bouhss, N. Josseaume, A. Severin, K. Tabei, J. E. Hugonnet, D. Shlaes, D. Mengin-Lecreulx, J. Van Heijenoort, M. Arthur, *J. Biol. Chem.* **2002**, *277*, 45935 – 45941; b) A. Bouhss, N. Josseaume, D. Allanic, M. Crouvoisier, L. Gutmann, J. L. Mainardi, D. Mengin-Lecreulx, J. van Heijenoort, M. Arthur, *J. Bacteriol.* **2001**, *183*, 5122 – 5127.
[24] J. Steger, D. Graber, H. Moroder, A. S. Geiermann, M. Aigner, R. Micura, *Angew. Chem. Int. Ed.* **2010**, *49*, 7470 – 7472; *Angew. Chem.* **2010**, *122*, 7632 – 7634.
[25] A. H. El-Sagheer, R. Kumar, S. Findlow, J. M. Werner, A. N. Lane, T. Brown, *ChemBioChem* **2008**, *9*, 50 – 52.
[26] a) M. Fonvielle, D. Mellal, D. Patin, M. Lecerf, D. Blanot, A. Bouhss, M. Santarem, D. Mengin-Lecreulx, M. Sollogoub, M. Arthur, M. Etheve-Quelquejeu, *Chem. Eur. J.* **2013**, *19*, 1357 – 1363; b) M. Fonvielle, I. Li de La Sierra-Gallay, A. H. El-Sagheer, M. Lecerf, D. Patin, D. Mellal, C. Mayer, D. Blanot, N. Gale, T. Brown, H. van Tilbeurgh, M. Etheve-Quelquejeu, M. Arthur, *Angew. Chem. Int. Ed.* **2013**, *52*, 7278 – 7281; *Angew. Chem.* **2013**, *125*, 7419 – 7422.
[27] M. Fonvielle, M. Chemama, R. Villet, M. Lecerf, A. Bouhss, J. M. Valery, M. Etheve-Quelquejeu, M. Arthur, *Nucleic Acids Res.* **2009**, *37*, 1589 – 1601.
[28] a) D. Panesso, P. J. Planet, L. Diaz, J. E. Hugonnet, T. T. Tran, A. Narechania, J. M. Munita, S. Rincon, L. P. Carvajal, J. Reyes, A. Londono, H. Smith, R. Sebra, G. Deikus, G. M. Weinstock, B. E. Murray, F. Rossi, M. Arthur, C. A. Arias, *Emerging Infect. Dis.* **2015**, *21*, 1844 – 1848; b) T. Schneider, M. M. Senn, B. Berger-Bachi, A. Tossi, H. G. Sahl, I. Wiedemann, *Mol. Microbiol.* **2004**, *53*, 675 – 685.

Received: July 14, 2016
Revised: September 3, 2016
Published online: ■■ ■■, ■■■■

